Valorization of paper waste into platform chemicals

Emmanuel Nzediegwu

Department of Bioresource Engineering

Faculty of Agricultural and Environmental Science

Macdonald Campus of McGill University

Ste-Anne-de-Bellevue, Québec, Canada

December 2022

A thesis submitted to McGill University

In partial fulfilment of the requirements of the degree of

Doctor of Philosophy

Abstract

In recent years, the use of lignocellulose has become a global alternative to fossil fuels to produce bio-based chemicals. They consist of inedible parts of plants, grasses, and forestry residues whose use will not cause food crisis. Among them, paper waste is one of the most prominent due to its abundance and environmental friendliness. The increase in paper consumption has created a huge reserve of paper waste, encouraging their transformation to valuable products in the biorefinery.

The primary focus of this study was the valorization of different types of paper products into platform chemicals. Specifically, newsprints and corrugated boxes were hydrolysed to produce levulinic acid, hydroxymethylfurfural, and furfural, depending on the selected reaction conditions. In the first instance (chapter 3), soft/hardwood pulps were decationized by dilute acid hydrolysis followed by thermo-chemical conversion to levulinic acid. The effects of the major reaction conditions including reaction temperature, time, and HCl concentration on the yield of levulinic acid were studied *via* a central composite design. Levulinic acid yields from softwood and hard wood pulps reached 50.3 mol% and 68.9 mol%, respectively, at optimum reaction conditions. When newsprints were tested using the optimized parameters for softwood and hardwood conversion, levulinic acid yields of 66.3 mol% and 79.7 mol% were obtained, respectively.

Chapter 4 focused on the effect of pretreatment on the conversion of newsprint wastes to levulinic acid. In this study, Box-Behnken design (BBD) was employed to optimize the yield of levulinic acid from HCl and Fenton pretreated newsprints (NP). With the optimum conditions for the conversion of HCl-NP and Fenton-NP as follow: T = 200 ^{o}C, t = 3.63 and 3.50 h, and [$FeCl_3.6H_2O$] = 0.118 and 0.100 M, the maximum yields of LA were 81.3 mol% and 84.0 mol%, respectively.

In chapter 5, an integrated mechanoenzymatic/catalytic approach was employed to produce furan-based platform chemicals from newsprint wastes. The holocellulose fraction of the newsprint was first hydrolyzed to monosaccharides using a commercial cellulase blend at 55 ^{o}C (enzyme loading of 45 mg/g of substrate or 4.55 w/w). The use of a moist-solid enzymatic reaction with a short period (15 min) of ball milling followed by 24 h of static incubation greatly enhanced hydrolysis, affording glucose and xylose yields of 52 mol% and 22 mol%, respectively. The sugars in the hydrolysate were next dehydrated using $AlCl_3.6H_2O$ (200 mg) as an eco-friendly catalyst. With stirring at 600 rpm and 150 ^{o}C, hydroxymethylfurfural and furfural were obtained in yields of 66 mol% and 67 mol%, respectively.

The last study in this thesis (chapter 6) proposed a simplified approach to produce hydroxymethylfurfural and furfural from corrugated boxes. A robust catalytic system comprising $AlCl_3.6H_2O$/LiCl/NaCl in H_2O/MIBK biphasic media was developed, affording HMF and FU in maximum yields of 98 mol% and 51 mol% at 160 ^oC and 40 min. Another aspect in the above-listed chapters were the detailed kinetic studies that followed, which provide deeper insights into the various stages necessary to enhance the yields of value-added products from paper waste. The information developed in this study can aid the production of biobased products as well as help the design of biorefinery which is still in the developmental stage.

Résumé

Ces dernières années, l'utilisation de la lignocellulose est devenue une alternative mondiale aux combustibles fossiles pour produire des produits chimiques d'origine biologique. Ils sont constitués de parties non comestibles de plantes, d'herbes et de résidus forestiers dont l'utilisation ne provoquera pas de crise alimentaire. Parmi eux, les déchets de papier sont l'un des plus importants en raison de leur abondance. L'augmentation de la consommation de papier a créé une énorme réserve de déchets de papier, encourageant leur transformation en produits de valeur.

L'objectif principal de cette étude était la valorisation de différents types de produits provenant de l'industrie papetière en produits chimiques de haute valeur. Plus précisément, des papiers journaux et des boîtes de carton ont été hydrolysés pour produire de l'acide lévulinique, de l'hydroxyméthylfurfural et du furfural. Dans le premier cas (chapitre 3), les pâtes de résineux/feuillus ont été traités par hydrolyse acide diluée suivie d'une conversion thermochimique en acide lévulinique. Les effets des principales conditions de réaction comprenant la température de réaction, le temps, et la concentration de HCl sur le rendement de l'acide levulinic ont été étudiés par l'intermédiaire d'un plan composite centré. Les rendements en acide levulinique des pâtes de bois résineux et de bois dur ont atteint 50,3 % en mole et 68,9 % en mole, respectivement, dans des conditions de réaction optimales. Lorsque les journaux ont été testés à l'aide des paramètres optimisés pour la conversion du bois résineux et du bois dur, des rendements d'acide lévulinique de 66,3 % en mole et de 79,7 % en mole ont été obtenus, respectivement.

Le chapitre 4 porte sur l'effet du prétraitement sur la conversion des déchets de papiers journaux en acide lévulinique (LA). Dans cette étude, la design Box-Behnken a été utilisée pour optimiser le rendement en acide levulinique à partir de HCl et de papiers journaux (NP) prétraité par la réaction de Fenton. Avec les conditions optimales pour la conversion de HCl-NP et Fenton-NP comme suit: T = 200 ^{o}C, t = 3,63 et 3,50 h, et [$FeCl_3.6H_2O$] = 0,118 et 0,100 M, les rendements maximaux de LA étaient 81,3% et 84,0 % en mole, respectivement.

Au chapitre 5, une approche mécano-enzymatique/catalytique intégrée a été utilisée pour produire des produits chimiques à base de furanes à partir de déchets de papier journal. La fraction holocellulosique du papier journal a d'abord été hydrolysée en monosaccharides à l'aide d'un mélange commercial de cellulase à 55 ^{o}C (charge enzymatique de 45 mg/g de substrat ou 4,55 p/p). L'utilisation d'une réaction enzymatique humide-solide avec une courte période (15 min)

dans un broyeur à boulet, suivie de 24 h d'incubation statique a considérablement augmenté l'hydrolyse, produisant des rendements de glucose et de xylose de 52% et de 22% en mole, respectivement. Les sucres présents dans l'hydrolysat ont ensuite été déshydratés en utilisant un catalyseur de $AlCl_3.6H_2O$ (200 mg). Sous agitation à 600 rpm et 150 ^oC, l'hydroxyméthylfurfural et le furfural ont été obtenus dans des rendements de 66% et 67% en mole, respectivement.

La dernière étude de cette thèse (chapitre 6) propose une approche simplifiée pour produire de l'hydroxyméthylfurfural et du furfural à partir de boîtes de carton. Un système catalytique robuste comprenant du $AlCl_3.6H_2O$/LiCl/NaCl dans les milieux biphasiques de H_2O/MIBK a été développé, offrant de l'hydroxymethylfurfural et du furfural dans des rendements maximaux de 98% et 51 % mole à 160 ^oC et 40 min. Un autre aspect des chapitres énumérés ci-dessus a été les études cinétiques détaillées qui ont suivi, qui fournissent des informations plus approfondies sur les différentes étapes nécessaires pour améliorer les rendements des produits à valeur ajoutée provenant des déchets de papier. Les informations développées dans cette étude peuvent aider à la production de produits d'origine biologique ainsi qu'à la conception de la bioraffinerie qui est encore au stade de développement.

Dedication

This thesis is dedicated to the Almighty God, for His divine protection, guidance, and above all, for His gift of life without which nothing is possible.

Acknowledgements

First of all, I sincerely thank and appreciate the Almighty God for bestowing on me wisdom, knowledge, a sound mind, and most importantly, good health, without which I would not have come this far. According to the bible (Ecc. 7:8), better is the end of a thing than the beginning thereof.

My unreserved appreciation goes to my indefatigable supervisor, Dr. Marie-Josée Dumont for accepting to supervise and fully fund my Ph.D. program. Your consistent and invaluable support helped me to be successful throughout my studies. I am most grateful for your words of hope and encouragement which were inspiring especially during the seemingly challenging times. I am forever grateful and indebted to have benefited from your wealth of knowledge, experience, and expertise. Thank you so much, Dr. Dumont.

I want to also commend the unwavering support of Dr. Agneev Mukherjee, a true friend who was a postdoc in Dr. Dumont's Lab when I started my studies. You painstakingly coached and cheerfully directed me to ensure that I was independent to carry out my research before you left. While away, you have consistently kept in touch, always asking about my progress per time. You are nothing but an embodiment of inspiration to me. Thank you, Dr. Agneev. I say a very big thank you to Surabhi Pandey, Karoline Dietrich, and other members of our group for their teamwork, dedication, and corporation. It was good having you all as part of the team.

I specifically thank Yvan Gariepy for his wealth of technical knowledge, always willing to assist and proffer solutions to problems as they come; Dr. Vijaya Raghavan, Dr. Valérie Orsat, Dr. Michael Ngadi and Dr. Karine Auclair of the Chemistry Department for their guidance as well as allowing me to work in their laboratories.

I met a lively community of Nigerian students and other friends during the course of my program; these great minds including - Valentine Okonkwo, Dare Oloruntoba, Izuchukwu John, Dr. Samuel Ihuoma, Gaurav Pradhan, Tolulope Abodunrin, and a host of others are highly appreciated for their moral and social support. I am also thankful to the entire family of Restoration House Montréal for her constant support, prayers, and love.

My special thanks go to my parents, especially to my late dad, Deacon Joshua Nzediegwu, whose aspirations inspired me throughout this program; to my lovely siblings, especially to Dr. Christopher Nzediegwu and family, for their love, prayers, and support.

Finally, to my lovely and dear wife, Josephine Ahiante (Ph.D.), who recently joined me in Canada, you have brought so much joy to me. Thank you for your love, moral and spiritual support. I sincerely appreciate and love you, girl.

Contribution of Authors

The excerpt from this thesis has been accepted in form of original papers or submitted for publication in peer-reviewed journals. The principal author, Emmanuel Nzediegwu, was responsible for developing protocols, designing, and performing the experiments, in addition to model development, data analysis, and manuscript composition. Dr. Marie-Josée Dumont contributed to all aspects of the research by providing supervisory insight, and intellectual guidance, and reviewing and correcting the manuscripts and thesis. Dr. Guillermo Alberto Portillo Perez assisted in writing and editing the manuscript. Dr. Karine Auclair and Dr. Mario Pérez Venegas contributed as part of a collaborative project on mechanochemistry, providing the use of their laboratory, as well as protocol designs, resources, writing, and reviewing of the manuscript. Details of the papers from this thesis are as follows:

1. E. Nzediegwu and M.-J. Dumont, "Chemo-catalytic Transformation of Cellulose and Cellulosic-Derived Waste Materials into Platform Chemicals," Waste Biomass Valoriz. Pp. 1-27, 2020.
2. E. Nzediegwu, G. Portillo-Perez, and M.-J. Dumont, "Valorization of decationized newsprint to levulinic acid," Cellulose, pp. 1-19, 2021.
3. E. Nzediegwu and M.-J. Dumont, "Optimization and mechanistic kinetic model: Toward newsprint waste conversion to levulinic acid, "J. Environ. Chem Eng. Vol.9, no. 6, p. 106637, 2021.
4. E Nzediegwu, M Pérez-Venegas, K. Auclair, and M.-J. Dumont, "Semisynthetic production of hydroxymethylfurfural and furfural: The benefits of an integrated approach," J. Environ. Chem. Eng., P. 108515, 2022.
5. E. Nzediegwu, M.-J. Dumont, "One-pot conversion of corrugated boxes for the co-synthesis of hydroxymethylfurfural and furfural in a biphasic media, Cellulose (accepted under the condition of revision).

Table of Contents

List of Figures

List of Schemes

List of Tables

List of Abbreviations

AC.....Activated Carbon

$AlCl_3.6H_2O$…….Aluminum Chloride Hexahydrate

ACN……..……Acetonitrile

AAEM…….Alkali and Alkaline Earth Metals

ADF……..……..……Acid Detergent Fiber

ADL…….……Acid Detergent Lignin

APPO ..... Aqueous Phase Partial Oxidation

[Bmim]Cl .....1-butyl-3-methyl imidazolium chloride

BSTFA……..……Bis(trimethylsilyl)trifluoroacetamide

CB……..…… Corrugated Boxes

CNT ..... Carbon Nanotubes

CNF.....Carbon Nanofibers

CaCO3……..…….Calcium Carbonate

$CaSO_4$..... Calcium Sulfate

COOH .....Carboxylic Acid

DEG .....Diethylene Glycol

DHA..... 1,3-dihydroxyacetone

DOE ..... Department of Energy

DMSO ..... Dimethyl Sulfoxide

DNS……..……3,5-dinitrosalicylic acid

EPN..... Environmental Paper Network

EG .....Ethylene Glycol

[Emim]Cl .....1-ethyl-3-methyl imidazolium chloride

[Epyr]Cl ..... 1-ethyl pyridinium chloride

FAO .....Food and Agriculture Organization

FA ..... Formic Acid

FDCA.....2,5-furan dicarboxylic acid

FT-IR……..……Fourier Transform-Infra Red

GC-MS……..……Gas Chromatography-Mass Spectrometry

GDP……. Gross Domestic Product

GVL ..... ϒ-valerolactone

GA……..……..Gluconic Acid

GLA……..……..Glyceraldehyde

Glc……..…….Glucose

He…….Helium

H_2O……Water

H_2O_2…….Hydrogen Peroxide

HCl……..……Hydrochloric Acid

HPLC…….……High-performance Liquid Chromatography

HSO_4 ..... Hydrogensulfate

HW……..…….Hard Wood

HMF……...……Hydroxymethylfurfural

HTC ..... Hydrothermal Processing Technology

OH.....Hydroxyl Group

ILs .....Ionic Liquids

FeCl3.6H2O……...……Iron(III) Chloride Hexahydrate

LiCl……..Lithium Chloride

$Ln(OTf)_3$ ..... Lanthanide Triflate

LG……..……Levoglucosan

LA .....Levulinic Acid

MTHF 2-Methyl-tetrahydrofuran

MCC.....Microcrystalline Cellulose

MC-Sn-CNS..... Microwave-treated Chestnut Shell

MEG..... Monoethylene Glycol

MIBK…….Methyl Isobutyl Ketone

MSW..... Municipal Solid Waste

NDF…….Neutra Detergent Fiber

NPs.....Nanoparticles

NREL……..….National Renewable Energy Laboratory

OMC .....Ordered Mesoporous Carbon

PW…….…….Paper Wastes

$LaCoO_3$ ..... Perovskite Metal Oxide

PS-PEG-OSO3H……Polystyrene-Poly(ethylene glycol)

PTSA-POM…….....p-toluene Sulfonic Acid and Paraformaldehyde

RAging……..…… Reactive Aging

RI…….……..Refractive Index

LG……..……Levoglucosan

PET ..... Polyethylene Terephthalate

SAPO…….Silicoaluminophosphate

SEM…….. Scanning Electron Microscope

SO_3H ..... Sulfonated Functional Group

CP-SO_3H .....Sulfonated Chloromethyl Polystyrene Resin

SDBS……..Sodium Dodecyl Benzene Sulfonate

NaOH……Sodium Hydroxide

Na_2SiO_3……..Sodium Silicate

SPPS.....Sulfonated Poly(phenylene sulfide)

SPTPA ..... Sulfonated Polytriphenylamine

SW…….,…….Soft Wood

TGA……Thermal Gravimetric Analyzer

TRS .....Total Reducing Sugar

TEG.....Triethylene Glycol

AlW..... Tungstated Alumina

ZrW..... Tungstated Ziconia

UNEP……..…….United Nation Environment Programme

WP ..... Tungstine Phosphide

VWD……..…….Variable Wavelength Detector

Xyl……..……..Xylose

1 Introduction

1.1 General introduction

The fourth industrial revolution has caused a profound effect on the global economy, reshaping the way we live, work, and interact [1]. However, the world's heavy dependence on fossil fuels could negatively impact the global life style due to their huge environmental impact. Recently, different groups of interest including policy makers and the scientific community have shifted their focus to the valorization of lignocellulosic biomass as a renewable and cleaner alternative to fossil fuel. It is mainly composed of cellulose, hemicellulose, and lignin that are non-edible, and may not compete with the food supply chain [2]. However, they have a complex composition, which is the reason for their huge processing difficulty in biorefinery. Pretreatment is a key step to fractionate, utilize, and efficiently transform lignocellulose into valuable products. An ideal pretreatment would among others, reduce the lignin content, increase the biomass surface area, as well as cause a concomitant reduction in cellulose crystallinity. Pretreatment as a costly and energy-intensive step could be a determinant factor of the economic viability of a biorefinery [3]. Pretreatment differs and is mild for paper wastes whose parent source (wood) is subjected to prehydrolysis before pulp formation during papermaking. Therefore, a strong case is made for the repurposing of paper wastes, to compensate for its abundance and relatively low cost.

Even with the high recycling activities, the majority of this refuse is either dumped or incinerated, which significantly increase the rate of environmental pollution. As paper consumption is increasing, the demand on the environment becomes more intense not only to produce more paper from trees but also to cope with the increasing amount of paper wastes. During thermochemical conversion, the holocellulose in the PW can be transformed into platform chemicals such as hydroxymethylfurfural (HMF), levulinic acid (LA), and furfural (FU), depending on the type of sugar and the selected reaction conditions. To begin, the hollocellulose is converted to sugars *via* acid or enzymatic hydrolysis. Although acid hydrolysis has existed since the 20^{th} century, it is the least employed in the industry [4, 5]. To hydrolyze cellulose in aqueous media, high temperatures (>140 ^{o}C) and strong acids (pKa < -3) are needed [6]. The overall reaction from cellulose to glucose is exothermic (-3 kcal mol^{-1} in water at 13 ^{o}C to 43 ^{o}C) [7], but has high energy barriers (30 to 40 kcal mol^{-1}) [8].

The first technology for the acid hydrolysis of cellulose was developed in 1920, known as Scholler's process [9]. The process allowed the passage of a 0.5 wt% H_2SO_4 solution through wood wastes in a percolator at 170 ^{o}C and 20 bar for about 45 min [9]. Sugars in yield of 50 %

was attained, and the remaining 50% liquor was a mixture of hydrolyzed oligosaccharides and furan derivatives. For the Bergius process, cellulose hydrolysis was performed in 40 wt% HCl at 25 ^{o}C [10]. Cellulose and hemicellulose were solubilized in the reaction medium, while lignin was insoluble. Cellulose was degraded into oligosaccharides and glucose within a few hours, with a little amount of degradation products, such as HMF and LA [10]. Hemicellulose was also hydrolyzed, producing mannose, xylose, galactose, glucose, and fructose. Similarly, cellulose was hydrolyzed using HCl in the presence of $CaCl_2$ or LiCl at 90 ^{o}C [4]. Sugars yields of up to 85% were reported and the swelling effect of the salt in the cellulosic fibers was the main cause of the improved hydrolysis rate. For the Madison wood-sugar process, wood was treated with a continuous flow of 0.5 to 0.6 wt% H_2SO_4 at 150 ^{o}C to 180 ^{o}C [11]. Compared to the Scholler process, hydrolysis was done in a shorter time because the produced sugars were removed more rapidly.

Freudenberg and Blomqvist reported a decreased rate of cellulose hydrolysis in 50 wt% H_2SO_4 at 18 ^{o}C and 30 ^{o}C as their degree of polymerization (DP) increased [12]. Cellulose activation energy being 125 kJmol^{-1} was quite higher than for 1,4-β-glucans (114-112 kJmol^{-1}). Saeman [13] reported an activation energy of 179 kJmol^{-1} from a detailed kinetic study of cellulose in dilute acid at 170-190 ^{o}C [13]. The hydrolysis was a first-order reaction depending on the concentration of H_3O^+. The high activation energy was attributed to a modification of the hydrolysis process by diffusion at the early stages, and then to a transient opening of the H-bonded structure that accompanies the rupture of the glycosidic bonds. From the literature, acidified cellulose hydrolysis in aqueous media has been well explored with different improvements made on reaction conditions. For instance, the decision on solvent (water, ionic liquids (ILs), and deep eutectic solvent) selection [14], the use of solid phase and metal catalysts instead of strong acids like H_2SO_4 or HCl [15], and the enhanced mixing in the form of mechanical ball milling [16] have enabled the use of cellulose from both economic and environmental standpoint.

Glucose, a product of cellulose hydrolysis, is a precursor for the synthesis of several platform chemicals such as HMF and LA. One important reaction is the isomerization of glucose to fructose [17]. Naturally, fructose occurs as a monomer of inulin or levan. Since 1967, fructose has been majorly produced as a component of high fructose syrups [18]. The process involves the breakdown of starch to glucose, prior to its isomerization to fructose in the presence of immobilized α-xylose ketoisomerase [18]. Following this route, the annual global production of fructose was estimated to be about 60,000 metric tons in 2006 [19]. However, the enzymatic production of fructose appears to be expensive owing to the following:

the high cost and low stability of enzymes, the need for glucose of high purity, and the use of buffer solutions. This has encouraged the design of suitable chemo-catalysts that could isomerize glucose to fructose. Chemically, the isomerization is carried out under basic or acidic condition as detailed below.

The use of a basic catalyst such as alkali and alkali earth hydroxides is traced to the year 1885 as the pioneer catalyst to isomerize glucose to fructose [20]. The reaction follows the Lobry de Bruyn-Alberda van Ekenstein rearrangement, named after the researchers for their discovery [20, 21]. For a long time, this reaction remained the simplest and most convenient method for the synthesis of a series of rare monosaccharides such as mannose, galactose and ribose. The two-step rearrangement reaction involves epimerization and aldose-ketose interconversion, occurring almost simultaneously. In the presence of the basic catalyst, a proton is eliminated from the O-1 of the glucose molecule, enabling ring opening of the glucose, prior to charge transfer to O-5, which subsequently extracts a proton from O-2, and finally forms an enediol anion. The final product being fructose is formed *via* electron pair movement through the carbon skeleton [21]. As stated above, previous studies mainly employed NaOH and $Ca(OH)_2$ as efficient catalysts. However, despite being very active, these chemicals generated numerous acidic byproducts, especially at high concentrations or increased reaction time and temperature [22]. This undesired reaction is a result of aldolization/retroaldolization, *β*-elimination, and benzillic rearrangement reactions that occur at the same time as isomerization [23].

Classical Lewis acids such as $AlCl_3$ and $FeCl_3$ are usually deactivated in water [20]. This is because water molecules coordinate with a metal cation and the obtained hydrated cation undergoes partial hydrolysis [24]. The negative effect of H_2O could be limited when the Lewis acid sites (e.g. Sn or Ti atoms) are implanted in the hydrophobic zeolite framework [25]. In addition, water is a solvent of choice for biomass valorization, considering its high polarity and poor solubility in organic solvents. The revealed catalytic activity of Lewis acids to isomerize sugars in bulk water has prompted much research interest. To begin, Moliner et al. pioneered the research on the catalytic efficiency of Sn silicalite with β zeolite topology for glucose-fructose isomerization in H_2O [26]. They reported that Sn-beta isomerized a 10 wt % of glucose solution to generate 31 wt % fructose at 110 ^oC. Remarkably, in an acidic environment (pH = 2, HCl), Sn-beta afforded fructose in yield of 33%. Surely, the ability to isomerize sugars at a low pH is needful to overcome some of the main drawbacks common with basic catalysts such as the neutralization of active sites by acidic by-products and the low stability of sugars in alkaline environments. The zeolite topology and the nature of the Sn site

were shown to significantly influence the catalytic activity. However, the isomerization reaction did not proceed with a medium pore zeolite structure. This is most likely because glucose molecules are not able to enter the smaller pores [27].

1.2 Hypothesis

1. Using hard/softwood pulp and newsprint wastes as feedstocks, and mineral acid (HCl) as a catalyst, it is possible to attempt the hydrothermal production of LA.

2. Newsprint wastes pretreated using HCl and Fenton reagent can both be effective for LA synthesis.

3. It is possible to convert untreated newsprint wastes to glucose and xylose by enzymatic hydrolysis followed by aluminum-catalyzed dehydration to generate HMF and FU under mild reaction conditions.

4. It is possible to valorize corrugated boxes using a robust catalytic system comprising of $AlCl_3.6H_2O$/LiCl/NaCl in H_2O/MIBK biphasic system to HMF and FU in a one-pot reaction.

1.3 Study Objectives

The objective of this work was to develop an efficient route for the utilization of paper waste in biorefinery other than for bioethanol production. In the first instance, the potential to produce LA from newsprint waste was evaluated based on trials performed on wood pulps using HCl as a catalyst. Thereafter, the newsprint was characterized to determine its morphology, chemical composition, functional groups, and thermal stability. Response surface methodology (RSM) was used to evaluate the reaction to optimize the conditions for maximum product yields. Another aspect was kinetic studies, which provided insights into the various steps necessary for the conversion of the newsprint into the products of interest. More specifically, the objectives are detailed as follows:

Objective 1 (Chapter 3)

a) To evaluate the potential to improve the yields of LA from decationized hard/softwood pulps using RSM.
b) To test the optimized condition from RSM on the production of LA from decationized newsprint.
c) To characterize the newsprint in terms of chemical composition and thermal stability.
d) To develop a kinetic model, fitting experimental data, to understand the various steps toward newsprint conversion to LA.

Objective 2 (Chapter 4)

a) To optimize and compares the yields of LA from HCl pretreated (HCl-NP) and Fenton pretreated (Fenton-NP) newsprints using RSM.
b) To develop a mechanistic model, fitting experimental data, to understand the various steps toward the conversion of HCl-NP and Fenton-NP.
c) To characterize and compare the morphology of the untreated, HCl, and Fenton pretreated newsprint.
d) To test the sustainability of the catalytic system ($FeCl_3.6H_2O$/LiCl) by comparing its reusability in MIBK or THF.

Objective 3 (Chapter 5)

a) To convert untreated newsprint to glucose and xylose by enzymatic hydrolysis followed by aluminum-catalyzed dehydration to generate HMF and FU under mild reaction conditions.
b) To compare the effect of enzymatic hydrolysis using a moist solid mixture with those achieved under a bulk solvent environment.
c) To develop a mechanistic model, fitting experimental data, to understand the various steps toward the conversion of the monomeric sugars from untreated newsprint to HMF and FU.

Objective 4 (Chapter 6)

a) To screen the catalytic activity of $FeCl_3.6H_2O$ and $AlCl_3.6H_2O$ for the one-pot conversion of corrugated boxes to HMF and FU in a biphasic media.
b) To improve the yields of HMF and FU based on a trade-off between the different process parameters such as $AlCl_3.6H_2O$/LiCl/NaCl in H_2O/MIBK biphasic media at a selected reaction temperature and time.
c) To characterize the corrugated boxes by studying their inherent functional group and chemical composition.
d) To develop a kinetic model, fitting experimental data, to understand the various steps toward corrugated boxes conversion to HMF and FU.

2 Literature review - Chemo-catalytic transformation of cellulose and cellulosic-derived waste materials into platform chemicals.

2.1 Abstract

The transformation of lignocellulosic biomass into valuable products is an important area of modern biotechnology. Lignocellulosic biomass wastes include industrial and municipal wastes, agricultural residues, forest residues, and natural herbaceous plants. They are mostly composed of cellulose, hemicellulose, and lignin. With cellulose being the most abundant biopolymer on earth, it has been identified as an alternative to the petroleum-based feedstock to produce platform chemicals. However, the use of cellulose is challenging due to its recalcitrance to dissolution. At present, the catalytic conversion of cellulose and cellulosic materials is studied by various research groups. This review outlines the procedures for the chemo-catalytic conversion of cellulose to help valorize paper wastes into platform chemicals. These platform chemicals include sorbitol, ethylene glycol, gluconic acid, lactic acid, LA, and HMF. Recent advances in the design and the use of novel homogenous and heterogenous catalysts have been reported. Special attention has been given to heterogenous catalysts due to their green status and scale-up potential. Moreover, the potential to recycle and reuse pulp and paper for bioprocessing has also been reviewed. Finally, the current and future market scenarios for these platform chemicals have been discussed. If economically competitive, these building block chemicals could overtake their fossil-based counterparts.

Keywords: Catalytic systems; cellulose; paper wastes; platform chemicals.

2.2 Introduction

The conversion of non-edible plant biomass to valuable bioproducts, biofuels, and/or biochemicals is an important area of modern biotechnology [28]. A vast number of these biomasses include industrial and municipal wastes, agricultural residues, forest residues, natural herbaceous plants, and so forth. Plant-based biomass from food and non-edible materials (e.g. paper materials/wastes) are abundant, renewable, and inexpensive sources of feedstock, which accumulate in the world in large amounts. For example, the estimated annual accumulation of biomass in the US is more than 1 trillion kg per year, with 30% coming from forestry residues [29]. Global paper production is continuously increasing and totalized 400 billion kg in 2015 [30, 31]. A small ratio of paper waste (PW) material is recycled, while most of the used materials are discarded in landfills or burned in an incinerator.

PW has been categorized as all manner of previously discarded paper or paperboard products including office papers, newsprints, cardboard, corrugated boxes, milk cartons, tissue paper, paper plates, and cups [32]. These wastes are also labeled as used-up papers that are no longer relevant for the purpose for which they were made, or that have already served such purpose and are meant to be discarded [33]. It is now obvious that paper and paper products in most developed and developing countries represent a great percentage of the municipal solid waste (MSW) stream. Predictions on global paper consumption indicate that a large amount of PW will continue to be generated in developing and developed countries [34]. A justification for this may be attributed to the increasing demand for paper and paperboard which invariably occurs with the growth of a country's GDP [35]. For several years, PW has continued to form one of the largest components of the MSW stream in the United States, Europe, and some parts of Asia [33].

The build-up of paper and cardboard wastes has increased continuously from 2007 to 2017 in Europe, as shown in Fig.2.1. In the US alone, the per-capita paper consumption was estimated to be approximately 317 kg/person in 2004, while that of China and the rest of Asia felt below 50 kg/person/year [36]. In 2015, the United Nation Environment Programme (UNEP) global outlook on annual per capital paper consumption showed that the waste amounted to 240 kg in North America, 140 kg in Europe, 40 kg in Asia, and 4 kg in Africa [37].

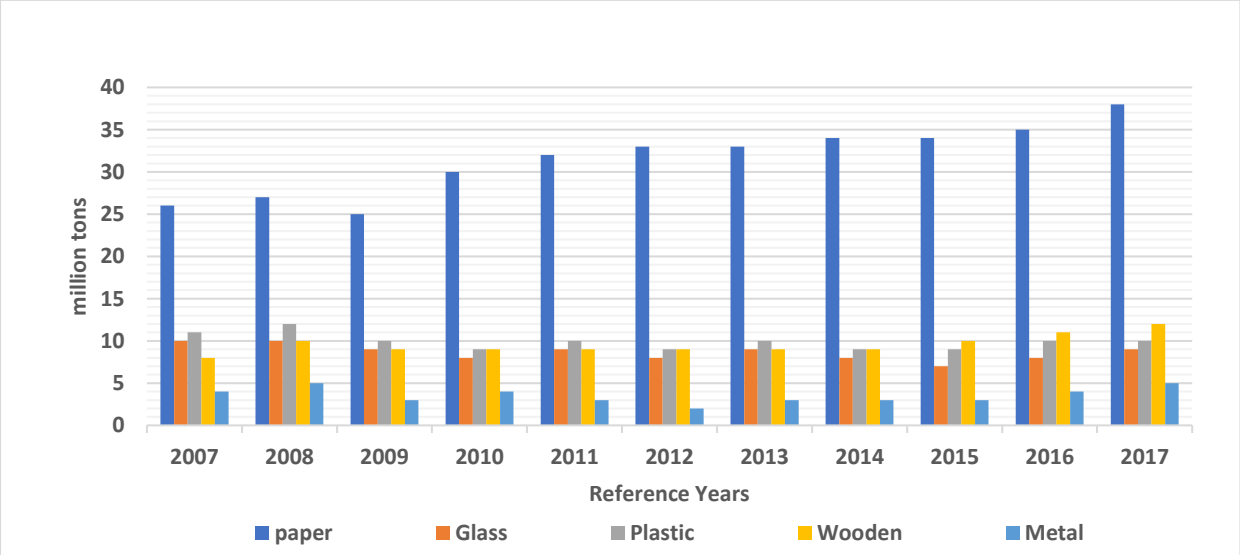

Fig.2.1: Various compositions of packaging wastes: a case study of Europe (2007-2017) [38].

The global demand for paper and paperboard materials is predicted to increase by 60%, from 368 billion kg recorded in 2005 to 579 billion kg forecasted by 2021 [39]. Despite the high

degree of recycling activities adopted in developed countries, there exists an estimated volume of 10 billion kg of paper and boards that are currently ending up in incineration plants or landfills. Notwithstanding the recycling rate of 71.7% achieved in 2012 [40], 48 billion kg of PW is being disposed of in the US [41]. These large amounts discarded could be a new dawn for the bioconversion of PW to other valuable products.

PW is the second most abundant lignocellulosic component of MSW after food waste, representing approximately 27% of the lignocellulosic fraction of MSW [42, 43]. In a biorefinery, these wastes are mainly utilized to produce biofuels. This review aims at combining and condensing the body of knowledge related to the transformation of these wastes into platform chemicals other than ethanol. A global perspective on the pulp and paper industry is first provided, and the market potentials for the chemicals presented in this review are discussed.

2.3 Pulp and paper: a global perspective

Pulp and paper production has become one of the largest world industries, contributing to a country's GDP [44]. In 2015, the Canadian pulp and paper industry accounted for about 39% of its forestry product which makeup 1.1% of the country's GDP [45] Most of this growth occurs in the packaging and tissue sectors [46]. Previously, 85% of the world's paper was manufactured and predominantly utilized in the US, Canada, Western Europe, and Japan [47]. Today, there is a decrease in global paper production in North America and Europe. This trend correlates with a report by the Environmental Paper Network (EPN) on the global paper industry. The report posits that one goal of the global paper's vision is to reduce total paper consumption [39]. However, the use of paper is increasing. Currently, Asia accounts for about half of the pulp and paper used worldwide [39]. China has taken over the US as the leading paper producer, generating more than a quarter of the world's paper [48]. Presently, fibres can be obtained from both wood and non-wood biomass. About 13 billion kg of pulp is generated from non-wood agricultural wastes [49]. In China, agricultural fibres account for more than 50% of the pulp. The non-wood pulp peaked at 10.5 billion kg in 2004 and decreased to about 3.5 billion kg in 2015 [50]. Since then, there has been a massive shift toward wood-based fibres for the manufacture of paper.

In 2014, about 172 billion kg of pulp were produced globally from virgin fibres, where North America and Europe were the major producers [51, 52]. One of the concerns regarding the increase in the production of pulp has been related to the rate of deforestation. Accordingly, between 2010 and 2015, the Food and Agriculture Organization (FAO) estimated the annual

forest loss at 7.6 million hectares with an annual forest gain of 4.3 million hectares [53]. To produce 1 ton of 100% virgin copy paper, 4000 kg of trees are necessary [47]. In contrast, no tree is required to make 1000 kg of 100% recycled copy paper [47]. The production of recycled paper also reduces energy use by 40%, greenhouse gases by more than 55%, hazardous air pollutants by nearly 30%, and solid wastes by 82%. In 2015, it was reported that the recovery of paper and paperboard in developed regions approached its peak, with nearly 70% achieved in the USA, and over 70% and 80% attained in Europe and Japan, respectively [50]. In 2012, the information and data firm (RISI) reported that globally, 57% of paper and paperboard were recovered and recycled. This trend is projected to increase to 64% by 2028 [54].

2.4 Platform chemicals from cellulose and paper wastes

Platform chemicals can serve as precursors to other valuable chemicals. In most cases, they contain 2-6 carbons [55]. In 2004, the US Department of Energy (DOE) identified 12 chemical building blocks derivable from biomass [56]. These chemicals can be produced *via* microbial fermentation, or by chemical processes which convert from sugars to other valuable products. In 2010, an updated version of the DOE list included a few novel biobased platform chemicals [57]. The major difference in the updated 2010 report was that some chemicals with lesser growth market were removed, and new chemicals with high industrial potential were added [57]. Since the first DOE report was published, a few biorefinery processes have been commercialized or are getting close to commercialization [58]. The most important factors for the commercialization of a biorefinery are that the process should be environmentally friendly and economically competitive with the petroleum refinery process. In this section, the current challenges, achievements, and progresses on the lab-scale production of some top value-added building blocks from cellulose and lignocellulosic biomass are reviewed. These building block chemicals include sorbitol, ethylene glycol (EG), gluconic acid (GA), lactic acid, LA, and HMF.

2.4.1 Polyol platform

2.4.1.1 Sorbitol

Sorbitol is a sugar alcohol with an annual production of 650 million kg [59]. It is a widely used sweetener in the food and pharmaceutical industries [56]. It can serve as a building block for other value-added chemicals such as glycols, lactic acid, isosorbide, 1,4-sorbitan, and L-sorbose [60]. Sorbitol may also be exploited to produce H_2 and liquid alkane fuels [61]. Previously, sorbitol and other polyols were produced by cellulose hydrolysis with mineral acids into glucose prior to hydrogenation (scheme 2.1) [62]. However, this process is not green and suffers from common problems associated with using mineral acids, such as reactor corrosion

and acid recovery or disposal. In attempts to solve these problems, various solid acids on different supports have been screened, with only a few reported on cellulose conversion to sorbitol (Table 2.1).

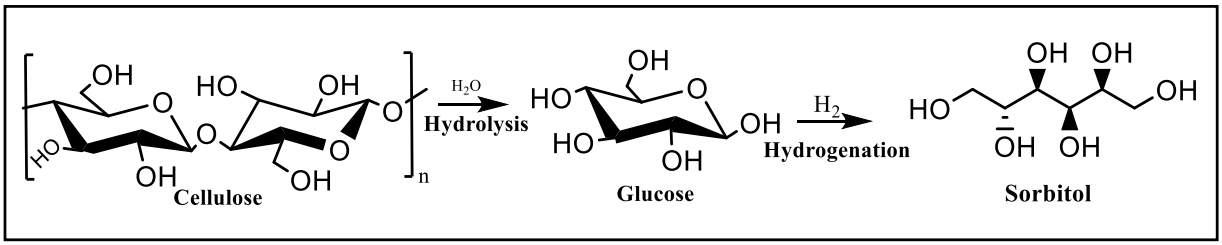

Scheme 2.1: Hydrolytic hydrogenation of cellulose to sorbitol via glucose

Table 2.1: Overview of cellulose conversion into sorbitol with different catalytic systems over various support

Substrate		Catalyst	Condition			Conv. (%)	Sorbitol yield (%)	Ref.
Type	Amount (g)		Temp. (K)	Time	H_2 pressure (MPa)			
MCC	0.16	Pt/ϒ-Al_2O_3	463	24 h	5	N.A.	25.0 mol%	[63]
MCC	1.00	Ru/C	518	5 min	6	39.0	30.8 wt%	[64]
MCC	0.16	1%Ru/CNT	458	24 h	5	N.A.	69.0 mol%	[65]
MCC	0.75	16%Ni_2P/AC	498	1.5 h	6	100	48.0 mol%	[66]
MCC	N.A.	1%Ir-5%Ni/MC	518	30 min	6	100	51.5 mol%	[67]
Cellulose	0.24	5%Ru/$NbOPO_4$	443	24 h	4	93.0	59.6 mol%	[68]
Cellulose	0.75	0.4%Ru/Ac	478	4 h	5	76.0	68.0 mol%	[69]
Cellulose	0.75	Ru-Ni/CNT	478	1 h	5	99.0	70.8 mol%	[70]
Cellulose	0.16	$Ni_{12}P_5$	503	40 min	5	92.0	62.0 mol%	[71]
Cellulose	1.00	3%Ni/CNF	463	24 h	6	92.0	50.3 wt%	[72]
Cellulose	0.25	Ru/SiO_2-SO_3H	423	10 h	4	91.0	61.0 mol%	[73]
Printing paper	0.3	Ru/CNT	478	5 h	5	50.0	7.0 mol%	[74]

MCC = microcrystalline cellulose, N.A. = not available

Pioneer work on the chemo-catalytic conversion of cellulose using Pt/ϒ-Al_2O_3 afforded sorbitol in a modest yield of 25 mol% [63]. The low yield was likely due to the robust structure

of cellulose and its limited access to surface acid sites [64]. Known as heat and water-tolerant supports, activated carbon (AC) and carbon nanotubes (CNT) have been extensively used as supports in cellulose conversion [75]. Luo [64] employed Ru/AC and reversibly generated H_3O^+ in hot water to catalyze cellulose conversion. Sorbitol in yield of about 30 wt% was obtained at 518 K in 5 min. Deng, et al. [65] used Ru nanoparticles (NPs) supported on CNT to catalyze the conversion of cellulose to sorbitol in yields of up to 69 mol%. The authors concluded that both the acidic functional groups and the higher concentration of adsorbed hydrogen species on CNT surfaces played key roles in sorbitol formation. Recently, a polyoxometalate-supported Ru bifunctional catalyst was used for cellulose conversion, affording sorbitol in a yield of 50 mol% [76]. The Brønsted acid sites generated *in situ* from H_2 played a crucial role in sorbitol formation. Xi, et al. [68] prepared a novel mesoporous niobium phosphate-supported Ru bifunctional catalyst ($Ru/NbOPO_4$) to transform cellulose processed by ball milling. Sorbitol in yield of about 60 mol% was afforded at 443 K in 24 h. It was observed that ball-milling pretreatment mainly promoted cellulose conversion rather than product distribution. It was also found that when cellulose and $Ru/NbOPO_4$ were mixed and then co-milled for 10 h, 69 mol% yields of sorbitol could be obtained. Similarly, Ribeiro [69] employed Ru/AC for the one-pot hydrolytic hydrogenation of cellulose. Again, the mixing and co-milling of both the substrate and the catalyst afforded sorbitol in yield of 68 mol%, whereas the separately ball-milled catalyst and cellulose provided only a 49 mol% yield of sorbitol. The mixing and co-milled treatment enhanced the contact between the cellulose and the catalyst. Two factors including ball-mill time and ball-mill frequency were responsible for the enhanced catalytic performance and sorbitol selectivity.

Recently, silica gel grafted with sulfonic acid followed by deposition of Ru NPs catalyzed the direct conversion of cellulose into sorbitol [73]. Cellulose conversion and sorbitol yield from the bifunctional Ru/SiO_2-SO_3H catalyst were 90.5% and 61.2 mol%, respectively. The interaction between SO_3H groups and proximate RU NPs through electron transfer in Ru/SiO_2-SO_3H was crucial for glucose hydrogenation to sorbitol. Studies on the effects of temperature showed that increasing temperature from 393 K to 423 K increased the sorbitol yields from 10.3 mol% to 61.2 mol%. Although a higher temperature of 453 K slightly favored cellulose conversion, the yield of sorbitol decreased to 39.8 mol% probably due to degradation. Though the catalyst was effective in cellulose conversion, it was found that SO_3H groups were leaching when in contact with hot water, thus limiting their recyclability.

Other inexpensive but highly efficient catalysts such as Ni have been screened [75]. For instance, Ni_2P/AC [66] and $Ni_{12}P_5$ [71] afforded sorbitol in yields of 48 mol% and 62 mol%

respectively, when microcrystalline cellulose (MCC) was used as feedstock. However, the drawbacks of these catalysts included phosphorous leaching and Ni sintering. In contrast, Ni supported on carbon nanofibers (CNF) was found to be stable, and afforded sorbitol in yield of 50.3 wt% with 92% cellulose conversion [72]. Efficient accessibility of the Ni catalyst particles grafted at the tip of the CNFs allowed for immediate hydrogenation of the released glucose units.

The studies described above were conducted with mono-metallic catalysts such as Pt, Ru, and Ni on various support systems. Optimization of these catalysts can be achieved by combining active sites, supports, and promoters. Bimetallic catalysts are portrayed as a promising option since the interaction between metals can modify the electronic and chemical properties of the catalyst [77]. As such, Pang, et al. [67] employed a Ni-Ir bimetallic catalyst on a mesoporous carbon (MC) support and reported a sorbitol yield of 51.5 mol%. The following three parameters contributed to the performance of Ir-Ni/MC: the high activity of MC for cellulose hydrolysis; the MC facilitated the reactant transportation; and the enhanced hydrogenation activity of the bimetallic catalyst. In another study, mix milling of bimetallic Ru-Ni/CNT increased the yield of sorbitol from 41.4 mol% to 70.8 mol% with 99.3% cellulose conversion in 1 h [70]. Recycling tests performed for the conversion of mix-milled cellulose with Ru-Ni/CNT showed that the catalyst was not deactivated.

From the above studies, successful manipulation of the catalytic process using heterogenous catalysts would be economical and environmentally viable if the use of chemicals, waste production, catalyst separation and recovery, and processing time are optimized. Accordingly, for scale-up, these studies could be replicated for the direct conversion of lignocellulose to sorbitol.

2.4.1.2 Ethylene glycol

Ethylene glycol (EG) is a polyol with diverse applications such as monomer for the polymer industry, functional additives for the food industry, as well as intermediates for the pharmaceutical industry. Currently, the commercial-scale production of EG is from petroleum-derived ethylene. To substitute the petroleum-based route, alternatives such as cost-effective cellulosic feedstock are gaining attention. Presently, only a few studies have been conducted on EG synthesis directly from cellulose (Table 2.2). The following reaction pathway (scheme 2.2) was proposed for EG synthesis from cellulose: (i) cellulose is hydrolyzed to glucose; (ii) glucose undergoes C–C dissociation, e.g., a retro-aldol reaction to glycol aldehyde and erythrose; (iii) the retro-aldol reaction of erythrose forms two molecules of glycol aldehyde, and (iv) glycol aldehyde is reduced to ethylene glycol. Ji, et al. [78] reported an EG yield of

27.4 wt% upon 98% cellulose conversion using W_2C. When W_2C was doped with Ni, an increased EG yield of 61 wt% was observed with complete cellulose conversion. The higher EG yield was partially due to weaker bonding between EG and Ni-promoted W_2C surface. A study showed that with an increase in temperature from 503 K to 523 K, the EG yield gradually increased until it attained its maximum value at 518 K, and then decreased at a higher reaction temperature [79]. In contrast, the cellulose conversion increased invariably with the reaction temperature. This study concluded that EG formation is not a thermally stable process, with EG undergoing further decomposition into smaller molecules at higher temperatures [79].

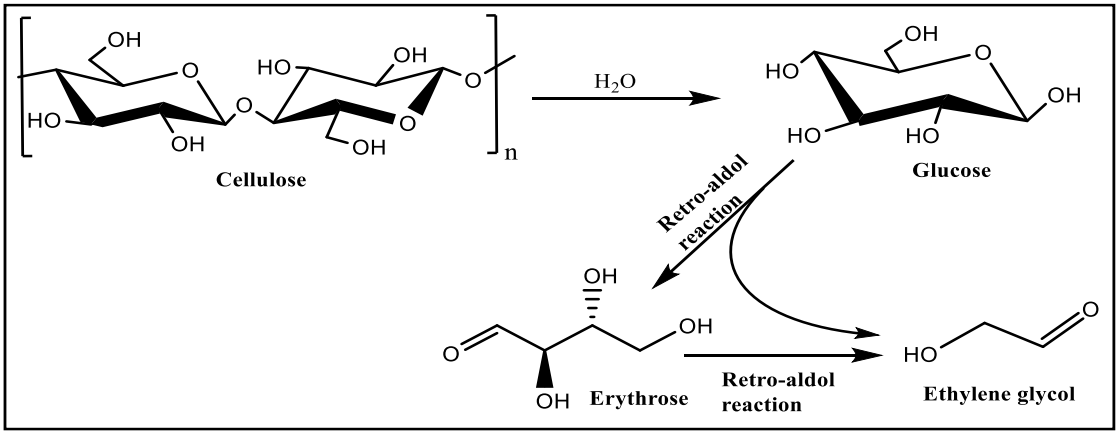

Scheme 2.2: Pathway toward EG synthesis from cellulose

Other factors, such as the methods used for the synthesis of the catalysts, could be detrimental to the catalytic conversion of cellulose and EG formation. For example, the Ni-W_2C/AC catalysts were prepared by co-impregnation, which involved simultaneous loading of Ni and W on the catalyst, prior to a carburization step [80]. The co-impregnation caused severe sintering of W_2C due to the methanation of the carbon support by Ni at an elevated temperature. To circumvent sintering, post-impregnation of the catalyst was performed, allowing for complete cellulose conversion with an EG yield of 73 wt% [80].

Table 2.2: Conversion of cellulosic materials into EG over different catalytic systems

Substrate				Condition				
Type	Amount (g)	Catalytic system	Conv. (%)	Temp. (K)	Time (min)	H_2 pressure (MPa)	EG yield	Ref.
MCC	0.5	30% W_2C/AC-1073	98	518	30	6	27.4 wt%	[78]
MCC	0.5	2% Ni-30%W_2C/AC-973	100	518	30	6	61.0 wt%	[81]
MCC	0.5	10% Ni-30% W_2C/AC	100	518	30	6	73.0 wt%	[80]
MCC	1.0	Ni5-$W_2$5/SBA-15	100	518	N.A.	6	75.4 wt%	[82]
MCC	1.0	3% Ni-15WO_3/SBA-15	100	503	360	6	70.7 wt%	[83]
MCC	0.3	Ru-Fe_3O_4-SiO_2	100	528	50	6	13.8 wt%	[84]
MCC	0.5	20% WP/AC	100	518	30	6	25.4 mol%	[85]
MCC	0.5	2% Ni-20%WP/AC	100	518	30	6	46.0 mol%	[85]
MCC	0.5	2% Ru-30%W_2C/AC	N.A.	518	30	6	63.5 wt%	[86]
MCC	1.0	Ru/C-WO_3/AC	23.0	478	30	6	51.5 wt%	[87]
MCC	0.8	0.8% Ru-30%W/CNT	100	478	180	5	40.0 mol%	[88]
MCC	0.5	Raney Ni+H_2WO_4	100	518	30	6	65.4 wt%	[89]
Cellulose	0.5	10% Ni-20%W/SBA-15	100	518	120	5	64.9 wt%	[90]
Cellulose	1.0	WC_x/MC	100	518	30	6	73.0 wt%	[91]
Corn stalk	0.5	2% Ni-W_2C	96.0	518	120	6	18.3 mol%	[92]

MCC = microcrystalline cellulose, N.A. = not available

It is well-known that both the activity and selectivity of a catalyst are largely dependent on the dispersion and accessibility of the active sites within the catalyst support. For example, conventional AC support has been studied extensively [93]. Despite their large surface area, their active sites are often poorly dispersed and are not easily accessed due to their microporous structure [78]. On the other hand, MC has the advantages of good accessibility and molecular

diffusion [94]. Also, MC supports have provided possibilities to manipulate the catalytic properties of bifunctional catalysts [95]. Recently, Zhang, et al. [91] prepared a novel MC support with three-dimensional interconnected mesopores *via* a nano-casting approach. The MC-supported WC_x catalyst (WC_x/MC) afforded a higher EG yield of 73 wt% as compared to WC_x/AC with an EG yield of 48 wt%, for the one-pot conversion of cellulose in an aqueous media. Interestingly, the WC_x/MC had better resistance to deactivation. Just like W_2C-based catalysts, tungsten phosphide (WP) catalyst was reported for cellulose conversion, affording EG in yield of 25 mol%. As previously observed for W_2C, the modification of the WP with Ni increased the EG yield to 46 mol%.

Beside the known W_2C catalysts, a series of bimetallic catalysts for cellulose conversion, including Ni-W, Pd-W, Pt-W, Ru-W, and Ir-W supported on different carriers, were employed for EG synthesis [96]. W hydrolyzed cellulose, while Ni, Pd, Ru, Pt, or Ir is responsible for the hydrogenolysis reaction of unsaturated intermediates. For example, Ni-W/SBA-15 afforded a maximum EG yield of 75.4 wt%. For this type of catalyst, ligand or strain effects are often considered important in enhancing their catalytic performance [97, 98]. To ensure that the performance of Ni-W/SBA-15 did not originate from the influence of a particular support, Ni-W/SiC and Ni-W/TiO_2 catalysts were prepared and tested with different carriers [96]. Although Ni-W/SiC and Ni-W/TiO_2 had much lower surface areas than Ni-W/SBA-15, they generated EG in yields of 45.3 wt% and 36.8 wt%, respectively [96]. Similarly, high catalytic activity was observed with 3%Ni-15WO_3/SBA-15 catalyst [83] and with 10%Ni-20%W/SBA-15 catalyst [90]. This indicated that EG yields could be modulated by varying the ratio of transition metals and metallic W [96].

Recently, a novel magnetically recoverable catalyst was reported [84]. The catalyst was synthesized by incorporation of magnetite (Fe_3O_4) NPs in mesoporous silica pores followed by blending with Ru NPs. For that study, cellulose was hydrolyzed in subcritical water through the formation of H_3O^+ [64]. Ru/SiO_2 alone was inactive in cellulose hydrogenolysis. However, for the Ru-Fe_3O_4-SiO_2 catalyst, since Fe_3O_4 and Ru NPs are in close range, their interaction in the SiO_2 pores facilitated an increase in EG yield, up to approximately 14 wt%. Moreover, upon the addition of 0.195 mol of $Ca(OH)_2$, the EG yield increased to 25 wt%. The increase in EG yield was due to the influence of $Ca(OH)_2$ as a cracking agent, participating in C-C cleavage [99]. Similarly, $Ca(OH)_2$ markedly improved the EG yield to 30.8 wt% using CuCr catalyst for cellulose and glucose conversion [100].

The studies above juxtapose the robustness of the various catalytic systems developed for cellulose conversion to EG. So far, the obtained EG yields confirmed that these systems are

potential routes for EG synthesis. Other catalytic systems, for example, Ru/C-WO_3/AC [86], Ru/C-WO_3/AC [87], and 0.8%Ru-30%W/CNT [88] gave reasonable yields of EG at 63.5 wt%, 51.5 wt%, and 40 mol%, respectively. However, using Ru can affect EG yields as follows: (1) Ru can promote the methanation of EG to other undesired products, thus reducing EG selectivity [89], and (2) the high cost of Ru limits its industrial application. Therefore, Raney Ni and tungstic acid (H_2WO_4) were employed [89]. Both components are low-cost and commercially available. Raney Ni can catalyze the hydrogenolysis of glycerol to EG [101]. Similarly, cellulose was converted using Raney Ni and H_2WO_4 catalyst, affording EG in yield of 65.4 wt%. The high EG yield obtained could be due to the high activity of Raney Ni for hydrogenolysis, as well as its inertness to further EG degradation [89].

MCC conversion for EG synthesis has been screened extensively for various catalytic systems (Table 2.2). These catalysts are quite promising, generating EG in yield up to 75 wt% for the most efficient of them. Even with these results, no alternative route has yet been developed to compete with the petroleum-based ethylene route from an economic point of view. For instance, 2% Ni-30% W_2C afforded a low EG yield of 18.3 mol% from corn stalks, even after pretreatment [92]. One major drawback of EG production from lignocellulosic biomasses is poor pretreatment. An inappropriate pretreatment can limit access to the available cellulose macromolecule needed for EG synthesis. Therefore, PW could be a desirable feedstock to scale up EG production for two reasons: (1) it has been subjected to a robust pretreatment during the paper-making process, making it a more flexible feedstock, and (2) the presence of $CaCO_3$ in paper materials could favor EG yield because it has been previously indicated that Ca containing compounds can facilitate C-C cleavage during cellulose hydrolysis [99]. Therefore, PW could be a new route toward chemo-catalytic EG production on an industrial scale.

2.4.2 Carboxylic acid platform

2.4.2.1 Gluconic acid

Gluconic acid (GA) was first discovered by Hasiwetz and Habermann in 1870 [102]. Globally, the demand for GA has steadily risen over the past years, reaching 60 million kg per year [103]. The neutralization products of GA, such as calcium gluconate or sodium gluconate, find broad applications in chemical, food, and construction industries, being a multifunctional carbonic acid [104]. Its complexing ability and its savory potential have been of relevance in the food sector. Due to its non-corrosiveness, it can be used in the cleaning and degreasing of ferrous and nonferrous metal ions such as Ca^{2+}, $Fe^{2+,}$ and Al^{3+} [104]. Also, GA has shown natural occurrence in plants, fruits, wine, honey, rice, and vinegar [105]. Several routes to

producing GA exist including chemical, electrochemical, biochemical, and bio-electrochemical approaches.

Presently, the fermentation route using the fungus *Aspergillus niger* dominates other routes for GA synthesis [106]. Although bacterial, yeast and immobilized enzymes have been explored, *A. niger* fermentation for GA production is well-established and provides high selectivity [107]. For example, a recent report using *A. niger* indicated a GA production of up to 96.5% theoretical yield (1.09 g/g) [108]. Nevertheless, the major shortcomings of the fermentation route toward GA synthesis are the long reaction times (15-24 h), restricted conditions (pH 6.0-6.5 and 307 K), and the high operational cost (0.4 MPa air pressure and stirring) [109]. Therefore, the chemical route appears to be a favorable substitute to the traditional fermentative pathway. Today, the interest is in developing an efficient catalytic system for GA production from lignocellulosic biomass to meet its rising demand.

Until now, studies on the catalytic conversion of cellulose to GA are scarce, however, few reports using cellobiose have been produced. Cellobiose, a D-glucose dimer connected by a β-1,4-glycosidic bond, is viewed as a simple model of cellulose. The first step in GA formation is to hydrolyze cellobiose to glucose (Scheme 2.3). Glucose possesses three different types of carbons: aldehyde, primary (1^0), and secondary (2^0) alcohol. All three positions can be oxidized, leading to different products. The oxidation of the aldehyde generates GA, whereas the 1^0 and 2^0 alcohol afford GA, keto-glucose, and keto-acid, respectively. Studies on the catalytic conversion of cellobiose could provide directives for developing efficient routes for cellulose transformation to GA (Table 2.3).

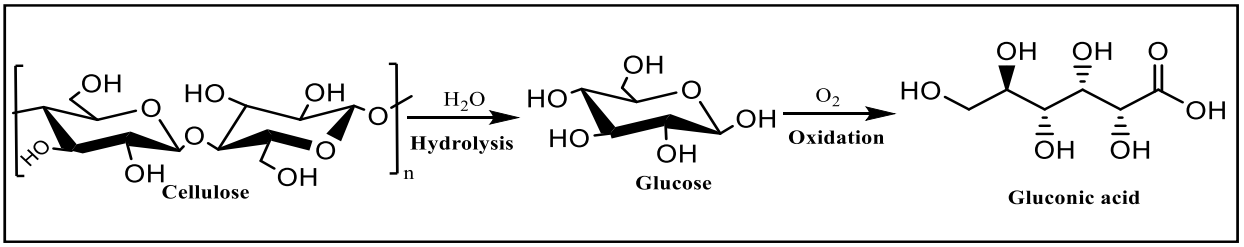

Scheme 2.3: Gluconic acid formation via C1 oxidation

Table 2.3: Overview of various catalytic systems for conversion of cellobiose and cellulose to GA

Substrate			Condition					
Type	Amount (g)	Catalyst	Temp. (K)	Time (h)	O_2 pressure (MPa)	Conversion (%)	GA yield (mol%)	Ref.
Cellobiose	0.10	Au/CNT	418	3	0.5	91.0	55.0	[110]
Cellobiose	0.10	Au/CNT-HNO_3	418	3	0.5	81.0	68.0	[110]
Cellobiose	0.10	Au/$Cs_2HPW_{12}O_{40}$	418	3	0.5	97.5	96.4	[111]
Cellobiose	0.10	Au/SiO_2+$H_3PW_{12}O_{40}$	418	3	0.5	77.2	76.0	[111]
Cellobiose	4.11	Au/$Cs_xH_{3-x}PW_{12}O_{40}$	418	3	0.5	96.6	90.0	[112]
Cellobiose	0.10	Au/TiO_2	418	3	0.5	97.9	N.A.	[113]
Cellobiose	4.11	Au/TiO_2	418	3	0.5	96.0	60.0	[112]
Cellobiose	0.20	Cu-Au/TiO_2	418	3	N.A.	100	N.A.	[114]
Cellobiose	0.20	Ru-Au/TiO_2	418	11	N.A.	98.5	N.A.	[114]
Cellobiose	0.20	Au/CNT	418	1	0.5	60.0	74.1	[115]
Cellobiose	0.20	Au/CX	418	1.25	0.5	45.0	53.7	[115]
Cellobiose	0.20	Au/OMC	418	1.25	0.5	N.A.	35.9	[115]
Cellobiose	0.77	Pd/C	418	3	0.5	N.A.	22.0	[116]
Cellobiose	0.05	Pt/AC-SO_3H	393	24	N.A.	N.A.	46.0	[117]
Ball-milled cellulose	0.05	$H_3PW_{12}O_{40}$-Au/$Cs_{30}PW_{12}O_{40}$	418	11	1.5	97.0	85.0	[112]
Avicel PH-101	0.25	$FeCl_3$	393	2	N.A.	100	50.0	[109]
Cellulose	0.50	$FeCl_3.6H_2O$/EG	393	1	N.A.	100	52.7	[118]

N.A. = not available

Reports on the catalytic conversion of cellobiose to GA have focused on using Pt, Pd, or Au NPs as catalysts, and O_2 from the air as an oxidant, under mild conditions [119]. Among them, Au has been considered the most competitive catalyst for glucose oxidation toward GA synthesis due to its high selectivity and steady activity [120]. In this view, recent studies using Au NPs have attracted attention. For example, the loading of Au NPs on various supports such as SiO_2, Al_2O_3, MgO, and CNT has been reported [110]. CNT was the best support over Au

NPs for the oxidation of cellobiose in an aqueous medium. Herein, fusing CNT with Au afforded GA in yield of 55 mol% at a reaction time of 3 h. The Au NPs assisted in both converting cellobiose and accelerating glucose oxidation to GA. Accordingly, an increased Au loading up to 0.5 wt% onto CNT remarkably enhanced cellobiose conversion to 91%. Subsequently, the GA yield reached 68 mol%, upon pretreating Au/CNT with HNO_3. HNO_3 pretreatment introduced an acidic site on the Au/CNT surface that improved its catalytic performance. These results revealed the key role played by the nature of the solid support and the type of metal catalyst in cellobiose conversion and selectivity towards GA.

To this end, it is believed that the Au NPs are a robust system to initiate cellobiose conversion on a solid support. Therefore, a novel heterogenous cesium hydrogen phosphotungstate-support Au catalyst ($Au/Cs_2HPW_{12}O_{40}$) was employed for the oxidation of cellobiose to GA [111]. $Cs_2HPW_{12}O_{40}$ was selected as a catalyst support because of its high acidity and strength [121]. The catalyst gave a cellobiose conversion of 97.5% with high selectivity of 98.9%, and thus a 96.4 mol% yield of GA. The high performance of the catalyst is due to the inertness of $Cs_2HPW_{12}O_{40}$ and its potential to fine-tune the oxidative activities of the Au NPs, and thus prevent GA from being further oxidized. To reaffirm the activity of phosphotungstic support, the oxidation of cellobiose was performed over Au/SiO_2 by introducing $H_3PW_{12}O_{40}$ [111]. GA in yield of 76 mol% with a selectivity of about 98% was reported.

Other support systems on Au NPs such as various metal oxides (e.g. HZSM-5 and $Cs_xH_{3-x}PW_{12}O_{40}$) were tested [112]. An average cellulose conversion of 96.6% and GA selectivity of 93% over Au catalyst loaded on $Cs_xH_{3-x}PW_{12}O_{40}$ were attained, being the catalyst with the highest performance activity for cellobiose conversion. Furthermore, $Au/Cs_xH_{3-x}PW_{12}O_{40}$ afforded GA in yield of 90 mol% at 418 K in 3 h. Au NPs have proven to be efficient catalysts on different support systems for the chemo-catalytic conversion of cellobiose to GA. Accordingly, Au NPs supported on TiO_2, CNT, and zeolite (HY) were reported for the oxidation of cellobiose [113]. TiO_2 outperformed the other supports and the bifunctionality of Au/TiO_2 showed the highest conversion and selectivity towards GA. When the cellobiose conversion was 97.9%, the Au/TiO_2 afforded a GA selectivity of 73.7% at 418 K. The conversion of cellobiose to GA catalyzed by Au/TiO_2 has been reported as a two-step reaction where cellobiose was first hydrolyzed to glucose, and subsequently oxidized in the presence of molecular O_2 to GA. In this process, the catalyst support (TiO_2) promoted the cellobiose conversion into glucose by hydrolysis, while Au NPs catalyzed the oxidation of glucose to GA.

Compared to pure metals, bimetallic catalysts are believed to be a promising option for the transformation of biomass into valuable products. They have been used for several reactions, including 2,3-dihydrofuran synthesis [122], partial oxidation of methanol [123], water-gas shift [124], and naphthalene hydrogenation [125]. In this view, a series of Au-M (where M = Cu, Co, Ru, and Pd) bimetallic catalysts supported on urea-treated TiO_2 were reported for cellobiose conversion [114]. The interactions between these metals could modify the surface and electronic properties of the resultant catalyst, thereby enhancing significantly their catalytic activity and stability [126]. Cu-Au/TiO_2 and Ru-Au/TiO_2 were reported as highly active in the oxidation of cellobiose. With Cu-Au/TiO_2, complete conversion of cellobiose with a GA selectivity of 88.5% was attained at 418 K in 3 h. Ru-Au/TiO_2 allowed a cellobiose conversion of 98.5% with a GA selectivity of 87.8% at 418 K in 11 h. Interestingly, the addition of Cu and Ru to Au NPs increased the activity and selectivity to GA by about 15% as compared to those of monometallic Au/TiO_2 previously reported under the same temperature, but at different reaction times.

Recently, the quest for more efficient catalytic systems for GA synthesis spurred research interests in the fabrication of cheap novel support materials for Au NPs. Core knowledge of the textural properties and surface chemistry of solid support systems gives insights into selecting/synthesizing catalytic systems toward GA synthesis. In this respect, Au supported on ordered mesoporous carbon (OMC), and carbon xerogel (CX), were reported for one pot cellobiose conversion [115]. The Au/OMC and Au/CX were compared in catalytic performance with well-known Au/CNT catalyst for GA production from cellobiose. The yield of GA obtained for Au supported on carbon materials increased following this trend CNT > CX > OMC. It was suggested that larger pore sizes of the carbon supports can render glycosidic bonds in cellobiose more accessible for activation, thus enhancing the final selectivity of the reaction. Additionally, the presence of phenolic groups on the functionalized carbon supports acts as weak Brønsted acid, influencing a higher rate of hydrolysis of cellobiose [127]. Also, the weak Brønsted acid was responsible for high selectivity towards GA.

Similarly, oxidative treatment was performed on CX to graft [$Pd(OAc)_2(Et_2NH)_2$] complex, in preparation of Pd/C catalyst for cellobiose conversion [116]. The oxygen groups on the surface of CXs were used as anchors for grafting Pd precursors to prepare bifunctional catalysts with redox and acid sites. Pd/C attained a yield of 22 mol% and selectivity of 100% toward GA. A different sulfonated activated carbon-supported Pt catalyst (Pt/AC-SO_3H) catalyzed the conversion of cellobiose in water under ambient air. A GA yield of 46 mol% was obtained at 393 K after 24 h. The high selectivity of Pt/AC-SO_3 was claimed to be provided by

AC with high surface area and high thermal stability. Moreover, AC-SO_3H provided strong acidity and water tolerance for the hydrolysis of saccharides in aqueous media [128]. Although GA selectivity was high for the two latter studies, the GA yield obtained from catalysts such as Au/CNT and Au/TiO_2 were higher than yields reported for Pt/AC-SO_3H and Pd/C. This suggests that Au metal is more efficient for sugar oxidation.

Identical catalytic systems used for cellobiose conversion were tested for cellulose. For instance, Au/$Cs_xH_{3.0-X}PW_{12}O_{40}$ could effectively catalyze the oxidative conversion of cellulose to GA with a selectivity of about 80% and a yield of around 60 mol% in water at 418 K [112]. However, the instability of Au/$Cs_xH_{3.0-X}PW_{12}O_{40}$ system over long-term hydrothermal conditions may result in its deactivation upon reuse. Overcoming deactivation required a combination with $H_3PW_{12}O_{40}$, which resulted in a GA selectivity and yield of 88% and 85 mol% using ball-milled cellulose as feedstock.

Generally, the drawback associated with noble metal-based catalytic systems is their high cost. Also, the necessary use of strong bases may hinder their industrial potential [129, 130]. Another consideration is that GA is very difficult to separate from the reaction systems since it is usually mixed with unreacted reactants and solvents. As an attractive alternative, the direct conversion of cellulose using 40% $FeCl_3$ was reported [109]. A yield of 50 mol% GA was generated at 393 K in 2 h. Nevertheless, the separation of GA and the reuse of $FeCl_3$ may restrict this method. To address the separation difficulty with the $FeCl_3$ systems, catalytic deep eutectic solvents (DESs) were proposed. DESs are a mixture of Lewis acids, Brønsted acids, and bases, forming a eutectic system which is liquid at low temperatures. DESs are used in applications such as in transition metal-catalyzed synthesis [131], and in separation processes [132] as a substitute for conventional ILs and organic solvents. The advantage of catalytic DESs lies in the fact that they can change a heterogeneous reaction into a homogenous reaction by dissolving reactants, which can improve the reactivity significantly [133]. Studies have shown that cellulose and starch are soluble in choline chloride DESs [134, 135]. Accordingly, $FeCl_3.6H_2O$/EG converted cellulose completely and afforded GA in yield of 52.7 mol% at 398 K [118]. The strong acidity of $FeCl_3.6H_2O$/EG with a molar ratio of 1:2 was crucial in cellulose hydrolysis, a key step in GA formation.

The chemo-catalytic synthesis of GA from cellulose in a sustainable fashion has been the interest of many research groups. Catalytic DESs seem promising as a novel and sustainable route toward GA synthesis [118]. This is due to the potential of the synthesized GA to precipitate from the reaction system without additional extraction of solvent [118]. Pure GA could be obtained by recrystallization in ethyl acetate to remove small amounts of $FeCl_3$ and

by-product contamination. Moreover, catalytic DESs are ecofriendly and can be reused without a decline in their catalytic activities. All these show the potential to commercialize GA production from cellulose and cellulosic materials such as PW.

2.4.2.2 Lactic acid

Lactic acid, $CH_3CH(OH)CO_2H$, is a chiral molecule composed of L- (+)-lactic acid or (*S*)-lactic acid, and D- (−)-lactic acid or (*R*)-lactic acid isomers. A mixture of both isomers in equal amounts is called DL-lactic acid or racemic lactic acid. Lactic acid has an extensive list of applications ranging from its use in food, cosmetics, pharmaceutical, leather, and textile industries [136, 137]. Also, it is used mainly to produce polylactic acid (PLA) for biodegradable and biocompatible lactate polymers [138]. At present, 90% of lactic acid is fermented from simple carbohydrates such as starch and sugar, which contributes 30% of the total production cost [137]. To reduce the cost, lignocellulosic biomass with scale-up potentials is being investigated [137]. Presently, only a few studies have been reported on the catalytic conversion of cellulose and lignocellulose to lactic acid (Table 2.4). As known, cellulose is first hydrolyzed to glucose and then the glucose isomerizes to fructose in the presence of a basic or Lewis acid catalyst (Scheme 2.4) [139]. The as-formed fructose is converted to glyceraldehyde (GLA) and 1,3-dihydroxyacetone (DHA) *via* a retro aldol reaction. Next, the GLA and 1,3-(DHA) dehydrate into pyruvaldehyde which then converts to lactic acid. The next section summarizes the conversion of cellulose to lactic acid using different catalysts.

Jin, et al. [140] attempted cellulose hydrolysis in a subcritical region and afforded lactic acid in a very low yield. Regardless of the yield, the authors posited that in the subcritical region, water can act as an effective alkaline catalyst. Accordingly, Yan, et al. [141] reported the alkaline hydrothermal treatment of cellulose with $Ca(OH)_2$ and obtained lactic acid in yield of 19.2 mol% at 573 K. Subsequently, Sánchez [142] performed the alkaline hydrothermal treatment of corn cobs. Lactic acid in yield of 44.8 mol% was achieved at 573 K in 30 min. In general, alkaline hydrothermal methods unavoidably entail the use of mineral acids to obtain lactic acid, which is almost the same problem prevalent with the fermentation broth. In addition, corrosion of equipment arising from the high alkaline concentration is inevitable. To address this problem, Chambon [143] used solid Lewis acids, such as tungstated zirconia (ZrW), and alumina (AlW), to depolymerize cellulose. AlW afforded lactic acid in yield of 27 mol% at 463 K in 24 h. The lactic acid yield was rather low, and a portion of the metal specie leached into the reaction solution.

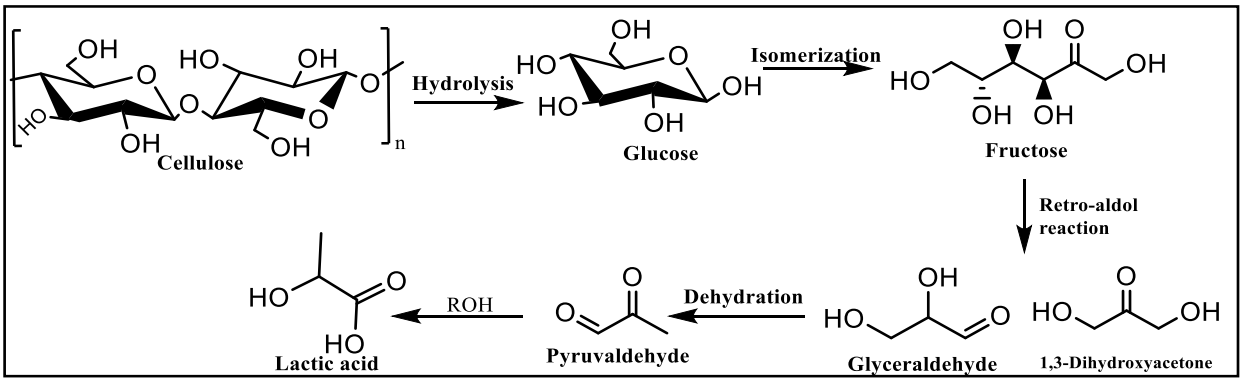

Scheme 2.4: Reaction pathway for the transformation of cellulose to lactic acid

Table 2.4: Overview of lactic acid yield from cellulose and lignocellulose in a typical catalytic system

Substrate		Catalyst	Condition			Conv. (%)	Lactic acid yield (mol%)	Ref.
Type	Amount (g)		Temp. (K)	Time	Pressure (MPa)			
Cellulose	0.10	$Ca(OH)_2$	573	15 min	N.A.	N.A.	19.2	[141]
Cellulose	1.60	AlW	463	24 h	$5/He_2$	47	27.0	[143]
Cellulose	1.60	ZrW	463	24 h	$5/He_2$	42	18.5	[143]
MCC	0.10	$Er(OTf)_3$	513	30 min	$2/N_2$	100	89.6	[144]
MCC	0.10	$ErCl_3$	513	30 min	$2/N_2$	100	91.1	[145]
MCC	0.30	Er/K10	513	30 min	$2/N_2$	100	67.6	[146]
MCC	0.20	$LaCoO_3$	513	1 h	$3/N_2$	14	24.9	[147]
Cellulose*	0.10	$PbCl_2$	463	4 h	$3/N_2$	60	68.0	[148]
Cellulose*	0.20	$VoSO_4$	453	2 h	$2/N_2$	N.A.	54 .0	[149]
Cellulose*	0.50	ZrO_2	473		$0.1/N_2$	87	21.2	[150]
Cellulose*	0.50	$10\%ZrO_2$-Al_2O_3	473	6 h	$0.1/N_2$	86	25.3	[151]
Filter paper	0.04	Zn/Ni/AC	573	5 min	N.A.	N.A.	42.2	[152]
Wheat stalk	0.10	$ErCl_3$	513	30 min	$2/N_2$	95	63.1	[145]
Corn cob	1.20	$Ca(OH)_2$	573	30 min	N.A.	N.A.	44.8	[142]

MCC = microcrystalline cellulose, N.A. = not available, Cellulose* = ball-milled cellulose.

Wang, et al. [144] investigated lanthanide triflate, $Ln(OTf)_3$, as a Lewis acid catalyst for cellulose conversion. It was found that $Ln(OTf)_3$ was stable and could act as Lewis acid in both aqueous and organic solvents [153]. These features are different for conventional Lewis acids such as $AlCl_3$, BF_3, and $SnCl_4$ which can decompose or deactivate in the presence of H_2O [154]. In addition, $Ln(OTf)_3$ is easy to recover and regarded as an eco-friendly catalyst [144]. Surprisingly, various $Ln(OTf)_3$ screened completely converted cellulose and afforded lactic acid in yields above 50 mol%, with the highest yield of 89.6 mol% observed for $Er(OTf)_3$. This result is interesting because cellulose was completely converted at a shorter reaction time of 30 min. However, the high cost of the catalyst can affect the total production cost of lactic acid. Lei, et al. [145] employed an inexpensive chemical compound erbium ($ErCl_3$) to transform cellulose. Lactic acid in yield of 91.1 mol% was obtained upon complete cellulose conversion. $ErCl_3$ exhibited high activity and stability and can be reused. Under similar conditions, lactic acid in a yield of 63.1 mol% was obtained from wheat stalk at a conversion rate of 94.7%. Accordingly, Wang, et al. [146] reported that erbium-exchanged montmorillonite (Er/K10) was efficient at hydrolyzing cellulose. The montmorillonite has both Lewis and Brønsted acid sites which enable its use as an alternative catalyst in acid-catalyzed organic transformation [155]. Er/K10 afforded lactic acid in yield of 67.6 mol% at 513 K in 30 min. Furthermore, Wang, et al. [148] combined Pb(II) ions with water to hydrolyze cellulose. Lactic acid in yield of 68 mol% was achieved at 60% cellulose conversion. However, the toxicity of Pb may hinder the practical application of this system.

Recently, vanadyl sulfate ($VOSO_4$) and perovskite metal oxide ($LaCoO_3$) were employed to depolymerize cellulose. $VOSO_4$, a cheaper and less toxic vanadium salt, afforded lactic acid in yield of 54 mol% at 453 K [149]. $LaCoO_3$ exhibited redox properties which were different from the acid/base properties of prevalently used catalysts for cellulose [156]. $LaCoO_3$ attained a lactic acid yield of about 24.9 mol% at 513 K [147]. However, about 2.4 mol% Co ions and 1.5 mol% La ions leached from the catalyst.

Overall, stability has been an issue for most solid acids in hydrothermal media. Only a few metal oxides such as ZrO_2, TiO_2, and α-Al_2O_3 exhibit acceptable stability for certain biomass conversion in subcritical water [147, 157, 158]. As such, Wattanapaphawong, et al. [150] investigated the potentials of ZrO_2 to depolymerize cellulose. ZrO_2 generated lactic acid in a yield of 21.2 mol% at 87.3% cellulose conversion. As anticipated, the ZrO_2 catalyst was stable in hot water and did not leach metal species into the reaction solution. Based on the performance of ZrO_2, it is believed that developing a mixed metal oxide catalyst could enhance the lactic acid yield. Accordingly, the dispersion of active ZrO_2 species on Al_2O_3 support was

demonstrated for cellulose conversion [151]. The combined effects of 10% ZrO_2-Al_2O_3 afforded lactic acid in yield of 25.3 mol% at 473 K in 6 h. The improved yield showed the important role of the Lewis acid sites of the catalyst on cellulose conversion [159]. Interestingly, when the catalyst was reused, the lactic acid yield increased to 31.7 mol%. The increase was attributed to the reactivation of the catalyst by calcination, which eliminated contaminants at its surface. However, some of the metal species in ZrO_2-Al_2O_3 leached into the reaction solution compared to the aforesaid ZrO_2 that did not leach metal species. Thus, an extensive study on the suitability of ZrO_2 and other metal oxides will be needful. Also, the optimization of reaction conditions using these oxides may further improve the yield of lactic acid from cellulose. Furthermore, the use of flexible feedstocks such as PW with these metal oxides will be a promising route toward large-scale lactic acid production.

2.4.2.3 Levulinic acid

Levulinic acid (LA) is one of the most important platform chemicals [160]. It is a keto-acid with two reactive functional groups, a carbonyl and a carboxyl group, which makes this molecule suitable for various chemical transformations [161]. In 1840, G.J. Mulder first synthesized LA by heating sucrose in the presence of mineral acids at an elevated temperature [162]. In 2004, the US DOE promoted LA as one of the 12 top precursors for biorefineries since it can be used in the production of various important chemicals such as levulinate esters, β-acetyl acrylic acid, diphenolic acid, δ-amino-LA (DALA), acrylic acid, 2-methyl-tetrahydrofuran (MTHF) and ϒ-valerolactone (GVL) [160]. The common route to LA synthesis involves one-pot biomass hydrolysis to glucose prior to dehydration (Scheme 2.5). This can in turn be converted to several derivatives, including HMF and FU, with the HMF being rehydrated to LA and formic acid (FA). LA synthesis from cellulose could be feasible since it takes about 2 kg of cellulose to generate 1 kg of LA [163]. Table 2.5 shows a comparative study of LA synthesis from cellulose under different reaction conditions. The next section will deal with reaction media for LA synthesis.

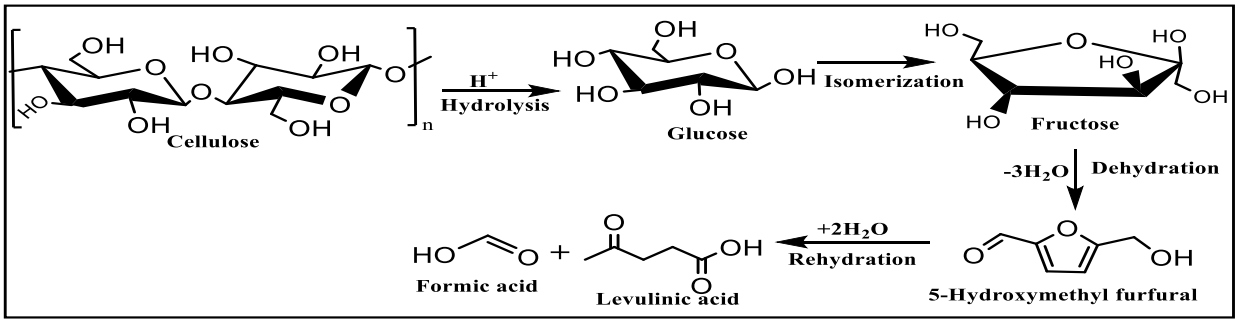

Scheme 2.5: Reaction path for cellulose conversion to levulinic acid

Table 2.5: Comparative study on LA synthesis from cellulosic feedstock under different reaction conditions

Substrate		Catalyst	Condition		LA yield	Ref.
Type	Amount		Temp. (K)	Time		
Avicel PH-101	2.00 wt%	0.927 M HCl	453-473	20 min	60.0% theoretical yield	[164]
Avicel PH-101	4.00 wt%	Amberlyst 70	433	8 h	28.0% of theoretical yield	[165]
MCC	0.50 g	SO_2	483	45 min	45.0 mol%	[166]
MCC	2.00 wt%	0.02 M $CrCl_3$	473	3 h	67.0 mol%	[167]
MCC	1.70 wt%	1 M H_2SO_4	423	2 h	60.0 mol%	[168]
MCC	2.00 g	ZrO_2	453	3 h	54.0 mol%	[169]
MCC	1.00 g	Ni-HMETS-10 Zeolite	473	6 h	91.0 mol%	[170]
MCC	2.00 wt%	Amberlyst 70	433	16 h	69.0%	[171]
MCC	0.10 g	CP-SO_3H	453	N.A.	65.5 mol%	[172]
MCC	5.30 wt%	1.25 M HCl	428	1.5 h	72.0 wt%	[173]
MCC	0.25 g	$[C_3SO_3Hmim]HSO_4$	433	30 min	44.5 mol%	[174]
MCC	0.05 g	$[BSmim]HSO_4$	393	2 h	39.4 wt%	[175]
MCC	0.15 g	$[C_3SO_3Hmim]HSO_4$	433	4 h	86.1 mol%	[176]
MCC	0.10 g	$[mimPS]H_2PW_{12}O_{40}$	413	12 h	63.1 mol%	[177]
Cellulose	2.00 g	Nafion SAC-13	463-473	5 days	72.0 mol%	[178]
Cellulose	5.00 wt%	Al-modified mesoporous NbP	453	24 h	52.9 mol%	[179]
Cellulose	0.03 g	$[C_4(mim)_2][(2HSO_4)(H_2SO_4)_2]$	373	3 h	55.0 mol%	[180]
Cellulose	1.00 g	ZrO_2	513	25 min	51.9 mol%	[181]
Cellulose*	1.50 g	$FeSO_4$-SBA-SO_3H	423	12 h	54.0 mol%	[182]
Paper sludge	1.75 g	37% HCl	473	1 h	77.0% of theoretical yield	[183]
Paper towel	0.50 g	1 M H_2SO_4	473	2.5 min	46.0 mol%	[184]

Paper towel	0.50 g	Amberlyst 36	423	20 min	34.0 mol%	[184]
Tobacco chops	1.75 g	37% HCl	473	30 min	82.5% of theoretical yield	[183]

MCC = microcrystalline cellulose, N.A. = not available, Cellulose* = ball-milled cellulose

2.4.2.3.1 Reaction media for LA synthesis

LA synthesis is conducted in aqueous media. A recent study showed that the hydrothermal decomposition of cellulose for a non-catalyzed reaction can selectively afford glucose and HMF at a high cellulose loading of 29 wt% and a temperature range of 463-573 K [165, 185]. The effect of water on these reactions has been studied extensively and has appeared as a central theme of various literature reviews [186-188]. This phenomenon is due to the distinct properties that water exhibits at elevated temperatures. For instance, the equilibrium constant for the ionization of water near the critical temperature is about 3 orders of magnitude higher than at ambient temperature, which can be advantageous for acid and base-catalyzed reactions [189]. However, the low selectivity toward LA resulted in the search for more viable solvent media. For this reason, a solvent such as ILs which can act as catalysts alongside their dissolution potential for cellulose was proposed [190].

It was found that $MnCl_2$ in sulfonated (SO_3H)-functionalized ILs was an effective catalyst for the synthesis of HMF and FU from cellulose; whereas LA was detected as a side product [191]. From these results, Ren, et al. [174] used SO_3H-functionalized ILs such as 1-methyl-3-(3-sulfopropyl) imidazolium hydrogen sulfate $[C_3SO_3Hmim]HSO_4$ for the selective conversion of cellulose to LA under microwave radiation. The cationic structure of the sulfonated IL had negligible influence on its catalytic performance. However, the anion HSO_4^- determined the acidity of the IL, generating LA in yield as high as 44.5 mol% at 433 K for 30 min. Recently, a dicationic acid IL composed of 1,1-bis(3-methylimidazolium-1-yl) butylene $[C_4(mim)_2]$ cation with hydrogensulfate (HSO_4) anion was synthesized and characterized for the catalytic conversion of cellulose to LA [180]. To enhance the acidity of HSO_4-based ILs, additional acidic sites were incorporated by adding a stoichiometric amount of H_2SO_4. The as-prepared $[C_4(mim)_2][(2HSO_4)(H_2SO_4)_2]$ afforded LA in yield of 55 mol% at 373 K in 3 h. The performance of the IL was attributed to its strong acidity, with HSO_4 anion enabling the cleavage of intra and intermolecular hydrogen bonding of cellulose. Also, the small size of HSO_4 experiences low steric hindrance and could access the cellulose moiety with ease. Other ILs, for example, heteropoly acid ILs $[mimPSH]H_2PW_{12}O_{40}$ gave LA in yield of 63.1 mol% at 413 K in 12 h [177]. The considerably high LA yields from these studies suggest that ILs

are suitable media for LA production. Nevertheless, issues of recyclability can be resolved by immobilizing ILs on a solid surface, with the resultant catalyst combining the benefits of both heterogeneous catalysts and ILs [192].

2.4.2.3.2 Catalytic systems

Extensive research on LA synthesis has been carried out in the presence of catalysts since cellulose conversion and product selectivity are very poor with non-catalytic systems. The catalytic systems have further been divided into two categories including homogenous and heterogeneous catalysts. When water-insoluble biomass is to be processed into platform chemicals, strong Brønsted homogenous acid catalysts are often used. These homogeneous catalysts including H_2SO_4, HCl, HBr, and H_3PO_4, deliver their catalytically active H^+ into cellulose [183]. The rate of HMF conversion and the LA yield is correlated to the H^+ concentration in the mineral acid-catalyzed reaction. H_2SO_4 and HCl are two of the majorly used catalysts in this category due to their low cost, readily availability, and ability to produce LA in high yields [186]. Girisuta, et al. [168] reported that cellulose conversion in an aqueous solution of H_2SO_4 afforded LA in yield of 60 mol% at 423 K. Detailed kinetic studies showed that the activation energy needed to produce LA is lower than that for glucose decomposition and humin formation. This suggests that high temperature favors humin formation. Shen [164] conducted a comparative study on cellulose conversion to LA catalyzed by HCl. Based on an optimized kinetic model, they generated LA at 60% of the theoretical yield at 453 K in 20 min. The debate has been to state which between H_2SO_4 and HCl is superior for cellulose conversion to LA, as their efficiency relies on the chosen reaction condition and the source of cellulose [166, 193]. So far, HCl has shown enormous potential for LA synthesis from cellulose [194]. Additionally, it has been demonstrated that HCl is very effective when refuse such as paper sludge and tobacco chops, which contain a high concentration of calcium salts, are to be transformed into LA [183]. Calcium sulfate ($CaSO_4$) is formed when H_2SO_4 is used, which can clog the reactor. Overall, the major drawbacks of homogenous acid-catalyzed reactions are related to the separation and reuse of the catalyst, corrosion hazard, and an additional processing step to achieve neutralization [182].

To address the problems associated with the use of homogenous catalysts, solid acids, particularly the ones containing SO_3H functional groups, were used to convert cellulose into LA. For instance, Amberlyst 70, a resin-bearing SO_3H group which has comparable activity to HCl, was reported to be efficient for cellulose conversion [165]. At an initial cellulose loading of 29 wt%, the two-step conversion process afforded LA at 28% of the theoretical yield at 443 K. In another study, the Amberlyst 70 catalytic system was modified with 90 wt% GVL

and 10 wt% H_2O to afford LA in yield of 69% at 433 K. The high yield of LA was attributed to GVL, which could solubilize cellulose and therefore, enhance the cellulose and solid catalyst interaction [173]. Also, Lai, et al. [182] synthesized a magnetic sulfonated mesoporous silica solid catalyst, Fe_3O_4-SBA-SO_3H, to transform cellulose into LA. The sulfonic acid ordered mesoporous material was found to be a good catalyst for esterification and acid-catalyzed reactions [195]. Fe_3O_4-SBA-SO_3H delivered LA in a yield of 54 mol% at 423 K after a prolonged reaction time of 12 h. The LA yield decreased from 54 mol% to 45 mol% when the acid concentration was changed from 0.10 mmol mL^{-1} to 0.72 mmol mL^{-1}, showing that stronger acidity is crucial to catalyze cellulose to LA [196]. Currently, research on SO_3H functionalized catalyst to produce LA from cellulose is gaining attention. Accordingly, Van de Vyver, et al. [197] employed sulfonated hyperbranched poly(arylene oxindole)s to depolymerize ball-milled cellulose, affording LA in yield of 27.1 mol% at 438 K for over 3 h.

Zuo, et al. [172] prepared a sulfonated chloromethyl polystyrene resin (CP-SO_3H) by partially substituting the Cl group of CP with the SO_3H group. This novel catalyst contained both acid sites (SO_3H) and cellulose binding sites (Cl). The catalyst generated LA in a yield of 65.5 mol% in a 90 wt% GVL/10 wt% H_2O biphasic medium. The high catalytic activity of CP-SO_3H was attributed to the high amount of SO_3H group and chlorine on the catalyst, which is needful to retain the affinity of the catalyst for cellulose.

The above studies have shown that solid acids bearing SO_3H groups are efficient for cellulose conversion to LA. These results counter the presumed low LA yields speculated for solid acids, owing to their limited interaction with the cellulose moiety [198]. However, the large-scale application of the sulfonated solid acids could be limited because of the leaching of the acidic group.

Accordingly, Potvin [178] hydrolyzed cellulose to glucose, which was further converted to LA in the presence of Nafion, a solid acid. When 25% of NaCl was added on Nafion, a 5-fold increase in LA yield, from 14 mol% to 72 mol%, was afforded. Xiang [170] designed a porous ETS-10 zeolite catalyst, to depolymerize cellulose. Remarkably, the catalyst converted cellulose completely and afforded LA in yield of 91.0 mol% at 473 K in 6 h. The moderate Lewis acidic centers of the heterogenous catalyst played a crucial role in activating cellulose and the reaction intermediates, enabling high catalytic activity.

Lin, et al. [181] converted cellulose directly into LA, *via* a ZrO_2-catalyzed aqueous phase partial oxidation (APPO) and afforded LA in yield of 51.9 mol% at 513 K in 25 min. The superoxide's species on the ZrO_2 surface was proposed to play a crucial role in breaking the glycosidic bonds in cellulose, enhancing LA formation. In this view, Joshi, et al. [169]

reported an efficient conversion of cellulose using ZrO_2 under hydrothermal conditions. Cellulose was completely converted to LA in a yield of 54 mol% at 453 K in 3 h. In general, the fact that the ZrO_2 catalyst could be recycled without being deactivated showed that they are viable from an economic standpoint. Another consideration is that ZrO_2 is non-toxic in nature. Thus, studies on ZrO_2 and other metal oxides such as TiO_2 should focus on optimizing the reaction conditions to further improve the LA yield.

2.4.3 Furan-based platform

2.4.3.1 Hydroxymethylfurfural production

HMF is a multifunctional and versatile molecule that can be further converted into high-value-added chemicals [199]. Previously, HMF has been listed as an intermediate toward LA synthesis (Scheme 2.5). Since HMF is a derivative of hexose (C-6) sugars, its potential as a feedstock in the biorefinery to obtain carbon neutrality is feasible. Moreover, the capability of undergoing several forms of reactions including esterification, reduction, oxidation, halogenation, nitration, sulphonation, and dehydration makes HMF a host of other derivatives such as 2,5-furan dicarboxylic acid (FDCA), 2,5-bis-hydroxymethylfuran, 5-hydroxy furoic acid, 2,5-dimethylfuran, 5-alkoxymethylfurfural and bis(5-methylfurfuryl) ether [200]. For example, HMF can be oxidized to FDCA which can favorably replace terephthalic acid in polyester production [201]. Due to its polyvalence, HMF is among the building block chemicals listed by US DOE [160]. Although studies on high HMF yields have been reported, the cost of fructose being the favored feedstock for HMF synthesis could prevent its economic viability [186]. For HMF price to be competitive, a cheap and readily available feedstock alongside the development of more efficient processes is necessary [202]. The above discussions have shown that HMF has tremendous market potential that needs to be explored. Table 2.6 gives a comparative study of HMF synthesis from cellulose using different reaction systems. The use of green chemistry techniques for HMF synthesis is of interest. The next section will deal with reaction media for HMF synthesis.

Table 2.6: Comparative studies of HMF synthesis from different reaction media and various reaction conditions

Substrate		Catalyst	Reaction media	Condition		HMF yield	Ref.
Type	Amount			Temp. (K)	Time		
MCC	2.00 g	H_2O-CO_2	N.A.	523	30 min	16.2 wt%	[203]
MCC	1.00 g	Subcritical water	N.A.	553	4 h	11.9 mol%	[204]
MCC	0.05 g	$CrCl_3$-LiCl	[Bmim]Cl	433	10 min	62.3 mol%	[205]
MCC	0.50 g	N.A.	[TMG]BF_4	473	2 h	17.2 wt%	[206]
MCC	0.25 g	Bimodal-HZ-5	H_2O	463	4 h	46 mol%	[207]
MCC	0.10 g	$ChH_2PW_{12}O_{40}$	H_2O/MIBK	413	8 h	75.0 wt%	[208]
MCC	0.10 g	Nb/C-50	THF/H_2O-NaCl	443	8 h	53.3 mol%	[209]
MCC	1.80 g	$AlCl_3$-H_3PO_4	DMOE/H_2O	453	2 h	49.4 mol%	[210]
MCC	1.00 g	$FePO_4$	H_2O/THF	433	1 h	48 mol%	[211]
MCC	1.00 g	$NaHSO_4$-$ZnSO_4$	H_2O/THF	433	1 h	53 mol%	[212]
MCC	0.50 g	$CrCl_3$	[Bmim]Cl	393	5 h	58.4 mol%	[213]
Cellulose	0.02 g	N.A.	[Emim]Cl/H_2O	393	3 h	21.0 mol%	[214]
Cellulose	5.00 wt%	HCl	[Emim]Cl	378	4 h	30.0 mol%	[215]
Cellulose	0.90 g	SO_3H-SPPS	[Emim]Br	453	2 h	68.2 mol %	[216]
Cellulose	0.03 g	$CrCl_3.6H_2O$	[C_4C_1im]Cl	423	1 h	58.0 mol%	[217]
Cellulose	0.10 g	$AlCl_3$	DMSO/[Bmim]Cl	423	9 h	54.9%	[218]
Cellulose	1.00 g	Acidic H_2O	N.A.	573	0 min	20.7 mol%	[219]
Cellulose	2.00 g	TiO_2-ZrO_2 /Amberlyst 70	THF/H_2O	453	3 h	25.5 mol%	[220]
Cellulose	0.20 g	Cr[(DS)]$H_2PW_{12}O_{40}$	H_2O/MIBK	423	2 h	52.7%	[221]
Cotton	0.50 g	$CrCl_3$-$AlCl_3$	[Bmim]Cl	393	3 h	59.5 mol%	[213]

MCC = microcrystalline cellulose, N.A. = not available

2.4.3.1.1 Reaction media for HMF synthesis

Various classes of solvent including H_2O, ILs, and dimethyl sulfoxide (DMSO) with respect to cellulose dissolution have been recently reviewed [222]. Sugar dehydration to HMF has long been studied, and early results which date back to 1947 showed that the process tends to be autocatalytic in an aqueous media [223, 224]. Similarly, HMF has been produced from cellulose under sub- and supercritical conditions. For instance, cellulose conversion of 99.3% at the subcritical region afforded HMF in yield of 10.9 mol% at 623 K [14]. Additionally, CO_2 reacts with H_2O to form H_2CO_3 with enhanced acidity to promote the degradation of cellulose [203]. The subcritical H_2O-CO_2 system afforded HMF in yield of 16.2 mol%. When the CO_2 mole fraction exceeded 5.0%, the HMF yield ceased increasing because H_2CO_3 is a weak acid with limited ionization potential. Overall, non-catalytic dehydration of cellulose in subcritical water is slower and less selective toward HMF synthesis than the catalytic processes.

ILs can dissolve cellulose [190]. For example, imidazole ILs such as [$C_x$mim]Cl were reported to solubilize cellulose fairly well, up to 25 wt % [225]. The unusual solubility of cellulose in [$C_x$mim]Cl was attributed to the disruption of hydrogen bonds in cellulose by the chloride anions of the IL. The action of the ILs includes dispersion, π-π, n-π, hydrogen bonding, dipolar, and ionic/charge-charge interactions [226]. Accordingly, Hsu [214] investigated the conversion of cellulose to HMF using three ILs including 1-ethyl-3-methyl imidazolium chloride [Emim]Cl, 1-butyl-3-methyl imidazolium chloride [Bmim]Cl, and 1-ethyl pyridinium chloride [Epyr]Cl. They pointed out that a longer dissolution time is needed for cellulose to dissolve in [Bmim]Cl with longer alkyl length, but that parameter was almost irrelevant with other ILs [214]. At optimum conditions of 393 K, 30 min dissolution time, and 3 h of reaction, [Emim]Cl generated the highest HMF yield of 21 mol%. [Epyr]Cl delivered a mild HMF yield of 3 mol% but transformed cellulose to monosaccharides at a 32% yield.

Jiang [227] studied cellulose hydrolysis over various acidic ILs and observed that the presence of sulfonic acid groups in [C_4SO_3Hmim]Cl and [C_4SO_3Hmim]HSO_4 ILs greatly increased the reaction rate. [C_4SO_3Hmim]Cl and [C_4SO_3Hmim]HSO_4 afforded a total reducing sugar (TRS) of 95% and 85% after complete cellulose hydrolysis in about 1 h. The major products of the cellulose transformation were glucose and HMF. Li and Zhao [228] reported a method to dissolve cellulose in [C_4mim]Cl catalyzed by H_2SO_4. A previous study showed that acid hydrolysis of cellulose under atmospheric pressure requires excess acid loading [229]. In contrast, Li and Zhao observed a progressive increase in the yield of TRS and glucose from 5% and 7%, to 43% and 77% upon a decrease in acid/cellulose mass ratio from 5 to 0.11. This

suggested that the synergy between [C_4mim]Cl and H_2SO_4 under mild conditions facilitated cellulose hydrolysis even without pretreatment.

To further investigate the influence of functional groups on ILs performance, [$BMIM^-$][Cl^-] was functionalized using sulfonated (SO_3), carboxylic acid (COOH), and hydroxyl group (OH) [230]. The Hammett acidity of these ILs followed this order: IL-SO_3 > IL-COOH > IL-OH. Consequently, 85% of TRS was obtained as the highest yield when 0.2 g of IL-SO_3 was used [230]. For better performance, these ILs were used as co-catalyst to most metal halides. For instance, $MnCl_2$ in sulfonated ILs generated HMF in a yield of 45.7 wt% at 423 K after 5 h [191]. It was further explained that the metal ions of the ILs form $[MClx(SO_4)n]^{2n-}$ complexes which can promote the rapid conversion of the α-anomer of glucose to β-anomer [231]. Additionally, the $MnCl_2$ can improve the rate of cellulose conversion and enhance product selectivity. [Emim]Cl acted as a co-catalyst to $FeCl_3$, generating HMF in a yield of 23.6 wt% [232]. Generally, Cl anion with both basic and nucleophilic properties can enhance the cleavage of β-1,4-glycosidic bonds of cellulose to yield glucose. [$C_x$mim] cation can stabilize HMF and avoid its decomposition [233]. The Cr halide salts like $CrCl_2$ and $CrCl_3$ can isomerize glucose to fructose, which further dehydrates to HMF [234]. Accordingly, $CrCl_3.6H_2O$ in the presence of [C_4C_1im]Cl effectively converted cellulose to HMF with a yield of 58 mol% [217]. Increasing the cellulose loading decreased the HMF yield to 45 mol%. This was due to issues of mass transfer that could limit the rate by which cellulose and the catalyst interacted. Also, $CrCl_3$ in [Bmim]Cl afforded HMF in yield of 58.4 mol% upon cellulose conversion [213]. A study to transform cellulose to HMF was conducted using [Bmim]Cl with $CrCl_3$ as a catalyst, and LiCl, LiBr, or $LaCl_3$ as co-catalysts [205]. The synergy between these metal halides was more efficient as compared to $CrCl_3$ alone. LiCl as co-catalyst to $CrCl_3$ in [Bmim]Cl gave the best HMF yield of 62 mol% [205]. In general, the use of chromium salt has delivered HMF in high yields, however, the perceived toxicity of chromium is a key issue against its commercial application.

Most recently, Li [216] reported that sulfonated poly(phenylene sulfide) (SPPS) in ILs can catalyze the effective conversion of cellulose to HMF. SPPS is chemically and thermally stable and has been employed as the base polymer for proton-conducting electrolytes [235]. As confirmed by density functional theory (DFT), the SO_3H group of SPPS acts as Brønsted acid that donates a proton, and also acts as a conjugate base which can accept a proton [236]. The catalyst afforded HMF in yield of 68.2 mol% at 453 K in 2 h. The high HMF yield was unexpected since the steric hindrance between the SPPS polymer and the cellulose moiety was speculated to impede the reaction [216]. However, the authors explained that the steric effect

was possibly weakened by the proton exchange between the IL and the SPPS [237]. The SPPS catalyst is heterogeneous, and can easily be separated from the product and reused. This shows that SPPS can be a novel route for large-scale HMF synthesis from cellulose and lignocellulosic biomass such as PW.

2.4.3.1.2 Catalytic systems for HMF synthesis

Homogenous catalysts are in the same phase as the reactants. Since most reactions are conducted in a liquid phase, if both the reactant and the catalyst are soluble, homogenous catalysis occurs [222]. Although homogenous Brønsted acids in terms of H_2SO_4 [238], HCl [239], and H_3PO_4 [240] acids prove to be effective in cellulose hydrolysis, they are rarely selective towards HMF. Presently, only a few studies have shown the influence of these acids on HMF synthesis in a given reaction media. For instance, Weingarten, et al. [241] reported 44 mol% HMF yield from cellulose using dilute H_2SO_4 in a water/tetrahydrofuran (THF) media. Also, cellulose in an acidic solution of HCl afforded HMF in yield of 20.7 mol% [203]. On the other hand, the combined effect of homogeneous Lewis acid and Brønsted acid has been reported for HMF synthesis. For instance, Binder and Raines [242] reported that 37 mol% of HMF was formed from cellulose using $CrCl_3$ and HCl as cocatalysts in the DMA-LiCl solvent. Also, Zhao [210] reported that $AlCl_3$-H_3PO_4 bifunctional catalyst produced HMF in a yield of 49.4 mol% in a single-phase reaction system of 1,2-dimethoxyethane and H_2O at 453 K in 2 h. Similarly, Leng [213] proposed the use of $CrCl_3$ and its cocatalyst $AlCl_3$ for HMF synthesis from cellulose with high degree of polymerization under mild oil-bath heating. Remarkably, the $CrCl_3$-$AlCl_3$ catalyst generated HMF in yield of 58.3 mol% at a markedly reduced reaction time. Overall, these homogenous catalysts suffered from the disadvantages of the separation of catalyst and products, the recovery of acids, and the corrosion of the reactor under harsh conditions [243]. Additionally, the production of a large amount of acid waste also causes severe environmental problems.

In this context, heterogeneous solid catalysts for the conversion of cellulose and lignocellulosic biomasses were proposed. These systems are usually composed of a liquid phase, including the reactants and a solid catalyst. They can be cheap, easily recycled, can hold adjustable properties, and function as molecular sieves [244]. Among others, zirconium phosphates [245], SO_4^{2-}/Ti-MCM-41 [246], and zeolites [207] have been studied for HMF synthesis in hot compressed water. Accordingly, Nandiwale [207] reported that a mesoporous H-ZSM-5 obtained by post-treatment of microporous H-ZSM-5 through desilication was efficient to transform cellulose. The reaction temperature was crucial for cellulose conversion to HMF. When the temperature was increased from 443 K to 473 K, cellulose conversion

increased from 37% to 77%. Other factors that influenced cellulose conversion are an increase in total surface area, the total pore volume, and the total acidity of the solid catalyst. Glucose dehydration was found to be accelerated at a temperature of 463 K, affording HMF in yield of 46 mol%. When the temperature was further increased from 463 K to 473 K, the HMF yield later decreased to 35 mol%. This was attributed to the conversion of HMF to undesired products such as LA and humins, at a higher reaction temperature.

A yield of about 27 mol% of HMF was obtained using TiO_2 from its chloride precursor [247]. With the aid of dihydric phosphates, a 31 mol% yield of HMF was obtained from cellulose hydrolysis in hot compressed steam [248]. Similarly, the decomposition behavior of several biomasses has been investigated under hot-compressed H_2O. Hemicellulose started decomposing at a temperature above 453 K, and cellulose decomposed above 503 K. However, cellulose decomposition in the presence of alkali and Ni catalysts under hot compressed H_2O showed that the alkali hindered the char formation, whereas Ni enhanced steam formation and methanation reactions [249].

HMF synthesis in aqueous media using solid acids is a promising route however, the poor stability and high solubility of HMF in water could affect HMF selectivity as well as product separation. Eventually, this can limit the practical application of simple aqueous systems. To solve this problem, the use of biphasic media is proposed and detailed in the section below.

2.4.3.1.3 Cellulose conversion to HMF in biphasic systems

A biphasic media comprises of aqueous and organic phases. Upon HMF formation in an aqueous phase, it can be transferred immediately into the organic phase *via* extraction [243]. Therefore, the issues of rehydration to LA or other side products can be circumvented, and HMF yield can be enhanced. The aqueous phase is usually H_2O or H_2O-DMSO mixture with an acid as a catalyst. The organic phase can be methyl isobutyl ketone (MIBK), a mixture of MIBK/2-butanol or THF [250]. Using these solvents, reasonable yields of HMF have been obtained over various heterogeneous catalysts. Herein, an inexpensive $FePO_4$ catalyst was reported for the conversion of cellulose into HMF in a water/THF biphasic media [211]. Fe^{3+} acted as a Lewis acid catalyst and promoted the isomerization of glucose to fructose. Moreover, H_3PO_4 generated from the hydrolysis of $FePO_4$ enhanced the dehydration of fructose to HMF. A 48 mol% yield of HMF was generated from cellulose at 433 K with H_2O/THF biphasic media in a ratio of 1:3. In the same fashion, it was shown that $CrPO_4$ can degrade cellulose to HMF, with a yield of 37 mol% obtained at 413 K in 15 min [251].

Similarly, H_2O/THF biphasic media was reported for cellulose conversion over the $NaHSO_4$-$ZnSO_4$ catalytic system [212]. $NaHSO_4$ alone delivered HMF in a yield of 36.7 mol%, which was attributed to the activity of the H^+ from $NaHSO_4$. When $ZnSO_4$ was added as a co-catalyst, the HMF yield increased to 56.2 mol%. The Zn^{2+} was effective in isomerizing glucose to fructose *via* a 1,2-hydride transfer [252]. Additionally, the added $ZnSO_4$ increased the volume of the aqueous solution and could regulate the acidity of the solution afterward. Therefore, increasing the volume of H_2O added to the aqueous system can influence the HMF yield. However, adding H_2O continuously is undesired and could cause poor cellulose degradation and a sharp decline in the catalyst concentration.

Polyoxometalate, the conjugate anion of a heteropoly acid, has been studied extensively for its unique catalytic activities [253]. Accordingly, when polyoxometalate is modified with a surfactant such as dodecyl sulfate, cellulose can be selectively transformed into HMF under mild conditions [221]. Therefore, the heteropoly acid containing both Brønsted and Lewis acid sites as well as a surfactant, i.e., $Cr[DS]H_2PW_{12}O_{40}]_3$ (DS = dodecyl sulfate, $OSO_3C_{12}H_{25}$), delivered HMF in yield of 52.7% at 423 K. The high catalytic activity was due to the combined effect of Brønsted and Lewis acid sites, and the micellar structure with hydrophobic groups. Here, the Brønsted acid site catalyzed the hydrolysis of cellulose into glucose. Meanwhile, the Lewis acid site accelerated the conversion of glucose into HMF *via* fructose dehydration. In addition, the micelles could provide a hydrophobic environment to protect HMF and prevent it from other undesired reactions. After HMF was extracted with MIBK, the $Cr[DS]H_2PW_{12}O_{40}]_3$ catalyst was present between the water and organic phases as an emulsion and could be easily separated.

Recently, Zhang, et al. [208] investigated a thermo-responsive heteropolyacid ($ChH_2PW_{12}O_{40}$) catalyst, prepared by $H_3PW_{12}O_{40}$ and choline chloride (ChCl) for cellulose hydrolysis in a one-pot conversion system. HMF in yield of 75.0 wt% was attained upon 87.0% cellulose conversion in the biphasic media of H_2O/MIBK. Compared to conventional $H_3PW_{12}O_{40}$, the high HMF yield could be due to the thermoregulation property and the Brønsted acidity of the prepared catalyst.

Overall, biphasic systems when combined with heterogenous catalysts could catalyze the conversion of cellulose into HMF in high yields. One factor that can limit its use on a large scale is the complicated separation of organic and inorganic phases. Core knowledge of how these two phases interact will be needful to assist the engineers in designing reactors that will be efficient for this purpose.

2.5 Market Potentials for Biobased Products

The total market for biobased platform chemicals is difficult to estimate [254]. There is a strong tendency to focus on markets where biobased products can favorably replace fossil-based products. Experts working for Cargill and McKinsey & Company believe that two-third of the total volume of chemicals could be produced from biobased materials, which would be valued at US$1 trillion/y [255]. This could be achieved based on the feedstock price, policy framework, and market attraction. Table 2.7 summarizes the market potentials of biobased platform chemicals [256]. Lactic acid is one of the chemicals that has gained momentum, dominating globally at US$684 million/y. This is mostly explained by the growing demand for PLA, which is expected to grow at a compound annual growth rate of about 4% until 2023 [257]. This trend is at about the same rate as petrochemical-derived polymers and plastics.

Table 2.7: Market potential for biobased platform chemicals adapted from [256]

	Biobased Market					
Product	Price (US$/kg)	Volume (kg/y)	Sales (m$/y)	% of total market	End-use	Key players
Sorbitol	0.72	164,000,000	107	assumed 100%	Toothpaste, surfactants, pharmaceuticals, and polyether polyols for polyurethane.	Cargill, ADM, Roquette Freres, SPI Pharma Inc., Ingredion Inc. and Lonza Inc.
EG	1.43-1.65	425,000,000	553-638	1.5%	Polyester resins, PET, antifreeze, explosives, textile fiber	AkzoNobel, Sinopec Group, BASF, Dow Inc., Royal Dutch Shell, and Reliance Industries Ltd.
GA	0.55-0.88	100,000,000	50-80	assumed 100%	Industrial cleaner, ink, paint, and dye	Roquette, BASF SE, Sigma-Aldrich, Bristol-Myers Squibbs
Lactic acid	1.60	472,000,000	684	100%	Preservative, antimicrobial agent, PLA	BASF, Corbion, CSM N.V., Dow Inc., Teijin, Nature Works LLC
LA	7.17	3,000,000	20	assumed 100%	Plasticizers, cosmetics, herbicides	Segetis, Biofine, DuPont, Incitor, GFBiochemicals
HMF	>2.93	20,000	0.05	20%	Flavors, fragrances, pharmaceuticals	AVA Biochem, Robinson Brothers, Penta Manufacturer, Treatt, and NBB Company.

Biobased EG is the second most attractive building block molecule reported. EG exists in three forms namely mono ethylene glycol (MEG), diethylene glycol (DEG), and triethylene glycol (TEG). Among them, MEG is the largest commodity chemical, accounting for over 90% of EG production, followed by DEG and TEG [258]. MEG is mainly used for the production of PET [258]. Antifreeze is the second largest application for MEG however, the market is still underdeveloped, representing only 7% of total MEG used in 2019 [258].

Products like sorbitol and GA have a significant market share based on their end-use [256]. Sodium gluconate, a GA derivative, accounts for more than 80% of the total GA market [105]. About 83% of the global sorbitol is sold as a 70 wt% aqueous syrup used in the formulation of syrups, solvents, and gels [259]. Sorbitol, in its crystalline form, is used as an additive to produce mint tablets, chewing gum, and polydextrose. The bulk prices for liquid and crystalline sorbitol are about US$0.55-US$0.65 per kg and US$1.61-US$2.26 per kg, respectively [260].

LA is one of the least valued platform chemicals with a relatively small market [261, 262]. In the last decade, the production volume of LA has been estimated by several authors [263]. In 2002, Meons estimated that about 1 million kg/y is produced by DSM but solely through a fossil-based route with a typical price for LA around US$11.02 per kg [264]. The development of bio-based routes *via* the Biofine process will serve as a potential way to increase the volume to 180 million kg/y [261]. In 2006, Hayes, et al. [265] reviewed the Biofine process with the LA market estimated at 500,000 kg/y at US$5 per kg. Using the Biofine process, LA has been produced in a pilot plant located at Glens Falls, New York, operating at 1000 kg per day dry mass of feedstock [265]. Recently, GFBiochemical has purchased an LA processing plant in Caserta, Italy, with a processing capacity of 50,000 kg of dry feedstock per day [261]. GFBiochemicals has announced plans to expand its production capacity to 50 million kg/y.

FDCA, an HMF derivative, has a market volume estimated at 500 million kg by the end of 2020 [266]. FDCA is expected to replace PET with about 322 million kg, followed by polyamides at 80 million kg [266]. Avantium, through collaborations with companies such as Coca-cola, Danone, Alpha, and Wifag-Polytype, became the key player in the development of FDCA [267]. Their long-term ambition is to sell licenses to build or retrofit plants, each producing 300-500 million kg/y of FDCA [267].

2.6 Conclusion

The thermochemical route for the transformation of cellulose involves hydrolysis to glucose prior to platform chemicals production. These chemicals include sorbitol, EG, GA, lactic acid, LA, and HMF. They have been synthesized from cellulosic biomass using homogenous and heterogeneous catalysts. Although homogenous catalysts were effective in transforming cellulose into the desired platform chemicals, these systems suffer the drawback of separation of catalyst and products, acid recovery, and the corrosion of the reactor under harsh conditions. Some of these acids are not selective as they generate undesired by-products, thus, affecting the yield of the targeted specie. The corrosive conditions demand the use of special materials to design the reactor. In turn, this increase the capital investment and operating costs of the biorefinery. Hence, the need to substitute the homogenous catalysts with their heterogeneous counterpart. Most of the heterogeneous catalysts screened converted cellulose and afforded platform chemicals in considerable high yield. The observed yields were against the speculation that the limited interaction of solid acids with cellulose will affect their catalytic performance. One problem plaguing the use of heterogeneous catalysts is the issue of stability. Some of the solid acids leach their metal species into the reaction solution, restricting their reuse. Another problem is related to downstream product separation. Effective product recovery depends on the mode and technology used for its production. Downstream processing significantly influences the process economies, owing to wastewater generation and energy requirement of the recovery process. This review thus juxtaposes studies conducted on various catalytic systems and reaction media to transform cellulose to the aforesaid platform chemicals. Plausible suggestions have been made to abet the production of these platform chemicals on a large scale. Also, a strong case has been made for PW, a flexible feedstock, which has been subjected to a robust pretreatment step during the paper-making process. Accordingly, section 2 detailed the global perspective of pulp and paper. The method these feedstocks are sourced could affect the operations of the biorefinery. A proper recovery and sorting system for these paper materials could enhance their use as well as reduce the cost of operating the biorefinery. Other sections of this review discussed the current and future market scenarios of these chemicals. If these biobased molecules are economically competitive, they could overtake their fossil-based counterparts.

Connecting Statement 1

Chapter 2 provides a concrete discussion on the chemocatalytic transformation of cellulose and cellulosic-derived waste to platform chemicals, focusing on paper wastes which are currently underutilized. Although cellulose from paper wastes has mainly been used for bioethanol production, this review aimed to expand the scope of the utilization of these refuses to produce platform chemicals. Studies on homogenous and heterogeneous catalysts for cellulose conversion have afforded platform chemicals in considerably high yields, with emphasis given to the latter, considering their green status. One major challenge in the use of these heterogeneous catalysts is their limited interaction with cellulose during hydrothermal processing. While fine-tuned electronic properties have helped to improve the catalytic activities of some of these catalysts, the interplay between solid matrix and other catalysts has enabled the depolymerization of cellulose. An emerging technique involving the co-mixing of catalyst and cellulose in a ball mill was highlighted, affording platform chemicals in high yields. Insights from the aforesaid studies will serve as a guide to valorize paper waste into platform chemicals. Since these wastes are cheap, readily available, and flexible, they have tremendous potential as biorefinery feedstocks.

The following chapter studied the thermochemical conversion of decationized newsprint to levulinic acid. The process parameters for newsprint conversion were based on conditions optimized for hard/softwood, using response surface methodology (RSM). The reaction kinetics was included to understudy the various steps toward the conversion of the newsprint to levulinic acid. The newsprint was characterized by TGA after its chemical composition was determined using the National Renewable Energy Laboratory (NREL) protocol. This chapter is an excerpt from the article published with Cellulose (2021), with permission from Springer. The article was co-authored by Dr. Marie-Joseé Dumont and Dr. Guillermo Alberto Portillo Perez.

3 Valorization of Decationized Newsprint to Levulinic Acid

3.1 Abstract

As of today, most chemical products are fossil-based. The environmental concerns of fossil resources due to their constant misuse have led to the exploration of bio-based alternatives. Biomass comprising industrial and municipal wastes, agricultural residues, forest residues, and natural herbaceous plants can favorably replace fossil fuels to produce chemicals. In this study, softwood and hardwood pulps were used to synthesize levulinic acid. Prior to a dilute acid hydrolysis step, the wood pulps were decationized overnight with 0.2 M HCl. The effects of the major reaction conditions including reaction temperature, time, and HCl concentration on the yield of levulinic acid were studied *via* a central composite design. Levulinic acid yields from softwood and hardwood pulps reached 50.30 mol% and 68.85 mol%, respectively, at optimum reaction conditions. When newsprints were tested using the optimized parameters for softwood and hardwood conversion, levulinic acid yields of 66.3 mol% and 79.7 mol% were obtained, respectively. A kinetic model was developed to predict the yields of glucose, hydroxymethylfurfural, and levulinic acid from the HCl-pretreated newsprint. The analysis of the kinetic parameters and the results of the response surface methodology experiments provided optimized conditions for levulinic acid production.

Keywords: levulinic acid; decationization; softwood; hardwood; newsprints.

3.2 Introduction

Biorefineries (modeled after fossil fuel refineries) are essential for a successful transition towards producing sustainable chemicals and materials from biomass. Ideally, biorefineries should be flexible and produce various chemicals from the agricultural, forest, and municipal residues using multiple conversion processes. These chemicals can be transformed into a range of other derivatives, like those derived in the petrochemical refinery. Among the known platform chemicals, levulinic acid (LA) is one of the most outstanding [268]. LA has two highly reactive functional groups that allow several forms of chemical transformation. The carbon atom of the carbonyl group is usually more subjected to nucleophilic attack than the carboxyl group [265]. As a keto-acid, it can act as a precursor to produce resins, plasticizers, textile, coatings, and fuel additives [269, 270].

The first step to produce LA from biomass is the hydrolysis of cellulose into glucose. For the acid-catalyzed hydrothermal process, the as-formed D-glucose isomerizes to fructose and subsequently converts to hydroxymethylfurfural (HMF). The outlined process is referred to as the Lobry de Bruyn-Alberda van Ekenstein rearrangement [271].

The transformation of monomeric sugars such as glucose and fructose into LA has been well-documented [272-277]. While sugars can be obtained directly from biomass, such as from saccharose present in sugar beet, or semi-directly from hydrolysis of starch from corn or other crops, there is a concern that such processes may compete with food supplies. Alternatively, glucose can be obtained from cellulose present in straw, grass, municipal solid wastes (MSW), and forestry products such as wood. Wood is a form of lignocellulose consisting primarily of cellulose (38-50%), hemicellulose (23-32%), and lignin (15-25%) [278]. The variation in the physicochemical properties of cellulosic biomass reveals the need for pretreatment to achieve efficient conversion of holocellulose into their monomeric sugars. In this process, lignin and hemicellulose, which surround the cellulose, are broken down. While the lignin is removed, the hemicellulose is degraded, and the crystalline structure of cellulose is altered to make it susceptible to hydrolysis. Cellulosic biomass also contains a small number of inorganics and extractives (ranging from less than 1% up to 15 %), depending on the biomass type. These inorganics are known as alkali and alkaline earth metals (AAEMs) such as Ca, K, Na, and Mg with a smaller amount of Fe, Al, Mn, S, and P. They contribute to process-related issues such as catalyst deactivation, equipment corrosion, and heat transfer reduction [279]. Such issues are prevalent even for biomass with relatively low AAEMs content and could alter the degradation rate and the reaction pathways during thermochemical conversion.

In practice, the catalytic activity of AAEMs can be mitigated by dilute acid washing (pretreatment) of the biomass prior to thermochemical conversion. Generally, the removal efficiency of the metal ions (Ca^{2+}, K^{+}, Mg^{2+}, and Na^{+}) in wood depends on a trade-off between temperature, process time, acid type, and acid concentration. Washing with hot deionized water alone can remove most of the Na, Mg, and K ions, but the Ca ion is only partly removed [280]. For acid washing, the factors selected should be such that a significant fraction of the volatile matter in the biomass is preserved. Scott, et al. [280] showed that acid washing with 0.1 wt% HNO_3 at 30 ^{o}C for 60 min removed most of the metal ions in the biomass, affording levoglucosan (LG) in yield of 17 wt%. Shafizadeh, et al. [281] reported 15-19 wt% LG yield for newsprint washed with H_2SO_4 or HCl. Piskorz, et al. [282] leached poplar wood with HCl and H_2SO_4 under hydrolysis conditions and afforded LG in yield of up to 30 wt%. Kuzhiyil [283] reported an 80% yield of LG due to the removal of AAEMs in cellulose with H_2SO_4 or H_3PO_4. Recently, a prior decationization of hardwood (HW) with 0.1 M HCl followed by rinsing with deionized water afforded HMF in yield of 50.4 mol% [284]. Acid-washed pine followed by rinsing delivered LG in higher yield than acid-washed pine without rinsing [285]. While acid washing could effectively remove a large portion of inorganics and disrupt the

chemical structure to a certain extent, rinsing biomass with deionized H_2O after acid washing can prevent LG conversion to levoglucosone [283].

Overall, pretreatment is a significant step during the thermochemical conversion of all lignocellulosic biomass. This treatment is expensive, especially for complex biomass (e.g. wood), and contributes to about 25% of the processing cost [286]. Therefore, a strong case is made for paper waste, which may only require mild pretreatments prior to use. Paper wastes comprising office papers, newsprints, cardboards, and corrugated boxes are major components of MSW, which account for more than 35% of total lignocellulosic wastes [287, 288].

As global paper consumption increases, a large number of paper waste continues to be generated in developing and developed countries. For newsprints, there has been an up rise in its exclusive production from paper wastes [289]. In 2015, the global production was about 24.9 million tons with a price worth US$12.7 billion [290]. Of this, 14% was produced in Canada, while the US contributed about 7%. In contrast, the US consumed 13% of the world's produced newsprints and Canada used only about 1%. To the best of the authors' knowledge, there is a dearth of information on the use of newsprint for platform chemical production other than ethanol. For LA synthesis, paper towel seems to be the only paper type recently hydrolyzed, affording LA yields of 32 to 40 mol% [291, 292].

In this study, HCl catalyzed the production of LA from softwood (SW) and HW pulps under a range of reaction conditions. Prior to the hydrolysis reaction, the pulps were decationized with 0.2 M HCl solution for 24 h, to eliminate pre-existing metal ions and to increase their cellulosic content. With cellulose as the most abundant component of the wood pulp, LA was the primary focus of this analysis. Besides, due to the abundance of paper wastes and their potential as biorefinery feedstock, the above protocol used for wood pulps was tested on newsprints. Furthermore, a kinetic study was performed to maximize the yield of LA from the HCl-pretreated newsprint.

3.3 Materials and methods

3.3.1 Chemicals

The mixed softwood pulp (spruce, pine, fir, 1:1:1), containing 84.8% glucan, 7.7% xylan, and 5.6% mannan, and the eucalyptus hardwood pulp with holocellulose comprising 86% glucan and 14% xylan were received from FPInnovations, Canada. Newspaper wastes were collected from a local store and deinked using hydrogen peroxide (H_2O_2), sodium dodecylbenzene sulfonate (SDBS), sodium hydroxide (NaOH), sodium silicate (Na_2SiO_3), and Triton^{TM} X-100 bought from Sigma-Aldrich Co. LLC, USA. The high-performance liquid chromatography (HPLC) mobile phase was prepared with HPLC-grade acetonitrile (≥ 99.9%)

and HPLC-grade water, both purchased from Sigma-Aldrich. Formic acid (FA) (≥ 95%) bought from Sigma-Aldrich was used to modify the HPLC mobile phase. Standards of glucose (99.5%), mannose (99%), galactose (99%), xylose (99%), arabinose (99%), LA (99%), furfural (FU) (95%) and HMF (≥ 95%) purchased from Sigma Aldrich were used to calibrate the HPLC. Thermo Fisher Scientific, USA, supplied the catalyst (HCl), neutralizing agent ($CaCO_3$, 99.0%), and sulphuric acid (H_2SO_4) used for structural carbohydrate determination. Pyridine, anhydrous (99.8%), and bis(trimethylsilyl)trifluoroacetamide (BSTFA) were purchased from Sigma-Aldrich and used to prepare samples for GC-MS analysis.

3.4 Experimental

The procedure to de-ink newsprints is described in section 3.4.1 meanwhile sections 3.4.2 and 3.4.3 are detailing the decationization and the hydrothermal treatment of the wood pulps and newsprints for LA production.

3.4.1 Deinking of newsprints

Newsprint (50 g) was shredded into pieces of 15 mm × 4 mm using a shredder. Then, a deinking agent comprising of 1.5 wt% NaOH, 3wt% H_2O_2, 5 wt% Na_2SiO_3, 1.5 wt% SDBS and 1.5wt% Triton^{TM} X-100 solution was dissolved in 1000 mL of deionized water [293]. The shredded newspapers were inserted in a flask (2000 mL), soaked in the deinking agent, and stirred for 30 min. Thereafter, the flask was vigorously shaken for about 30 min until its contents turned into a slurry. While the chemical agents and the shredded newsprints were mechanically agitated, the ink was disentangled from the pulp. Subsequently, the pulps were washed with deionized water through a fine mesh (US standard sieve, No. 30) to remove ink and impurities. The deinked pulps were then vacuum filtered to remove water followed by air-drying for about 24 h, before storing in an airtight container for use.

3.4.2 Decationization of wood pulps and paper wastes

Decationization to remove the pre-existing metal ions and to increase the cellulosic content of the wood pulps and deinked newsprint was implemented using a procedure adapted from [284]. This involved the impregnation of about 5 g of the substrate overnight in a 500 mL aqueous solution of 0.2 M HCl. Afterward, the pulps were rinsed with deionized water until the pH of the solution turned neutral. Then, the samples were inserted into a vacuum filter to eliminate water prior to air drying for 24 h. When drying was completed, the samples were placed in an airtight container and stored in a desiccator for further analysis.

3.4.3 Batch experimental procedure for the synthesis of LA

Cylindrical batch reactors (capacity of about 5 mL) consisting of Pyrex tubes fitted with high-temperature seals were used for LA production from pulps. Appropriate amounts of pulps (from wood or deinked newsprints), HCl, and deionized H_2O were inserted into the tubes and totalized a volume of 4 mL. The tubes were capped tightly with the seal prior to heating in a Fisher Scientific High Temp Bath 160-A. The reaction was conducted under constant stirring with a magnetic stirrer. The heating medium was silicone oil from Acros Organics, Morris Plains, NJ, USA. The oil bath temperature was monitored using a K-type thermocouple, with deviations maintained within ± 1 ^oC. At the set reaction time, the tubes were removed and simultaneously placed in an ice bath to quench the reaction. When the temperature dropped to the ambient level, the tubes were opened, and their content was filtered using filter paper (Fisherbrand; qualitative P8; flow rate: fast). Before analytical work, the acid in the filtrate was neutralized with calcium carbonate to a pH of 5 to 6, and the suspension was centrifuged (Thermo Scientific, Legend X1R) at 10000 rpm for 10 min. The supernatant was then filtered with a 0.2 µm filter (Whatman RC 30) into a vial for HPLC analysis. To validate if LA was present in the biomass hydrolysate as seen in the HPLC chromatogram, GC-MS analysis was performed.

3.4.4 Structural carbohydrate determination for deinked newsprint

The monomeric sugars of the deinked newsprint pulps were evaluated following the two-step hydrolysis procedure of the National Renewable Energy Laboratory (NREL) [294]. The pulps from the deinked newsprints (300 mg) were hydrolyzed with 3 mL of 72% H_2SO_4 at 30 ^oC for 1 h. After completing the first hydrolysis, the acid was diluted to 4% by adding 84 mL of deionized H_2O prior to autoclaving at 121 ^oC for 1 h. The resultant solution was cooled to room temperature and then filtered using a vacuum filter. To evaluate the monomeric sugars, the filtrate was neutralized with $CaCO_3$ to a pH within 5-6. Subsequently, the solution was passed through a 0.2 µm micro syringe filter into a vial for HPLC analysis. Sugars including glucose, galactose, mannose, xylose, and arabinose were separated and analyzed with a Hi-Plex Ca (Duo), 300 x 6.5 mm column at 65 ^oC using HPLC water as the mobile phase at a flow rate of 0.6 mL/min, and a refractive index (RI) detector.

3.4.5 Sample preparation for GC-MS analysis

The first step involved LA recovery using liquid-liquid extraction, for which 3 mL of the acidic aqueous solution and methyl isobutyl ketone (MIBK), in a ratio of 1:1, was prepared. The solution was then sealed in a tube and vortexed (Corning LSE, USA) to allow for proper mass transfer of LA between the organic and aqueous phases. After 30 min of settling, 0.5 mL

of the organic phase was transferred into a glass tube and used for derivatization. Derivatization was done by adding 300 µL of BSTFA and 1 mL of pyridine. While the silyl group in BSTFA enabled the replacement of the active hydrogen in LA, pyridine facilitated the dissolution of the LA and BSTFA [295]. Thereafter, the solution was heated at 60 ^{o}C for 45 min prior to filtration using a microfilter of 0.2 µL into a vial for GC-MS analysis.

3.4.6 Analysis of substrates and products

A thermogravimetric analyzer (TGA) (Q50, TA Instruments, New Castle, DE, USA) was used to study the thermal behavior of the pulps from wood and newsprints. About 10 to 20 mg of the air-dried pulps were used for each run. The analyses were performed under a stream of nitrogen at a flow rate of 60 mL/min. The heating rate of the sample was 5 ^{o}C/min at a temperature range of 20 ^{o}C to 800 ^{o}C. The LA concentration of the samples for each completed conversion reaction was analyzed with an Agilent 1260 HPLC system. The system was fitted with a Zorbax Eclipse plus C18 (4.6 x 100mm, 3.5 mm) column and a variable wavelength detector (VWD) set at 274 nm. The mobile phase was a mixture of HPLC H_2O: acetonitrile (ACN) at a ratio of 90:10 with 0.1% formic acid. The flow rate, injection volume, and temperature were maintained at 1 mL/min, 10 µL, and 30 ^{o}C, respectively. The calibrations were conducted using LA, FU, and HMF analytical standards (Sigma Aldrich).

An Agilent 6890N GC system equipped with a MS detector was used for qualitative analysis of LA. The flow rate of the carrier gas (He) was set at 1.3 mL/min with an Agilent HP-5 column (30 m x 0.25 mm x 0.25 µm) used for LA separation. The oven temperature was kept at 80 ^{o}C for 3 min and rose to 280 ^{o}C at a heating rate of 20 ^{o}C/min. The injection volume was 1 µL and the splitless direct injection mode was used. The product yields (in mol%) were extracted from a calibration curve plotting the concentration of pure analytes (LA, FU & HMF) in H_2O against areas displayed on the chromatogram. Equation 3.1 was used to calculate the LA yield of pulps from hard/softwood pulps and newsprints [284].

$$LA\ yield\ (mol\%) = \frac{Weight\ of\ LA\ produced\ (mg)}{Weight\ of\ wood\ \ (mg)} \times \frac{162\ g/mol}{116 g/mol} \times \frac{1}{Xc \times Xg} \times 100 \qquad (3.1)$$

From the equation, Xc and Xg are the holocellulose and C6 contents of the newsprint, and the hard/softwood pulps. The molecular weights of the anhydroglucose and LA are 162 g/mol and 116 g/mol, respectively. A similar equation was used to generate kinetic data for HMF and glucose with their molecular weight given as 126 g/mol and 180 g/mol. The newsprint conversion (X_{NP}) and the selectivity to LA (X_{LA}) were calculated using equations 3.2 and 3.3 below.

$$Newsprint\ conversion\ (\%) = \frac{weight\ of\ reacted\ cellulose\ in\ NP\ (mg)}{weight\ of\ initial\ cellulose\ in\ NP\ (mg)} \times 100 \quad (3.2)$$

$$LA\ selectivity\ (\%) = \frac{Weight\ of\ LA\ produced\ (mg)}{Weight\ of\ reacted\ cellulose\ (mg)} \times 100 \quad (3.3)$$

3.4.7 Kinetic model development for the degradation of newsprints to LA.

Kinetic experiments were performed in duplicate at the following conditions: 180 °C, 190 °C, and 200 °C, 1.6 M HCl concentration, and reaction time of 0 to 100 min at an interval of 20 min. A kinetic model was developed to understand the degradation pattern of the newsprint to LA. First, the cellulose in newsprint hydrolysed to glucose, which then dehydrated to HMF and finally to LA. As shown in the model, the formation of humins, a dark insoluble by-product, invariably occurred during the dehydration of glucose to HMF. In addition, an increase in humins can occur via a prolonged reaction time.

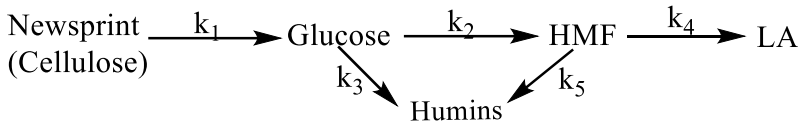

Fig. 3.1: Simplified reaction scheme used for kinetic modeling of cellulose in newsprint to LA.

This model assumes that the step from cellulose conversion to glucose is a pseudo-homogenous irreversible first-order reaction, whereas the other steps are irreversible first-order [296]. The model was employed to generate the corresponding rate equations as shown below.

$$-\frac{dC}{dt} = k_1 C \quad (3.4)$$

$$\frac{dG}{dt} = k_1 C - k_2 G - k_3 G \quad (3.5)$$

$$\frac{dHMF}{dt} = k_2 G - k_4 C_{HMF} - k_5 C_{HMF} \quad (3.6)$$

$$\frac{dLA}{dt} = k_4 C_{HMF} \quad (3.7)$$

Integration of equations 3.4-3.7 with the following initial conditions: C = Co and G = HMF = LA = 0 at t = 0, gave the following expressions (equations 3.8-3.11) for which C, G, HMF, and LA represent the concentrations of cellulose, glucose, HMF, and LA. Other kinetic parameters such as k_1, k_2, k_3, k_4 and k_5 are used to express the reaction rate constants.

$$C = C_o e^{k_1 t} \tag{3.8}$$

$$G = \frac{C_O k_1}{k_G - k_1}\left[e^{-k_1 t} - e^{-k_G t}\right] \tag{3.9}$$

$$HMF = k_2 k_1 C_o \left[\frac{e^{-k_1 t}}{(k_G - k_1)(k_{HMF} - k_1)} - \frac{e^{-k_G t}}{(k_G - k_1)(k_{HMF} - k_G)} + \frac{e^{-k_{HMF} t}}{(k_{HMF} - k_G)(k_{HMF} - k_1)}\right] \tag{3.10}$$

$$LA = k_4 k_2 k_1 C_o \left[\frac{1 - e^{-k_1 t}}{k_1 (k_G - k_1)(k_{HMF} - k_1)} - \frac{1 - e^{-k_G t}}{k_G (k_G - k_1)(k_{HMF} - k_G)} + \frac{1 - e^{-k_{HMF} t}}{k_{HMF} (k_{HMF} - k_G)(k_{HMF} - k_1)}\right] \tag{3.11}$$

3.5 Results and discussion

3.5.1 Thermal analysis of wood pulps and newsprint

Pulps from wood (SW and HW) and newsprint were hydrothermally converted into platform chemicals. These polymer matrixes with components such as cellulose, hemicellulose, and lignin are expected to withstand a temperature of approximately 200 ^{o}C. Therefore, it was important to identify the thermal degradation profile of fibers to be used for hydrothermal processing. Temperature, processing time, and water content among other factors are important to consider. The water content of wood has an impact on its thermal softening. Water content depends on properties such as dry weight, and size stability of wood. Fig. 3.2 shows the derivative thermogravimetric (DTG) data corresponding to the decationized pulps from soft/hardwood (SW and HW), HCl decationized newsprint (HCl-NP), and non-decationized newsprint (NP). Holocellulose values for the soft/hardwood pulps and newsprint were calculated *via* TGA as 82 wt%, 80 wt%, and 61.5 wt%, respectively. The thermal softening temperatures of all samples started at around 180 ^{o}C. The conversion of wood components into pyrolysis degradation products started at 270 ^{o}C and increased with increasing temperatures above 450 ^{o}C.

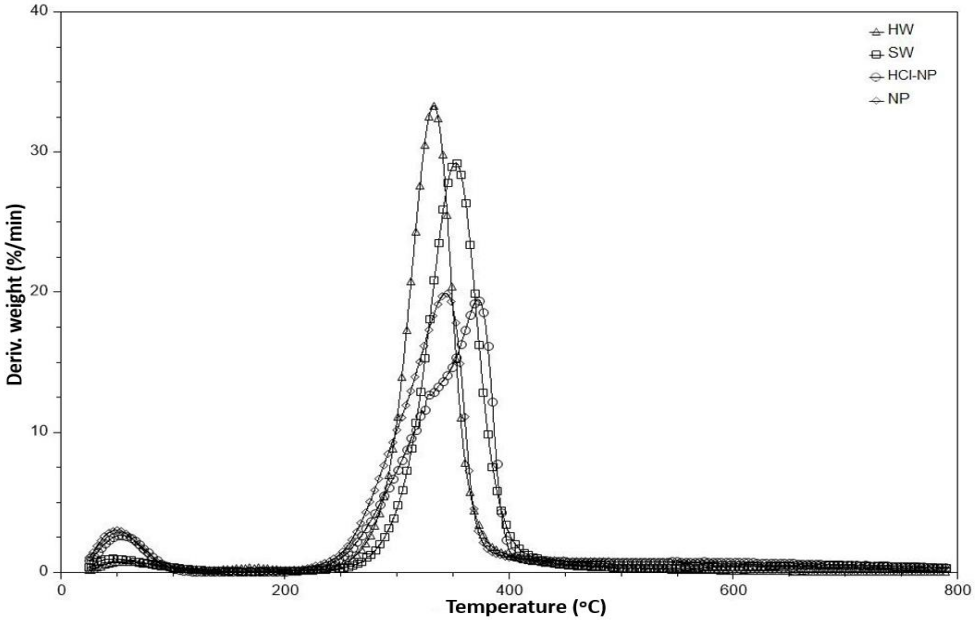

Fig. 3.2: DTG curves comparison for decationized pulps from wood and newsprint and non-decationized pulps from newsprint.

The first step in these degradation processes is the evaporation of water, occurring at around 150 ºC [297]. Holocellulose, which encompasses cellulose and hemicellulose, had the lowest degradation peak temperature of all compounds, due to the ease of decomposition of hemicellulose. The degradation of holocellulose occurred between 200 ºC and 410 ºC and peaked at about 375 ºC, corresponding to cellulose degradation. Lignin degradation started at a relatively low temperature and increased to around 400 ºC. HW and SW showed similar heating profiles (Fig. 3.2). Although both samples present a single peak in the degradation zone of cellulose and hemicellulose, the peak of HW is slightly tilted to a lower temperature. The slightly tilted HW peak could probably be due to the low degradation temperature of hemicellulose (200-350 ºC) as compared to cellulose (300-390 ºC) [297, 298]. This suggests a higher hemicellulose content in the HW as compared to the SW pulp. The HCl-NP and untreated NP have a lower peak height, corresponding to the degradation of cellulose. At the beginning of the thermo-degradation process, the weight loss between pulps from wood and newsprint was obvious. This weight loss could be due to water content and might explain why HW and SW pulps have a larger peak than their newsprint counterpart does. The peak deformation of the HCl-NP in the temperature range of 320 ºC to 350 ºC showed the degradation of hemicellulose. This confirmed the effect of pretreatment on newsprint. Overall, the evolution of the lignin content is similar for all the biomass species investigated.

3.5.2 Transformation of wood pulps into LA

The decationized wood pulps were subjected to hydrothermal treatment using an oil-bath as described in section 3.4.3. The HPLC chromatogram (Fig. 3.3) shows LA retention at 1.66 min, which appears before FU and HMF at 1.95 min and 2.70 min, respectively. The difficulty of LA retention on a reversed-phase column led to the modification of the mobile phase (H_2O: ACN, 90:10) with 0.1% of FA. The added FA in the mobile phase caused the formation of ionic pairs (neutral pairs of LA and FA) that can be retained in the HPLC column. The LA yields were derived based on the glucan and mannan content of the newsprint and the pulps from soft/hardwood. The C6 composition (section 3.4.5) of the newsprint was calculated as 60%. Data (LA yields) collated from HPLC runs were then used for statistical analysis.

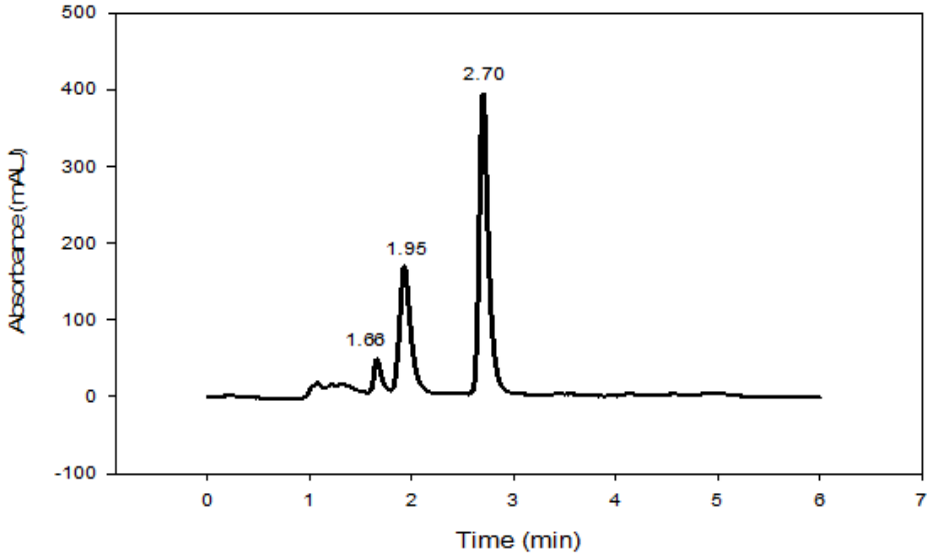

Fig. 3.3: HPLC chromatogram for levulinic acid, furfural, and hydroxymethylfurfural synthesis from softwood hydrolysate, a representation of hardwood and newsprint chromatogram.

3.5.3 Experimental design and analysis

For the statistical experimental design, a 5-level 3-factor central composite rotatable design (CCRD) was employed using JMP® (SAS institute). This method required 18 experiments, which included eight factorial points, six axial points, and four central points to provide an overall measure of a pure experimental error [299]. The three independent variables were the reaction time, the reaction temperature, and the catalyst (HCl) concentration. Table 3.1 shows the coded and uncoded independent variables (X_i). Multiple regression and analysis of variance (ANOVA) were used to predict and evaluate the statistical model.

Table 3.1: Factors and their levels in the central composite design for soft/hardwood pulps

Variable	Symbol	Coded factor levels				
		-1.68	-1	0	1	1.68
Tempe (^oC)	X_1	173.18	180.00	190.00	200.00	206.82
Time (min)	X_2	34.77	45.00	60.00	75.00	85.22
HCl C. (M)	X_3	0.53	0.80	1.20	1.60	1.87

3.5.4 Statistical Analysis

Table 3.2 shows the experimental data for SW and HW conversion to LA. A quadratic model was fitted to the experimental data for LA yield as follows:

$$Y_1 = 28.05 + 5.71X_1 + 2.19X_2 + 6.60X_3 + 2.77X_1^2 + 5.05X_2^2 - 0.19X_3^2 - 4.66X_1X_2 - 5.02X_1X_3 - 6.85X_2X_3 \quad (3.12)$$

$$Y_2 = 59.18 + 1.77X_1 + 7.33X_2 + 5.92X_3 - 1.06X_1^2 - 6.27X_2^2 - 6.27X_3^2 - 1.29X_1X_2 - 2.8X_1X_3 + 6.94\ X_2X_3 \quad (3.13)$$

Y_1 and Y_2 represent the responses (LA yields from SW/HW pulps) for the independent variables in coded units, i.e., temperature (X_1), time (X_2), and HCl concentration (X_3).

Table 3.2: Experimental design and results for SW and HW conversion to LA

Run	Temp., X_1 (^oC)	Time, X_2 (min)	HCl, X_3 (M)	LA Yield, Y_i (mol %)	
				SW	HW
1	180.00	75.00	0.80	36.35	39.99
2	190.00	60.00	1.20	26.36	59.89
3	190.00	85.22	1.20	42.43	50.37
4	190.00	60.00	1.20	29.97	59.00
5	180.00	75.00	1.60	39.27	68.14
6	180.00	45.00	0.80	2.21	29.90
7	200.00	75.00	1.60	38.39	68.85
8	206.82	60.00	1.20	41.50	56.22
9	190.00	34.77	1.20	38.96	29.81
10	180.00	45.00	1.60	42.72	39.31
11	190.00	60.00	1.20	30.50	59.66
12	200.00	75.00	0.80	45.37	42.88
13	190.00	60.00	0.53	12.97	32.31
14	173.18	60.00	1.20	27.02	53.43
15	190.00	60.00	1.20	25.94	58.63
16	200.00	45.00	0.80	40.05	46.95
17	190.00	60.00	1.87	38.79	47.87
18	200.00	45.00	1.60	50.30	37.15

SW = softwood, HW = hardwood

For SW (Fig. 3.4), the R^2 and adjusted R^2 were 0.94 and 0.88, respectively. This shows that the studied factors account for almost all of the variation in the response. A similar result was obtained for HW, with a R^2 of 0.97 (Fig. 3.5). From the values of the coefficient of determinations (R^2 and adjusted R^2), the agreement between actual and predicted LA yield was verified, providing a good estimate of response within the region of study [300].

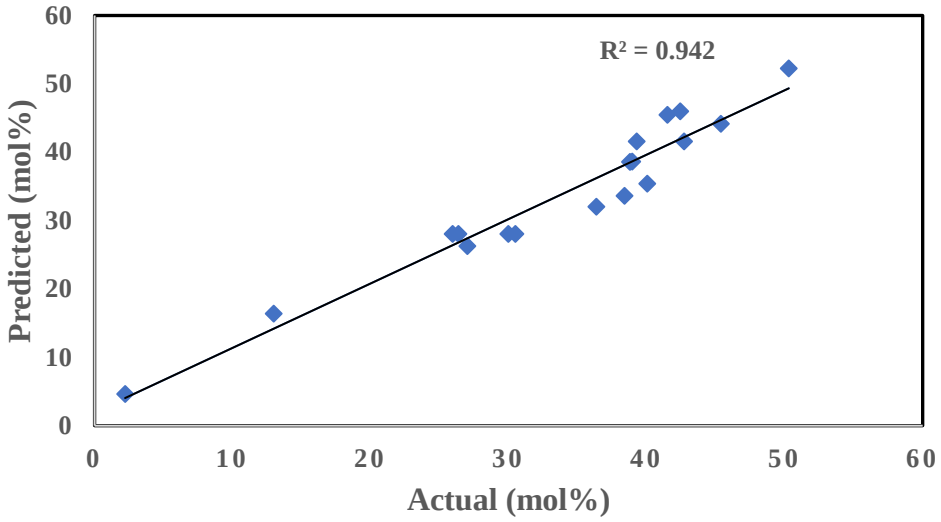

Fig. 3.4: Plot of predicted versus actual values for levulinic acid yields from softwood.

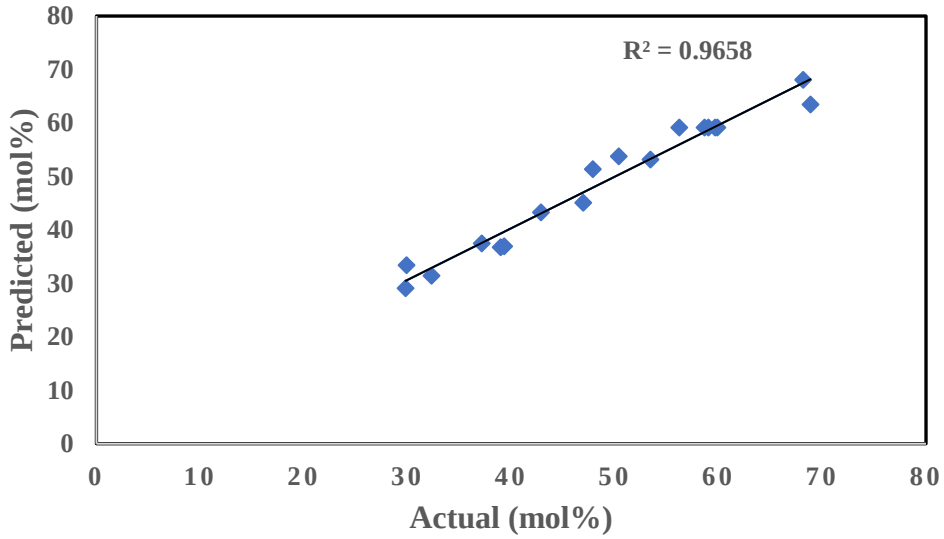

Fig. 3.5: Plot of predicted versus actual values for levulinic acid yields from hardwood.

The coefficients obtained from Equations 3.12 and 3.13 are tabulated below (Table 3.3). The estimated parameters show the coefficients and significance of the linear, quadratic and interactive terms on each response. From the table, absolute magnitudes in relation to the statistical significance p-level of 0.05 are shown for SW and HW. For instance, reaction temperature (X_1) and catalyst concentration (X_3) for SW had the clearest effects on the yield of LA, displaying the smallest p-values (0.001 and 0.0004). HW followed a similar trend,

however, with the smallest p-values (<0.0001 and 0.0002) observed for variables such as reaction time (X_2) and acid concentration (X_3). In addition, the entire model's interactive effects and the quadratic effects of temperature (X_1^2) and time (X_2^2) significantly affected SW pulp conversion to LA. For HW, two interactive effects where the concentration combined with the temperature (X_1X_3) and time (X_2X_3), and the quadratic effect of time (X_2^2) and concentration (X_3^2) had a significant effect on LA yields. These observations showed that the three main effects were of relevance to producing LA from SW and HW pulps.

Table 3.3: Regression coefficient and its significance as per LA yield

Variables	Regression coefficient		Standard error		t-value		Significant level, p-value	
	SW	HW	SW	HW	SW	HW	SW	HW
Intercept	28.05	59.18	2.08	1.68	13.47	35.23	0.0005*	<0.0001*
X_1	5.71	1.77	1.13	0.91	5.05	1.95	0.0010*	0.0611
X_2	2.19	7.33	1.13	0.91	1.94	8.05	0.0875	<0.0001*
X_3	6.60	5.92	1.13	0.91	5.84	6.51	0.0004*	0.0002*
X_1X_2	-4.66	-1.29	1.47	1.19	-3.17	-1.08	0.0133	0.3109
X_1X_3	-5.02	-2.80	1.47	1.19	-3.41	-2.35	0.0092*	0.0464*
X_2X_3	-6.85	6.94	1.47	1.19	-4.66	5.83	0.0016*	0.0004*
X_1^2	2.77	-1.06	1.17	0.95	2.35	-1.12	0.0454*	0.2933
X_2^2	5.05	-6.27	1.17	0.95	4.32	-6.63	0.0026*	0.0002*
X_3^2	-0.19	-6.27	1.17	0.95	-0.16	-6.63	0.8741	0.0002*

*Significant variables, SW = softwood, HW = hardwood

The response surface plot is shown in Fig. 3.5, in which the corresponding contour indicated the significance level for the interactions between variables. Elliptical contours can be achieved when the interaction between independent variables is strong [301]. ANOVA (Table 3.4) was performed to test the significance of the regression models that expresses the relationship between dependent and independent variables. The ANOVA with probability as low as 0.0005 and <0.0001 for SW and HW pulps indicated that the fitted model was of high significance.

Table 3.4: ANOVA to test the significance of the regression model fitted for LA production

Source	DF		Sum of squares		Mean square		F-value		Prob > F		R^2	
	SW	HW	SW	HW	SW	HW	SW	HW	SW	HW	SW	HW
Model	9	9	2249.4	2557.2	249.94	284.1	14.4	25.1	0.0005	<0.0001	0.94	0.97
Error	8	8	138.6	90.5	17.3	11.3					0.88*	0.93*
C total	17	17	2387.9	2647.6								

*Adjusted R^2, DF = degree of freedom, SW = softwood, HW = hardwood

Fig. 3.6a-f shows the response surface plots obtained from equations 3.12 and 3.13. These 3D response surfaces and their corresponding contour plots are used to highlight the interactive effects between the independent variables on the response. The maximum predicted LA yield is depicted by the surfaces surrounding the smallest ellipse.

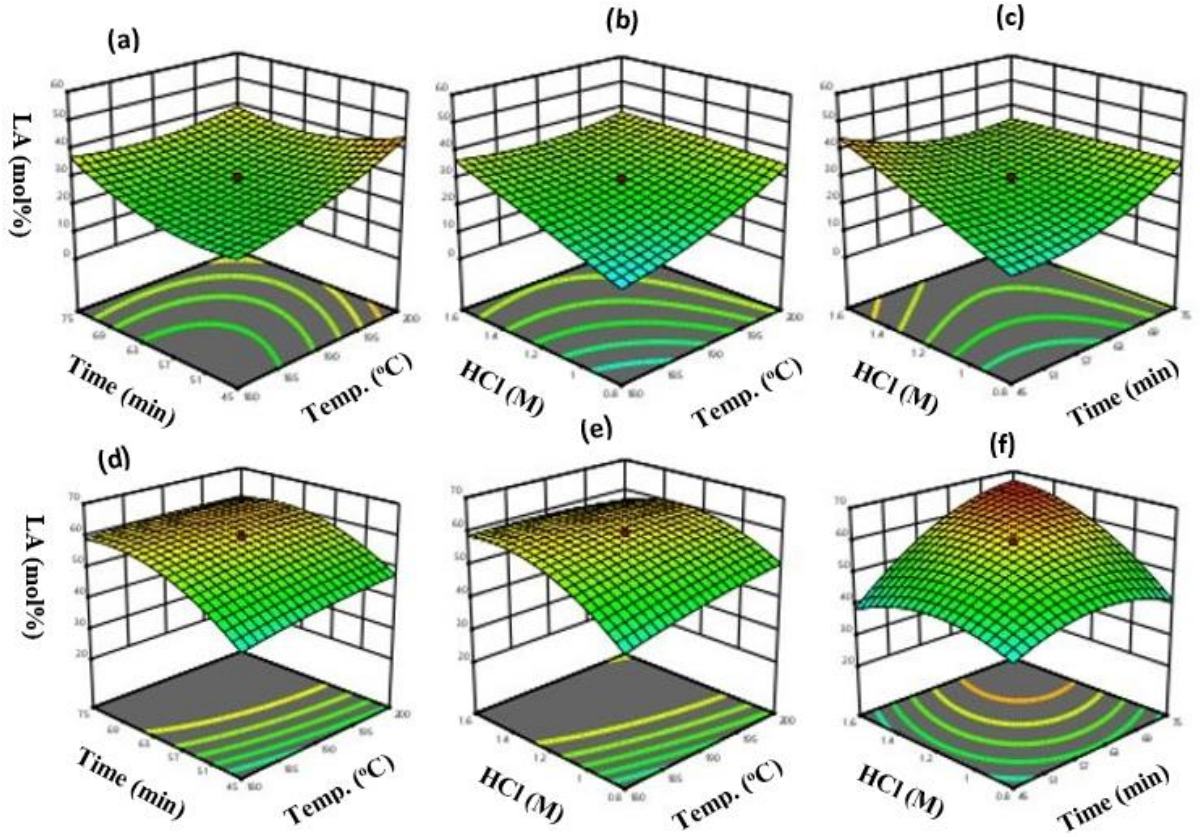

Fig. 3.6: 3D response surface plot for the optimization of levulinic acid (LA) yield from softwood (SW) and hardwood (HW) pulps: (a) LA yield versus reaction time and temperature for SW; (b) LA yield versus catalyst concentration and temperature for SW; (c) LA yield versus catalyst concentration and reaction time for SW, (d) LA yield versus reaction time and temperature for HW; (e) LA yield versus catalyst concentration and temperature for HW; (f) LA yield versus catalyst concentration and reaction time for HW.

While Fig. 3.6a and b show the effect of temperature on LA synthesis from SW, Fig. 3.6d and e show the data for HW. As known, temperature is a major factor that influences the

rate of acid hydrolysis. In this study, the main and quadratic effect of temperature is significant for SW, participating in the disruption of the rigid structure of the wood pulps as confirmed by a previous study [302]. The main effect of temperature for HW conversion was almost significant; however, the quadratic effect was not. With temperatures in the range of 180 ^{o}C to 200 ^{o}C, a maximum yield of LA for both pulps can be achieved at around 200 ^{o}C. Nevertheless, HW afforded LA in yield of 68.1 mol% at 180 ^{o}C, showing that HW can as well be converted at a milder temperature. The interactive effect of temperature in combination with time and HCl concentration was significant for SW. For this specimen (SW), higher temperature and shorter reaction time were required to afford LA in high yields and vice versa. For instance, LA yield as high as 50.3 mol% was achieved at a high temperature of 200 ^{o}C for only 45 min. However, a reaction duration of 60 min at 206.8 ^{o}C would only result in a 41.5 mol% yield of LA. For HW, the interactive effect of temperature was only significant when combined with the concentration. Hence, at a temperature of 200 ^{o}C and a catalyst (HCl) concentration of 0.8 M, LA in a maximum yield of 68.9 mol% was delivered. A 3.41% increase in temperature was detrimental to HW conversion, thus lowering LA yield to 56.2 mol%. According to the literature, a further increase in the temperature favors humin formation that occurs at activation energy of 161.41 kJ/mol, which is higher than the 152.14 kJ/mol needed for HMF formation [303].

Fig. 3.6a and c show the effect of reaction time on LA yield for SW pulp. The main effect of reaction time in addition to its combined effects with temperature and concentration was significant. As expected, the interactive effect of reaction time and temperature afforded LA in high yield. However, higher reaction time and temperature could be detrimental, leading to an increase in the rate of hydrolysis and the generation of side products [300]. Thus, an optimum condition of reaction time of only 45 min was necessary, affording LA in a high yield of 50.3 mol% from SW. This phenomenon can also be the same for catalyst interaction with reaction time, for which the catalyst will enhance LA yield until a given reaction time. On the other hand, Fig. 3.6d and f illustrate the effect of reaction time on LA yield from HW pulps. The main effect of time in conjunction with its combined effect with temperature was significant, confirming the LA yield of 68.9 mol% at 200 ^{o}C for 75 min. Besides, the quadratic effects of reaction time were highly significant for both pulps, promoting LA yield. However, longer reaction time favored the formation of humins and other unwanted products.

Fig. 3.6b and c show that catalyst concentration is relevant for LA formation from SW pulp, for which its linear and interactive terms are significant. Initially, the LA yield increased with the increase in catalyst concentration, which invariably influenced the rate of hydrolysis.

For example, starting at 0.8 M of HCl, the hydrolysis rate increased and a LA yield of 45.4 mol% was afforded. When the catalyst concentration exceeded its optimum value (1.6 M, HCl), the LA yield decreased. Fig. 3.6e and f explained the effect of catalyst concentration on LA yield from HW pulp. Both the linear and quadratic effect of HCl and its combined effects with temperature and time were highly significant. This can be verified by the average increase in LA yields (39.9 mol%, 52.6 mol%, and 54.4 mol%) for low (0.8 M), medium (1.2 M), and high (1.6 M) HCl concentrations. However, LA yield decreased to 47.9 mol% at a higher HCl concentration (1.87 M). According to Yang et al., higher catalyst concentration does not favor LA formation due to dehydration reaction [304].

3.5.4 Effect of decationization on LA yields from wood and newsprint pulps

In a recent study, Mukherjee, et al. [284] detailed the effect of the removal of metal cations from hardwood pulp. While cations such as Ca^{2+}, $K^{+,}$ and Mg^{2+} are the most prevalent, cations of Fe and Mn occur only in trace amounts. For eucalyptus pulps, the Ca^{2+}, K^{+} and Mg^{2+} contents can range from 500-2700 mg/kg, 400-900 mg/kg, and 75-800 mg/kg, whereas cations such as Na^{+}, Al^{3+}, and Mn^{2+}, occur in amounts below 200 mg/kg dry wood [305]. The existing metal ions could hinder the activity of the HCl catalyst during hydrothermal processing thus reducing the LA yield.

As described in section 3.4.2, the decationization of the pulps from SW and HW was done by dilute acid (HCl, 0.2 M) washing. The maximum LA yields of the decationized SW and HW pulps were 50.3 mol% and 68.9 mol%, respectively (Table 3.5). When newsprint was deinked, decationized, and tested following the optimum condition for SW and HW conversion, LA in yields of 66.3 mol% and 79.7 mol% were attained. In this study, the optimum condition for HW conversion afforded LA in higher yield from newsprint. With newsprint as a blend of both HW and SW pulps, Petroudy and Resalati [306] gave the composition of HW in the blend as 83% whereas that of SW accounted for only 17%. This high composition of HW in this blend could be the reason for the higher LA yield from newsprint. In addition, the effect of decationization and the extensive pulping process that removed lignin and exposed the cellulosic fibers of the newsprint could also enhance the LA yield. Another author used aqueous extraction to remove water-soluble extractives from Pinus Pinaster wood prior to hydrothermal conversion, affording LA in yield of 56.4 mol% [307]. To confirm the effect of decationization on LA yield, hydrothermal treatment was performed in triplicate on non-decationized pulps from newsprint. At an optimum condition for HW conversion, a LA yield of 73.4 mol% was achieved. The 7.83% reduction in LA yield from non-decationized newsprint

as compared to its decationized counterpart showed that decationization is an important step in the chemo-catalytic conversion of newsprint to LA.

Among others, factors that could affect LA yield include incomplete cellulose hydrolysis due to too mild or uncontrolled HMF decomposition from too harsh reaction conditions. For this study, LA production depends majorly on the interplay between temperature, reaction time, and catalyst concentration. Conditions of low and intermediate severities have delivered LA in high yield. For instance, the central point replicated for HW conversion afforded LA in yields above 55 mol% in addition to the high yields of 68.1 mol% and 68.9% in runs 5 and 7 (Table 3.2), respectively. This finding confirmed that the experimental range selected for this study is more suitable for HW conversion.

Table 3.5: Levulinic acid yield from wood and wood products at different reaction conditions

Substrate		Catalyst	Condition		LA yield (mol%)	Refs.
Type	Amount		Temp. (^{o}C)	Time (min)		
Softwood pulp*	0.03 g	1.6 M HCl	200.0	45.0	50.3	This work
Hardwood pulp*	0.03 g	1.6 M HCl	200.0	75.0	68.9	This work
Decationized newsprint*	0.03 g	1.6 M HCl	180.0	75.0	79.7 ± 3.85	This work
Non-decationized newsprint*	0.03 g	1.6 M HCl	180.0	75.0	73.4 ± 3.45	This work
Paper sludge	1.75 g	37% HCl	200.0	60.0	77.00	[308]
Paper towel	0.5 g	1 M H_2SO_4	200.0	2.5	46.00	[292]
Paper towel	0.5 g	Amberlyst 36	150.0	20.0	34.00	[292]
Paper towel	5 wt%	0.135 M H_2SO_4	200.0	5.0	32.00	[291]
Pinus Pinaster	1 g	1.0 wt% HCl	192.2	18.9	56.40	[307]

Both HW and SW pulps were tested using the same apparatus and reaction conditions to exclude any variability other than the type of pulp. These wood pulps served as a modeled feedstock for newsprint conversion, being the major reason for this study. The maximum yield of LA from SW pulp based on experimental data was 50.30 mol%. The predicted optimum conditions (for SW), comprising temperature (200.0 ^{o}C), reaction time (45.0 min) and HCl concentration (1.6 M) afforded LA in yield of 66.3 mol% from decationized newsprint. HW on the other hand afforded LA in maximum yield of 68.9 mol%. When decationized newsprint

was hydrothermally converted at the predicted optimum conditions (T=180.0 ^{o}C, t= 75.0 min, and HCl =1.60 M) for HW conversion, LA in yield of 79.7 mol% was attained. As observed, the different optimized conditions used for SW and HW conversion afforded LA yields that are even higher for newsprints.

3.5.5 LA-profile for HCl pretreated newsprints at different temperatures and reaction times.

Fig. 3.7 presents the results for the LA yields obtained for the experiments performed at 180 ^{o}C, 190 ^{o}C, and 200 ^{o}C using 1.6 M HCl as a catalyst.

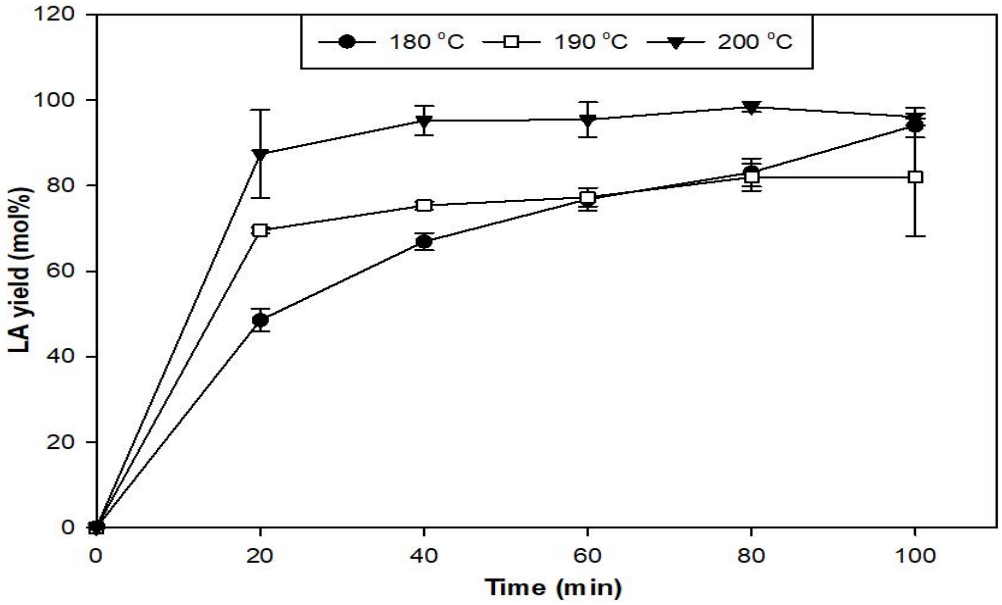

Fig. 3.7: LA yield from HCl pretreated newsprint at different temperatures and reaction times.

While the different temperatures had similar effects on the degradation of the newsprint, the LA yields followed a related variation pattern, reaching higher yields under conditions of higher severities. At all reaction temperatures (180-200 ^{o}C) studied, the LA yield increased with time from 20 to 60 min and then plateaued (89.8 and 98.4 mol%) at 80 min for the newsprints heated at 190 and 200 ^{o}C. For the newsprint processed at 180 ^{o}C, there was a sharp increase in LA yield (94.1 mol%) after 80 min, showing that elongated time is beneficial, promoting the further interaction of the newsprint with the HCl catalyst. These findings correlate with the study of Shen and Wyman [296] who reported that the time required to reach maximum LA yield was 20 min at 180 ^{o}C and only 3 min at 200 ^{o}C. It can also be seen that there was no significant increase in LA yield from 40 to 100 min at 200 ^{o}C, as the difference was in the region of 0.9% to 3.4 % only.

Generally, LA yield could be improved by increasing the temperature or prolonging the reaction time. For instance, LA yield of 95.2 mol% attained at 200 ^{o}C in 40 min was similar to

the yield of 94.1 mol% achieved at a lower temperature of 180 ^{o}C in 80 min. The high temperature of 200 ^{o}C may have contributed to a decrease of the cellulose crystallinity, leading to an improved rate of cellulose hydrolysis, which consequently led to a higher LA yield. The high temperature could also decrease the effects of the reaction media viscosity and reduce the mass transfer limitation, thus enhancing the rate of cellulose depolymerization [309]. As such, the production of LA at a higher temperature and a shorter reaction time could be preferred. However, the LA yield decreased when the reaction time was further elongated above the optimum point, owing to the unwanted side reactions produced. For instance, increasing the reaction time from 80 to 100 min was detrimental as seen for the newsprint heated at 190 ^{o}C and 200 ^{o}C, leading to an 8.74% and 2.40% decrease in LA yield, respectively.

3.5.6 Kinetic modeling of HCl-pretreated newsprints to LA

The yields of the different reaction products from the hydrothermal conversion of HCl pretreated newsprint were experimentally determined and reported. Fig. 3.8 shows the fits between the experimental and predicted data for cellulose, glucose, HMF, and LA under different reaction conditions. A MATLAB SIMULINK (version R2019b) program was used to simulate the model in equations 3.4-3.7 with the corresponding rate constants reported in Table 3.6. Except for k_2, the rate constants did not change monotonically with increasing temperature. Table 3.6 shows that there is an obvious difference between the k_1 values for the three temperatures as compared to the other k-values (k_2, k_3, k_4,k_5). The observed variations between these values (Table 3.6) did not significantly affect the overall fit of the system. As seen, the rate constant increased following this order $k_1 > k_4 > k_2 > k_3 > k_5$. The high values of k_1, which is about 73, 9, and 25 times higher than k_4 at 180, 190, and 200 ^{o}C, show the rapid degradation of cellulose occurring at a time of around 5 or 10 min earlier than the initial reaction time of 20 min. At 20 min, the degradation of cellulose afforded glucose only in low yields with the highest being 14.72%, 6.93%, and 5.45 % for newsprint hydrolyzed at 180 ^{o}C, 190 ^{o}C, and 200 ^{o}C, respectively. The k_4 values were the second highest, suggesting that the rehydration of HMF to LA was not the rate-determining step in the overall synthesis of LA from newsprint. As soon as the HMF is formed, it is instantaneously transformed to LA such that the detected yield is always low with the highest being around 3 mol% for the newsprint heated at 180 ^{o}C. The low HMF yield could also suppress humin formation and might be the reason for the low values of k_5, which for this study were very close to zero.

Table 3.6: Kinetic parameters for the hydrothermal conversion of newsprint at different temperatures

T (°C)	k_1 (min^{-1})	k_2 (min^{-1})	k_3 (min^{-1})	k_4 (min^{-1})	k_5 (min^{-1})
180	38.6900	0.0783	0.0075	0.52873	7.21×0^{-6}
190	4.5994	0.1267	0.0071	0.5217	1.18×10^{-4}
200	15.3920	0.1429	0.0019	0.6038	7.21×10^{-6}

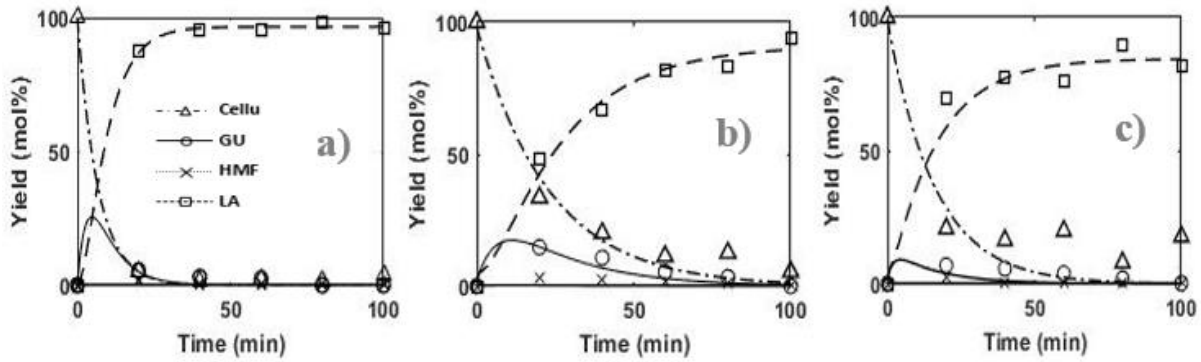

Fig. 3.8: Experimental and modeled yield profiles for the degradation of HCl-pretreated newsprint at (a): 180 °C, (b): 190 °C, and (c): 200 °C.

3.5.7 Catalytic conversion of HCl pretreated newsprint at different reaction conditions

The newsprints pretreated with HCl were hydrolyzed at temperatures of 180 °C, 190 °C, and 200 °C with 1.6 M HCl. After an initial reaction time of 20 min, cellulose conversions of 66.42%, 79.24%, and 93.99% and LA yields of 48.5%, 69.5%, and 87.4% were achieved (Table 3.7).

Table 3.7: Comparison between conversions of newsprint (X_{NP}), selectivities (S_{LA}), and yields (Y_{LA}) of LA obtained at different temperatures

Time (min)	HCl-NP at 180 °C			HCl-NP at 190 °C			HCl-NP at 200 °C		
	X_{NP} (%)	S_{LA} (%)	Y_{LA} (%)	X_{NP} (%)	S_{LA} (%)	Y_{LA} (%)	X_{NP} (%)	S_{LA} (%)	Y_{LA} (%)
20	66.4 ± 2.02	73.0 ± 1.82	48.5 ± 2.69	79.4 ± 2.14	87.8 ± 1.53	69.5 ± 0.664	94.0 ± 4.95	92.8 ± 3.54	87.4 ± 10.28
40	79.9 ± 0.28	83.7 ± 2.26	66.9 ± 2.04	83.6 ± 2.54	92.4 ± 0.47	77.3 ± 1.97	98.2 ± 0.61	96.7 ± 3.04	95.2 ± 3.37
60	88.7 ± 2.08	92.1 ± 0.95	81.7 ± 2.70	80.1 ± 1.58	94.9 ± 0.84	76.0 ± 2.18	96.9 ± 1.76	97.4 ± 2.17	95.4 ± 4.04
80	87.7 ± 1.75	95.1 ± 1.82	83.1 ± 3.25	92.0 ± 3.49	97.6 ± 0.31	89.8 ± 3.65	99.7 ± 0.19	99.8 ± 0.01	98.4 ± 1.24
100	94.5 ± 2.73	99.5 ± 0.13	94.1 ± 2.84	82.7 ± 3.21	99.6 ± 0.03	82.0 ± 3.16	96.3 ± 2.05	99.8 ± 0.002	96.1 ± 2.04

While the selectivity of LA rose above 70% in all cases, the highest value (99.8%) was observed for the newsprint hydrolyzed at 200 °C for 100 min, which afforded LA yield of 96.1 mol%. This could be due to the substrate type and the effect of the pretreatment, which enabled

the efficient hydrolysis of the newsprint. In addition, a previous study showed that the acid type (HCl), acid amount, and acid strength could influence the selectivity of LA from cellulose or glucose conversion [179]. Furthermore, the selectivity to LA from this study is relatively high and except for LA and furfural as a by-product, no other products were detected in the reaction solution.

3.6 Conclusion

This study shows an alternative way to use paper waste effectively other than for ethanol production. To begin, SW and HW pulps were used as modeled feedstocks to produce LA at a given range of temperature, reaction time, and HCl concentration. The LA produced from the SW and HW were analysed using the RSM. This enabled the selection of optimum conditions (T = 200.0 ^{o}C, t = 45.0 min and HCl = 1.6 M) and (T = 180.0 ^{o}C, t = 75.0 min and HCl = 1.6 M) for SW and HW pulps that could deliver LA in maximum yields. At these reaction conditions, newsprint was hydrolyzed, affording LA yields of 66.3 mol% and 79.7 mol%, being higher than the yields from the modeled feedstocks. A kinetic model was also developed to understand the degradation process of the cellulose in newsprint into glucose, HMF, and LA. Overall, this study provides a better knowledge of the fundamental steps toward newsprint conversion followed by the optimized parameters required to improve LA yield.

Connecting Statement 2

The previous chapter highlighted the hydrothermal conversion of deinked newsprint to levulinic acid based on trials performed on both hard and softwood pulps as modelled feedstocks. In the first instance, the wood pulps and the newsprint were decationized using dilute acid washing to remove alkali and alkaline earth metals, which contribute to process-related issues such as catalyst deactivation, equipment corrosion, and heat transfer reduction. Pretreatment also assisted in altering the crystalline structure of cellulose, making it susceptible to hydrolysis to enhance the product yield. Another aspect was to characterize the newsprint to elucidate its chemical composition as well as its thermal stability.

Chapter 4 focused on comparing the levulinic acid yield from HCl and Fenton pretreated newsprint. The reaction was performed in an acidic aqueous solution of $FeCl_3.6H_2O$/LiCl at selected reaction temperature and time and optimized for improved levulinic acid yield using response surface methodology. An additional kinetic study was performed to compare the degradation stages of the HCl and Fenton pretreated newsprints and both were characterized by SEM. This chapter is an excerpt from the article published in the Journal of Environmental Chemical Engineering (2021), with permission from Elsevier. The article was co-authored by Dr. Marie-Joseé Dumont.

4 Optimization and mechanistic kinetic model: toward newsprint waste conversion to levulinic acid

4.1 Abstract

In this study, Box-Behnken design (BBD) was employed to optimize the yield of levulinic acid from HCl pretreated (HCl-NP) and Fenton pretreated (Fenton-NP) newsprints. Experiments were performed in a 5 mL Pyrex tube batch reactor at the following conditions: 180-200 ^{o}C of reaction temperature (T), 3.5-4.5 h of reaction time (t), 0.1-0.2 M of catalyst concentration ([$FeCl_3.6H_2O$]), and 20-wt% LiCl, which served as a promoter. With the optimum conditions for conversion of HCl-NP and Fenton-NP as follow: T = 200 ^{o}C, t = 3.63 and 3.50 h, and [$FeCl_3.6H_2O$] = 0.118 and 0.100 M, the predicted maximum yields of LA were 83.4 mol% and 86.4 mol %, respectively. This showed that the optimal conversion of HCl and Fenton-NP occurred at different processing conditions. A mechanistic model was developed where the experimental concentrations of cellulose, glucose, hydroxymethylfurfural, and levulinic acid were simulated to generate the model's kinetic parameters. This provides a deeper insight into the various stages necessary to improve levulinic acid yields from newsprints wastes.

Keywords: levulinic acid; pretreatment; newsprints; kinetic model.

4.2 Introduction

The search for alternatives to fossil resource use has prompted the use of renewable resources as feedstock for various industrial processes. The valorization of biomass residues and wastes is considered a promising route for the production of liquid fuels, chemicals, and polymers. Among others, paper waste (PW) is one component of municipal and industrial solid wastes, accounting for more than 35% of the total lignocellulosic fraction [287]. Besides being renewable, abundant, and inexpensive, PW conversion into a commodity and fine chemicals can help in attaining carbon neutrality. Although more than 400 million tons of these wastes are generated annually, only about 50-65% end up being recycled [288].

Levulinic acid (LA), a keto acid with both carbonyl and carboxyl functional groups, can be derived from PW in high yields when pretreated [310, 311]. Such pretreatment enables the breaking of the compact cellulosic structure of PW, increasing the accessibility of the available cellulose in its pulp. The use of alkali and liquid hot water are methods, which have been investigated for biomass pretreatment [312-314]. While the former requires a longer processing time, the latter is capital-intensive due to a high energy cost, a high-pressure demand, and a large amount of water supplied to the system.

In this study, the Fenton reagent and dilute acid (HCl) were used to pretreat fibers of deinked newsprint (NP) prior to hydrothermal conversion. Although the use of dilute HCl for biomass pretreatment has been reported in the literature, Fenton-pretreatment for biomass valorization is still emerging. Fenton chemistry provides non-selective oxidation of organic compounds [315]. It is considered environmentally benign since it does not require conditions of high temperature, pressure, or concentration. Although the catalytic effect of Fe^{2+} on H_2O_2 was first observed by Fenton in 1894, the role of hydroxyl radical ($HO^{\cdot}$) was proposed by Haber and Weiss in 1934 [316]. H_2O_2 is a powerful oxidant, but its reaction kinetics is very slow at low concentrations. However, when ferrous salt is added to H_2O_2, its oxidative strength increases dramatically [317]. The ferrous ions catalyze the decomposition of H_2O_2 to hydroxyl radicals and ferric ions at pH 3-5 (Eq. 4.1). The ferric ion further reacts with hydrogen peroxide, regenerating ferrous ions (Eq. 4.2).

$$Fe^{2+} + H_2O_2 = Fe^{3+} + OH^- + HO^{\cdot} \quad (4.1)$$

$$Fe^{3+} + H_2O_2 = Fe^{2+} + {}^{\cdot}OOH + H^+ \quad (4.2)$$

$HO^{\cdot}$ can enhance the degradation of polysaccharides, which leads to a decrease in molecular weight as well as the formation of carboxyl groups [318]. These highly reactive electrophilic species react with cellulose by abstracting a hydrogen atom to form reactive organic radicals that can lead to depolymerization. The hydrogen abstraction activity of the hydroxyl radicals depends on the strength of R-H bonds in the substrate, which can be defined by the difference between the bond formation energy of the product (HO-H), and the bond dissociation energy of the substrate (R-H) [319].

Mineral acids such as HCl and H_2SO_4 have been extensively studied as catalysts for the conversion of both simple sugars and lignocellulose to LA. However, these acids have drawbacks such as equipment corrosion and recycling difficulty [320]. Although heterogeneous catalysts can overcome these challenges, constraints take place due to the solid-solid mass transfer limitation when lignocellulose is used as feedstock [269]. Other limitations of heterogeneous catalysts include the ease of deactivation, high preparation cost, and long reaction times. Recently, inorganic salts such as $FeCl_3.6H_2O$ were employed as catalysts for the conversion of lignocellulose to LA. For instance, Wang et al. used $FeCl_3$/NaCl catalyst for the conversion of xylose residues, affording LA in yield of 68 mol% [321]. Zhi et al. used $FeCl_3$ to facilitate the conversion of corn stalks and afforded LA in yield of 49 mol% [322]. Therefore, for the first time, this study aimed at enhancing the conversion of NP pretreated with HCl (NP-HCl) and Fenton reagent (NP-Fenton) into LA using $FeCl_3.6H_2O$ as a catalyst

and LiCl as a promoter. Like NaCl, LiCl is an inorganic salt that can swell or even dissolve NP slurry, thus increasing the cellulose hydrolysis by $FeCl_3.6H_2O$. The ions of LiCl behave similarly to ions of ionic liquids, which can penetrate the cellulose fibers and disrupt the hydrogen bond network [323].

4.3 Materials and Method

4.3.1 Chemicals

Newspaper waste (NP) was sourced from a nearby store and deinked using hydrogen peroxide (H_2O_2), sodium dodecyl benzene sulfonate (SDBS), sodium hydroxide (NaOH), sodium silicate (Na_2SiO_3), and Triton^{TM} X-100 bought from Sigma-Aldrich Co. LLC, USA. The high-performance liquid chromatography (HPLC) mobile phase was prepared with HPLC-grade methanol (≥ 99.9%), HPLC-grade acetonitrile (ACN) (≥ 99.9%), and HPLC-grade water, supplied by Sigma-Aldrich. Formic acid (FA) (≥ 95%) bought from Sigma-Aldrich was employed as the mobile phase modifier. Standards of glucose (99.5%), mannose (99%), galactose (99%), xylose (99%), arabinose (99%), LA (99%), furfural (FU) (95%) and hydroxymethylfurfural (HMF) (≥ 95%) purchased from Sigma Aldrich were used to calibrate the HPLC. The organic solvents used for LA extraction are tetrahydrofuran (THF) (≥ 99.9%) and methyl isobutyl ketone (MIBK) (≥ 99.9%), from Sigma-Aldrich. Other chemicals supplied by Sigma-Aldrich include the catalyst ($FeCl_3.6H_2O$), its co-promoter (LiCl), H_2SO_4, and $CaCO_3$ used for neutralization.

4.4 Experimental

The following procedures comprising deinking and HCl decationization of NP have been detailed in previous studies [284, 324]. Before hydrothermal processing, all samples were pulverized using a cyclone mill (MODEL 3010-030, UDY Corp., Fort Collins, CO) to obtain a uniform particle size reduction, and for proper interaction between samples and aqueous acidic solution. While section 4.4.1 explains the Fenton pretreatment of NP (Fenton-NP), section 4.4.2 details the oil-bath procedure for NP conversion to LA.

4.4.1 Experimental procedure for Fenton pretreatment of NP

In a typical Fenton pretreatment experiment, 50 g of deinked NP pulps were inserted in an Erlenmeyer flask (1000 mL), followed by the addition of 100 mL of 6% H_2O_2 and 100 mL of 1.25 mM $FeCl_2.4H_2O$ [325]. To avoid H_2O_2 volatilization, the flask was sealed with parafilm prior to incubating at 25 ^oC in an orbital shaker (Max Q^{TM} 4000 series, Thermo Fisher) at 30 rpm for 24 h. After the reaction, the slurry was filtered, with the obtained pulp sequentially

washed with a 5-wt% oxalic acid solution. The washing step was performed using deionized water until a neutral pH was attained, and the obtained solid was subsequently dried for 24 hrs.

4.4.2 Experimental procedure for LA synthesis using oil-bath

Pyrex tube reactors (capacity of about 5 mL) fitted with high-temperature seals were employed for LA synthesis from deinked NP. The catalyst comprising a solution of 4.5 mL of $FeCl_3.6H_2O$/LiCl in a ratio of 3:1 and 20 mg of NP was transferred into the tube. Prior to hydrothermal treatment, the tubes were vortexed (Corning LSE, USA), enabling proper mixing of the NP and the solvent media. The tubes were then sealed and placed in a silicone oil bath (Fisher Scientific High Temp Bath 160-A). A thermocouple probe placed inside the oil-bath and connected to a digital indicator was used to monitor the temperature. After the reaction, the reaction tubes were quenched in an ice-bath. The hydrolysate was filtered using filter paper (Fischerbrand; qualitative P8; flow rate: fast). Afterward, the filtrate was passed through a 0.2 µm filter (Whatman RC 30) prior to HPLC analysis.

4.4.3 Product quantification and sample characterization

LA, its intermediate (HMF), and co-product (FU), as well as glucose, were analyzed using an Agilent 1100 HPLC system. A Supelco Analytical C18 (25 cm × 4.6 mm, 5 µm) column and a variable wavelength detector (VWD) set at 267 nm were used to quantify LA, HMF, and FU. The column temperature was set at 30 ^oC, and the mobile phase was an isocratic 80:20 (v/v) blend of HPLC water and methanol plus 0.1% of formic acid. The injection volume, flow rate, and running time were 5 µL, 0.6 mL/min, and 15 min, respectively. The glucose yields were evaluated using a Zorbax Carbohydrate analysis column (4.6 × 150 mm, 5 µL) with a refractive index detector (RID) being used to obtain the glucose concentration. The column, as well as the RID temperature, were set at 30 ^oC, and the mobile phase was an isocratic 75:25 (v/v) blend of ACN and HPLC water. The injection volume, flow rate, and run-time were 5 µL, 1.4 mL/min, and 10 min, respectively. The product (LA, HMF, FU, and glucose) yields were expressed in mol% and extracted from a calibration curve plotting the concentration of pure analytes in H_2O against areas displayed on the chromatogram. While the LA yield, which is based on C6 sugar, is calculated from equation 4.3, the FU yield, a C5 sugar derivative, is derived from equation 4.4.

$$LA\ yield\ (mol\%) = \frac{Weight\ of\ LA\ produced\ (mg)}{Weight\ of\ newsprint\ fed\ (mg)} \times \frac{162\ g/mol}{116 g/mol} \times \frac{1}{Xc \times Xg} \times 100\% \quad (4.3)$$

$$FU\ yield\ (mol\%) = \frac{Weight\ of\ FU\ produced\ (mg)}{Weight\ of\ wood\ (mg)} \times \frac{132\ g/mol}{96\ g/mol} \times \frac{1}{Xc \times Xy} \times 100\% \quad (4.4)$$

With the holocellulose (Xc) value of the NP calculated using the TGA [311], its C6 (Xg) and C5 (Xy) compositions were determined following the NREL two-step hydrolysis procedure [294]. The molecular weights of the anhydroglucose, LA, anhydroxylose, and FU are 162 g/mol, 116 g/mol, 132 g/mol, and 96 g/mol, respectively. A similar approach (Eq. 4.3) was employed to calculate the HMF, and glucose yields, with their molecular weights, denoted as 126 g/mol and 180 g/mol, respectively.

The morphology of the untreated, HCl, and Fenton pretreated NP were investigated using a scanning electron microscope (SEM) (TM 3000, Hitachi High-Technologies Co., Tokyo, Japan) at an accelerating voltage of 5 kV.

4.4.4 Experimental design

The Box-Behnken design (BBD) and the response surface methodology (RSM) were employed to investigate the impact of three factors including reaction temperature, reaction time, and $FeCl_3.6H_2O$ concentration on LA yield. The selected ranges of temperature (180-200 ^oC), reaction time (3.5-4.5 h), $FeCl_3.6H_2O$ concentration (0.1-0.2 M), and a constant LiCl amount of 20-wt% were deemed appropriate for NP conversion to LA based on previous work and preliminary analysis (Table 4.1). The design was performed with the JMP® software (SAS institute) and the factors were studied at three different levels, totaling 17 experiments.

Table 4.1: Factors and their levels in the BBD for newsprint conversion to levulinic acid

Variable	Symbol	Ranges and levels		
		-1	0	1
Temperature (^oC)	X_1	180	190	200
Reaction time (h)	X_2	3.5	4	4.5
$FeCl_3.6H_2O$ (M)	X_3	0.1	0.15	0.2

The center point of the design was replicated five (5) times to estimate the errors. The coded and uncoded levels of each independent variable are shown in Table 4.1. The LA yield from the experiment was statistically analysed and fitted to a second-order polynomial model (Eq. 4.5).

$$Y = b_o + \sum_{i=1}^{k} b_i x_i + \sum_{i=1}^{k} b_{ii} x_i^2 + \sum_{i=1}^{k} \sum_{j>1}^{k} b_{ij} x_i x_j + \delta \quad (4.5)$$

Herein, Y is the predicted response, x_i represents the independent variables, k is the number of variables, and b_o, b_i, $b_{ii,}$ and b_{ij} are the coefficients of each independent variable, quadratic effect, and interactive effect.

4.4.5 Kinetic model development and parameter estimation

In this section, reaction temperature, time and $FeCl_3.6H_2O$/LiCl were the independent variables necessary for LA synthesis from NP. The temperature investigated was within the range of 180 to 200 ^oC, whereas the reaction time started from 0 to 240 min. While the catalytic system is a combination of 0.15 M $FeCl_3.6H_2O$ and 20-wt% LiCl, 20 mg of NP was used for each conversion. In total, 12 experiments were performed in duplicate with each tube heated at an interval of 20 min for glucose, HMF, and LA synthesis. The collated data was used to develop the kinetic model reported in this study. Fig. 4.1 shows the scheme employed to develop the kinetic model for the hydrothermal degradation of NP.

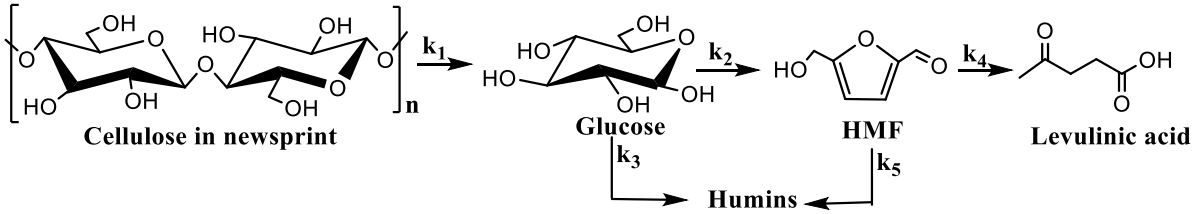

Fig. 4.1: Simplified kinetic model for the hydrolysis of cellulose in newsprint to levulinic acid.

Based on the developed kinetic model, the derivative rate laws for each conversion step were determined as follows:

$$-\frac{dC}{dt} = k_1 C \tag{4.6}$$

$$\frac{dG}{dt} = k_1 C - k_2 G - k_3 G \tag{4.7}$$

$$\frac{dHMF}{dt} = k_2 G - k_4 C_{HMF} - k_5 C_{HMF} \tag{4.8}$$

$$\frac{dLA}{dt} = k_4 C_{HMF} \tag{4.9}$$

$$k_2 + k_3 = k_G \tag{4.10}$$

$$k_4 + k_5 = k_{HMF} \tag{4.11}$$

Where C, G, HMF, and LA are the concentrations of cellulose, glucose, HMF, and LA and k_{1-5} are the rate constants for each of the reactions.

As shown below, the relationship between the reaction rate constant and the activation energy was expressed by the Arrhenius model.

$$k = A \times exp\left(-\frac{Ea}{RT}\right) \quad (4.12)$$

With A and Ea denoted as the frequency factors (min^{-1}) and activation energies ($Jmol^{-1}$), R and T are the universal gas constant (8.314 $J(mol\ K)^{-1}$) and reaction temperature (K).

To test the reusability of $FeCl_3.6H_2O$/LiCl, MIBK and THF were selected as solvents to extract LA from the aqueous acidic solution based on previous work [321]. With Fenton-NP selected as the most efficient substrate for LA synthesis, THF and MIBK were investigated as organic solvents for LA extraction. The study was conducted following these conditions: NP amount = 20 mg, reaction time = 100 min, temperature = 200 ^oC, $FeCl_3.6H_2O$ = 0.15 M and LiCl = 20-wt%. After each reaction, the mixture was filtered followed by LA extraction (5X) into the organic solvent from the aqueous acidic solution in a ratio of 2:1. The resultant aqueous acidic solution was then reused for subsequent hydrothermal conversion of NP to produce LA.

4.5 Results and discussion

4.5.1 Newsprint composition and SEM analysis

The holocellulose (Xc) value for the NP was reported as 61.5 wt%, with their C6 (Xg) and C5 (Xy) contents obtained as 60% and 30% (Section 4.4.3). SEM was used to examine the effect of pretreatment on the morphology of NP. Fig. 4.2 (a, b, & c) presents a SEM image of HCl-NP, Fenton-NP, and untreated NP along with a high-resolution image of their surfaces in Fig. 4.2 (d, e, & f). SEM images indicated that most of the untreated newsprint fibers were intact, dense, and well-packed, exhibiting a ribbon-like shape. Each of the untreated-NP fibers appears to be unconstrained, extending from one end to the other, without a notable fiber break. Although the fibers of the HCl and Fenton NP share some similarities with the untreated NP, they are shorter in appearance and are randomly packed. In addition, both HCl and Fenton pretreatments rendered NP fibers fluffy and soft, fully exposing them and creating more sites for hydrolysis. The HCl pretreatment resulted in the peeling of the fiber's surface and could enhance hydrolysis. Moreover, the Fenton pretreated NP showed more and clearer pit than its untreated counterpart.

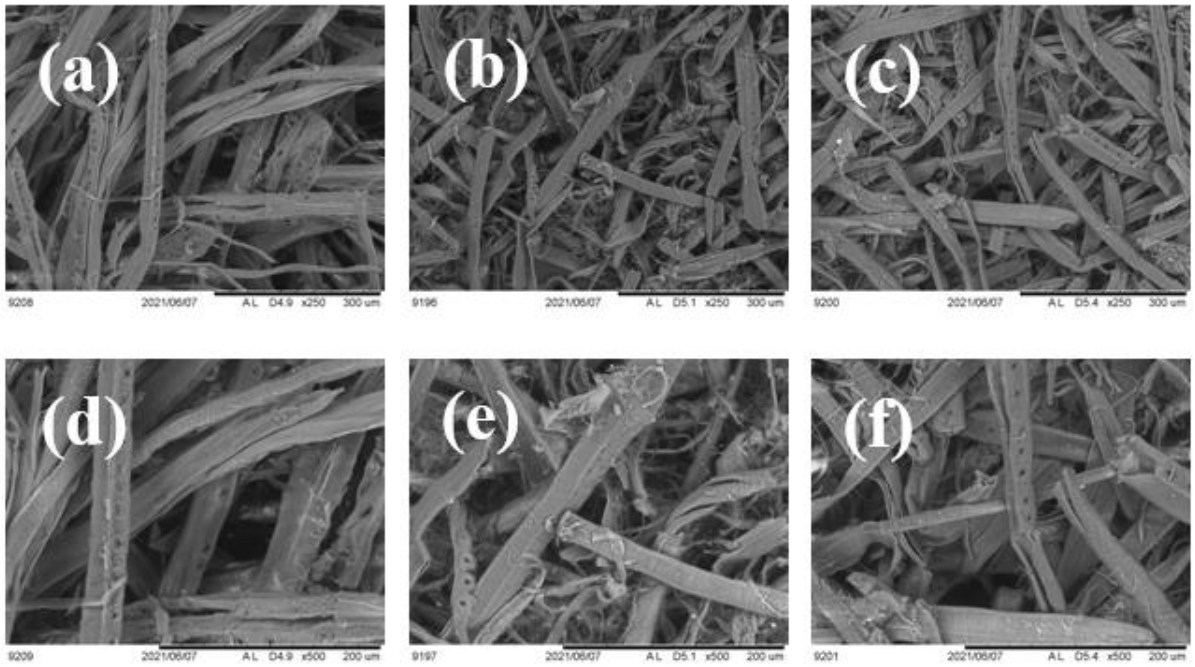

Fig. 4.2: SEM images of untreated newsprint (a), HCl-NP (b), and Fenton-NP (c) at ×250 magnification, and their corresponding images (d), (e), and (f) at ×500 magnification.

4.5.2 Preliminary analysis for HCl and Fenton-NP conversion to LA

Prior to the experimental design, 0.15 M of $FeCl_3.6H_2O$, 20-wt% of LiCl, and a combination of $FeCl_3.6H_2O$/LiCl were screened as catalysts for the conversion of NP to LA. The analysis was carried out in duplicate in batch reactors loaded with 5 mg and 30 mg of NP, respectively. Each of the reactors was heated in an oil-bath at a temperature of 190 ^oC for 100 min. LA was not detected for the reactors with 5 mg of NP. This is probably due to the low starting quantity of NP, which resulted in a LA concentration below the detection limit of the HPLC. The reactor with 30 mg of NP afforded LA in the order of 24.5 mol%, 29.5 mol%, and 33.7 mol% from LiCl, $FeCl_3.6H_2O$, and $FeCl_3.6H_2O$/LiCl catalytic systems, respectively. Since the combined effect of $FeCl_3.6H_2O$ and LiCl was explicit for NP conversion, the reaction system ($FeCl_3.6H_2O$/LiCl) was then selected for LA production. To upgrade the catalytic system and improve the LA yield, the $FeCl_3.6H_2O$: LiCl ratio was modified from 1:1 to 3:1. Subsequently, other reactions were performed using a constant amount of LiCl (20 wt%) while varying the $FeCl_3.6H_2O$ concentration. The amount of NP inserted into the reactor was also reduced from 30 mg to 20 mg, possibly reducing the mass transfer limitation. At a longer reaction time (6 h), the LA yield was improved significantly (56 mol%). Furthermore, the LA yields for two different concentrations of $FeCl_3.6H_2O$ (0.15 M and 0.325 M) were investigated at reaction times of 4 h, 5 h, and 6 h. As shown in Fig. 4.3, the use of $FeCl_3.6H_2O$ at a concentration of 0.15 M led to a LA yield of about 72 mol% after 4 h of reaction. Therefore,

the following reaction conditions were selected to design the experiments: temperature (180 - 200 °C), reaction time (3.5 - 4.5 h), $FeCl_3.6H_2O$ (0.1 – 0.2 M) and a constant concentration of LiCl (20 wt%).

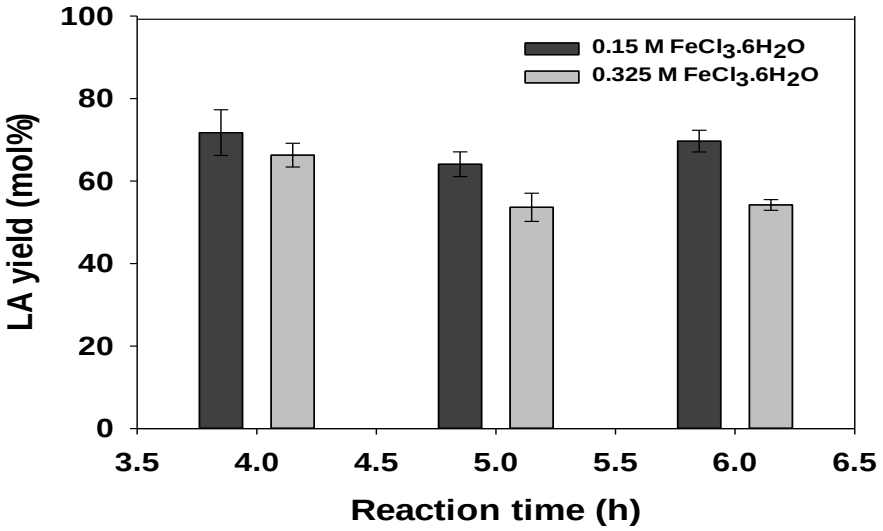

Fig. 4.3: Preliminary study of LA synthesis from NP using different concentrations of $FeCl_3*6H_2O$ at a temperature of 190 °C.

4.5.3 Optimization of LA yield from newsprint pretreated with HCl and Fenton Reagent

BBD (17 experiments) and RSM were employed to study how temperature, reaction time, and $FeCl_3.6H_2O$/LiCl concentration can improve the LA yield. The study was performed by applying the same process parameters for the conversion of HCl and Fenton-NP to various products (LA, HMF, and FU) as reported in Table 4.2. To model the system behavior accurately, logit transformation was used to reduce the ratio of maximum to minimum response. While values for the lower bounds of LA yields are selected as 29 mol% and 33 mol% for the HCl and Fenton- NP respectively, an upper bound of 100 mol% was used for both, being the maximum yield of LA to expect.

The polynomial expressions as obtained from the experimental data are represented accordingly (Eq. 4.13 and 4.14).

$$\text{Logit}(Y_1) = \ln(Y_1\text{-}29.00)/(100.00\text{-}Y_1) = -548.92 + 5.01X_1 + 15.09X_2 + 351.58X_3 - 0.09X_1X_2 - 1.75X_1X_3 + 15.36X_2X_3 - 0.01X_1^2 + 0.19X_2^2 - 233.30X_3^2 \quad (4.13)$$

$$\text{Logit}(Y_2) = \ln(Y_2\text{-}33.00)/(100.00\text{-}Y_2) = -459.10 + 4.36X_1 - 2.20X_2 + 411.49X_3 - 0.01X_1X_2 - 2.35X_1X_3 + 14.29X_2X_3 - 0.01X_1^2 + 0.27X_2^2 - 36.85X_3^2 \quad (4.14)$$

Where Y_1 and Y_2 are the LA yields as a function of temperature (X_1), reaction time (X_2), and $FeCl_3.6H_2O$ concentration (X_3) for the HCl and Fenton-NP.

Table 4.2: Experimental design and results for the conversion of HCl and Fenton-NP to LA

Run	Temp (°C)	Time (h)	$FeCl_3$ (M)	HCl-Pretreated NP			Fenton-Pretreated NP		
				LA (mol%)	HMF (mol%)	FU (mol%)	LA (mol%)	HMF (mol%)	FU (mol%)
1	200	4.0	0.10	78.0	0.9	5.3	89.1	1.5	5.9
2	190	4.0	0.15	68.7	2.0	3.7	60.3	2.1	3.0
3	200	4.0	0.20	66.0	0.1	0.7	70.9	0.2	0.8
4	190	4.0	0.15	63.1	2.3	4.5	74.3	2.2	4.4
5	190	3.5	0.10	53.3	2.7	9.5	59.8	3.8	11.4
6	180	4.0	0.10	29.8	2.0	11.2	33.5	2.3	9.3
7	190	4.0	0.15	71.0	2.2	4.6	57.2	1.7	2.7
8	180	4.0	0.20	40.3	1.9	1.8	45.2	2.2	1.5
9	190	4.0	0.15	75.1	2.5	5.7	74.6	2.3	4.5
10	190	4.5	0.20	82.4	0.9	1.9	82.5	1.1	2.1
11	200	3.5	0.15	81.0	0.3	2.7	65.0	0.5	2.0
12	190	4.0	0.15	77.3	2.7	6.3	69.8	2.1	3.9
13	180	3.5	0.15	33.7	1.9	5.9	36.1	2.3	5.0
14	180	4.5	0.15	43.0	2.2	5.1	43.1	2.0	3.0
15	190	3.5	0.20	56.0	1.1	1.6	68.5	0.6	1.3
16	190	4.5	0.10	54.2	2.5	7.6	52.2	2.7	7.2
17	200	4.5	0.15	70.0	0.1	1.8	82.8	0.1	1.6

The transformed data from the proposed model (Eq. 4.13) gave a R^2 and adjusted R^2 values of 0.97 and 0.94 for HCl-NP. The R^2 value shows that this model can explain 97.3% of the variability in the response. In addition, equation 4.14 gave a similar R^2 value of 0.96 with an adjusted R^2 value of 0.91 for the Fenton-NP.

Table 4.3 shows the ANOVA result for the Logit transformed data to test the significance of the regression model parameters. Values of $p < 0.05$ depict a significant model term. As such, the main effects of reaction temperature (X_1) and $FeCl_3.6H_2O$ concentration

(X_3) with p-values of <0.0001 and 0.0065 (for HCl-NP) as well as <0.0001 and 0.0120 (for Fenton-NP) were significant for LA production. Additionally, two interactive effects comprising temperature in combination with time (X_1X_2) and catalyst concentration (X_1X_3) and the quadratic effects of temperature (X_1^2) and catalyst concentration (X_3^2) greatly improved LA yields from HCl-NP. Only the quadratic effect of temperature (X_1^2) and its combination with $FeCl_3.6H_2O$ concentration (X_1X_3) positively affected LA yield for the Fenton-NP. While the above analysis shows that, the proposed models are suitable for representing the experimental data, the reaction time for both HCl and Fenton-NP were insignificant, suggesting that the LA yield may increase even for a prolonged time.

Table 4.3: ANOVA results for the logit-transformed data of LA yields from NP pretreated with HCl and Fenton reagent

ANOVA results				
Factors	HCl pretreated NP		Fenton pretreated NP	
	F-test	P-value	F-test	P-value
Model	27.72	0.0001*	19.60	0.0004*
X_1	143.78	<0.0001*	112.64	<0.0001*
X_2	4.52	0.0710	4.70	0.0668
X_3	14.67	0.0065*	11.32	0.0120*
X_1X_2	7.01	0.0330*	0.0246	0.8799
X_1X_3	23.11	0.0020*	25.49	0.0015*
X_2X_3	4.43	0.0733	2.36	0.1686
X_1^2	38.82	0.0004*	19.42	0.0031*
X_2^2	0.07	0.7987	0.0880	0.7753
X_3^2	10.77	0.0135*	0.1650	0.6968

*significant variables, NP = newsprint.

Fig. 4.4 shows the interactions of the response surface with the corresponding contour plots among the three variables on LA yields. All the interactions for temperature in combination with time and catalyst concentration showed a better curvilinear relationship. The following are the mid-point values of the independent variables applicable to both substrates: temperature (190 ^oC), reaction time (4 h), and $FeCl_3.6H_2O$ concentration (0.15 M). In Fig. 4.4 (a & d) (with $FeCl_3.6H_2O$ = 0.15 M), the predicted LA yield of 42.7 mol% from HCl-NP is higher than 39.6 mol% of LA from Fenton-NP at 180 ^oC for 4.5 h (run 14). When the temperature increased to 200 ^oC at a reduced time of 3.5 h, the product yield increased further, much in favor of HCl-NP with a LA yield of 81.5 mol% (run 11).

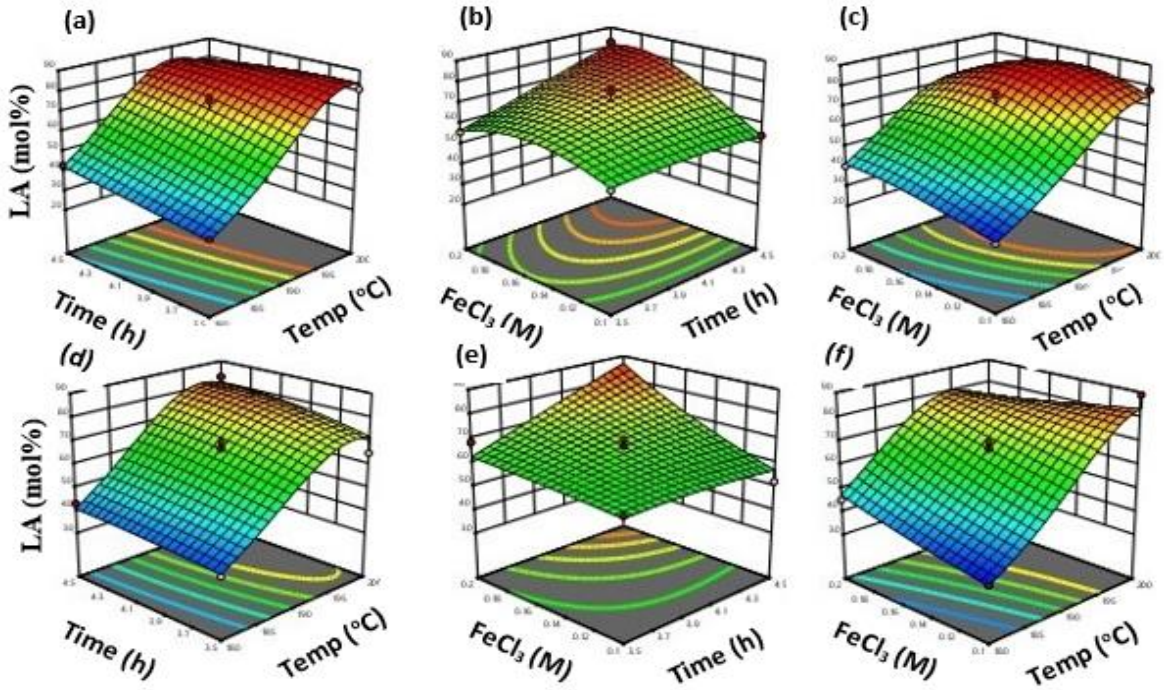

Fig. 4.4: RSM plots of LA yields against different variables from HCl (a-c) and Fenton (d-f) pretreated newsprint

Fig. 4.4 (b & e) highlights the effects of varying reaction time and $FeCl_3.6H_2O$ concentration, at a constant reaction temperature of 190 ^oC. As observed, the LA yield increased gradually over time, starting from a low $FeCl_3.6H_2O$ concentration (0.1 M) and reaching a yield of 55.4 mol% for the HCl-NP (run 5). The Fenton-NP afforded LA in yield of 57.3 mol%, representing a slight increase of about 3.41%. As $FeCl_3.6H_2O$ increased to 0.2 M, the LA yield from HCl and Fenton-NP were reported as 59.0 mol% and 63.3 mol% for a reaction time of 3.5 h (run 15). Continuously increasing the reaction time was advantageous, affording LA yields of 80.4 mol% and 84.1 mol% (run 10). These high yields of LA from both substrates could be due to the following: (1) high activity of the catalytic system ($FeCl_3.6H_2O$/LiCl); (2) high surface area of the HCl, and Fenton-NP.

In Fig. 4.4 (c & f), the interaction between reaction temperature and $FeCl_3.6H_2O$ concentration was examined at a reaction time of 4 h. The combination of the highest temperature (200 ^oC) and the lowest $FeCl_3.6H_2O$ concentration (0.1 M) gave LA yields of 74.8 mol% and 84.5 mol% (run 1). The improved LA yield could be due to the positive interaction between both variables for the two forms of pretreated NP. As expected, increasing the $FeCl_3.6H_2O$ concentration at 200 ^oC was not beneficial, decreasing the LA yields to 64.6 mol% and 72.6 mol% for HCl and Fenton-NP, respectively. It has been suggested that an increase in catalyst concentration could improve the rate of NP hydrolysis [292]. A negative side to this is the polymerization reaction between intermediate products, restricting the LA yield and

increasing humins formation [326]. Overall, the effective hydrolysis of NP to LA was observed to be a trade-off between reaction temperature, time, and catalyst concentration [327]. With the temperature range (180 – 200 ^{o}C) selected for this study similar to a previous study [328], the reaction time (3.5 – 4.5 h) is quite long. A justification for this could be due to the nature of the catalytic system ($FeCl_3.6H_2O$/LiCl), which when compared to a catalyst such as HCl (with pKa = -4.04 to -3.46) [329], requires a longer time to interact with the NP.

The quadratic model used to fit the experimental data was employed to predict LA yield from HCl and Fenton-NP under conditions of reaction temperature, time, and $FeCl_3.6H_2O$ concentration. The optimum conditions for conversion of HCl-NP and Fenton-NP were as follow: reaction temperature of 200 ^{o}C, reaction times of 3.63 and 3.50 h, and $FeCl_3.6H_2O$ concentrations of 0.118 and 0.100 M. Under these conditions, the predicted maximum yields of LA were 83.4 mol% and 86.4 mol %, respectively. This showed that the optimal conversion of HCl and Fenton-NP occurred at different processing conditions.

Following these conditions, two parallel tests performed on hydrolysis of HCl-NP and Fenton-NP afforded actual LA in yields of 81.3 mol% and 84.0 mol%, respectively. The percent error between the actual and predicted values of LA yield was calculated as 2.50 % and 4.49 %, respectively. Therefore, the empirical models developed were reasonably accurate, especially for HCl-NP. This shows that RSM is somewhat of a useful tool to predict and optimize the synthesis of LA from NP.

Another product detected alongside LA is FU, confirming the presence of C5 sugars in the newsprint. It is well known that furfural can be produced from hemicellulose under milder reaction conditions as compared to conditions for LA synthesis from cellulose [326]. In this study, the low FU yield detected by HPLC analysis can be due to the smaller hemicellulose fraction of the NP. In addition, the severity of the conditions under which cellulose in NP was converted could accelerate humin formation from hemicellulose, which then hinders the formation of FU [330]. In a recent study, FU was detected in low yield (7.3 mol%) at optimum conditions for the conversion of NP to LA (79.7 mol%) using HCl as a catalyst [311]. For this study, the highest FU yields for HCl and Fenton-NP were 11.2 mol% and 11.4 mol%, respectively.

4.6 Kinetic study

4.6.1 Degradation products of newsprint conversion

As mentioned above, glucose, HMF, and LA are the major degradation products of newsprint conversion under an aqueous acidic solution. At first, the cellulosic fraction of the newsprint hydrolyzes, forming glucose at the selected reaction conditions. The temperature dependence of the reaction is obvious for the three selected temperatures, where the HCl and Fenton-NP at 180 ^{o}C afforded maximum glucose yields of 48.2 and 50.8 mol%, respectively. More than 45 mol% of the cellulosic residues were observed for the newsprint heated at 180 ^{o}C even after a prolonged reaction time of 240 min. At elevated temperatures of 190 and 200 ^{o}C, cellulose degradation was enhanced such that merely about 30 mol% and 20 mol% of cellulosic residue remained after 240 min of reaction. This notable increase in cellulose hydrolysis is due to temperature adjustment, leading to a decrease in cellulose crystallinity. According to Yan et al., a complete dissolution of cellulose was possible at 200 and 220 ^{o}C for only 30 and 10 min respectively, using 1 wt% of H_2SO_4 as a catalyst [331]. Xiang et al. also demonstrated that increasing temperature could enhance the hydrolysis of cellulose to glucose with 0.07 wt% H_2SO_4 [332]. In all cases, the HMF yields were low since it is an intermediate that is rapidly converted into LA. Fig. 4.5 presents the yield of LA as a function of reaction time from HCl and Fenton-NP at different temperatures. All runs were conducted in duplicate, with the standard deviation being $\leq$ 9.5. At the studied temperatures (180-200 ^{o}C), the LA yield from the Fenton-NP was higher than from the HCl-NP. Furthermore, the condition that gave the maximum LA yield from Fenton-NP also afforded a high yield that is only about 0.52% lesser than the maximum yield from HCl-NP. When untreated NP was hydrolyzed at this condition, a LA yield of 69.4 mol%, representing a decrease of 15.70 % and 20.16 % from HCl and Fenton-NP respectively, revealed that pretreatment is of significance for the hydrothermal conversion of NP to LA.

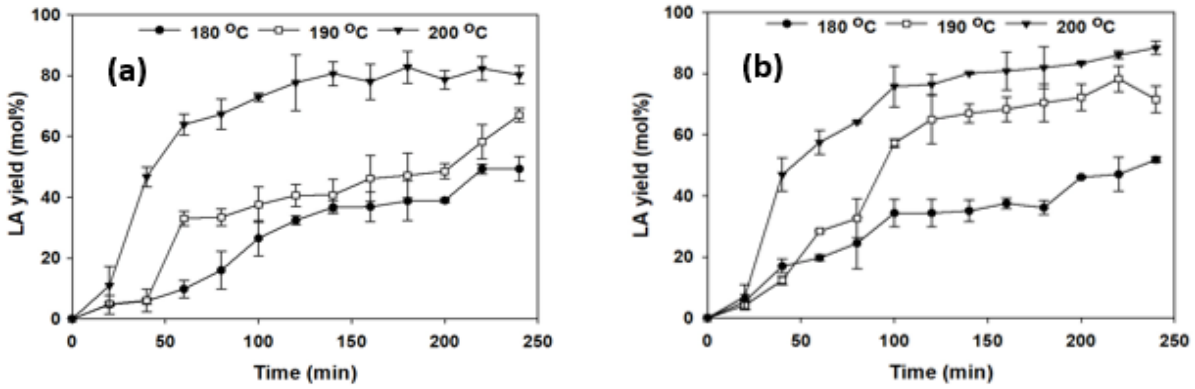

Fig. 4.5: Experimental LA yields versus time at three different temperatures for (a) HCl-NP and (b) Fenton-NP degradation. Conditions: 0.15 M $FeCl_3.6H_2O$, 20-wt% LiCl, and 20 mg of substrate.

As the temperature increased from 180 to 200 ^{o}C, the maximum LA yield increased from 49.3 to 82.8 mol%, and from 51.8 to 88.4 mol% for the HCl and Fenton pretreated NP, respectively. Since the reaction rate is a function of temperature, the time to attain maximum LA yield is shortened with increasing temperature. For instance, at 120 min, both Fenton and HCl-NP heated at 200 ^{o}C gave high LA yields above 70 mol% such that there was no significant change in the LA yield at a longer reaction time. One demerit of the increasing reaction temperature is that it could accelerate the occurrence of side reactions, leading to a decrease in LA yield. At 180 ^{o}C, the LA yield increased and could only reach around 50 mol% at a reaction time of 240 min. This shows that LA production from NP depends more on temperature than reaction time. On the contrary, Girisuta et al. performed a study where LA yield decreased from 61% at 150 ^{o}C to 42 % at 200 ^{o}C [168]. The difference between both studies may be due to the following: (1) the effect of pretreatment that could enhance the depolymerization of the NP to LA, (2) the lesser amount of NP (20 mg) used, and (3) the flexibility of the paper type due to the rigorous processing steps during papermaking.

4.6.2 Kinetic modeling of LA synthesis from HCl and Fenton pretreated newsprints

Fig. 4.6 depicts the experimental and fitted curves of NP degradation products as described by the kinetic model in section 4.4.5. The resulting set of rate equations (4.6-4.9) was simultaneously solved using the LSQCURVEFIT function from the optimization toolbox of MATLAB (R2020b) to generate the kinetic parameters (Table 4.4).

As observed, the values of the reaction rate constants ($k_{1\text{-}5}$) increase with temperature rise, suggesting the significance of high temperatures in enhancing the hydrolysis of NP to LA. Noteworthy, the values of k_1/k_G are less than 1, showing that the rate constant of glucose degradation is higher than for cellulose depolymerization. From the kinetic scheme in Fig. 4.1, improving the LA yield depends on the values of k_1, k_2, and k_4. Table 4.4 shows that most values of k_1 are smaller when compared to k_2 or k_4, showing that the hydrolysis of the NP to glucose is most likely the rate-limiting step. Except for the NP heated at 200 ^{o}C, the values of k_2 were lower than k_4, explaining the rapid rate of HMF rehydration to LA, which is higher than the transformation of glucose to HMF.

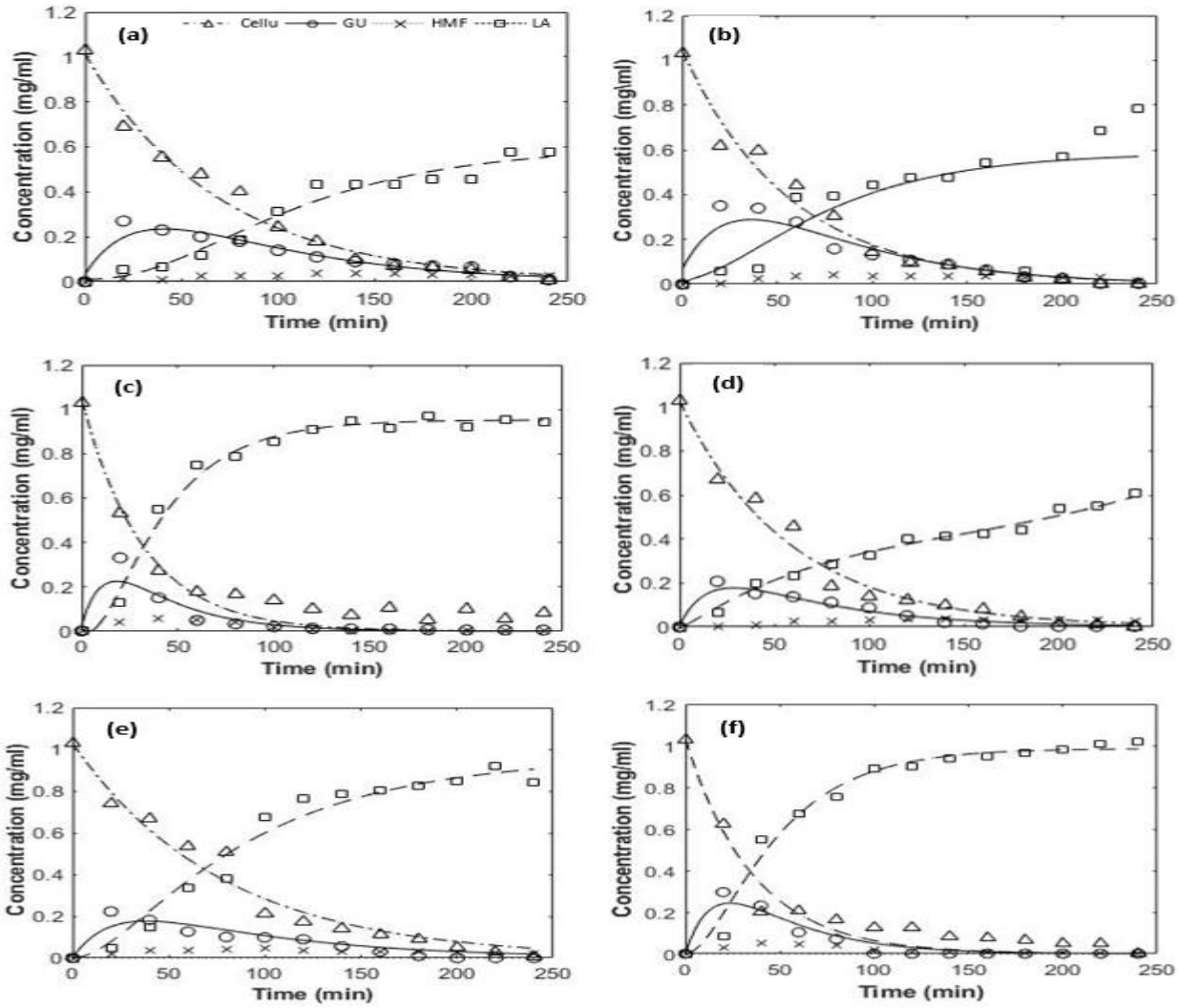

Fig. 4.6: Concentration-time plots for HCl-newsprint degradation products at (a) 180 °C, (b) 190 °C, and (c) 200 °C, a representation of Fenton pretreated newsprint (d, e, and f). Reaction conditions: $FeCl_3.6H_2O$ = 0.15 M, LiCl = 20 wt% and substrate amount = 20 mg.

Table 4.4: Kinetic rate constants (min^{-1}) for LA production from HCl and Fenton pretreated newsprints

Parameters	180 °C		190 °C		200 °C	
	HCl-NP	Fenton-NP	HCl-NP	Fenton-NP	HCl-NP	Fenton-NP
k_1	0.99940	0.01697	1.00114	0.81358	3.15964	2.29936
k_2	1.69223	0.02223	2.02649	0.52623	3.28162	4.22070
k_3	0.93431	0.03488	1.59515	0.35621	2.23562	1.13622
k_4	1.71429	0.16094	2.29918	0.94195	2.57788	1.13159
k_5	0.61189	0.03989	1.03019	1.01395	2.83561	17.0000
k_G	2.6254	0.05711	3.62164	0.88244	5.51724	5.35692
k_{HMF}	2.32618	0.20083	3.32937	1.9559	5.41349	18.13159

Despite not being the rate-limiting step, values of k_{HMF}, which are about 1.7-11.3 and 1.3-9.0 times greater than those of k_1 and k_2 respectively, can enhance the LA yield. k_3 and k_5 are the terms for the side reactions yielding humin and other by-products (Fig. 4.1). The high value of k_5 at 200 ^oC confirms the ease of humin formation, which did not impede the yield of LA (from Fenton-NP) in the reaction solution. Other values of k_5 and k_3 are comparable to those of k_2 and k_4 being terms for the main reaction. This trend remained constant for the two forms of pretreated NP at different temperatures.

Table 4.5: Activation Energy values (kJ/mol) for the synthesis of LA from HCl and Fenton pretreated newsprints

Pretreatment	Ea_1	Ea_2	Ea_3	Ea_4	Ea_5	Ea_G	Ea_{HMF}
HCl-NP	10.18	58.79	77.83	36.45	136.25	66.07	75.14
Fenton-NP	438.99	467.92	310.99	174.71	539.50	405.02	401.05

According to the Arrhenius model (Eq. 4.12), the calculated activation energy (Ea) values for the HCl and Fenton-NP are reported in Table 4.5. All the Ea values for the Fenton-NP were higher than for HCl-NP, showing that the former is more sensitive to temperature. The higher Ea values for the Fenton-NP imply that more kinetic energy is required to break their bonds. This hydrogen bond network, which appears within the crystalline domain of cellulose, could be more closely compacted for the Fenton-NP than their HCl counterpart. It can be observed that the activation energy for k_1 is the least for HCl-NP, and among the highest for the Fenton-NP. This shows that the initial step in the degradation of the HCl-NP is less energy-intensive. The E_{HMF} value for the HCl-NP is higher than for the combination of the first two steps, suggesting the high-temperature dependence of the HMF degradation. On the contrary, the E_{HMF} value for the Fenton-NP was lower than E_1 and E_2, showing a higher degree of difficulty in hydrolyzing cellulose in addition to glucose degradation. Although high temperature favors LA yield, the high activation energy values for k_5 prove that a higher temperature will generate more humins. Therefore, a study for reaction temperature above 200 ^oC was not conducted.

4.6.3 Comparison with previous kinetic models

Table 4.6 presents some kinetic studies for the conversion of cellulose or lignocellulose to LA. From the literature, factors that could influence the broad range of Ea include substrate type, solvent system, catalyst, and reaction temperature [333]. For this study, pretreatments

prove to be another significant factor, affecting the overall degradation process of the cellulose in NP.

Table 4.6: Activation energies (kJ/mol) from cellulose and lignocellulosic biomass

Substrate	Temp (°C)	Ea_1	Ea_2	Ea_3	Ea_4	Ea_5	Ref
Cellulose	150-200	151.5	152.2	164.7	110.5	111.3	[168]
Bagasse	150-200	144.9	152.1	161.4	101.6	na	[334]
Corn cob	160-180	116.0	96.0	120.0	84.5	na	[335]
Cornstalk	160-200	77.6	93.3	94.0	42.9	na	[336]
Corn cob	170-190	48.2	46.0	57.0	76.3	67.3	[328]

na = not available

A comparison of the Ea values in Table 4.5 shows that the values for the HCl-NP largely correlate with those reported in the literature (Table 4.6). The only slight variation is that the HCl-NP with Ea_1 and Ea_4 as low as 10.18 and 36.45 KJ/mol (Table 4.5) as compared to literature reports (Table 4.6) depicts how rapid the cellulose and HMF are transformed into glucose and LA, respectively. On the other hand, Fenton-NP exhibits high Ea values. Since the crystallinity of the two pretreated NP differs, that could influence their heating profile, thus affecting their product formation by varying the Ea values of the different reactions. The idea that the Ea values for the HCl-NP are identical to those in literature (Table 4.6) is justifiable since most of these feedstocks might have been mildly pretreated using mineral acid prior to hydrothermal conversion. The lack of a previous kinetic model on Fenton-NP conversion to LA makes it difficult to compare its high Ea values with others.

4.7 Catalyst reusability

Several experiments regarding catalyst reusability were performed to test the sustainability of the $FeCl_3.6H_2O$/LiCl system (Section 4.4.5). Using THF as the extracting solvent, the recycled catalyst attained a LA yield of 77.3 mol% after the first recycle (Table 4.7). Further hydrolysis with the reused catalyst showed a continued decline in LA yield, with the fourth run yielding only about 20.0 mol% of LA. One justification for the drop in yield could be due to the miscibility of the THF that enabled the distribution of some of the catalysts to the organic phase [321]. This then reduced the activity of the resultant aqueous acidic solution needed for subsequent runs. Another issue of THF miscibility is the limited number of runs that could be achieved due to the reduction in the volume of the catalyst after each run. For the MIBK, the decrease in LA yield was about 8.2% from the first to the fourth run, which is lesser when compared to THF with a 75.5% decrease in LA yield for the same number of

runs. Since the MIBK appears to be more selective than THF, one more run was performed, affording LA in yield of 64.8 mol%, representing a slight decrease of only 2.6%. The use of MIBK for extraction shows that $FeCl_3.6H_2O$/LiCl can be used up to 5 times without a significant loss in LA yield.

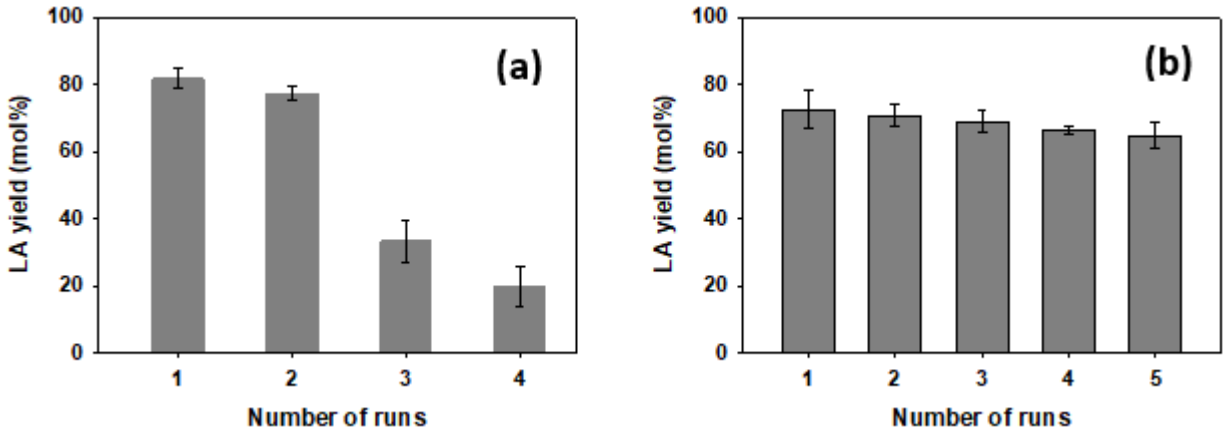

Fig. 4.7: LA yield obtained for catalyst recycling using: (a) THF and (b) MIBK as solvent. Reaction conditions: temperature = 200 °C, time = 100 min, $FeCl_3.6H_2O$ = 0.15 M, LiCl = 20 wt%, and substrate amount = 20 mg.

4.8 Proposed reaction pathway for newsprint degradation to levulinic acid

Based on the catalytic system ($FeCl_3.6H_2O$/LiCl) and the product distribution from this work, a reaction pathway for the depolymerisation of cellulose in Np was proposed. The hydrolysis of cellulose is enhanced in an acidic solution as displayed in the chemical equation that follows:

$$xFe^{3+} + yH_2O = Fe_x(OH)y^{(3x-y)} + yH^+ \quad (4.15)$$

As the Fe^{3+} dissociates into complex ions in an aqueous environment, they form a coordinate covalent bond with water, generating more H^+. The rise in H^+ with an increase in Fe^{3+} concentration can effectively degrade the glycosidic bond between the anhydroglucose units (AGU). The H^+ then diffuses into the amorphous region and surfaces of the crystalline region of cellulose to break the intramolecular glycosidic bonds. Other than physical swelling, the process causes chemical degradation that can enhance LA yield. Li et al. explained that cellulose in its crystalline region is more difficult to access due to its orderly packed structure [337]. Such differences in their structural arrangement could affect the selectivity during acid hydrolysis. The Fe^{3+} can increase the rate of acid hydrolysis in the amorphous regions [338]. Also, the high activity of cellulose is observed in the O(5) and C(2, 3, and 6) positions of the AGU. A plausible mechanism for the $FeCl_3$ catalyzed conversion of cellulose to LA in water is shown in Scheme 4.1 [339]. At first, oxygen readily adsorbs Fe^{3+} to form an annular

intermediate complex that will then increase the pyranose ring bond angle and bond length, and lower the activation energy of the reaction. The coordinated water molecules from the hydrated $FeCl_3$ act as a nucleophile to help break glycosidic bonds with the formation of glucose. During the glucose degradation process, the hydrated complex of $FeCl_3$ could facilitate the mutarotation of glucose from α-anomer to β-anomer through hydrogen bonds of Cl^- with the OH groups of glucose. Then, the hemiacetal portion of β-glucopyranose converts to an Fe(III) enolate anion complex that enables glucose-fructose isomerization prior to dehydration to HMF. HMF, being an unstable intermediate, rehydrates into LA.

Moreover, LiCl, an inorganic colorless salt, is expected to act as a co-promoter with $FeCl_3.6H_2O$ to produce LA from NP. LiCl, which easily dissolves in water, has a major influence on the reaction mechanism In a $FeCl_3.6H_2O$/LiCl solvent system, Cl^- bonds with the hydroxyl functional group of cellulose and form a new structure by replacing the OH…O bonds between cellulose with the O…Cl^- bonds [340]. With the original hydrogen bond network of cellulose crystalline lattice degraded, the solvating action of $FeCl_3.6H_2O$/LiCl improves, causing the molecular chains of the cellulose to be separated and dissolved.

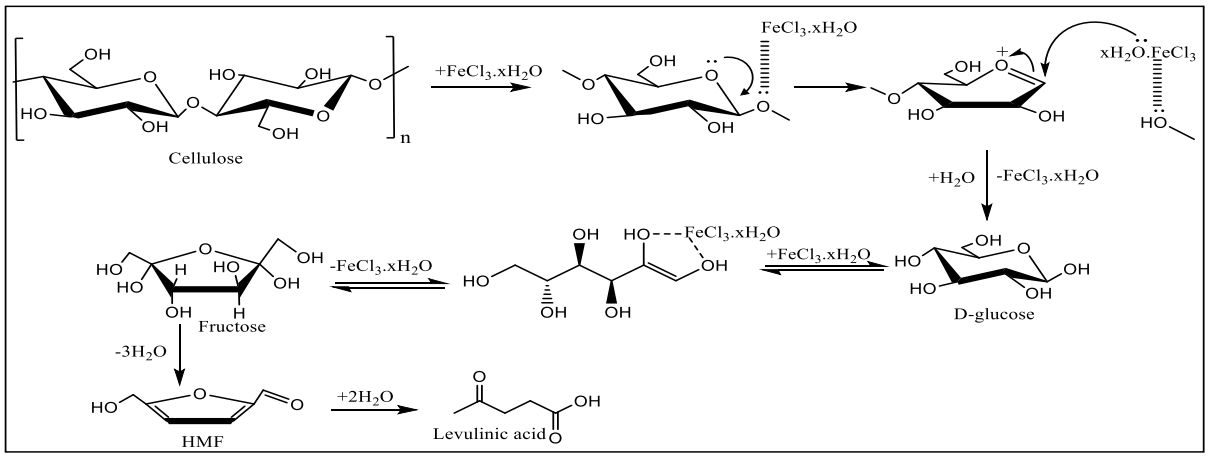

Scheme. 4.1: Reaction path for the conversion of the cellulose in newsprint to levulinic acid via $FeCl_3$

4.9 Conclusion

LA yields from the HCl and Fenton pretreated NP were optimized using the BBD at different ranges of temperature (180-200 ^oC), reaction time (3.5-4.5 h), $FeCl_3.6H_2O$ concentration (0.1-0.2 M), and a fixed amount of LiCl (20 wt-%). The optimum conditions for the conversion of the HCl and Fenton-NP are as follow: T = 200 ^oC, t = 3.63 α 3.50 h and [$FeCl_3.6H_2O$] = 0.118 α 0.100 M. The predicted maximum yields of LA were 83.4 mol% and 86.4 mol %, respectively. This revealed that the optimal conversion of HCl and Fenton-NP occurred at different process conditions. Following these conditions, two parallel tests

performed on hydrolysis of HCl-NP and Fenton-NP afforded actual LA in yields of 81.3 mol% and 84.0 mol%, respectively. This shows that RSM is somewhat a useful tool to predict and optimize the synthesis of LA from NP. In addition, a kinetic model was developed to understand the conversion process from cellulose to glucose, HMF, and LA. The results revealed that the Fenton-NP was more efficient during hydrolysis, affording a maximum LA yield of 88.4 mol% at 200 ^{o}C and 240 min. The study of the model's parameters and the interactive effects of temperature, time, and $FeCl_3.6H_2O$ concentration provided sufficient information to improve the LA yield from the newsprint.

SEM imaging showed that the HCl and Fenton newsprints shared some similarities with the untreated newsprints however; both are fluffy and shorter in appearance. The HCl pretreatment resulted in the peeling of the fiber's surface and could enhance hydrolysis and the Fenton-NP showed more and clearer pit than its untreated counterpart.

A recyclability test was performed using MIBK and THF as solvents to extract LA from the aqueous acidic solution of $FeCl_3.6H_2O$/LiCl. MIBK appeared to be more selective than THF for LA recovery such that the reuse of $FeCl_3.6H_2O$/LiCl was up to 5 times without a significant loss in LA yield.

Connecting Statement 3

The previous chapter provides a detailed comparison between HCl and Fenton pretreated newsprint. The RSM revealed that the optimal conversion of HCl and Fenton-NP occurred at different process conditions. In addition, a kinetic model was developed to understand the conversion process from cellulose to glucose, HMF, and LA. The results revealed that the Fenton-NP was more efficient during hydrolysis, affording a maximum LA yield of 88.4 mol% at 200 ^{o}C and 240 min.

While enzymatic hydrolysis remains a key step to sustainably transform newsprint to bioethanol, integrating this step toward the sustainable production of HMF and LA is still emerging and needs further research. Chapter 5 focused on the semisynthetic production of HMF and FU from untreated newsprint. Herein, a chemoenzymatic cascade process was established, starting with enzymatic hydrolysis of the newsprint to glucose and xylose, followed by aluminum-catalyzed dehydration to generate HMF and FU under mild reaction conditions. This chapter is an excerpt from the article published in the Journal of Environmental Chemical Engineering (2022), with permission from Elsevier. The article was co-authored by Dr. Marie-Joseé Dumont, Dr. Mario Pérez-Venegas, and Dr. Karine Auclair.

5 Semisynthetic production of hydroxymethylfurfural and furfural: The benefits of an integrated approach.

5.1 Abstract:

In this study, an integrated mechanoenzymatic/catalytic approach was employed to produce furan-based platform chemicals from newsprint wastes. The holocellulose fraction of the newsprint was first hydrolyzed to monosaccharides using a commercial cellulases blend at 55 ^{o}C (enzyme loading of 45 mg/g of substrate or 4.5% w/w). Working with a moist-solid enzymatic reaction with a short period (15 min) of ball milling followed by 24 h of static incubation greatly enhanced hydrolysis, affording glucose and xylose yields of 52 mol% and 22 mol%, respectively. The sugars in the hydrolysate were next dehydrated using $AlCl_3.6H_2O$ (200 mg) as an eco-friendly catalyst. With stirring at 600 rpm and 150 ^{o}C, hydroxymethylfurfural and furfural were obtained in yields of 66 mol% and 67 mol%, respectively. Another aspect was the first-order kinetic model with two consecutive reactions which was sufficient to predict the decomposition of sugars (glucose and xylose) into hydroxymethylfurfural and furfural, respectively.

Keywords: Cellulase; Mechanoenzymatic; Newsprint; Hydroxymethylfurfural; furfural; kinetic model.

5.2 Introduction

Biorefinery is recognized as a promising candidate to replace petroleum refinery. Biomass production has the advantage of fixing inorganic carbon through photosynthesis, thus reducing CO_2 emissions [341]. Lignocellulosic material, with an estimated annual production of 1 x 10^{12} tons, has the greatest potential for biorefinery development [342]. The conversion of biomass to platform chemicals is however challenging, in part due to the chemical recalcitrance, poor solubility, and limited access to its (major) cellulose component [343]. Paper waste (PW) is a lignocellulosic material that has undergone various treatment steps and is therefore significantly more reactive. With an estimated global production of 400 million tons in 2015, this inexpensive waste can serve as feedstock for the production of ethanol, as well as chemical building blocks such as hydroxymethylfurfural (5-HMF) and furfural (FU) [311, 343]. According to the US Department of Energy, furan-based derivatives are among the top twelve value-added chemicals from biomass [344]. For PW transformation, its holocellulose content (comprising cellulose and hemicellulose) can be hydrolyzed into C6 and C5 sugars before dehydration to yield 5-HMF and FU [345].

5-HMF is a multifunctional and versatile molecule that serves as a precursor for high-value chemicals such as 2,5-furandicarboxylic acid, 2,5-dimethylfuran, and levulinic acid [346-348]. The aromatic aldehyde, primary alcohol, and furan ring of 5-HMF allow its derivatization by way of a wide-range of reactions, including esterifications, oxidations, rearrangements, and condensations [349]. The simpler FU molecule can be used as a feedstock in the production of levulinate esters and biofuels such as 1, 5-pentanediol, and ɣ-valerolactone [350]. In addition, FU and furfural alcohol are used to make resins, either individually or in combination with phenol, acetone, or urea [351]. Notably, the FU derivatives 2-methyl furan, 2,5-dimethylfuran, and methyl tetrahydrofuran are primary components of biofuels [345]. These biofuels are known to have higher energy density and octane rating than conventional ethanol.

Earlier production methods of 5-HMF and FU from biomass employ strong acids at moderate to high temperatures [345, 352]. The drawbacks of these processes include reactor corrosion, generation of wastewater and unwanted products, and high-energy consumption. As a renewal, nontoxic, and selective catalyst active under mild reaction conditions, enzymes are gaining popularity in the development of more sustainable alternative methods. Herein, we investigated a chemoenzymatic process for the production of 5-HMF and FU from PW. Whereas saccharification by cellulases and hemicellulases has already found use in several industrial processes, enzymatic biomass transformation typically requires chemical pretreatment of the raw material to make the biopolymer more accessible to the enzymes.

The ability to use enzymes in solvent-free or moist-solid mixtures with gentle mechanical mixing (also known as mechanoenzymology) is an emergent area of research that is especially promising with poorly soluble substrates [353-358]. In this context, reactive aging, or RAging [359], a technique which involves static incubation with intermittent mechanical mixing, is rapidly gaining attention. Remarkably, enzymatic reactions in moist-solid mixtures treated to RAging were found to be more efficient and more selective than in typical dilute aqueous solutions or slurries, while avoiding the need for pretreatment of the raw material, as demonstrated for lignocellulosic biomass [342, 359-361], chitinous biomass [362], and even plastics [354]. It was envisaged that RAging could be harnessed for biorefinery development. To the best of our knowledge, this study represents the first insight into integrated mechanoenzymatic and catalytic approaches for newsprint conversion. Herein, we establish a chemoenzymatic cascade process starting with enzymatic hydrolysis of PW to glucose (Glc) and xylose (Xyl), followed by aluminum-catalyzed dehydration to generate 5-HMF and FU under mild reaction conditions.

5.3 Material and methods

5.3.1 Materials

Water from a MilliQ system with a specific resistance of 18.2 MΩcm at 25 ^{o}C was used for all sample preparations. The Cellic CTec2 cellulase blend (SAE0020) and high-performance liquid chromatography (HPLC) mobile phase comprising of HPLC-grade acetonitrile (ACN) (≥ 99.9%), HPLC-grade methanol (≥ 99.9%), and HPLC-grade water, were supplied by Sigma-Aldrich. Standards of glucose (99.5%), mannose (99%), galactose (99%), xylose (99%), arabinose (99%), purchased from Sigma Aldrich were used to calibrate the HPLC. Other reagents including formic acid and $AlCl_3.6H_2O$ were supplied by Sigma-Aldrich and used without further purification. Newspaper waste (PW) was sourced from a nearby supermarket and shredded to 15 mm × 4 mm pieces. Reagents such as hydrogen peroxide (H_2O_2), sodium dodecyl benzene sulfonate (SDBS), sodium hydroxide (NaOH), sodium silicate (Na_2SiO_3), and Triton^{TM} X-100 were purchased from Sigma-Aldrich and used to deink the PW.

5.3.2 Biomass preparation

Deinking was performed according to a method described by Nzediegwu et al. [311] and Lei et al. [293]. Briefly, the PW and the deinking agent comprising of 1.5 wt% NaOH, 3 wt% H_2O_2, 5 wt% Na_2SiO_3, 1.5 wt% SDBS, and 1.5 wt% Triton^{TM} X-100 solution were dissolved in 1000 mL of deionized water and soaked for 30 min inside a 2000 mL Erlenmeyer flask. The flask was vigorously shaken for about 30 min until its contents turned into a slurry. As the chemical agent and the shredded PW were mechanically agitated, the ink was disentangled from the pulp. This was followed by a continuous washing of the pulp with deionized water until the attainment of a neutral pH. The deinked pulps were then vacuum filtered to remove water followed by air-drying for about 24 h. The PW was then milled to a size of < 250 µm before storing it in a desiccator for further use.

5.3.3 Enzymatic and mechanoenzymatic hydrolysis of PW

The protein content of the Cellic CTec2 cellulases blend was analyzed using the Bradford method, and calculated to be 97.7 mg/mL [362]. The Glc contained in the cellulases preparation was quantified using HPLC and this amount was subtracted from all reaction product measurements. Xyl was not detected in the cellulases blend. Traditional in-solution enzymatic reactions were performed by adding 100 mg of PW and an appropriate amount of enzymes (45 mg/g) to make up 2 mL of the aqueous solution. Samples were collected in a 2.5 mL Eppendorf tube, then incubated at 55 ^{o}C with shaking at 180 rpm for a period of 24 h. After lyophilization, the samples were diluted in water (1 mL), vortexed (5 sec), sonicated (5 min),

and centrifuged at 21,100 g for 5 min. Next, the supernatant (200 µL) was heated to 100 ^{o}C for 5 min after the addition of 3, 5-dinitrosalicylic acid (DNS, 100 µL) to quantify reducing sugars. The color change from yellow to brown, as measured by UV-Vis spectroscopy (540 nm) was used to approximate the total amount of soluble sugars in the hydrolysate. HPLC analysis was also used to quantify the different sugars in the reaction solution (see section 5.3.5).

During enzymatic reactions in moist-solids, mechanical mixing was achieved with a ball mill (FormTech Scientific FTS1000 shaker mill from FormTech Scientific) set at a frequency of 30 Hz, using SmartSnap stainless steel jars (15 or 30 mL), containing two stainless steel balls (7 or 15 mm in diameter). Static incubation (or aging) was performed in an IsoTemp vented oven from Fischer Scientific set to 55 ^{o}C. A milling duration of 15 min was typical for most experiments, with a total reaction duration ranging from 1-7 days. All experiments were run at least in triplicates with the results presented as average with standard deviation.

5.3.4 Analysis of the chemical composition of newsprint samples

The cellulose and hemicellulose content of the PW samples was determined through the ANKOM filter bag technique using the ANKOM 200i fiber analyzer (ANKOM Technologies, Inc., Fairport, NY, USA). From each sample, 0.5 g of powdered PW was taken into the ANKOM fiber bags for subsequent digestion by the fiber analyzer [363]. The measured parameters were neutral detergent fiber (NDF), acid detergent fiber (ADF), and acid detergent lignin (ADL). The analyses were performed with the portion of hemicellulose (X_h = 16 wt%) calculated as NDF-ADF, whereas that of cellulose (X_c = 54 wt%) was obtained from ADF-ADL.

5.3.5 Enzymatic saccharification and quantification of the monosaccharide products by HPLC analysis

In most cases, the milling reactions were performed using 100 to 300 mg of PW in a 15 mL stainless steel jar equipped with two 7 mm stainless steel balls. The substrate was mixed with the CTec2 cellulases (4 to 60 mg per g of the substrate) diluted in the appropriate amount of H_2O (final reaction mixture η = 20 µL/mg). The reaction mixture was milled at 30 Hz for 15 min, homogenized, and weighed (25 mg) using a precision balance into an Eppendorf tube. The tubes were transferred to a vented oven set to 55 ^{o}C and incubated for 24 h. Following lyophilization of the sample, a known amount of water (1 mL) was added, followed by vortexing (5 sec), sonication (5 min), and centrifugation at 21,100 g for 10 min. The supernatant was collected by filtration (0.22 µm nylon filter, Chromspec, Brockville, ON, Canada). Glc and Xyl were quantified by HPLC with refractive index detection (RID) using an Agilent 1100

HPLC system. Separation was achieved using a Zorbax Carbohydrate analysis column (4.6 mm × 150 mm, 5 µm). While the column and the RID were set at an identical temperature of 30 ^{o}C, the mobile phase consisting of a blend of HPLC grade acetonitrile (ACN) and water (75:25) was applied in an isocratic mode. With the injection volume and flow rate given as 5 µL and 1.4 mL/min, the retention times for Glc and Xyl were 5.82 min and 4.67 min, respectively. The Glc and Xyl yields (Eq. 5.1 & 5.2) calculated from a calibration curve (concentration of pure analytes in the mobile phase against the areas displayed on the chromatogram) are given in mol%.

$$Glc\ yield\ (mol\%) = \frac{Weight\ of\ Glc\ produced\ (mg)}{Weight\ of\ newsprint\ fed\ \ (mg)} \times \frac{162\ g/mol}{180 g/mol} \times \frac{1}{X_c} \times 100\% \qquad (5.1)$$

$$Xyl\ yield\ (mol\%) = \frac{Weight\ of\ Xyl\ produced\ (mg)}{Weight\ of\ newsprint\ fed\ \ (mg)} \times \frac{132\ g/mol}{150 g/mol} \times \frac{1}{X_h} \times 100\% \qquad (5.2)$$

These equations take into account X_c and X_h, the cellulosic and hemicellulosic fractions of the PW, respectively (measured as in section 5.3.4). While 162 g/mol and 180 g/mol denote the molecular weights of anhydroglucose and Glc, 132 g/mol and 150 g/mol represent the molar masses of anhydroxylose and Xyl, respectively.

5.3.6 Conversion of glucose and xylose to 5-HMF and furfural

The Glc and Xyl mixture produced enzymatically from PW was next catalytically dehydrated by hydrothermal conversion using $AlCl_3.6H_2O$. In a typical experiment, the sugar mixture, catalyst, and an appropriate volume (4.5 mL) of a solvent blend comprising of H_2O and methyl isobutyl ketone (MIBK) (1:3 v/v) were placed in a 10 mL Pyrex tube reactor. MIBK was used to extract 5-HMF from the acidic aqueous solution *in situ* and prevent further reaction with water. It has also been reported in the literature that organic solvents like MIBK with inherent aprotic properties can improve product yield [364]. To initiate the conversion process, a magnetic stir bar was inserted into the reactor, which was fitted with a high-temperature seal and placed in an oil bath (130-150 ^{o}C) on a stirring hotplate (Thermo Fisher Scientific). A K-type thermocouple was used to monitor the temperature of the oil bath with a deviation of ± 1 ^{o}C. Once the reaction was completed, the tubes were removed before being immersed in an ice bath to quench the reaction. Partitioning the mixture between aqueous and organic phases allowed for the separation of the starting materials and products. After allowing the phases to separate, the organic layer was collected and filtered before HPLC analysis to quantify 5-HMF and FU after separation on a Phenomenex C-18 column (4.6 mm × 150 mm, 5 µm). The mobile phase was an isocratic 90:10 (v/v) mixture of HPLC-grade water and methanol, both containing

0.1% (v/v) formic acid. Detection was achieved using a variable wavelength detector (VWD) set to 267 nm. With the injection volume and flow rate of 5 µL and 0.6 mL/min respectively, the retention times for 5-HMF (Eq. 5.3) and FU (Eq. 5.4) were 5.85 min and 8.66 min, respectively.

$$HMF\ yield\ (mol\%) = \frac{Weight\ of\ HMF\ produced\ (mg)}{Weight\ of\ Glc\ fed\ (mg)} \times \frac{180\ g/mol}{126\ g/mol} \times 100\% \quad (5.3)$$

$$FU\ yield\ (mol\%) = \frac{Weight\ of\ FU\ produced\ (mg)}{Weight\ of\ Xyl\ fed\ (mg)} \times \frac{150\ g/mol}{96\ g/mol} \times 100\% \quad (5.4)$$

With respect to the above equations, 126 g/mol denotes the molecular weight of 5-HMF whereas 150 g/mol and 96 g/mol are those of Xyl and FU.

5.3.7 Kinetics studies

The reaction was performed in a biphasic media of H_2O: MIBK (1:3v/v) using 200 mg of $AlCl_3.6H_2O$ as the catalyst. The degradation of Glc and Xyl was investigated at temperatures ranging from 130 to 150 ^oC at different time intervals (0 to 100 min). Based on the experimental observation, a kinetic model (Eq. 5.5) was developed to describe the transformation of Glc and Xyl to 5-HMF and FU.

$$R_i \xrightarrow{k_{i1}} P_i \xrightarrow{k_{i2}} D_i \quad (5.5)$$

Whereas R_i is the reactant (Glc or Xyl) and P_i is the product (5-HMF or FU), D_i is the degradation product (mainly humins).

This model showed a similar degradation pattern for Glc and Xyl with the overall rate equation as below.

$$\frac{dR}{dt} = -k_{i1}[R_i] \quad (5.6)$$

$$\frac{dP}{dt} = k_{i1}[R_i] - k_{i2}[P_i] \quad (5.7)$$

where R_i depicts the concentration of Glc or Xyl while P_i shows that for 5-HMF or FU. The rate constants for each of the reactions are denoted as k_{i1} and k_{i2}, respectively. The temperature dependence of the reaction rate constant is described using the Arrhenius equation.

$$k = A\exp(-Ea/RT) \quad (5.8)$$

where k is the reaction rate constant, A is the frequency factor, and Ea is the activation energy.

5.4 Results and discussion

5.4.1 Enzymatic hydrolysis of the holocellulose content of PW

Prior to the enzymatic hydrolysis, the PW was deinked to increase its enzyme digestibility as well as reduce enzyme consumption [365]. Initially, the 3,5-dinitrosalicylic acid (DNS reagent) was used to quantify the concentration of reducing sugars in the reaction mixtures, allowing the rapid approximation of the reaction progress and optimization. Herein, the enzyme loading is given as the mass of protein added to the reaction mixture per mass of cellulose in the PW (mg of protein per g of the substrate). The activity of the Ctec 2 cellulases during PW hydrolysis was first tested under standard dilute aqueous conditions at 55 ^{o}C for 24 h at an enzyme concentration of 45 mg/g, affording a Glc yield of 27 mol%. Other than cellulases, this enzyme blend is also known to contain xylanases [342], which were found to hydrolyze the hemicellulose of PW to 11 mol% Xyl. Control depolymerisation of PW in water without enzyme did not generate Glc or Xyl. Next, the reaction was performed under mechanoenzymology at low enzyme loading (4 mg/g) and η = 20 μL/mg using a stainless steel jar fitted to a ball mill with 15 min milling at 30 Hz before static incubation at 55 ^{o}C for 24 h. Glc and Xyl in similar yields of 6 mol% were afforded. Next, the enzyme loading was optimized to further improve the yields under these conditions. During the experimental design, it was hypothesized that if the enzyme loading is gradually increased, there would be a point where the reaction rate would no longer increase as observed in Michaelis-Menten kinetics. The optimum enzyme loading was found to be 45 mg/g (Fig. 5.1), consistent with a previous report by Hammerer et al. [342]. At this enzyme loading, the Glc and Xyl yields were 47 mol% and 16 mol%, respectively, *i.e.* significantly higher than in standard dilute aqueous conditions. Beyond 45 mg/g, there is reduced sugar (Glc and Xyl) yields due to protein agglomeration at higher enzyme loading. This reduces the efficiency of enzymatic hydrolysis by limiting the contact between the enzyme and substrate [366].

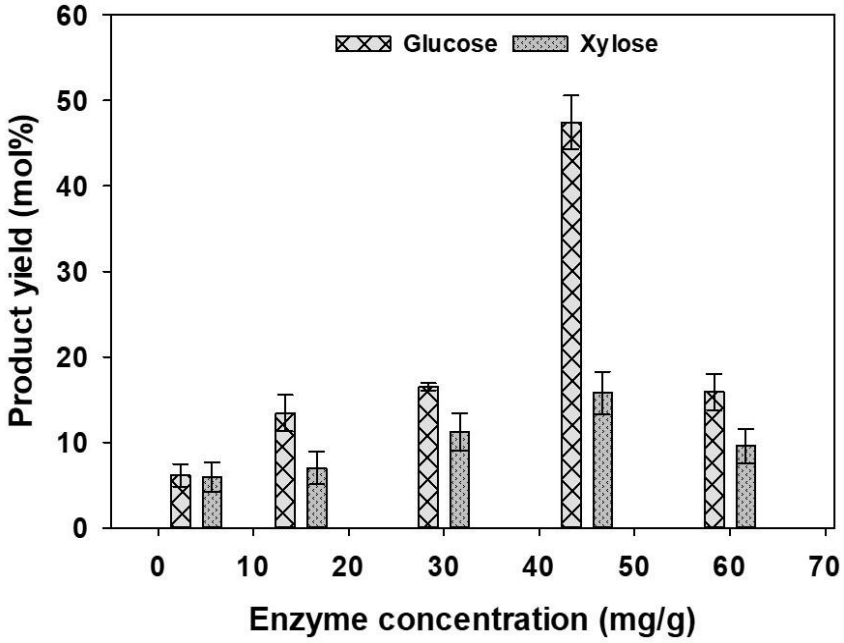

Fig. 5.1: Optimization of the enzyme loading for the conversion of PW to Glc and Xyl in moist-solid reaction mixtures. The reaction mixture consisted of 100 mg of PW, water (η = 20 µL/mg), and enzyme (4-60 mg/g), treated to ball milling once (15 min at 30 Hz) followed by static incubation at 55°C for 24 h. Reactions were performed in triplicates and the error bar is the standard deviation.

5.4.2 Impact of η-values on glucose and xylose yields from PW

In moist-solid reaction mixtures, the amount of water added to the mixture is typically defined as η, *i.e.* the volume of water added over the weight of solid substrate used in µL/mg. Under the liquid-assisted grinding (LAG) regime as defined in mechanochemistry [367], η is typically < 2 µL/mg, conditions previously shown to be optimal for cellulases [342, 359, 361]. Under such a regime, the water added was adsorbed completely, forming a moist-solid mixture that differed from a slurry or a solution. Our study was designed to capture a wider range of η, ranging between 1.5 to 20 µL/mg (Fig. 5.2).

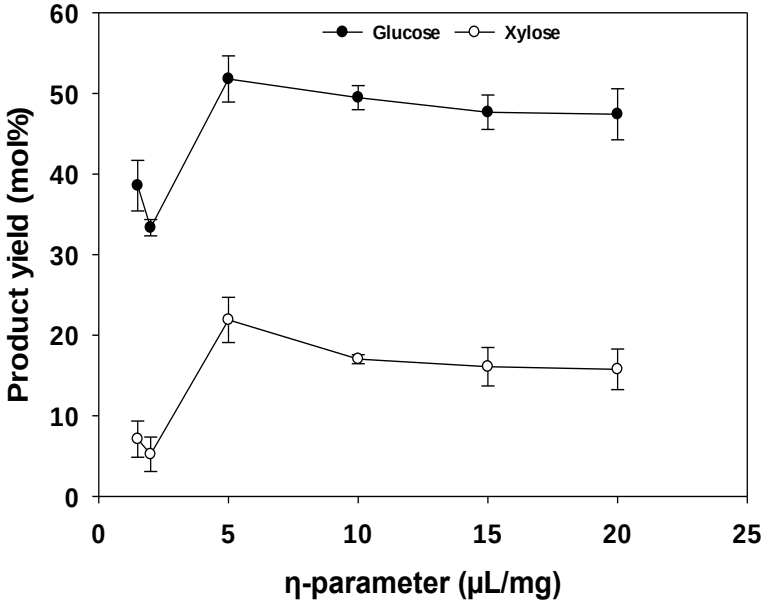

Fig. 5.2: Optimization of η for the enzymatic depolymerisation of PW holocellulose to Glc and Xyl. The reactions were performed in a stainless-steel jar equipped with two stainless steel balls, and the mixture consisted of 100 mg of PW, an appropriate amount of water (η = 1.5 to 20 μL/mg), and an enzyme loading of 45 mg/g, treated to ball milling once (15 min at 30 Hz) followed by static incubation at 55 °C for 24 h. Reactions were performed in triplicates and the error bar is the standard deviation.

An η = 1.5 μL/mg was previously reported to be optimal for *Trichoderma longibrachiatum* cellulases [342], which here gave a Glc yield of 39 mol%. This yield was further improved at η = 5 μL/mg (52 mol%) however, conditions that were also optimal of Xyl production (22 mol% yield). Further increase of the water content was not beneficial, and was even somewhat detrimental, with Glc yields of 48 and 47 mol% at η-values of 15 and 20 μL/mg, respectively. Therefore, η = 5 μL/mg was selected for subsequent experiments.

5.4.3 Effect of the milling jar material on the Glc and Xyl yields

Some factors often affect the optimization of mechanochemical reactions. These factors such as the number of milling balls and their diameters, weight, and density, as well as the shape and volume of the milling jar and its material are of significance [368]. Regardless, Halasz et al. posited that increasing the number of milling balls or their size can restrict movement and acceleration within the mill, thus causing a weak impact and insufficient mixing [368]. So far, all reactions in moist-solid mixtures involved ball milling in 15 mL stainless steel milling jars containing two stainless steel balls (7 mm). Considering that milling jars and balls of various materials may provide different reaction conditions, we next compared the yields of Glc and Xyl from reactions performed in stainless steel or in Teflon milling jars using either stainless steel or zirconia balls (Fig. 5.3). Recent studies have revealed a strong dependence of the reaction kinetics on the milling jar temperature [369]. This is peculiar to stainless steel

milling jars and may not apply to Teflon milling jars as its polymer lining has a poor heat transfer factor. In a typical mechanochemical operation where the ball mill heats up, the collisions of the milling balls also cause an increase in the temperature of the milling assembly [370]. The milling jar material also affects the elasticity of the collisions and the motion of the balls, influencing heat transfer from the balls to the wall of the jar. While temperature sensitivity is of particular interest during the kinetic study, the side-by-side coupling of the ball mill to a Raman monitoring setup is still emerging [371]. Moreover, whereas stainless steel is a harder (Vickers hardness = 2000 MPa) material with potential catalytic properties, Teflon is softer (Vickers hardness = 30 MPa) and more chemically inert [372]. Results from our study show that the reaction progresses to higher Glc yields in the stainless steel than in the Teflon jars, even when both are used with stainless steel balls. In stainless steel jars, the Glc yield reached 52 mol% after 24 h, and 54 mol% after 96 h. In contrast, in the Teflon jars, a 43 mol% yield of Glc was obtained after 24 h, compared to 51 mol% after 96 h. The production of Glc decreased when Teflon jars were used with zirconium balls (44 mol% after 1 week of reaction). In contrast, the production of Xyl was much less affected by the milling jar and ball types selected. The combination of stainless-steel jar and balls provided the highest yield (22 mol%) of Xyl after 24 h of incubation. Consequently, the stainless steel jar equipped with stainless steel balls was used in all subsequent experiments.

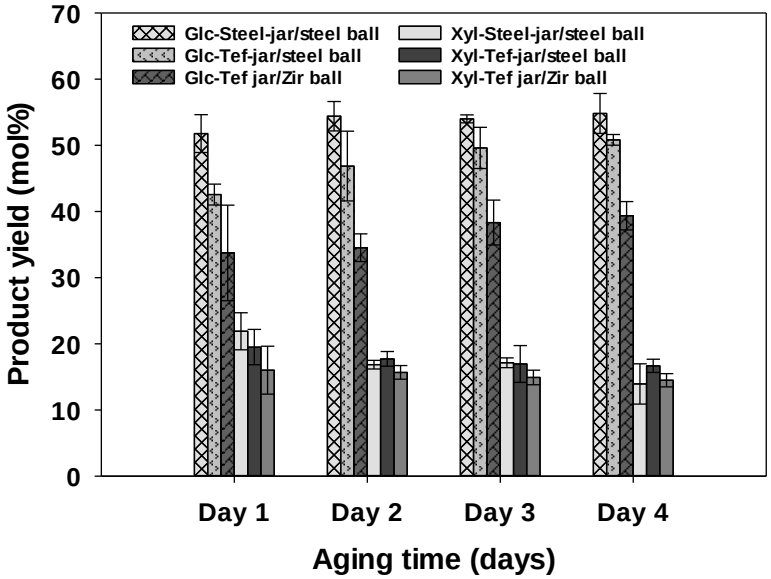

Fig. 5.3: Comparative study using jars and balls of different materials (Steel: stainless steel, Tef: Teflon, and Zir: zirconia) for the PW conversion to Glc and Xyl. The reaction mixture consisted of 300 mg of PW, water (η = 5 µL/mg), and an enzyme loading of 45 mg/g, together treated to ball milling once (15 min at 30 Hz) followed by static incubation at 55°C. Reactions were performed in triplicates and the error bar shows the standard deviation.

5.4.4 RAging conditions to enhance the yields of Glc and Xyl

To further increase the yield of PW saccharification, RAging conditions were explored next [342, 361, 362]. RAging involves intermittent milling of the reaction mixture, in between periods of static incubation. The RAging cycle can be optimized by varying the duration of the milling and the aging steps. Here, however, the RAging cycles were fixed to 5 minutes of milling and 55 minutes of static incubation based on previous studies that have demonstrated this regime to be optimal for cellulases [342, 359]. As observed in Fig. 5.4, the Glc yield was found to increase from one RAging cycle to another, although reaching only 38 mol% after 12 cycles (12 h). In this reaction, the Xyl yield was however only 13 mol%. Although RAging afforded lower yields of sugars than previous experiments, RAging was only performed for 12 h when earlier reactions lasted at least 24 h. To better understand the effect of RAging here, enzyme kinetics were performed.

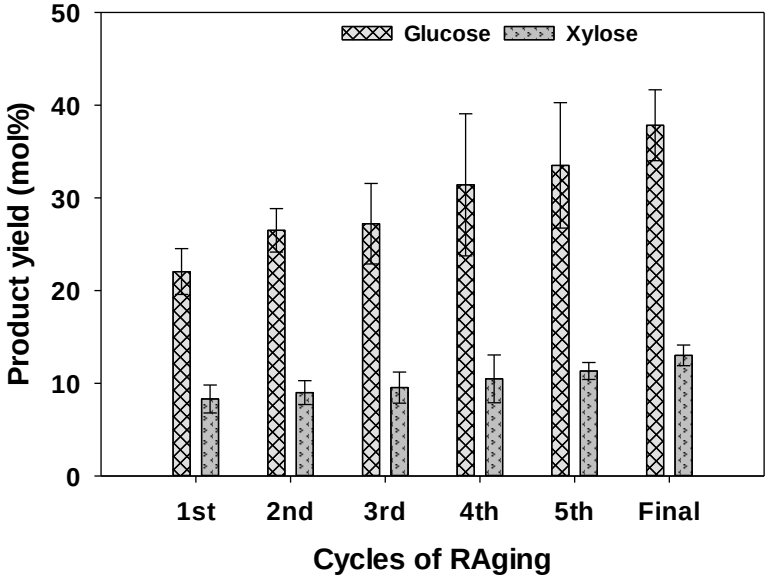

Fig. 5.4: Enzymatic PW depolymerization to Glc and Xyl in moist-solid reaction mixtures under RAging conditions. The reaction mixture consisted of 300 mg of PW, water (η = 5 µL/mg), and an enzyme loading of 45 mg/g, and was treated to 6 cycles of ball milling (5 min) and incubation (55 min) consecutively for a total of 12 h. Reactions were performed in triplicates and the error bars represent the standard deviation.

5.4.5 Evaluation of Glc and Xyl yields at different aging times

The kinetics of aging after 15 min of milling was studied to determine when the optimal yield was obtained (Fig. 5.5). After milling, the samples were allowed to incubate at 55 ^{o}C for different durations. As expected, the reaction showed a hyperbolic kinetic profile with a plateau in Glc yield being reached after ca. 24 h. The yield of Glc rose from 18 mol% after 30 min to 52 mol% after 24 h. Extending the incubation period to 48 h only provided a small yield

increase (54 mol%). It took one week for the Glc yield to reach 61 mol%. The yield of Xyl followed a similar trend, with a maximum 22 mol% reached after 24 h of incubation. Further increasing the incubation time was not beneficial. This result shows that xylanase is stable for 24 h of static incubation at 55 ^{o}C. Despite not using bulk water, analysis under a moist solid environment did not favor Xyl yield because enzymes of the same family like cellulases and xylanases can have different preferences for optimal activity. Under a solventless condition, the enzymatic hydrolysis of hemicellulose was consistent with the natural environment of xylanases, affording a high xylose yield (68 mol %), even after 72 h of incubation [361]. In summary, the solvent-less conditions can offer a more seemly platform for optimal performance of xylanase. For this study, Xyl is a minor product, which is consistent with the enzyme preparation being sold as a cellulases blend, not xylanases.

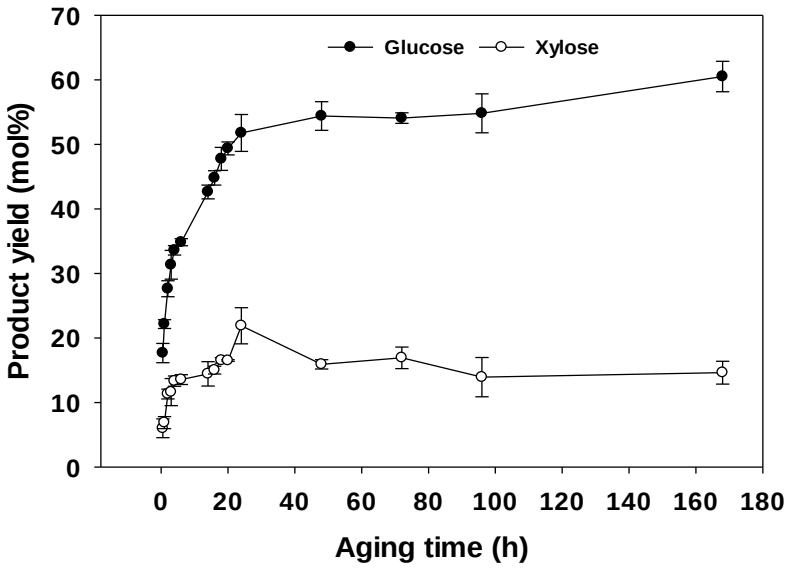

Fig. 5.5: Enzyme kinetics studies during aging for the enzyme-catalyzed saccharification of PW in moist-solid reaction mixtures. The reaction mixture consisted of 300 mg of NP, water (η = 5 µL/mg), with an enzyme loading of 45 mg/g, and treated to ball milling once (15 min at 30 Hz) followed by static incubation at 55 ^{o}C. Reactions were performed in triplicates and the error bar shown represents the standard deviation.

5.4.6 5-HMF and FU from the dehydration of the Glc and Xyl produced from mechanoenzymatic reactions

The catalytic conversion of Glc and Xyl for the co-synthesis of 5-HMF and FU were studied with varying amounts of $AlCl_3.6H_2O$. A sample from the crude mixture of Glc and Xyl (9 mg and 2 mg) obtained from enzymatic hydrolysis of PW was used as the substrate here. As shown in Figure 5.6, $AlCl_3.6H_2O$ was tested at 25 mg, 50 mg, 100 mg, 150 mg, 200 mg and 250 mg. Even with the lowest amount of catalyst (25 mg), Glc and Xyl were transformed to 5-

HMF and FU in yields of 4 mol% and 25 mol%, respectively. Increasing the catalyst loading was beneficial, with 200 mg affording the highest yield of 5-HMF (60 mol%), and 150 mg being optimal for FU (64 mol%). Beyond 250 mg of catalyst, the 5-HMF and FU yield decreased, as observed by Roy Goswami et al. [373] and Liu et al. [374] during starch hydrolysis by $AlCl_3.6H_2O$/DMSO/B[MIM]Cl. It has been suggested that excess $AlCl_3.6H_2O$ may induce additional side reactions [373]. An optimal concentration of 200 mg $AlCl_3.6H_2O$ was selected for further investigation.

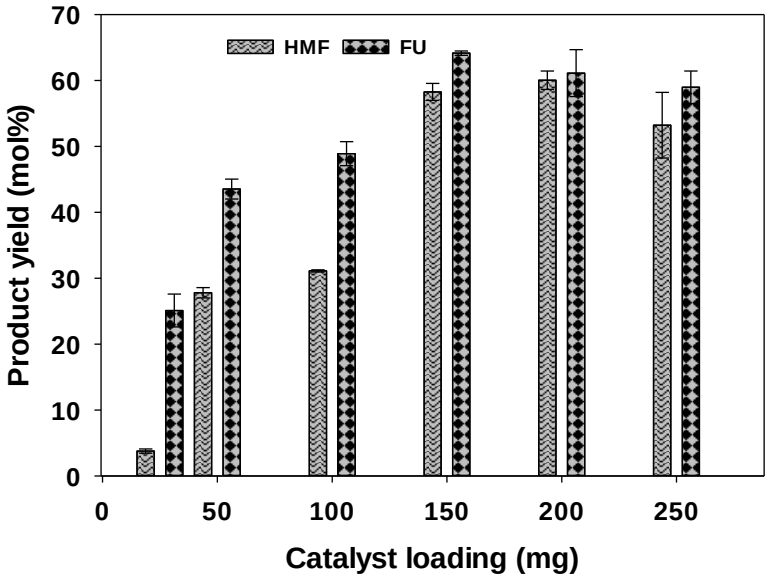

Fig. 5.6: Effect of catalyst ($AlCl_3.6H_2O$) loading on the co-synthesis of 5-HMF and FU from the crude Glc and Xyl produced from PW. The reaction mixture consisted of Glc (9 mg), Xyl (2 mg), and catalyst in 4.5 mL of H_2O/MIBK (1:3) at 140 °C for 60 min. Reactions were performed in triplicates and the error bars report the standard deviation.

5.4.7 Effect of reaction duration and temperature on the yields of 5-HMF and FU

Initially, the synthesis of 5-HMF and FU was studied under constant conditions (140 °C, 600 rpm, and 200 mg of $AlCl_3.6H_2O$), while varying the reaction duration from 10 to 100 min (Fig. 5.7). While the conversion to Glc was near completion in most experiments, only approximately half of the hemicellulose was cleaved to Xyl, as expected from the trace xylanases present in the commercial cellulases blend used. The yields of 5-HMF from Glc increased from 1 mol% at 10 min to a maximum of 63 mol% at 80 min, before decreasing to 57 mol% at 100 min, probably due to further transformation of 5-HMF to humins. The FU yield from Xyl followed a similar trend, starting from 5 mol% at 10 min and reaching 61 mol% at 60 min, and further increasing the reaction time to 100 min was detrimental, causing a decline in FU yield to 58 mol%.

It should be noted that levulinic acid was not detected in this study, most likely due to the mild reaction temperature (140 ^{o}C) selected and the reduced volume of water (1.125 mL) in the biphasic media. Two additional reaction temperatures (130 and 150 ^{o}C) were investigated. After 10 min at 130 ^{o}C, 5-HMF and FU were not detected. Increasing the duration to 20 min gave 5-HMF and FU yields of 2 mol% and 10 mol%, respectively. The 5-HMF and FU yields further increased to 41 mol% and 52 mol%, respectively, after 100 min. At 150 ^{o}C, the 5-HMF yield kept increasing from 12 mol% at 10 min, to a maximum of 66 mol% after only 40 min. Longer reaction times did not have a positive effect on the yield. Moreover, the brown color of the reaction solution after 40 min at 150 ^{o}C is indicative of humins formation. Therefore, higher temperatures were not tested. The FU yield at 150 ^{o}C rose from 30 mol% after 10 min of reaction to 67 mol% after 40 min, with a slight decrease after 100 min. The decline in FU yield could be due to its transformation to other compounds. During Xyl dehydration, undesired reactions including fragmentation, decomposition, condensation, and resinification have been reported to reduce the FU yield [375].

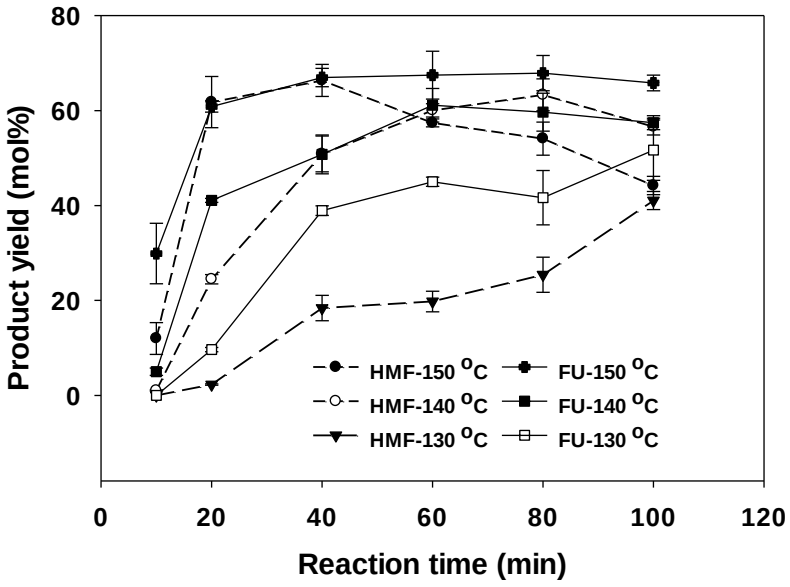

Fig. 5.7: Yields of 5-HMF and FU from a mixture of Glc and Xyl. The reaction mixture consists of Glc (9 mg), Xyl (2 mg), and $AlCl_3.6H_2O$ (200 mg) in 4.5 mL of H_2O/MIBK (1:3). Reactions were performed in triplicates and the error bar is the standard deviation.

5.4.8 Kinetic modelling for glucose and xylose degradation

Fig. 5.8 shows a typical concentration profile of compounds involved in the degradation of Glc and Xyl. The LSQCURVEFIT function from the optimization toolbox of MATLAB (R2020b) was used to integrate the rate equations (section 5.3.7), to generate the kinetic parameters (Table 5.1). The reaction temperature was varied to understand its effect on the kinetic parameters. The temperature had a strong influence on Glc consumption, seen from its

rate constant (k_{i1}). For instance, the value of k_{i1} increased from 0.00555 min^{-1} to 0.03114 min^{-1} as the temperature was increased from 130 to 150 ^{o}C. The same was observed during Xyl conversion with an increase in k_{i1}-value from 0.0169 min^{-1} to 0.02538 min^{-1}. A comparison of the observed rate constants of Glc dehydration and 5-HMF decomposition indicates that the former process was much faster. This was contrary to the dehydration of Xyl, with values of rate constant lower than that of FU decomposition, suggesting the high sensitivity of FU to temperature.

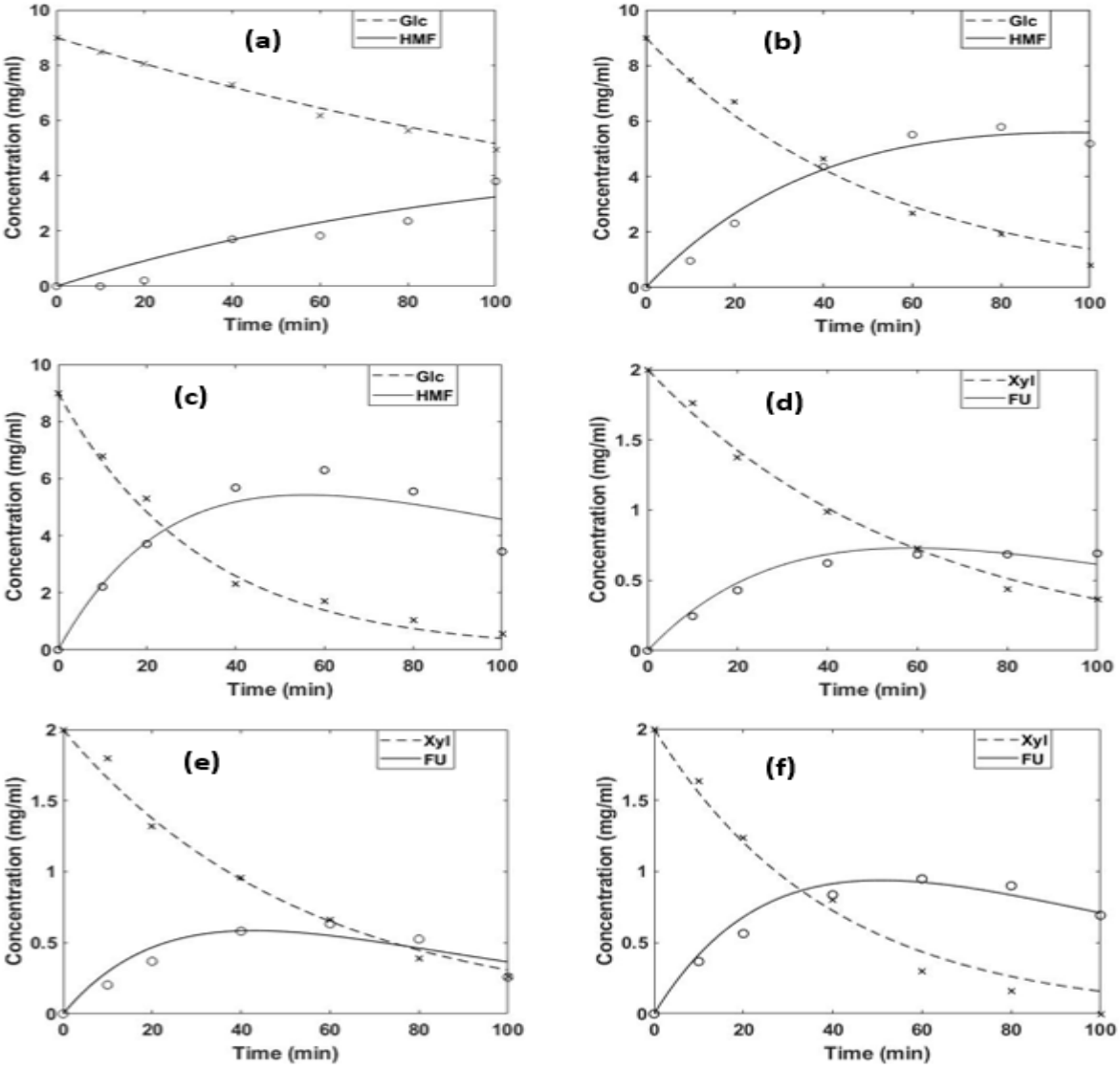

Fig. 5.8: Concentration-time graphs for glucose and xylose degradation at 130 ^{o}C (a & d), 140 ^{o}C (b & e), and 150 ^{o}C (c & f). The reaction mixture consists of Glc (9 mg), Xyl (2 mg), and $AlCl_3.6H_2O$ (200 mg) in 4.5 mL of H_2O/MIBK (1:3).

Table 5.1: Estimated rate constants (min^{-1}) for glucose and xylose conversion

Temperature (^oC)	Glucose		Xylose	
	k_{i1} (min^{-1})	k_{i2} (min^{-1})	k_{i1} (min^{-1})	k_{i2} (min^{-1})
130	0.00555	0.00319	0.01698	0.01721
140	0.01869	0.00492	0.01871	0.02865
150	0.03114	0.00904	0.02538	0.02990

The apparent activation energies (Ea) of the subreactions were deduced using the Arrhenius equation and presented in Table 5.2. The high Ea_{i1} value for the conversion of Glc (123 kJ/mol) indicates that the decomposition of Glc is favored at high temperatures. This value is comparable to that of Antal et al. [376] and Van et al. [377] who reported an Ea_{i1} of 100 kJ/mol and 114 kJ/mol from the dehydration of Glc. These values are higher than that reported by Qi et al. (74 kJ/mol) [378], who posited that the high acidity of their catalytic system might have promoted Glc conversion. The higher Ea_{i2} of 73.9 kJ/mol relative to 56-64 kJ/mol [379, 380] in water confirms the ease of 5-HMF decomposition in an acidic aqueous media. It has been reported that Glc dehydrates less rapidly than Xyl [381]. This is because Xyl (36.9 kJ/mol) expressed lower Ea_i for its dehydration compared to Glc (123.6 kJ/mol). The measured apparent Ea_i for FU decomposition is 39.3 kJ/mol. These values are more than two times lower than those reported in the literature. For instance, Lamminpää et al. reported the formic acid catalyzed Xyl degradation with estimated Ea_{i1} and Ea_{i2} values of 152 kJ/mol and 161 kJ/mol, respectively [382]. Similarly, the Ea_i calculated by Chen et al., was 108.6 kJ/mol and 105 kJ/mol for k_{i1} and k_{i2}, respectively, when acetic acid was employed for Xyl degradation in a high-pressured reactor [383]. Overall, the comparison of kinetic results with published literature is appropriate but challenging because of the discrepancies in experimental conditions.

Table 5.2: Activation energy values for glucose and xylose degradation

Rate constant (min^{-1})	Glucose		Xylose	
	Ea (kJ/mol)	A (min^{-1})	*Ea* (kJ/mol)	A (min^{-1})
k_{i1}	123.6	6.4×10^{13}	36.9	9.6×10^{2}
k_{i2}	73.9	1.2×10^{7}	39.3	2.2×10^{3}

5.4.9 Controlling water to optimize the production of 5-HMF and FU

Water is a product in the co-synthesis of 5-HMF and FU from Glc and Xyl. Acidic aqueous conditions are also known to lead to the decomposition of 5-HMF [384]. To further optimize the production of 5-HMF and FU, the amount of water was next optimized. The

reaction of Glc and Xyl in the presence of $AlCl_3.6H_2O$ (200 mg) in water only afforded low 5-HMF (1.5 mol%) and FU (13 mol%) yields (Table 3, entry 1). In contrast, the reaction in MIBK only was superior, with 2.4 mol% 5-HMF and 26 mol% FU (Table 3, entry 2), which are still low but about twice as high as in water alone, together showing that a monophasic media is not efficient for the co-synthesis of 5-HMF and FU. We next explored biphasic media comprising various ratios of water and MIBK (Table 5.3, entries 3-5). Whereas the 5-HMF yield followed the order MIBK:H_2O (3:1) > MIBK:H_2O (1:1) > MIBK:H_2O (1:3), the trend for the FU yield differed with a preference for MIBK:H_2O (1:1). The increase in FU yield at MIBK:H_2O ratio of 1:1 (Table 5.3, entry 4) may be due to the higher miscibility of MIBK in H_2O, leading to faster degradation of Xyl to FU. Also, MIBK:H_2O ratio of 1:1 for FU synthesis could be better for industrial applications due to the moderate volume of organic solvent required. Regardless, the MIBK:H_2O of 3:1 that favored 5-HMF synthesis was selected for subsequent analysis. The biphasic conditions likely afford higher yields by minimizing the degradation reaction that takes place more readily under aqueous conditions.

Table 5.3: Study of the effect of solvent media on the yield of 5-HMF and FU

Entry	Reaction media	Time (min)	Temperature (^oC)	5-HMF yield (mol%)	FU yield (mol%)
1	H_2O	40	150	1.5 ± 0.61	12.8 ± 0.52
2	MIBK	40	150	2.4 ± 0.21	25.5 ± 2.4
3	H_2O/MIBK (3:1)	40	150	27.9 ± 2.9	10.9 ± 3.1
4	H_2O/MIBK (1:1)	40	150	38.9 ± 1.8	73.4 ± 4.4
5	H_2O/MIBK (1:3)	40	150	60.0 ± 1.4	61.1 ± 3.6

5.4.10 Effect of stirring speed on the yields of 5-HMF and FU

Magnetic stir bar mixing efficiency strongly depends on the establishment of a liquid flow that is induced by centrifugal forces. Apart from the axial flow component, the radial and tangential flow components of a stirred vessel contribute most to liquid dispersion. Accordingly, a suitable stirring speed can agitate the sample solution to accelerate the mass transfer between phases, thus potentially enhancing the extraction efficiency of the products out of the aqueous layer. The effect of stirring speed was investigated in an attempt to further increase the yields (Fig. 5.9). The selected stirring modes were static (no stirring), low agitation (100-200 rpm), medium agitation (400-600 rpm), and vigorous agitation (800-1000 rpm).

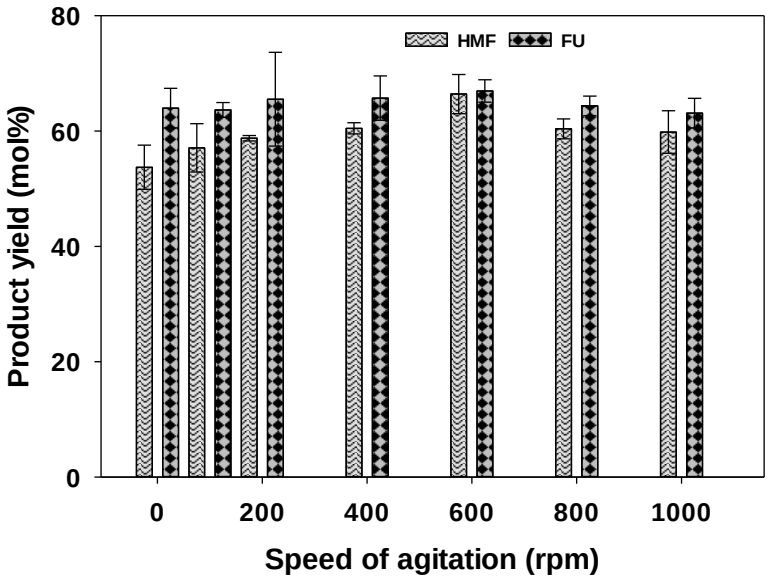

Fig. 5.9: Product (5-HMF and FU) yield as a function of stirring speed (rpm). The reaction mixture consisted of Glc (9 mg), Xyl (2 mg), and $AlCl_3.6H_2O$ (200 mg) in 4.5 mL of H_2O/MIBK (1:3). Reactions were performed in triplicates and the error bar presents the standard deviation.

The 5-HMF yield was found to increase with stirring speed up to 600 rpm. In the absence of stirring, a 54 mol% yield of 5-HMF was obtained, which rose to 66 mol% at 600 rpm. Higher stirring speeds were slightly detrimental, with 60 mol% 5-HMF at 800 rpm. The FU yield was less affected by the speed of stirring, ranging from 64 mol% without stirring and reaching a maximum (67 mol%) at 600 rpm. This could be attributed to the difference in solubility between the less-substituted furan ring of FU than that of HMF [385].

From this study, the optimal conditions for 5-HMF and FU co-synthesis from C6 and C5 sugars consist of a stirring speed of 600 rpm, a reaction time of 40 min, a temperature of 150 ^oC and 200 mg $AlCl_3.6H_2O$ for 9 mg of Glc and 2 mg of Xyl.

5.5 Conclusion

Here, we established a chemoenzymatic process for the transformation of PW to 5-HMF and FU. In the first step, we took advantage of an enzymatic transformation in a moist-solid mixture instead of the typical harsh reagents and conditions. In this process, the minor xylanases component of the commercial cellulases preparation also depolymerized hemicellulose to xylose. The reaction was optimally performed in a milling jar made of stainless steel equipped with two stainless steel balls, with milling once for 15 minutes, followed by static incubation for 24 h, which afforded Glc and Xyl in yields of 52 mol% and 22 mol%, respectively, from the calculated holocellulose content of the PW used. In a second step, the sugars were dehydrated into the furan-based platform chemicals 5-HMF and FU under mild chemical conditions with the catalyst $AlCl_3.6H_2O$ at 150 ^oC, to generate 5-HMF and FU

in yields as high as 66 mol% and 67 mol%, respectively, in 40 min. The renewable nature of the enzyme, which is non-toxic and the less water waste produced with moist-solid mixture makes this process an attractive alternative for future biorefineries. Another aspect was the first-order kinetic model with two consecutive reactions which was sufficient to estimate the decomposition of sugars (Glc and Xyl) into HMF and FU, respectively.

Connecting Statement 4

The preceding study established a chemoenzymatic process to efficiently convert untreated newsprint to HMF and FU. In the first step, the newsprint was hydrolysed to sugars in a moist solid environment, taking advantage of enzymes instead of the typical harsh reagents and conditions. In the second step, the sugars were dehydrated under mild chemical conditions with the $AlCl_3.6H_2O$ catalyst at 150 ^oC, to generate HMF and FU in yields as high as 66 mol% and 65 mol%, respectively, in 40 min.

The renewable nature of the enzyme, which is non-toxic, and the low amount of water used with moist-solid mixture makes this process an attractive alternative for future biorefinery. Another aspect is the inexpensive cost and low toxicity of $AlCl_3.6H_2O$ which has been investigated for HMF and FU production from monosaccharides (glucose and fructose) and cellulosic biomass. The combination of $AlCl_3.6H_2O$ with LiCl as a co-catalyst is beneficial, improving the selectivity and yield of HMF and FU from cellulosic biomass. Also, the presence of a biphasic media improved the product yield further, reducing the rate of degradation of HMF and FU to unwanted products.

Chapter 6 evaluates the one-pot conversion of untreated corrugated boxes to HMF and FU using $AlCl_3.6H_2O$/LiCl/NaCl in a H_2O/MIBK biphasic media. This Chapter is based on a manuscript submitted for publication. The article was co-authored by Dr. Marie-Josée Dumont.

6 One-pot conversion of corrugated boxes for the co-synthesis of hydroxymethylfurfural and furfural in a biphasic media

6.1 Abstract

This study proposes a simplified approach to produce hydroxymethylfurfural (HMF) and furfural (FU) from corrugated boxes. A robust catalytic system comprising of $AlCl_3.6H_2O$/LiCl/NaCl in H_2O/MIBK biphasic media was developed, affording HMF and FU in maximum yields of 98 mol% and 51 mol% at 160 ^oC and 40 min. The detailed kinetic model fits well with the experimental data, providing deep insights to the various steps necessary for the conversion of the corrugated boxes. The kinetic study also confirms that the biphasic media could effectively protect the HMF and FU from further degradation, thus improving their yield.

Keywords: Corrugated boxes; hydroxymethylfurfural; furfural; biphasic media; kinetic model.

6.2 Introduction

Furanic derivatives including furfural (FU) and hydroxymethylfurfural (HMF) are among the degradation products of simple sugars (C5 and C6) from lignocellulose. They are classified as platform chemicals from which liquid fuels and other important compound can be derived.

FU, also known as 2-formylfuran, furan-2-aldehyde or 2-furancarboxaldehyde is a furan based aromatic heterocyclic aldehyde. Its solubility varies depending on the solvent media and is higher for most polar organic solvent [386]. As a promising building block, it can be used for synthesizing different molecules such as furfuryl alcohol, levulinic acid, and tetrahydrofuran. The reaction of FU with nitrogen containing nucleophiles such as NH_3 or primary amines produces hemiaminals as intermediate which then dehydrates to furfural imines. Both the product and intermediate are useful in the manufacture of drugs, herbicides, pesticides, fibers and perfumes [387]. In the presence of molecular oxygen, the aldehyde group in FU is oxidized to furoic acid using Ag_2O/CuO as catalyst [388]. FU is also used to synthesize green solvents and fuel additives such as methyl tetrahydrofuran, valerate esters, and methyl furan with better properties than traditional fuels.

HMF with an additional hydroxyl group on C5 has a richer chemistry than FU. The CH_2OH group of HMF not only serve as an alkylating agent but also reacts with acids and halogens to form esters and halides [389]. The hydroxyl group of HMF can be easily halogenated to 5-bromomethylfurfural or 5-chloromethylfurfural. The latter which can as well

be obtained directly from sugar dehydration is currently been studied as a platform chemical [390]. The hydroxyl functional group is also important because it provides an easy grasp for attachment to a solid support [389]. This solid supported HMF with an unsubstituted carbonyl group might be a helpful framework in combinatorial chemistry [389]. The carbonyl group in HMF together with other heterocyclic moiety is used in the synthesis of libraries of complex compound necessary for bioactivity testing [391]. The aromatic aldehyde acts as an electrophile, reacting with nucleophiles to generate various value-added molecules. The oxidative conversion of the carbonyl group in HMF to nitrile was successful by using iodine in aqueous ammonia. HMF together with L-alamine has been transformed to an enantiopure salt of pyridinium ((S)-alapyridaine) by reductive amination in the presence of Br_2/MeOH/H_2O. Other applications are in the Diels-Alder reactions where the HMF-derived biscaminomethylfurans, bis(alkoxymethyl)furans and maleic anhydride could serve as dienophile to replace norcantharidin drug formulation for cancer treatment [392]. HMF can also be employed as a suitable candidate that is yet to be explored as a key reactant in wood adhesives [393].

A typical problem during the co-synthesis of HMF and FU is humins formation emanating from side reactions in aqueous media. Generally, the reaction mixture can be adjusted by adding an organic solvent to create a biphasic media which can improve the reaction selectivity and enhance the product yield [394]. In this study, methyl isobutyl ketone (MIBK) in a blend with acidified aqueous solution enhanced the continuous extraction of HMF and FU [395]. MIBK as a green solvent is cheap with a relatively lower boiling point than dimethyl sulfoxide (DMSO), making it easier to separate HMF and FU [396, 397]. Among the metal salts tested for lignocellulose biomass conversion to HMF and FU, Al(III) salts outperformed their Brønsted acid counterparts (e.g., H_2SO_4 and HCl). For instance, Roy Goswami et al. reported a modest HMF yield of 59.8 wt% from corn starch under $AlCl_3.6H_2O$ catalysis in a microwave [373]. Yang et al. also revealed a HMF and FU yield of 26 mol% and 51 mol% when $AlCl_3.6H_2O$ was employed to hydrolyze Poplar under similar heating mode [398]. As a Lewis acid that is cheap and less toxic, $AlCl_3.6H_2O$ can generate Brønsted acid in solution, making it conducive for rapid biomass conversion to HMF and FU [399]. Another aspect was the use of LiCl which served as a co-catalyst to increase the [H^+] activity of the catalytic system [400].

Corrugated boxes (CB) are used as packaging in a variety of sectors, providing temporary protection to products during all aspect of the distribution process [401]. As a result

of its low cost and biodegradability, CB is preferred as a packaging material over polyethylene from petrochemicals. In 2014, the global CB market was speculated to increase at a growth rate of 4%, reaching US$ 173.6 million by 2020 [402]. The largest market for CB packaging is North America, followed by Europe and Asia-Pacific. In China alone, the use of CB rose from 9.9 billion in 2015 to 14.4 billion in 2016, representing an increment of 45.2% [403]. CB demand is predicted to rise due to the growing pace of fast moving consumer goods (FMCG) industry along with the increase demand for fast food. Additionally, the paradigm shift toward internet shopping is stirring an increase on the overall consumption of CB which has limited end-use application. To the best of the authors' knowledge, this is a pioneer study to investigate the co-synthesis of HMF and FU from CB using $AlCl_3.6H_2O$ and LiCl as catalyst and co-catalyst. In this study, the influence of biphasic media, catalyst and co-catalyst dosage, biomass dosage, reaction temperature and time on the efficient conversion of CB was detailed. Reaction kinetics was also performed to understand the different steps toward CB conversion to HMF and FU.

6.3 Materials and Methods

6.3.1 Materials

D-glucose (99.5%), xylose (≥ 99%), 5-hydroxymethylfurfural (99%), furfural (99%), levulinic acid (98%), methyl isobutyl ketone (MIBK) (99%), $AlCl_3.6H_2O$ (99%, ACS reagent), $FeCl_3.6H_2O$ (97%, ACS reagent), LiCl (≥ 99.98%, ACS reagent), methanol (≥ 99.9%, HPLC grade), NaCl (≥ 99%, ACS reagent), acetonitrile (ACN) (≥ 99.9%, HPLC grade), and HPLC water were purchased from Sigma Aldrich (Canada). D-fructose (99.9%) was bought from Alfa Aesar (USA). All the materials and solvents were utilized as supplied without any purification.

6.3.2 Feedstock preparation

CB wastes were sourced at the MacDonald campus of McGill University, Canada. After removing non-fibrous contaminants such as stickers, glues, and staples, samples were cut to sizes of 20 mm × 5 mm. They were then dried overnight at 80 ^oC, and ball-milled (< 250 µm) for 5 min at 30 Hz before storing for further use.

6.3.3 Characterization of corrugated boxes

FT-IR analysis was performed with a Nicolet IS10 (Thermofisher, MA, USA) to determine the difference between the functional groups on untreated CB to that of the hydrothermally processed sample. The spectra were collected at 40 scans at a range of 400-4000 cm^{-1} and a resolution of 4 cm^{-1}.

6.3.4 Thermochemical conversion

All experiments were performed under oil-bath heating in a digital hotplate magnetic stirrer (Thermo Orion Inc., 22 Alpha Road, Chelmsford, MA 01824, US), using a 10 mL Pyrex tube reactor equipped with a magnetic stir bar. The agitation speed of 600 rpm was maintained throughout the reaction to enhance mass transfer. The temperature (with deviation of ± 1 ^{o}C) of the oil-bath was monitored with a K-type thermocouple. In a typical experiment, a 10 mL Pyrex tube reactor was filled with 50 mg of powdered CB, catalyst, co-catalyst, and the required volume (4 mL) of reaction medium made up of H_2O and MIBK. After a set reaction duration, the reaction was stopped by submerging the tube in an ice bath. Another aspect was the concentration of the products (HMF and FU) by recovery from the organic phase using a rotary evaporator under vacuum at 40 ^{o}C. Samples were placed in vials for HPLC analysis after being filtered using a 0.22 m nylon filter (Chromspec, Brockville, ON, Canada). All samples were reported in triplicate with data given as average ± standard deviation.

6.3.5 Quantification of glucose, xylose and their degradation products

C6 and C5 sugars, including their degradation products (HMF and FU) were assayed using HPLC (1260 Infinity Agilent). Zorbax Carbohydrate column (4.6 × 150 mm, 5uL) was used to separate and quantify the glucose and xylose in an HPLC equipped with a RID detector. The RID and the column were both kept at a constant temperature of 30 ^{o}C. ACN (HPLC grade) and water (75:25) were combined as the mobile phase, with injection volume and flowrate of 5 µL and 1.4 mL/min, respectively. The glucose (Eq. 1) and xylose (Eq. 2) yields in mol% were calculated using the calibration curves derived from the corresponding standard solutions at retention times of 5.82 min and 4.67 min, respectively. The molecular weights for glucose, anhydroglucose, xylose, and anhydroxylose are 180 g/mol, 162 g/mol, 150 g/mol and 132 g/mol, respectively. The HMF and FU on the organic phase were filtered followed by separation through a Phenomenex C-18 column (4.6 mm × 150 mm, 5 µm). The eluent (mobile pahse) is made up of methanol and HPLC grade water (10:90) acidified with 0.1% formic acid. The flowrate, injection volume and column temperature were adjusted to 0.6 mL/min, 5 µL, and 30 ^{o}C, respectively. The HMF and FU were detected at retention times of 5.85 min and 8.66 min using a UV detector set at 267 nm. The molecular weights for HMF and FU are 126 g/mol and 96 g/mol, respectively.

$$Glc\ yield\ (mol\%) = \frac{Weight\ of\ Glc\ produced\ (mg)}{Weight\ of\ newsprint\ fed\ \ (mg)} \times \frac{162\ g/mol}{180 g/mol} \times \frac{1}{X_c} \times 100\% \qquad (6.1)$$

$$Xyl\ yield\ (mol\%) = \frac{Weight\ of\ Xyl\ produced\ (mg)}{Weight\ of\ newsprint\ fed\ \ (mg)} \times \frac{132\ g/mol}{150 g/mol} \times \frac{1}{X_h} \times 100\% \qquad (6.2)$$

$$HMF\ yield\ (mol\%) = \frac{Weight\ of\ HMF\ produced\ (mg)}{Weight\ of\ corrugated\ boxes\ fed\ \ (mg)} \times \frac{180\ g/mol}{126\ g/mol} \times 100\% \qquad (6.3)$$

$$FU\ yield\ (mol\%) = \frac{Weight\ of\ FU\ produced\ (mg)}{Weight\ of\ corrugated\ boxes\ fed\ \ (mg)} \times \frac{150\ g/mol}{96\ g/mol} \times 100\% \qquad (6.4)$$

6.3.6 Kinetic model development for the co-synthesis of HMF and furfural

The kinetic study for HMF and FU from CB were demonstrated as a function of time (0-100 min) and temperature (150-170 ^{o}C). The hydrolysis of the cellulose and hemicellulose of CB was done using 0.15 mmol $AlCl_3 \cdot 6H_2O$ and 100 mg of LiCl in a reaction medium comprising of H_2O/MIBK (1:7). The concentration of glucose, xylose, HMF, and FU were evaluated to develop kinetic models (Fig. 6.1) as suggested by Saeman [404]. The models neglected the isomerization of glucose and xylose as well as the degradation of HMF and FU, which are constantly extracted into the organic phase. The proposed kinetic models assume the degradation of the cellulose and hemicellulose in CB as follow:

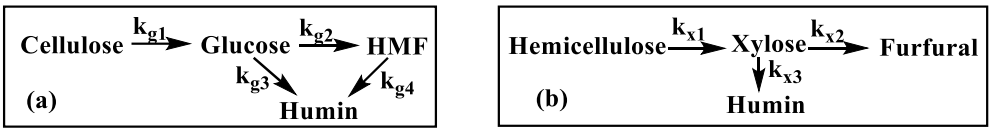

Fig. 6.1: Simplified kinetic model for the conversion of the (a) cellulose and (b) hemicellulose in corrugated boxes to HMF and furfural.

From Fig. 6.1 (a), the derivative rate law for each step in cellulose conversion is as follow:

$$\frac{dC}{dt} = -k_{g1}C \qquad (6.5)$$

$$\frac{dGlc}{dt} = k_{g1}C - \left[k_{g2}Glc + k_{g3}Glc\right]` \qquad (6.6)$$

$$\frac{dHMF}{dt} = k_{g2}C - k_{g4}HMF \qquad (6.7)$$

here, C, Glc, and HMF represent the concentrations of cellulose, glucose, and HMF with k_{g1-4} as the rate constants, respectively. As seen, the model did not account for the rehydration of HMF because levulinic acid was not detected in the reaction. The next scheme (Fig. 6.1b) with its corresponding rate equations describes the conversion steps for hemicellulose.

$$\frac{dH}{dt} = -k_{x1}H \qquad (6.8)$$

$$\frac{dXyl}{dt} = k_{x1}H - \left[k_{x2}Xyl + k_{x3}Xyl\right] \tag{6.9}$$

$$\frac{dFU}{dt} = k_{x2}Xyl \tag{6.10}$$

where H, Xyl, and FU are the concentrations of hemicellulose, xylose, and furfural, and k_{x1-3} are the rate constants for each step of the reaction.

The formation of humins during the dehydration of glucose $\left(k_{g3}\right)$ and xylose $\left(k_{x3}\right)$ were accounted for in the above models. The temperature dependence of the obtained kinetic parameters were evaluated using the Arrhenius model (6.11).

$$k = Ae^{-\frac{E_a}{RT}} \tag{6.11}$$

where $\left(E_a\right)$ and $\left(A\right)$ are expressions for activation energy and frequency factor, while R and T represent the universal gas constant $(8.314 J/mol.K)$ and the reaction temperature $\left(K\right)$, respectively.

6.4 Results and discussion

6.4.1 Sample preparation and FT-IR characterization

The activation by mechanical ball milling reduced both the crystallinity and degree of polymerization of cellulose, as well as enhanced the porosity of the CB [405]. Fig. 6.2 presents the FT-IR spectra of untreated and hydrothermally treated CB. The analysis was conducted to investigate the structural changes in the biomass moiety due to hydrothermal processing. The broad peak from 3659 cm^{-1} to 3010 cm^{-1} of the untreated CB is attributed to the O–H vibration in compounds such as phenol, alcohol, and carboxylic acid whereas the hydrothermally treated CB had sharp and intense peaks narrowing from 3586 cm^{-1} to 3331 cm^{-1}. The apparent shift in peak is probably due to the limited hydrogen bond network which could reduce the crystallinity of cellulose after hydrothermal processing. In the case of untreated CB, the presence of bands near 2915 cm^{-1} to 2350 cm^{-1} are ascribed to the axial and intense distortion of the C-H group in the holocellulose. However, a stronger vibrational streching of $–CH_2$ and $–CH_3$ emanated from C–H group in the hydrothermally treated CB with stretched band ranging from 2950 to 2300 cm^{-1}. The hydrothermally treated CB has a sharper and more intense peak (1741 cm^{-1}–1537 cm^{-1}) that is ascribed to the perturbation of the carbonyl group in the structure lignin as well as those in the structured carbohydrates. The disruption of the carbonyl group created

spaces that could facilitate the hydrolysis of more carbohydrate monomers into HMF and FU [406]. The vibrational stretching between 1500 cm^{-1} and 1150 cm^{-1} for the C=O and C=C groups in the holocellulose and lignin revealed the impact of delignification. The untreated CB exhibited an apparent peak near 1180 cm^{-1} to 830 cm^{-1} [407], together with a systematic breaking of the CH_2 and C-O-C bonds which most likely disappeared for the treated CB. The difference between the peaks in these spectra reveals the successful conversion of most of the crystalline domain in cellulose to the amorphous region. The reduced crystallinity, and the internal structural changes played key role in increasing cellulose accessibility to catalyst which eventually improved the hydrolysis efficiency and enhanced the product yield [408].

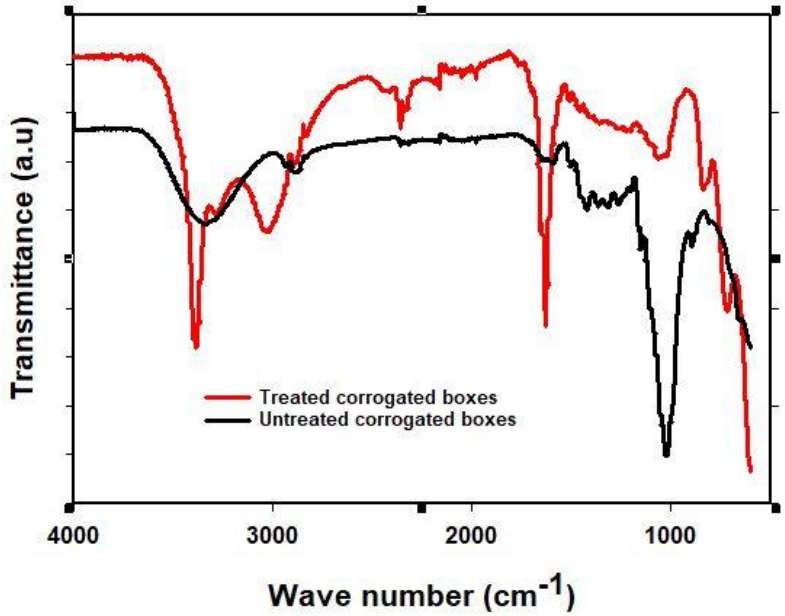

Fig. 6.2: FT-IR spectra of untreated (black) and treated (red) corrugated boxes.

6.4.2 Preliminary study to screen the catalytic performance of $FeCl_3.6H_2O$ and $AlCl_3.6H_2O$

In a preliminary study, the catalytic performance of $FeCl_3.6H_2O$ and $AlCl_3.6H_2O$ were screened for CB conversion to HMF and FU under different solvent media (Table 6.1). The yields of HMF and FU from CB were based on the hexose and pentose content of 19 wt% and 16 wt%, respectively. In most cases, the reaction mixture develops from colorless to dark brown, due to sugar (xylose and glucose) decomposition to insoluble humins [409]. The CB conversion in aqueous solution of $FeCl_3.6H_2O$ or $AlCl_3.6H_2O$ revealed negligible HMF and FU yields (Table 6.1, entries 1 and 2). The perceived poor performance is due to the instability of HMF in an acidic aqueous solution or environment. Also, the substrate was observed to float on water thus reducing the contact with the catalytic solution. Experiments using pure MIBK

also gave negligible yields of HMF and FU since glucose and xylose have been confirmed to be insoluble in such organic solvent [410].

MIBK was selected as an organic phase to supress humin formation and prevent HMF and FU from rehydration [411]. The use of a biphasic system comprising H_2O/MIBK performed better, expressly increasing the HMF and FU yields using $FeCl_3.6H_2O$ or $AlCl_3.6H_2O$ as catalyst (Table 6.1, entries 3 and 4). To further increase the partition coefficient, an additive in form of NaCl was added to the aqueous phase to create a salting-out effect [412]. In the first instance where only a monophasic system (H_2O or MIBK) was tested in combination with NaCl, no HMF and FU was detected (Table 6.1, entries 5 and 6). A similar study showed that the presence of NaCl reduced the yield of HMF by increasing its rate of rehydration to levulinic acid [413]. However, NaCl together with the biphasic system improved the HMF and FU yields using $FeCl_3.6H_2O$ or $AlCl_3.6H_2O$ as catalyst (Table 6.1, entries 7 and 8). Similarly, Yang et al. revealed an improved HMF yield of 61 mol% employing $AlCl_3.6H_2O$ catalyst in a H_2O/THF biphasic blend [398]. The type of the ionic interaction between all components of the reaction system determines the magnitude of the salting-out effect [414]. Other factors that could affect the salting-out effect are the reaction temperature and pressure in addition to the catalyst concentration [415]. NaCl as an electrolyte could regulate the intermolecular interaction between liquid components, reducing the mutual solubility of the biphasic media. In all cases, $AlCl_3.6H_2O$ performed better than $FeCl_3.6H_2O$. The higher HMF and FU yields obtained with $AlCl_3.6H_2O$ relative to $FeCl_3.6H_2O$ can be attributed to its smaller atomic radii which is responsible for a stronger electrostatic interaction with glucose [416]. Moreover, the $[Al(OH)_2(aq)]^+$ formed as a result of the dissociation of $AlCl_3$ in the presence of H_2O enhanced the rate of glucose-fructose isomerization. Therefore, $AlCl_3.6H_2O$ was selected for further analysis.

Table 6.1: Study of different Lewis acid and solvent media on HMF and FU yield

Entry	Catalyst	Solvent	Temp. (^{o}C)	Time (min)	HMF (mol %)	FU (mol %)
1	$FeCl_3.6H_2O$	H_2O	150	40	0.04 ± 0.02	0.01 ± 0.002
2	$AlCl_3.6H_2O$	H_2O	150	40	1.0 ± 0.3	3.4 ± 0.3
3	$FeCl_3.6H_2O$	H_2O/MIBK (1:3)	150	40	4.4 ± 0.8	13.2 ± 3.3
4	$AlCl_3.6H_2O$	H_2O/MIBK (1:3)	150	40	18.8 ± 0.4	19.3 ± 0.5
5	$FeCl_3.6H_2O$	H_2O + NaCl	150	40	ND	ND
6	$AlCl_3.6H_2O$	H_2O + NaCl	150	40	ND	ND
7	$FeCl_3.6H_2O$	H_2O/MIBK /NaCl	150	40	16.5 ± 0.3	35.7 ± 0.2
8	$AlCl_3.6H_2O$	H_2O/MIBK/NaCl	150	40	45.1 ± 3.1	37.4 ± 4.5

ND = not detected

6.4.3 Effect of varying the ratio of the biphasic media

The evaluated reaction system comprising of $AlCl_3.6H_2O$, NaCl and H_2O/MIBK (1:3) was investigated by varying the volume of H_2O/MIBK from 1:1 to 1:7. From Fig. 6.3, it is seen that by keeping other parameters fixed, the HMF yields increased as follows: H_2O/MIBK (1:7) > H_2O/MIBK (1:3) > H_2O/MIBK (1:1). The reduced HMF yield at H_2O/MIBK (1:1) is due to an increasing amount of water that resulted in lower concentration of the active sites [417]. Increasing the amount of organic solvent in the biphasic media could reduce the likelihood of HMF interaction with water, preventing its degradation as well as its rehydration [414]. However, FU yield followed a slightly different sequence with a preference for H_2O/MIBK (1:3). This is consistent with the findings of Mittal et al. who observed a considerable drop in FU yield after raising the solvent-to-aqueous ratio in a dioxane/H_2O system from 1:1 to 1:9 [416]. The higher miscibility of xylose in H_2O/MIBK (1:3) may have increased its degradation rate which eventually was beneficial for FU synthesis [418]. This demonstrates that FU, a less substituted furan derivative, might have a different preference for optimization than HMF.

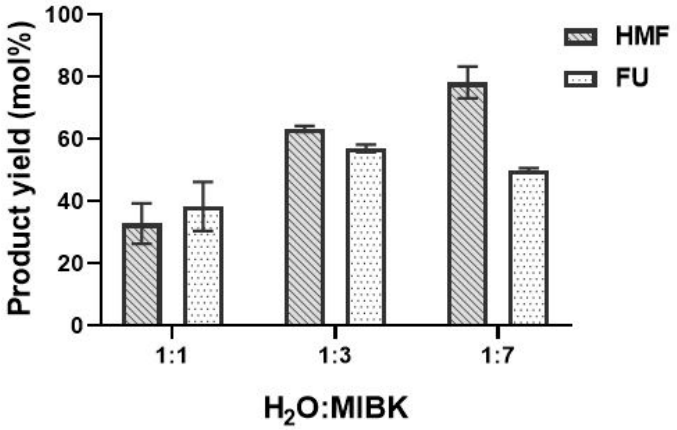

Fig. 6.3: Effect of varying the ratio of the biphasic mixture on the co-production of HMF and FU. The reaction mixture consist of 50 mg of CB, $AlCl_3.6H_2O$ (0.1 mmol) and NaCl (300 mg) heated at 150 °C for 40 min. The presented data are mean of triplicates ± standard deviation.

6.4.4 Studying the influence of catalyst dosage on both HMF and FU

The effect of $AlCl_3.6H_2O$ dosage on HMF and FU yield is shown in Fig. 6.4. When the dosage of $AlCl_3.6H_2O$ was only 0.025 mmol, the yield of HMF and FU were 50 mol% and 42 mol%, indicating the superior catalytic activity of the metal salt. Moreover, HMF (63 mol%-84 mol%) and FU (48 mol%-53 mol%) reached a reasonable yield by increasing the $AlCl_3.6H_2O$ amount from 0.05 mmol to 0.15 mmol. Ding et al. attributed this to the abundance of catalytically active sites [419]. Regardless, Zhang et al. observed a decrease in HMF production due to polymerization caused by excessive acid sites at higher catalyst loadings [420]. Similarly, increasing the catalyst amount from 3.6 wt% to 6 wt% was not beneficial for corncob conversion to FU, causing a decline in yield as a result of undesired side reactions [421, 422]. As a result, an optimal catalyst dosage of 0.15 mmol was chosen, corresponding to a loading ratio of 0.72 g catalyst/g CB.

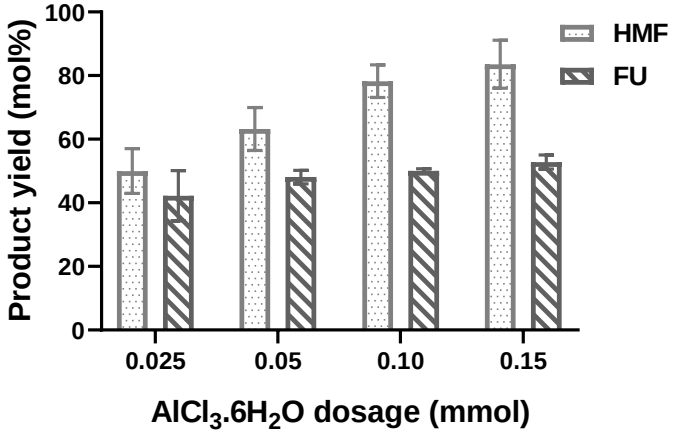

Fig. 6.4: Effect of catalyst amount on both HMF and FU. The reaction mixture consist of 50 mg of CB, NaCl (300 mg), LiCl (100 mg), and H_2O/MIBK (1:7), heated at 150 °C for 40 min. The analysis were triplicated with result presented as average ± standard deviation.

6.4.5 Effect of co-catalyst amount on HMF and FU production

The influence of LiCl on both HMF and FU from CB is presented in Fig. 6.5. Firstly, HMF and FU were not identified using LiCl (50 mg) and NaCl (300 mg) for the hydrolysis of 50 mg of CB in the absence of $AlCl_3.6H_2O$ at 150 ^oC for 40 min. Similarly, LiCl gave negligible yields of HMF when the conversion of glucose, cellulose, and starch were performed in isopropanol [423, 424]. However, LiCl was beneficial for the conversion of simple sugars, affording HMF yields of 79.1 mol% and 30.3 mol% from fructose and sucrose, respectively. Yuriy et al. reported modest HMF selectivity (72%) with LiCl in 1-butanol, but the test was only performed for fructose conversion [415]. This confirms that the inherent Brønsted acidity of LiCl could transform fructose to HMF, but lacked the Lewis acidity required for the isomerization of glucose to fructose [425]. The effect of LiCl (25 mg) together with $AlCl_3.6H_2O$/NaCl in H_2O/MIBK resulted in HMF and FU yields of 58 mol% and 49 mol%, respectively. Furthermore, increasing the LiCl dose to 100 mg dramatically expedited CB conversion with HMF and FU rising to 84 and 53 mol%. According to Binder et al., the LiCl/DMA system aided in enhancing HMF yields from fructose, glucose, and cellulose substrates using CrCl2 or CrCl3 as catalyst [426]. Chen and Lin [427] reported an acceptable yield of HMF (55-67 mol%), which was promoted by LiCl in the presence of metal salts such as $CrCl_2$, $SnCl_4$, or $SnCl_2$. LiCl acts best as auxiliary to $AlCl_3.6H_2O$ in stabilizing targeted products, as well as improving selectivity as confirmed by results of this study (HPLC chromatogram), where HMF and FU were the most significant peaks. The HMF and FU extracted into the MIBK phase was further concentrated by distillation, resulting to distinct peak areas.

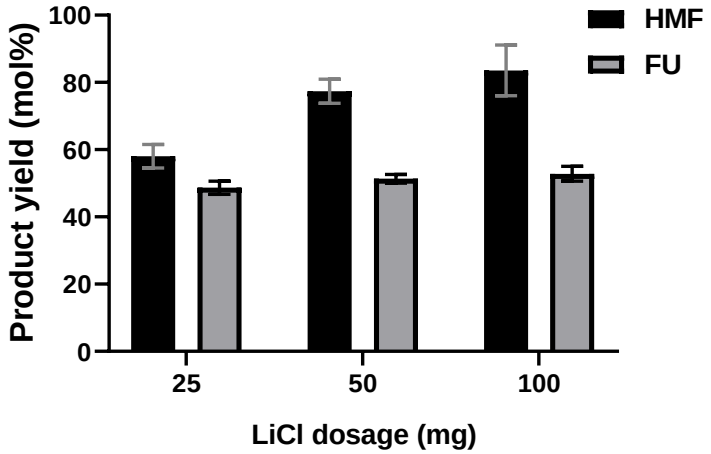

Fig. 6.5: Effect of co-catalyst (LiCl) dosage on the HMF and FU produced. The reaction mixture consist of 50 mg of CB, NaCl (300 mg), $AlCl_3.6H_2O$ (0.15 mmol), and H_2O/MIBK (1:7), heated at 150 ^oC for 40 min. The reported values are average of triplicates ± standard deviation.

6.4.6 Effect of biomass loading on HMF and FU synthesis

The influence of biomass amount on the production of HMF and FU was evaluated by increasing the CB dose in the reaction mixture from 50 mg to 100 mg (Fig. 6.6). Employing CB loading of 50 mg afforded HMF and FU in maximal of 84 mol% and 53 mol%. The CB conversion had no positive effects for HMF or FU after 50 mg. For instance, when CB was 100 mg, the yields of HMF and FU declined to 60 mol% and 45 mol% respectively, representing a decrease of about 29% and 15%, respectively. Sweygers et al. found a reduction in HMF and FU yields under identical conditions by increasing the substrate (bamboo) loading from 25 mg to 400 mg [428]. This could be attributed to high biomass loadings, which resulted in stirring difficulty and limited interaction between the biomass and the catalyst, hence decreasing the product yield. The viscosity of the biphasic system may also increase at high biomass loading, and may result to a non-uniform heating in the reactor. Therefore, biomass loading of 50 mg was selected to study other process parameters that may improve the yields of HMF and FU.

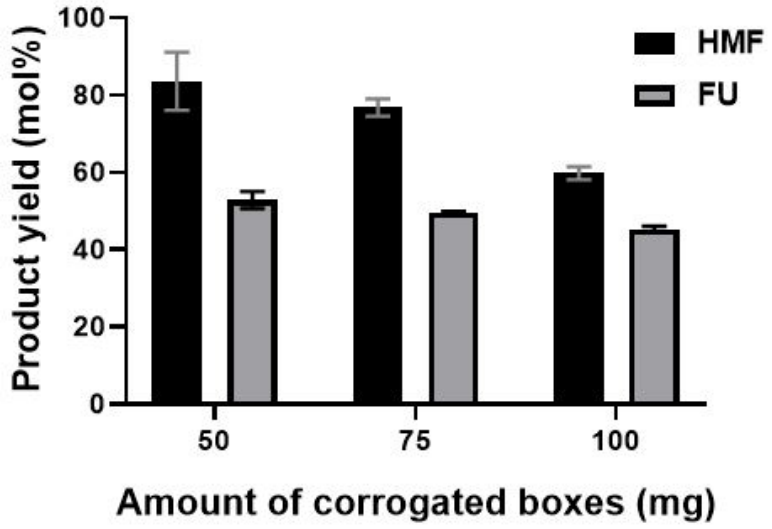

Fig. 6.6: Effect of biomass amount on the yield of HMF and FU. The reaction mixture consist of $AlCl_3.6H_2O$ (0.15 mmol), LiCl (100 mg), NaCl (300 mg) and H_2O/MIBK (1:7), heated at 150 °C for 40 min. The experiments were repeated three times with data given as average ± standard deviation.

6.4.7 The influence of reaction temperatures and times on HMF and FU

The effects of reaction temperatures (150-170 °C) on HMF and FU were investigated at selected time intervals (0-100 min), while keeping other parameters fixed. The results in Fig. 6.7 reveal that temperature has a significant influence on the HMF and FU yields. For instance, at a selected temperature of 150 °C, the HMF and FU yields gradually increased, reaching a maximum of 87 mol% and 54 mol% in about 80 min. The yields then decreased to 79 mol% and 50 mol% after a reaction duration of 100 min. When the temperature was set to 160 °C, the HMF production grew dramatically to approximately 98 mol% after 40 minutes, and then fell

to around 71 mol% after 100 minutes. After 60 minutes of reaction time at the same temperature of 160 ^{o}C, the FU production reached a high of 53 mol%. There was no significant difference in FU yield between 160 ^{o}C and 150 ^{o}C, or across reaction times of 40-100 min, indicating that temperature was more sensitive to HMF synthesis. The reaction pattern at 170 ^{o}C is more similar to that at 160 ^{o}C with maximum HMF and FU yields of 97 mol% and 55 mol% at only 40 min, respectively. The time required to achieve maximal HMF yield decreased from 80 minutes at 150 ^{o}C to 40 minutes at 160 and 170 ^{o}C, indicating that a trade-off between shorter reaction time and higher temperature is desirable for HMF synthesis. Beyond 40 min at 170 ^{o}C, the HMF yield decreased significantly to 38 mol%, probably due to humin formation while FU may have transformed to phenols or other organic moiety *via* fragmentation [429, 430]. The reaction system was sufficient to completely convert the CB at all selected reaction condition. However, from the mass balance, there are instance where unidentical products restricts the holistic evaluation of products. The proposed reaction mechanism for the catalytic system ($AlCl_3.6H_2O$/LiCl/NaCl) of this study is similar to that reported by Nzediegwu and Dumont [431], where $FeCl_3.6H_2O$ and LiCl acted as catalyst and co-catalyst for the hydrothermal conversion of newsprint to levulinic acid.

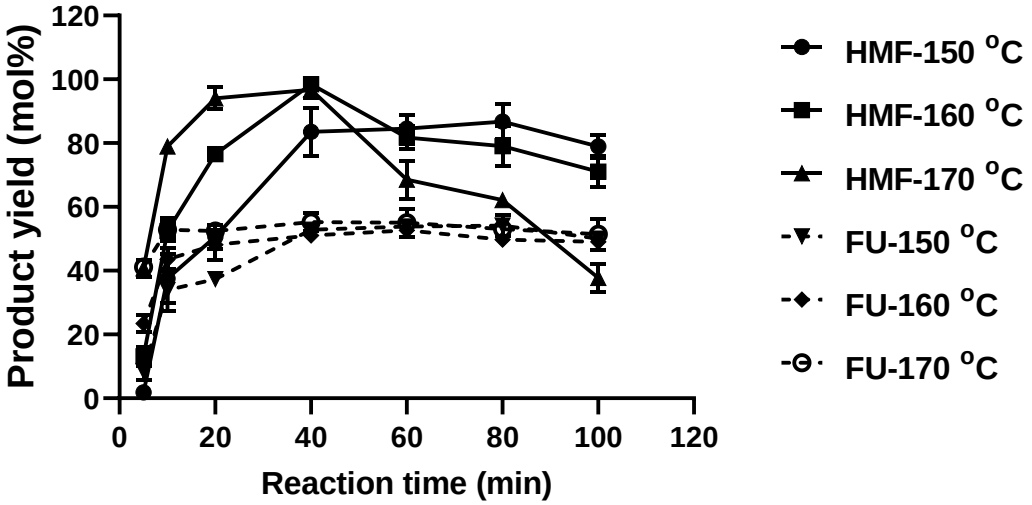

Fig. 6.7: Effect of reaction temperatures (150-170 °C) and times (0-100 min) on HMF and FU yields from corrugated boxes in the biphasic media composed of H_2O/MIBK (1:7) and a catalytic system comprising of $AlCl_3.6H_2O$ (0.15 mmol), LiCl (100 mg) and NaCl (300 mg). Data were presented as mean ± standard deviation.

6.4.8 Comparison with previous hydrothermal conversion using heterogonous catalysts

Heterogeneous catalysts have gainfully been explored for the conversion of lignocellulosic biomass into furan-based platform chemicals. Table 6.2 shows the unique acidities of these

catalysts, facilitating the valorization of biomass into HMF and FU in moderate to high yields. However, the difficult interaction between the catalyst and the biomass could be the reason while most of the reactions (Table 6.2) occurred at an elongated reaction time which was only 40 min for this study. Also, the SO_3H functional group of most of the heterogonous catalyst is a limitation that could affect their reusability because of the leaching of the acidic group. Overall, the developed catalytic system ($AlCl_3.6H_2O$/LiCl/NaCl) for this study gave the highest HMF and FU yields of 98 mol% and 56 mol%.

Table 6.2: Comparative studies of biomass conversion to HMF and FU using heterogonous catalyst in a biphasic media

Substrate	Catalyst	Solvent	Temp. (°C)	Time (min)	HMF (mol%)	FU (mol%)	Ref.
CB	$AlCl_3.6H_2O$/LiCl	MIBK-H_2O	160	40	98	56	This study
Cellulose	Sn-beta	THF-H_2O	190	70	32	NA	[432]
Corncob	SPTPA	GVL	175	30	32.3	73.9	[433]
Cornstalk	PTSA-POM	GVL	190	100	19.5	83.5	[434]
Wheat straw	Sulfamic acid	GVL-H_2O	180	180	28.5	26.1	[435]
Hemicellulose	SAPO-44	Toluene-H_2O	170	480	NA	63	[436]
Corncob	MC-Sn-CNS	MIBK-H_2O	180	15	NA	64.4	[437]
Cornstalk	SO_4^{2-}/SnO2-CS	ChCl:EG-H_2O	170	30	NA	68.2	[438]
Cellulose	Sn-Mont	THF-H_2O	160	180	39.1	NA	[395]
Cellulose	PS-PEG-OSO_3H	DMSO-H_2O	120	60	54	NA	[439]

CB = corrugated boxes, NA = not available, PS-PEG-OSO3H = polystyrene-poly (ethylene glycol), SPTPA = sulfonated polytriphenylamine, PTSA-POM = p-toluene sulfonic acid and paraformaldehyde, SAPO = silicoaluminophosphate, MC-Sn-CNS = microwave-treated chestnut shell.

6.4.9 Kinetic modelling for CB conversion to HMF and FU

Experimental data were used to determine the kinetic parameters for the conversion of the structural carbohydrates (cellulose and hemicellulose) in CB to HMF and FU. The resultant reaction rate constants (Table 6.3) were calculated with the LSQCURVEFIT function from MATLAB's optimization toolbox (R2020b). As a rule of thumb, the mass of the holocellulose in the CB decreases with the proceeding hydrolysis while the glucose and xylose reached maximum at 5-10 min before decreasing after a prolonged reaction time. The reaction profile for HMF and FU followed similar trends to that of glucose and xylose. However, the higher k_{i2} values during CB conversion indicates that glucose and xylose are both intermediates that are rapidly transformed to HMF and FU in parallel. As shown in Fig. 6.8, the predicted (solid line) and actual (point) results correspond well, indicating that the model was useful in

characterising the influence of reaction time and temperature on HMF and FU production. For all the reaction temperatures (150-170 ^{o}C) selected to convert the cellulose in CB, the reaction rate increased systematically, indicating the temperature dependence of the various steps toward CB conversion.

Table 6.3: Estimated cellulose and hemicellulose conversion rate constants (min^{-1})

Temp (^{o}C)	Cellulose				Hemicellulose		
	Reaction rate constant (min^{-1})						
	k_{g1}	k_{g2}	k_{g3}	k_{g4}	k_{x1}	k_{x2}	k_{x3}
150	0.13651	0.15399	0.02114	0.00092	0.15244	0.05454	0.04307
160	0.34633	0.27059	0.02199	0.00301	0.34393	0.09945	0.08743
170	0.36003	1.49518	0.14070	0.00908	0.45516	0.26343	0.21006

The values of k_{g1} and k_{g2} were higher than those of k_{g3} and k_{g4}, implying that the formation of glucose and HMF was favoured over humin formation. Apart from the CB conversion at 160 ^{o}C where k_{g1} is slightly higher than k_{g2}, all the rate constant increased with increasing temperature as follows: $k_{g2} > k_{g1} > k_{g3} > k_{g4}$. Notably, the degradation rate of HMF was higher at 170 ^{o}C with a higher rate constant (0.00908 min^{-1}). This supports the claim of a reduced HMF yield probably due to humin formation at a higher temperature and a prolonged reaction time.

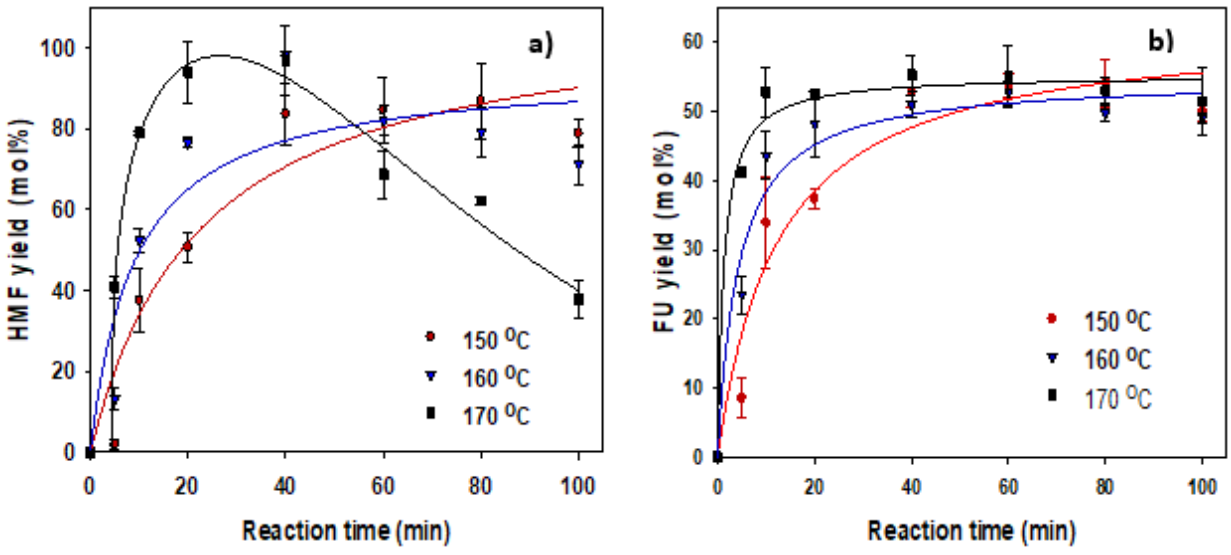

Fig. 6.8: Modelled yield of (a) HMF and (b) FU from the hydrolysis of corrugated boxes. Experimental data is represented by points while the predicted data is denoted by solid lines.

Just as for cellulose, the rate constant for transforming the hemicellulose in CB increased invariably with temperature, showing that temperature was beneficial to accelerate the reaction. The rate constant k_{x1} for the conversion of the hemicellulose in CB is substantially greater than that of the corresponding k_{x2}, implying that the rate-determining step of the reaction was the synthesis of FU from xylose. The k_{x3} values were about 1.2 times lower than the values of k_{x2}, showing that the degradation of xylose to FU could be much easier than the decomposition of FU to humins. This research indicated that the biphasic blend could successfully reduce the interference of side reactions, hence increasing HMF and FU production.

The natural logarithm of the reaction rate constants is inversely proportional to the temperature as depicted in Fig. 6.9, from which the associated activation energies were determined using linear interpolation. As shown in Table 6.4, the E_a from cellulose to glucose was 75.98 kJ/mol which is lower compared to that reported (156.51 kJ/mol) by Huang et al. who used [Bmim]HSO_4/H_2O/1,4-dioxane for biomass hydrolysis [440]. The decline in E_{a1} for this study revealed a significant change in the composition of CB, probably due to the creation of more amorphous regions during the rigorous pretreatment of paper manufacturing. During the conversion of glucose, its pyranose form is reversibly transformed into the furanose form before dehydration to HMF [441], making the E_a (175.74 kJ/mol) for this step higher than for the conversion of glucose to humins. This is comparable to the findings of Wang et al. [425] who found 160.96 kJ/mol and 23.45 kJ/mol for the identical reaction steps, validating the robustness of the model developed in this study.

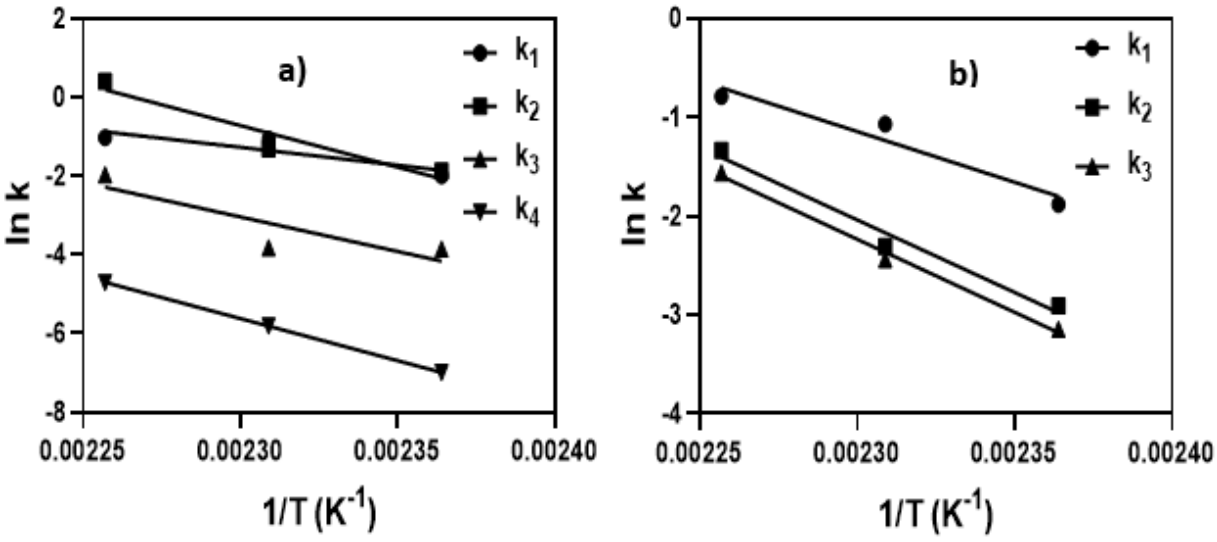

Fig. 6.9: The Arrhenius plots for the conversion of corrugated boxes to (a) HMF and (b) FU.

The E_{a1} value for hemicellulose hydrolysis is 85 kJ/mol, which is in range with that obtained for aspen wood (97 kJ/mol) [442] and bagasse (83.8 kJ/mol) [443] hydrolysis, showing the efficiency of the catalytic system in transforming the hemicellulose in CB to FU. The value of FU synthesis in this study is 122.07 kJ/mol in H_2O/MIBK system, which is lower than the value in water (154.15 kJ/mol) reported by Li et al [444], showing that the biphasic media might promote FU synthesis while also preventing its dehydration. The E_{a3} value of 122.96 kJ/mol, though identical to E_{a2}, could be detrimental for xylose decomposition due to the high energy barrier. Therefore, a compromise involving lowering temperature for optimum xylose yield is necessary.

Table 6.4: Activation energies for the HMF and FU yields from CB

Rate constant (min^{-1})	Cellulose		Hemicellulose	
	E_a (kJ/mol)	A (min^{-1})	E_a (kJ/mol)	A (min^{-1})
k_{i1}	75.98	3.79×10^8	85.36	5.75×10^9
k_{i2}	175.74	6.38×10^{20}	122.07	6.03×10^{13}
k_{i3}	145.92	1.63×10^{16}	122.96	6.37×10^{13}
k_{i4}	177.90	8.59×10^{18}	NA	NA

NA = not available

6.5 Conclusion

This study presented a platform for the effective utilization of CB which has limited end-use applications. The FTIR analysis shows that the hydrothermal treatment impacted the internal structure of the CB by creating more amorphous domain that could interact easily with the catalytic system. The hydrothermal treatment started by screening the catalytic activity of $FeCl_3.6H_2O$ or $AlCl_3.6H_2O$ for CB conversion to HMF and FU under different solvent media. $AlCl_3.6H_2O$ performed better than $FeCl_3.6H_2O$ due to its smaller atomic radii, which is responsible for a stronger electrostatic interaction with glucose. Next, a catalytic system leveraging on the synergy between $AlCl_3.6H_2O$ and LiCl (as co-catalyst) in H_2O/MIBK was developed to enhance the CB conversion process. Optimized reaction conditions were established based on a trade-off between the different process parameters such as $AlCl_3.6H_2O$/LiCl/NaCl in H_2O/MIBK biphasic media, affording HMF and FU in maximum yields of 98 mol% and 51 mol%, at 160 ^oC and 40 min, respectively. Kinetic study was performed to better understand how the different reaction steps could influence the CB

conversion process. The kinetic study also confirmed that the biphasic media could effectively protect the HMF and FU from further degradation, alongside with improving their yields.

7 General conclusions and recommendations

7.1 General conclusions and summary

The focus of this study was to repurpose paper wastes which are currently underutilized into platform chemicals. Although the processes to utilize these refuses for bioethanol synthesis have been well documented in the literature, there is only a hand full of data on their conversion to platform chemicals. Regardless of the paper type, selecting an appropriate reaction condition is the basic requirement necessary for their conversion. These conditions include reaction temperature, time, reaction media, catalyst type, and concentration. The choice of a catalyst will depend on the factor(s) that will impact the overall process economically, technically, and environmentally. The preference for heterogeneous catalysts against homogenous ones is more related to their eco-friendliness and ease of separation from the product stream. However, the use of heterogeneous catalysts is limited by their poor thermal stability and weak interaction with cellulose during hydrothermal conversion. Overall, these issues can be circumvented by employing an efficient pretreatment method which will reduce the crystallinity of the cellulose and make them susceptible to catalytic attack. To test this, wood pulps and paper wastes were pretreated by washing overnight with dilute HCl. This step which is also known as decationization helps to eliminate inorganics such as alkali and alkaline earth metals which could deactivate the catalyst, corrode reactors, as well as reduce heat transfer. In the next step, RSM was used to optimize the reaction condition for hard/softwood conversion. LA yields of 68.9 mol% and 50.3 mol% were obtained, followed by 79.7 mol% and 66.3 mol% from the pretreated newsprint, respectively. The optimized condition for hardwood conversion gave a LA yield of 73.4 mol% from the untreated newsprint, representing a 7.8% reduction. The observed reduction in LA yield shows that decationization is an important step in the chemo-catalytic conversion of newsprint to LA.

Next, LA yields from HCl and Fenton pretreated NP were optimized and compared using RSM at different ranges of temperature (180-200 ^{o}C), reaction time (3.5-4.5 h), $FeCl_3.6H_2O$ concentration (0.1-0.2 M), and a fixed amount of LiCl (20 wt-%). The predicted maximum yields of LA were 83.4 mol% and 86.4 mol%, respectively, followed by an actual yield of 81.3 mol% and 84.0 mol % for the HCl and Fenton pretreated newsprint, revealing a better performance of the Fenton newsprint in terms of yield. Also, the Fenton newsprint is more sensitive to temperature as confirmed by its activation energy (Ea) values which are higher than those of HCl newsprint. The higher Ea values for the Fenton-NP imply that more kinetic energy is required to break their bonds. SEM imaging showed that the HCl and Fenton

newsprints shared some similarities with the untreated newsprints, however, both are fluffy and shorter in appearance.

Next, an integrated approach leveraging the use of enzymes, followed by a mild acidic aqueous solution was investigated for the conversion of untreated newsprint. In the first step, the newsprint was hydrolysed to sugars in a moist solid environment, taking advantage of enzymes instead of the typical harsh reagents and conditions. In the second step, the sugars were dehydrated under mild chemical conditions with the $AlCl_3.6H_2O$ catalyst at 150 ^oC, to generate HMF and FU in yields as high as 66 mol% and 65 mol%, respectively in 40 min. The renewable nature of the enzyme, which is non-toxic and the less water waste produced with moist-solid mixture makes this process an attractive alternative for future biorefinery. Another aspect is the use of $AlCl_3.6H_2O$, an inexpensive and less toxic catalyst which was sufficient to dehydrate the sugars in the presence of a biphasic media.

Finally, the catalytic activities of $FeCl_3.6H_2O$ and $AlCl_3.6H_2O$ were screened for the valorization of untreated corrugated boxes with limited end-use application. $AlCl_3.6H_2O$ outperformed $FeCl_3.6H_2O$ due to its smaller atomic radii, which is responsible for a stronger electrostatic interaction with glucose. $AlCl_3.6H_2O$ further combines with LiCl as a co-catalyst, improving the selectivity and yield of HMF and FU. Optimized reaction conditions were established based on a trade-off between $AlCl_3.6H_2O$/LiCl/NaCl in H_2O/MIBK biphasic media, affording HMF and FU in maximum yields of 98 mol% and 51 mol%, at 160 ^oC and 40 min, respectively. Also, kinetic study reveals that the biphasic system could effectively avoid the occurrence of side reactions, thus enhancing the yield of HMF and FU.

7.2 Contributions to knowledge

Despite the extensive research on LA, HMF, and FU production from C6 and C5 sugars, there is a lack of data on the use of paper wastes for this purpose. By attempting the decationization and dilute acid hydrolysis of wood pulp, paper waste was valorised, following a similar route. Since these wastes are cheap and widely available, they have tremendous potential to not only reduce the operational cost of the biorefinery, but also to extend their product portfolio. While most research on paper waste has focused on its valorization to bioethanol, this work is among the few on the chemo-catalytic conversion of these refuses. The following is the knowledge contributed to this field:

1. To the best of the author's knowledge, this work is the first to valorize newsprint and corrugated boxes into platform chemicals.
2. This work reveals the effectiveness of pretreatment on paper waste conversion to LA.
3. This work evaluates the hydrolysis of newsprint to sugars using enzymes prior to HMF and FU production in the presence of a low concentration of $AlCl_3.6H_2O$.
4. This work also presented various kinetic models, providing deeper insights on the various elementary stages necessary for paper waste conversion to the products of interest.

7.3 Recommendations for future research

The effective valorization of paper waste opens several opportunities that can facilitate developing a modular biorefinery, however, some recommendations are as follows:

1. The focus on lignocellulose biomass poses no threat to the food supply, making them a viable feedstock for the biorefinery. Among them, paper waste stands out because it is cheap and readily available; however, it requires preliminary screening and sorting, followed by deinking (in most cases) to ensure that it is suitable for use. These steps may add extra units to the biorefinery and may in turn increase its operating cost.

2. Pretreatment is another essential prerequisite to enhance the susceptibility of the lignocellulose to catalytic attack. An ideal pretreatment would among others, reduce the lignin content, increase the biomass surface area and concomitantly reduce the cellulose crystallinity. While some pretreatments are energy intensive, others have moderate to high environmental impact. Therefore a trade-off between these factors must be placed into consideration when making a decision.

3. The strategy of an integrated biological and chemical approach was introduced in this study. The remarkable advantage of this process is its ability to produce HMF and FU in a relatively high yield. This study provides a new route for HMF and FU preparation, which avoids the use of expensive solvents and thus significantly reduced its operating cost. However, the process parameters need further optimization to improve its accuracy and enhance product yields.

4. Lastly, studies on the downstream processing of HMF and FU is still emerging, existing more on a lab-scale. Since such a process is complex; contributing majorly to the cost of operating the biorefinery, additional process intensification on an industrial scale is inevitable if the production of HMF and FU will be competitive.

8 List of References

[1] M. Elheddad, C. Benjasak, R. Deljavan, M. Alharthi, and J. M. Almabrok, "The effect of the Fourth Industrial Revolution on the environment: The relationship between electronic finance and pollution in OECD countries," *Technological Forecasting and Social Change*, vol. 163, p. 120485, 2021.

[2] H. Chen *et al.*, "A review on the pretreatment of lignocellulose for high-value chemicals," *Fuel Processing Technology*, vol. 160, pp. 196-206, 2017.

[3] W.-C. Tu and J. P. Hallett, "Recent advances in the pretreatment of lignocellulosic biomass," *Current opinion in green and sustainable chemistry*, vol. 20, pp. 11-17, 2019.

[4] C. Loerbroks, "Acid Hydrolysis of Cellulose and the Anomeric Effect: A Computational Study," 2014.

[5] K. S. Alongi and G. C. Shields, "Theoretical calculations of acid dissociation constants: a review article," in *Annual reports in computational chemistry*, vol. 6: Elsevier, 2010, pp. 113-138.

[6] C. Li, Q. Wang, and Z. K. Zhao, "Acid in ionic liquid: An efficient system for hydrolysis of lignocellulose," *Green Chemistry*, vol. 10, no. 2, pp. 177-182, 2008.

[7] Y. B. Tewari and R. N. Goldberg, "Thermodynamics of hydrolysis of disaccharides. Cellobiose, gentiobiose, isomaltose, and maltose," *Journal of Biological Chemistry*, vol. 264, no. 7, pp. 3966-3971, 1989.

[8] J. H. Q. Pinto and S. Kaliaguine, "A Monte Carlo analysis of acid hydrolysis of glycosidic bonds in polysaccharides," *AIChE journal*, vol. 37, no. 6, pp. 905-914, 1991.

[9] W. Faith, "Development of the Scholler process in the United States," *Industrial & Engineering Chemistry*, vol. 37, no. 1, pp. 9-11, 1945.

[10] F. Bergius, "Conversion of wood to carbohydrates," *Industrial & Engineering Chemistry*, vol. 29, no. 3, pp. 247-253, 1937.

[11] E. E. Harris and E. Beglinger, "Madison Wood Sugar Process," *Industrial & Engineering Chemistry*, vol. 38, no. 9, pp. 890-895, 1946.

[12] K. Freudenberg and G. Blomqvist, "Die Hydrolyse der Cellulose und ihrer Oligosaccharide," *Berichte der deutschen chemischen Gesellschaft (A and B Series)*, vol. 68, no. 11, pp. 2070-2082, 1935.

[13] J. F. Saeman, "Kinetics of wood saccharification-hydrolysis of cellulose and decomposition of sugars in dilute acid at high temperature," *Industrial & Engineering Chemistry*, vol. 37, no. 1, pp. 43-52, 1945.

[14] M. Sasaki, Z. Fang, Y. Fukushima, T. Adschiri, and K. Arai, "Dissolution and hydrolysis of cellulose in subcritical and supercritical water," *Industrial & Engineering Chemistry Research*, vol. 39, no. 8, pp. 2883-2890, 2000, doi: https://doi.org/10.1021/ie990690j.

[15] R. Rinaldi, N. Meine, J. vom Stein, R. Palkovits, and F. Schüth, "Which controls the depolymerization of cellulose in ionic liquids: the solid acid catalyst or cellulose?," *ChemSusChem: Chemistry & Sustainability Energy & Materials*, vol. 3, no. 2, pp. 266-276, 2010.

[16] H. Kobayashi, T. Komanoya, S. K. Guha, K. Hara, and A. Fukuoka, "Conversion of cellulose into renewable chemicals by supported metal catalysis," *Applied Catalysis A: General*, vol. 409, pp. 13-20, 2011.

[17] A. A. Rosatella, S. P. Simeonov, R. F. Frade, and C. A. Afonso, "5-Hydroxymethylfurfural (HMF) as a building block platform: Biological properties, synthesis and synthetic applications," *Green Chemistry*, vol. 13, no. 4, pp. 754-793, 2011.

[18] J. M. Rippe, "Fructose, high fructose corn syrup, sucrose, and health: modern scientific understandings," in *Fructose, High Fructose Corn Syrup, Sucrose and Health*: Springer, 2014, pp. 3-12.
[19] B. Kamm, P. R. Gruber, and M. Kamm, *Biorefineries-industrial processes and products* (no. 1). Wiley-VCH Weinheim, 2006.
[20] I. Delidovich and R. Palkovits, "Catalytic Isomerization of Biomass-Derived Aldoses: A Review," *ChemSusChem*, vol. 9, no. 6, pp. 547-561, 2016.
[21] S. J. Angyal, "The Lobry de Bruyn-Alberda van Ekenstein Transformation and Related Reactions," in *Glycoscience: Epimerisation, Isomerisation and Rearrangement Reactions of Carbohydrates*, A. E. Stütz Ed. Berlin, Heidelberg: Springer Berlin Heidelberg, 2001, pp. 1-14.
[22] V. Choudhary, A. B. Pinar, R. F. Lobo, D. G. Vlachos, and S. I. Sandler, "Comparison of homogeneous and heterogeneous catalysts for glucose-to-fructose isomerization in aqueous media," *ChemSusChem*, vol. 6, no. 12, pp. 2369-2376, 2013.
[23] C. J. Knill and J. F. Kennedy, "Degradation of cellulose under alkaline conditions," *Carbohydrate polymers*, vol. 51, no. 3, pp. 281-300, 2003.
[24] S. Kobayashi, "Scandium triflate in organic synthesis," *European journal of organic chemistry*, vol. 1999, no. 1, pp. 15-27, 1999.
[25] R. Gounder and M. E. Davis, "Monosaccharide and disaccharide isomerization over Lewis acid sites in hydrophobic and hydrophilic molecular sieves," *Journal of catalysis*, vol. 308, pp. 176-188, 2013.
[26] M. Moliner, Y. Román-Leshkov, and M. E. Davis, "Tin-containing zeolites are highly active catalysts for the isomerization of glucose in water," *Proceedings of the National Academy of Sciences*, vol. 107, no. 14, pp. 6164-6168, 2010.
[27] W. R. Gunther *et al.*, "Sn-Beta zeolites with borate salts catalyse the epimerization of carbohydrates via an intramolecular carbon shift," *Nature communications*, vol. 3, no. 1, pp. 1-8, 2012.
[28] M. Ioelovich and E. Morag, "Study of enzymatic hydrolysis of mild pretreated lignocellulosic biomasses," *BioResources*, vol. 7, no. 1, pp. 1040-1052, 2012.
[29] S. Paul and A. Dutta, "Challenges and opportunities of lignocellulosic biomass for anaerobic digestion," *Resources, Conservation and Recycling*, vol. 130, pp. 164-174, 2018, doi: https://doi.org/10.1016/j.resconrec.2017.12.005.
[30] FAO. "2012 Global Forest Products Facts and Figures." (accessed.
[31] D. Chakraborty, S. Dahiya, K. Amulya, V. Srivastav, and S. V. Mohan, "Valorization of paper and pulp waste: Opportunities and prospects of biorefinery," in *Industrial and Municipal Sludge*: Elsevier, 2019, pp. 623-656.
[32] S. El-Haggar and A. Samaha, "Sustainable Utilization of Municipal Solid Waste," in *Roadmap for Global Sustainability—Rise of the Green Communities*: Springer, 2019, pp. 189-203.
[33] O. M. Okeyinka, "THE APPLICABILITY OF RECYCLED WASTE PAPER AS LIGHTWEIGHT BUILDING MATERIALS," 2016.
[34] D. Hoornweg and P. Bhada-Tata, "What a waste: a global review of solid waste management," 2012.
[35] J. Larson, J. Baker, G. Latta, S. Ohrel, and C. Wade, "Modeling international trade of forest products: Application of PPML to a gravity model of trade," *Forest Products Journal*, vol. 68, no. 3, pp. 303-316, 2018.
[36] S. G. Kinsella, G Mills, V Rycroft, N Ford, J Sheehan, K Martin, J "The State of the Paper Industry Monitoring the Indicators of Environmental Performance," *Environmental Paper Network*, 2007.
[37] D. C. Wilson *et al.*, *Global waste management outlook*. UNEP, 2015.

[38] Eurostat, "Packaging waste statistics https://ec.europa.eu/eurostat/statistics-explained/pdfscache/10547.pdf," 2020.
[39] Environmental Paper Network, "The State of the Global Paper Industry Shifting Seas: New Challenges and Opportunities for Forests, People and the Climate," 2018.
[40] Confederation of European Paper Industries, *Strategy on Recycling: the Paper Industry's Point of View: The Confederation of European Paper Industries (CEPI)'s Contribution to the Thematic Strategy on Waste Recycling*. 2003.
[41] B. Nepal and V. Aggarwal, "Papercrete: A study on green structural material," *International Journal of Applied Engineering Research*, vol. 9, no. 3, pp. 253-260, 2014.
[42] U. EPA, "Municipal solid waste generation, recycling, and disposal in the United States: facts and figures for 2012," *US Environ. Prot. Agency*, pp. 1-13, 2014.
[43] T. Yamada, M. Asari, T. Miura, T. Niijima, J. Yano, and S.-i. Sakai, "Municipal solid waste composition and food loss reduction in Kyoto City," *Journal of Material Cycles and Waste Management*, vol. 19, no. 4, pp. 1351-1360, 2017/10/01 2017, doi: https://doi.org/10.1007/s10163-017-0643-z.
[44] R. Toczyłowska-Mamińska, "Limits and perspectives of pulp and paper industry wastewater treatment – A review," *Renewable and Sustainable Energy Reviews*, vol. 78, pp. 764-772, 2017/10/01/ 2017, doi: https://doi.org/10.1016/j.rser.2017.05.021.
[45] T. Ochuodho, C. Johnston, and P. Withey, "Assessing economic impacts of internet adoption through reduced pulp and paper demand," *Canadian Journal of Forest Research*, vol. 47, no. 10, pp. 1381-1391, 2017.
[46] T. J. Rainey and G. Covey, *Pulp and paper production from sugarcane bagasse*. John Wiley & Sons, Inc., Hoboken, NJ, USA, 2016.
[47] S. Neil, "Working Partner Update: Conservatree, Inc https://ilsr.org/working-partner-update-conservatree-inc/," 2018.
[48] "Pulp and Paper Technology," *https://www.pulpandpaper-technology.com/articles/top-largest-paper-producing-companies-in-the-world*.
[49] K. Schaefer and V. Fiber, "Outlook for the World Paper Grade Pulp Market," ed, 2015.
[50] L. Oliver, "The displacement of China's non-wood pulp capacity https://www.hawkinswright.com/news-and-events/blog/post/hawkins-wright-blog/2016/03/23/the-displacement-of-china," 2016.
[51] Environmental Paper Network, "The State of the Paper Industry : Monitoring the Indicators of Environmental Performance https://environmentalpaper.org/wp-content/uploads/2017/08/state-of-the-paper-industry-2007-executive.pdf," 2007.
[52] M. Haggith, *Paper Trails: From Trees to Trash-the True Cost of Paper*. Random House, 2008.
[53] C. Staub, "Resource Recycling : China's Sword effort continues to rattle market," 2017.
[54] E. W. Peter, Moore, "The Challenges, Opportunities and Solutions to Increasing Paper Recovery in Developing Countries: The New Paper Chase," 2013.
[55] Y. S. Jang *et al.*, "Bio-based production of C2–C6 platform chemicals," *Biotechnology and bioengineering*, vol. 109, no. 10, pp. 2437-2459, 2012, doi: https://doi.org/10.1002/bit.24599.
[56] T. Werpy and G. Petersen, "Top value added chemicals from biomass: volume I--results of screening for potential candidates from sugars and synthesis gas " National Renewable Energy Lab., Golden, CO (US), 2004.
[57] J. J. P. Bozell, Gene R "Technology development for the production of biobased products from biorefinery carbohydrates—the US Department of Energy's "Top 10" revisited," *Green Chemistry*, vol. 12, no. 4, pp. 539-554, 2010, doi: https://doi.org/10.1039/B922014C.

[58] S. Choi, C. W. Song, J. H. Shin, and S. Y. Lee, "Biorefineries for the production of top building block chemicals and their derivatives," *Metabolic Engineering*, vol. 28, pp. 223-239, 2015, doi: https://doi.org/10.1016/j.ymben.2014.12.007.

[59] H. Kobayashi, Y. Yamakoshi, Y. Hosaka, M. Yabushita, and A. Fukuoka, "Production of sugar alcohols from real biomass by supported platinum catalyst," *Catalysis Today*, vol. 226, pp. 204-209, 2014, doi: https://doi.org/10.1016/j.cattod.2013.09.057.

[60] W. Deng, H. Zhang, L. Xue, Q. Zhang, and Y. Wang, "Selective activation of the C–O bonds in lignocellulosic biomass for the efficient production of chemicals," *Chinese Journal of Catalysis*, vol. 36, no. 9, pp. 1440-1460, 2015, doi: https://doi.org/10.1016/S1872-2067(15)60923-8.

[61] D. A. Sladkovskiy, L. I. Godina, K. V. Semikin, E. V. Sladkovskaya, D. A. Smirnova, and D. Y. Murzin, "Process design and techno-economical analysis of hydrogen production by aqueous phase reforming of sorbitol," *Chemical Engineering Research and Design*, vol. 134, pp. 104-116, 2018, doi: https://doi.org/10.1016/j.cherd.2018.03.041.

[62] J. Li, A. Spina, J. A. Moulijn, and M. Makkee, "Sorbitol dehydration into isosorbide in a molten salt hydrate medium," *Catalysis Science & Technology*, vol. 3, no. 6, pp. 1540-1546, 2013, doi: https://doi.org/10.1039/C3CY20809E.

[63] A. Fukuoka and P. L. Dhepe, "Catalytic conversion of cellulose into sugar alcohols," *Angewandte Chemie International Edition*, vol. 45, no. 31, pp. 5161-5163, 2006, doi: https://doi.org/10.1002/anie.200601921.

[64] C. W. Luo, Shuai Liu, Haichao, "Cellulose conversion into polyols catalyzed by reversibly formed acids and supported ruthenium clusters in hot water," *Angewandte Chemie International Edition*, vol. 46, no. 40, pp. 7636-7639, 2007, doi: https://doi.org/10.1002/anie.200702661.

[65] W. Deng, X. Tan, W. Fang, Q. Zhang, and Y. Wang, "Conversion of cellulose into sorbitol over carbon nanotube-supported ruthenium catalyst," *Catalysis Letters*, vol. 133, no. 1-2, p. 167, 2009, doi: https://doi.org/10.1007/s10562-009-0136-3.

[66] L. N. W. Ding, Ai-Qin Zheng, Ming-Yuan Zhang, Tao "Selective transformation of cellulose into sorbitol by using a bifunctional nickel phosphide catalyst," *ChemSusChem*, vol. 3, no. 7, pp. 818-821, 2010, doi: https://doi.org/10.1002/cssc.201000092.

[67] J. Pang *et al.*, "Catalytic conversion of cellulose to hexitols with mesoporous carbon supported Ni-based bimetallic catalysts," *Green Chemistry*, vol. 14, no. 3, pp. 614-617, 2012, doi: https://doi.org/10.1039/C2GC16364K.

[68] J. Xi *et al.*, "Direct conversion of cellulose into sorbitol with high yield by a novel mesoporous niobium phosphate supported Ruthenium bifunctional catalyst," *Applied Catalysis A: General*, vol. 459, pp. 52-58, 2013, doi: https://doi.org/10.1016/j.apcata.2013.03.047.

[69] L. S. Ó. Ribeiro, José JM Pereira, Manuel Fernando R "Enhanced direct production of sorbitol by cellulose ball-milling," *Green Chemistry*, vol. 17, no. 5, pp. 2973-2980, 2015, doi: https://doi.org/10.1039/C5GC00039D

[70] L. S. Ribeiro, J. J. Delgado, J. J. Órfão, and M. F. R. Pereira, "Carbon supported Ru-Ni bimetallic catalysts for the enhanced one-pot conversion of cellulose to sorbitol," *Applied Catalysis B: Environmental*, vol. 217, pp. 265-274, 2017, doi: https://doi.org/10.1016/j.apcatb.2017.04.078.

[71] P. K. Yang, Hirokazu Hara, Kenji Fukuoka, Atsushi, "Phase change of nickel phosphide catalysts in the conversion of cellulose into sorbitol," *ChemSusChem*, vol. 5, no. 5, pp. 920-926, 2012, doi: https://doi.org/10.1002/cssc.201100498.

[72] S. G. Van de Vyver, Jan Dusselier, Michiel Schepers, Hans Vosch, Tom Zhang, Liang Van Tendeloo, Gustaaf Jacobs, Pierre A Sels, Bert F "Selective bifunctional catalytic conversion of cellulose over reshaped Ni particles at the tip of carbon nanofibers," *ChemSusChem*, vol. 3, no. 6, pp. 698-701, 2010, doi: https://doi.org/10.1002/cssc.201000087.

[73] W. Zhu *et al.*, "Efficient hydrogenolysis of cellulose into sorbitol catalyzed by a bifunctional catalyst," *Green Chemistry*, vol. 16, no. 3, pp. 1534-1542, 2014, doi: https://doi.org/10.1039/C3GC41917G.

[74] L. S. Ribeiro, J. J. de Melo Órfão, and M. F. R. Pereira, "Direct catalytic production of sorbitol from waste cellulosic materials," *Bioresource Technology*, vol. 232, pp. 152-158, 2017, doi: https://doi.org/10.1016/j.biortech.2017.02.008.

[75] M. Yabushita, H. Kobayashi, and A. J. A. C. B. E. Fukuoka, "Catalytic transformation of cellulose into platform chemicals," *Applied Catalysis B: Environmental*, vol. 145, pp. 1-9, 2014, doi: https://doi.org/10.1016/j.apcatb.2013.01.052.

[76] M. Liu, W. Deng, Q. Zhang, Y. Wang, and Y. Wang, "Polyoxometalate-supported ruthenium nanoparticles as bifunctional heterogeneous catalysts for the conversions of cellobiose and cellulose into sorbitol under mild conditions," *Chemical Communications*, vol. 47, no. 34, pp. 9717-9719, 2011, doi: https://doi.org/10.1039/C1CC12506K.

[77] R. Mu *et al.*, "Synergetic Effect of Surface and Subsurface Ni Species at Pt–Ni Bimetallic Catalysts for CO Oxidation," *Journal of the American Chemical Society*, vol. 133, no. 6, pp. 1978-1986, 2011/02/16 2011, doi: https://doi.org/10.1021/ja109483a.

[78] N. Ji *et al.*, "Direct catalytic conversion of cellulose into ethylene glycol using nickel-promoted tungsten carbide catalysts," *Angewandte Chemie International Edition*, vol. 47, no. 44, pp. 8510-8513, 2008, doi: https://doi.org/10.1002/anie.200803233.

[79] N. Ji *et al.*, "Catalytic conversion of cellulose into ethylene glycol over supported carbide catalysts," *Catalysis Today*, vol. 147, no. 2, pp. 77-85, 2009, doi: https://doi.org/10.1016/j.cattod.2009.03.012.

[80] N. Ji, M. Zheng, A. Wang, T. Zhang, and J. G. Chen, "Nickel-Promoted Tungsten Carbide Catalysts for Cellulose Conversion: Effect of Preparation Methods," *ChemSusChem*, vol. 5, no. 5, pp. 939-944, 2012, doi: https://doi.org/10.1002/cssc.201100575.

[81] N. Ji *et al.*, "Direct catalytic conversion of cellulose into ethylene glycol using nickel-promoted tungsten carbide catalysts," *Angewandte Chemie*, vol. 120, no. 44, pp. 8638-8641, 2008, doi: https://doi.org/10.1002/anie.200803233.

[82] M. Y. W. Zheng, Ai-Qin Ji, Na Pang, Ji-Feng Wang, Xiao-Dong Zhang, Tao "Transition metal–tungsten bimetallic catalysts for the conversion of cellulose into ethylene glycol," *ChemSusChem: Chemistry Sustainability Energy & Material*, vol. 3, no. 1, pp. 63-66, 2010, doi: https://doi.org/10.1002/cssc.200900197.

[83] Y. W. Cao, Junwei Kang, Maoqing Zhu, Yulei, "Efficient synthesis of ethylene glycol from cellulose over Ni–WO3/SBA-15 catalysts," *Journal of Molecular Catalysis A: Chemical*, vol. 381, pp. 46-53, 2014/01/01/ 2014, doi: https://doi.org/10.1016/j.molcata.2013.10.002.

[84] O. V. Manaenkov *et al.*, "Ru-Containing Magnetically Recoverable Catalysts: A Sustainable Pathway from Cellulose to Ethylene and Propylene Glycols," *ACS Applied*

Materials & Interfaces, vol. 8, no. 33, pp. 21285-21293, 2016/08/24 2016, doi: https://doi.org/10.1021/acsami.6b05096.

[85] Z. Guanhong, M. Zheng, W. Aiqin, and T. Zhang, "Catalytic conversion of cellulose to ethylene glycol over tungsten phosphide catalysts," *Chinese Journal of Catalysis*, vol. 31, no. 8, pp. 928-932, 2010.

[86] Z. Z. Tai, Junying Wang, Aiqin Zheng, Mingyuan Zhang, Tao, "Temperature-controlled phase-transfer catalysis for ethylene glycol production from cellulose," *Chemical Communications*, vol. 48, no. 56, pp. 7052-7054, 2012, doi: https://doi.org/10.1039/C2CC32305B.

[87] Y. Liu, C. Luo, and H. Liu, "Tungsten Trioxide Promoted Selective Conversion of Cellulose into Propylene Glycol and Ethylene Glycol on a Ruthenium Catalyst," *Angewandte Chemie International Edition*, vol. 51, no. 13, pp. 3249-3253, 2012, doi: https://doi.org/10.1002/anie.201200351.

[88] L. l. S. O. r. o. Ribeiro, Joana de Melo Órfão, José J. Pereira, M. Fernando R., "Hydrolytic hydrogenation of cellulose to ethylene glycol over carbon nanotubes supported Ru-W bimetallic catalysts," *Cellulose*, vol. 25, no. 4, pp. 2259-2272, 2018, doi: https://doi.org/10.1007/s10570-018-1721-7.

[89] Z. Tai, J. Zhang, A. Wang, J. Pang, M. Zheng, and T. Zhang, "Catalytic Conversion of Cellulose to Ethylene Glycol over a Low-Cost Binary Catalyst of Raney Ni and Tungstic Acid," *ChemSusChem*, vol. 6, no. 4, pp. 652-658, 2013, doi: https://doi.org/10.1002/cssc.201200842.

[90] Z.-q. Xiao, J.-w. Mao, J.-b. Ji, R.-y. Sha, F. Yu, and X. Chuang, "Preparation of nano-scale nickel-tungsten catalysts by pH value control and application in hydrogenolysis of cellulose to polyols," *Journal of Fuel Chemistry and Technology*, vol. 45, no. 6, pp. 641-650, 2017, doi: https://doi.org/10.1016/S1872-5813(17)30033-6.

[91] Y. Zhang, A. Wang, and T. Zhang, "A new 3D mesoporous carbon replicated from commercial silica as a catalyst support for direct conversion of cellulose into ethylene glycol," *Chemical Communications*, vol. 46, no. 6, pp. 862-864, 2010, doi: https://doi.org/10.1039/B919182H.

[92] J. Pang, M. Zheng, A. Wang, and T. Zhang, "Catalytic Hydrogenation of Corn Stalk to Ethylene Glycol and 1,2-Propylene Glycol," *Industrial & Engineering Chemistry Research*, vol. 50, no. 11, pp. 6601-6608, 2011/06/01 2011, doi: https://doi.org/10.1021/ie102505y.

[93] S. Wong, N. Ngadi, I. M. Inuwa, and O. Hassan, "Recent advances in applications of activated carbon from biowaste for wastewater treatment: a short review," *Journal of Cleaner Production*, vol. 175, pp. 361-375, 2018, doi: https://doi.org/10.1016/j.jclepro.2017.12.059.

[94] X. Zhao *et al.*, "Activated Carbon and Ordered Mesoporous Carbon-Based Catalysts for Biomass Conversion," *Nanoporous Catalysts for Biomass Conversion*, pp. 17-54, 2017.

[95] R. Wang, C. Tian, L. Wang, B. Wang, H. Zhang, and H. Fu, "In situ simultaneous synthesis of WC/graphitic carbon nanocomposite as a highly efficient catalyst support for DMFC," *Chemical Communications*, no. 21, pp. 3104-3106, 2009, doi: https://doi.org/10.1039/B901089K.

[96] M. Y. Zheng, A. Q. Wang, N. Ji, J. F. Pang, X. D. Wang, and T. Zhang, "Transition metal–tungsten bimetallic catalysts for the conversion of cellulose into ethylene glycol," *ChemSusChem: Chemistry & Sustainability Energy & Materials*, vol. 3, no. 1, pp. 63-66, 2010.

[97] D. Y. Jo, M. W. Lee, C. H. Kim, J. W. Choung, H. C. Ham, and K.-Y. Lee, "Interplay of ligand and strain effects in CO adsorption on bimetallic Cu/M (M= Ni, Ir, Pd, and

Pt) catalysts from first-principles: Effect of different facets on catalysis," *Catalysis Today*, 2019, doi: https://doi.org/10.1016/j.cattod.2019.05.031.
[98] F. Liu, C. Wu, and S. Yang, "Strain and Ligand Effects on CO2 Reduction Reactions over Cu–Metal Heterostructure Catalysts," *The Journal of Physical Chemistry C*, vol. 121, no. 40, pp. 22139-22146, 2017, doi: https://doi.org/10.1021/acs.jpcc.7b07081.
[99] Z. Xiao, S. Jin, M. Pang, and C. Liang, "Conversion of highly concentrated cellulose to 1, 2-propanediol and ethylene glycol over highly efficient CuCr catalysts," *Green Chemistry*, vol. 15, no. 4, pp. 891-895, 2013, doi: https://doi.org/10.1039/C3GC40134K.
[100] Z. Xiao, S. Jin, G. Sha, C. T. Williams, and C. Liang, "Two-step conversion of biomass-derived glucose with high concentration over Cu–Cr catalysts," *Industrial & Engineering Chemistry Research*, vol. 53, no. 21, pp. 8735-8743, 2014, doi: https://doi.org/10.1021/ie5012189.
[101] A. Perosa and P. Tundo, "Selective hydrogenolysis of glycerol with raney nickel," *Industrial & Engineering Chemistry Research*, vol. 44, no. 23, pp. 8535-8537, 2005, doi: https://doi.org/10.1021/ie0489251.
[102] M. Roehr, C. P. Kubicek, and J. c. Komínek, "Gluconic acid," *Biotechnology: Products of Primary Metabolism*, pp. 347-362, 1996.
[103] P. Pal, R. Kumar, and S. Banerjee, "Manufacture of gluconic acid: A review towards process intensification for green production," *Chemical Engineering and Processing: Process Intensification*, vol. 104, pp. 160-171, 2016/06/01/ 2016, doi: https://doi.org/10.1016/j.cep.2016.03.009.
[104] S. Ramachandran, P. Fontanille, A. Pandey, and C. Larroche, "Gluconic acid: Properties, applications and microbial production," *Food Technology & Biotechnology*, vol. 44, no. 2, 2006.
[105] L. P. Vandenberghe, S. G. Karp, P. Z. de Oliveira, J. C. de Carvalho, C. Rodrigues, and C. R. Soccol, "Solid-state fermentation for the production of organic acids," in *Current Developments in Biotechnology and Bioengineering*: Elsevier, 2018, pp. 415-434.
[106] F. Tarekegn and S. A. Jabasingh, "Gluconic acid production from cane molasses using Aspergillus carneus," *Emerging Trends in Chemical Engineering*, vol. 6, no. 3, pp. 37-44, 2019.
[107] H. Zhang, J. Zhang, and J. Bao, "High titer gluconic acid fermentation by Aspergillus niger from dry dilute acid pretreated corn stover without detoxification," *Bioresource Technology*, vol. 203, pp. 211-219, 2016, doi: https://doi.org/10.1016/j.biortech.2015.12.042.
[108] F. Lu *et al.*, "Enhancing gluconic acid production by controlling the morphology of Aspergillus niger in submerged fermentation," *Process Biochemistry*, vol. 50, no. 9, pp. 1342-1348, 2015, doi: https://doi.org/10.1016/j.procbio.2015.04.010.
[109] H. L. Zhang, Ning Pan, Xuejun Wu, Shubin Xie, Jun "Direct Transformation of Cellulose to Gluconic Acid in a Concentrated Iron (III) Chloride Solution under Mild Conditions," *ACS Sustainable Chemistry Engineering*, vol. 5, no. 5, pp. 4066-4072, 2017, doi: https://doi.org/10.1021/acssuschemeng.7b00060.
[110] X. D. Tan, Weiping Liu, Mi Zhang, Qinghong Wang, Ye "Carbon nanotube-supported gold nanoparticles as efficient catalysts for selective oxidation of cellobiose into gluconic acid in aqueous medium," *Chemical Communications*, no. 46, pp. 7179-7181, 2009, doi: https://doi.org/10.1039/B917224F.
[111] J. Zhang, X. Liu, M. N. Hedhili, Y. Zhu, and Y. Han, "Highly selective and complete conversion of cellobiose to gluconic acid over Au/Cs2HPW12O40 nanocomposite catalyst," *ChemCatChem*, vol. 3, no. 8, pp. 1294-1298, 2011, doi: https://doi.org/10.1002/cctc.201100106.

[112] D. An, A. Ye, W. Deng, Q. Zhang, and Y. Wang, "Selective Conversion of Cellobiose and Cellulose into Gluconic Acid in Water in the Presence of Oxygen, Catalyzed by Polyoxometalate-Supported Gold Nanoparticles," *Chemistry - A European Journal*, vol. 18, no. 10, pp. 2938-2947, 2012, doi: https://doi.org/10.1002/chem.201103262.
[113] P. N. L. Amaniampong, Kaixin Jia, Xinli Wang, Bo Borgna, Armando Yang, Yanhui "Titania-supported gold nanoparticles as efficient catalysts for the oxidation of cellobiose to organic acids in aqueous medium," *ChemCatChem* vol. 6, no. 7, pp. 2105-2114, 2014, doi: https://doi.org/10.1002/cctc.201402096.
[114] P. N. J. Amaniampong, Xinli Wang, Bo Mushrif, Samir H Borgna, Armando Yang, Yanhui, "Catalytic oxidation of cellobiose over TiO 2 supported gold-based bimetallic nanoparticles," *Catalysis Science & Technology*, vol. 5, no. 4, pp. 2393-2405, 2015, doi: https://doi.org/10.1039/C4CY01566E.
[115] K. Morawa Eblagon, M. F. R. Pereira, and J. L. Figueiredo, "One-pot oxidation of cellobiose to gluconic acid. Unprecedented high selectivity on bifunctional gold catalysts over mesoporous carbon by integrated texture and surface chemistry optimization," *Applied Catalysis B: Environmental*, vol. 184, pp. 381-396, 2016/05/05/ 2016, doi: https://doi.org/10.1016/j.apcatb.2015.10.011.
[116] N. Mager, N. Meyer, A. F. Léonard, N. Job, M. Devillers, and S. Hermans, "Functionalization of carbon xerogels for the preparation of palladium supported catalysts applied in sugar transformations," *Applied Catalysis B: Environmental*, vol. 148, pp. 424-435, 2014, doi: https://doi.org/10.1016/j.apcatb.2013.11.028.
[117] A. Onda, T. Ochi, and K. Yanagisawa, "New direct production of gluconic acid from polysaccharides using a bifunctional catalyst in hot water," *Catalysis Communications*, vol. 12, no. 6, pp. 421-425, 2011, doi: https://doi.org/10.1016/j.catcom.2010.10.023.
[118] F. Liu, Z. Xue, X. Zhao, H. Mou, J. He, and T. Mu, "Catalytic deep eutectic solvents for highly efficient conversion of cellulose to gluconic acid with gluconic acid self-precipitation separation," *Chemical Communications*, vol. 54, no. 48, pp. 6140-6143, 2018, doi: https://doi.org/10.1039/C8CC03798A.
[119] H. Zhang, B. Dai, X. Wang, L. Xu, and M. Zhu, "Hydrochlorination of acetylene to vinyl chloride monomer over bimetallic Au–La/SAC catalysts," *Journal of Industrial and Engineering Chemistry*, vol. 18, no. 1, pp. 49-54, 2012, doi: https://doi.org/10.1016/j.jiec.2011.11.075.
[120] A. Onda, T. Ochi, K. Kajiyoshi, and K. Yanagisawa, "A new chemical process for catalytic conversion of D-glucose into lactic acid and gluconic acid," *Applied Catalysis A: General*, vol. 343, no. 1-2, pp. 49-54, 2008, doi: https://doi.org/10.1016/j.apcata.2008.03.017.
[121] K.-i. Shimizu, H. Furukawa, N. Kobayashi, Y. Itaya, and A. Satsuma, "Effects of Brønsted and Lewis acidities on activity and selectivity of heteropolyacid-based catalysts for hydrolysis of cellobiose and cellulose," *Green Chemistry*, vol. 11, no. 10, pp. 1627-1632, 2009, doi: https://doi.org/10.1039/B913737H.
[122] X. Zhu, M.-Y. Han, P. Li, and L. Wang, "Photoinduced difunctionalization of 2, 3-dihydrofuran for the efficient synthesis of 2, 3-disubstituted tetrahydrofurans," *Organic Chemistry Frontiers*, vol. 4, no. 8, pp. 1640-1646, 2017, doi: https://doi.org/10.1039/C7QO00242D.
[123] Q. Sun, Y. Men, J. Wang, S. Chai, and Q. Song, "Support effect of Ag/ZnO catalysts for partial oxidation of methanol," *Inorganic Chemistry Communications*, vol. 92, pp. 51-54, 2018, doi: https://doi.org/10.1016/j.inoche.2018.04.001.
[124] D. Pal, R. Chand, S. Upadhyay, and P. Mishra, "Performance of water gas shift reaction catalysts: A review," *Renewable and Sustainable Energy Reviews*, vol. 93, pp. 549-565, 2018, doi: https://doi.org/10.1016/j.rser.2018.05.003.

[125] J. Escobar, M. C. Barrera, V. Santes, and J. E. Terrazas, "Naphthalene hydrogenation over Mg-doped Pt/Al2O3," *Catalysis Today*, vol. 296, pp. 197-204, 2017, doi: https://doi.org/10.1016/j.cattod.2017.04.064.
[126] W. Huang, Z. Zuo, P. Han, Z. Li, and T. Zhao, "XPS and XRD investigation of Co/Pd/TiO2 catalysts by different preparation methods," *Journal of Electron Spectroscopy and Related Phenomena*, vol. 173, no. 2-3, pp. 88-95, 2009, doi: https://doi.org/10.1016/j.elspec.2009.05.012.
[127] O. M. Gazit and A. Katz, "Understanding the role of defect sites in glucan hydrolysis on surfaces," *Journal of the American Chemical Society*, vol. 135, no. 11, pp. 4398-4402, 2013, doi: https://doi.org/10.1021/ja311918z.
[128] A. Takagaki, C. Tagusagawa, and K. Domen, "Glucose production from saccharides using layered transition metal oxide and exfoliated nanosheets as a water-tolerant solid acid catalyst," *Chemical Communications*, no. 42, pp. 5363-5365, 2008, doi: https://doi.org/10.1039/B810346A.
[129] T. Moreno, G. Kouzaki, M. Sasaki, M. Goto, and M. J. Cocero, "Uncatalysed wet oxidation of d-glucose with hydrogen peroxide and its combination with hydrothermal electrolysis," *Carbohydrate Research*, vol. 349, pp. 33-38, 2012, doi: https://doi.org/10.1016/j.carres.2011.12.005.
[130] D. Rinsant, G. Chatel, and F. Jérôme, "Efficient and Selective Oxidation of D-Glucose into Gluconic acid under Low-Frequency Ultrasonic Irradiation," *ChemCatChem*, vol. 6, no. 12, pp. 3355-3359, 2014, doi: https://doi.org/10.1002/cctc.201402604.
[131] J. García-Álvarez, "Deep eutectic mixtures: Promising sustainable solvents for metal-catalysed and metal-mediated organic reactions," *European Journal of Inorganic Chemistry*, vol. 2015, no. 31, pp. 5147-5157, 2015, doi: https://doi.org/10.1002/ejic.201500892.
[132] B. Tang, H. Zhang, and K. H. Row, "Application of deep eutectic solvents in the extraction and separation of target compounds from various samples," *Journal of Separation Science*, vol. 38, no. 6, pp. 1053-1064, 2015, doi: https://doi.org/10.1002/jssc.201401347.
[133] N. Guajardo, C. Carlesi, R. Schrebler, and J. Morales, "Applications of Liquid/Liquid Biphasic Oxidations by Hydrogen Peroxide with Ionic Liquids or Deep Eutectic Solvents," *ChemPlusChem*, vol. 82, no. 2, pp. 165-176, 2017, doi: https://doi.org/10.1002/cplu.201600594

[134] Q. B. Zhang, Maud De Oliveira Vigier, Karine Barrault, Joël Jérôme, François "Green and inexpensive choline-derived solvents for cellulose decrystallization," *Chemistry–A European Journal*, vol. 18, no. 4, pp. 1043-1046, 2012, doi: https://doi.org/10.1002/chem.201103271.
[135] A. Biswas, R. L. Shogren, D. G. Stevenson, J. L. Willett, and P. K. Bhowmik, "Ionic liquids as solvents for biopolymers: Acylation of starch and zein protein," *Carbohydrate Polymers*, vol. 66, no. 4, pp. 546-550, 2006/11/23/ 2006, doi: https://doi.org/10.1016/j.carbpol.2006.04.005.
[136] A. Yadav, A. Chaudhari, and R. Kothari, "Bioconversion of renewable resources into lactic acid: an industrial view," *Critical Reviews in Biotechnology*, vol. 31, no. 1, pp. 1-19, 2011, doi: https://doi.org/10.3109/07388550903420970.
[137] L. D. Gottumukkala, K. Haigh, F.-X. Collard, E. van Rensburg, and J. Görgens, "Opportunities and prospects of biorefinery-based valorisation of pulp and paper sludge," *Bioresource Technology*, vol. 215, pp. 37-49, 2016/09/01/ 2016, doi: https://doi.org/10.1016/j.biortech.2016.04.015.

[138] M. Karamanlioglu, R. Preziosi, and G. D. Robson, "Abiotic and biotic environmental degradation of the bioplastic polymer poly (lactic acid): a review," *Polymer Degradation and Stability*, vol. 137, pp. 122-130, 2017, doi: https://doi.org/10.1016/j.polymdegradstab.2017.01.009.
[139] S. Yamaguchi, K. Motokura, K. Tanaka, and S. Imamura, "Catalytic processes for utilizing carbohydrates derived from algal biomass," *Catalysts*, vol. 7, no. 5, p. 163, 2017.
[140] F. Jin, Z. Zhou, H. Enomoto, T. Moriya, and H. Higashijima, "Conversion mechanism of cellulosic biomass to lactic acid in subcritical water and acid–base catalytic effect of subcritical water," *Chemistry Letters*, vol. 33, no. 2, pp. 126-127, 2004, doi: https://doi.org/10.1246/cl.2004.126.
[141] X. Yan, F. Jin, K. Tohji, A. Kishita, and H. Enomoto, "Hydrothermal conversion of carbohydrate biomass to lactic acid," *AIChE journal*, vol. 56, no. 10, pp. 2727-2733, 2010, doi: https://doi.org/10.1002/aic.12193.
[142] C. E. Sánchez, Itziar García, Araceli Llano-Ponte, Rodrigo Labidi, Jalel, "Lactic acid production by alkaline hydrothermal treatment of corn cobs," *Chemical Engineering Journal*, vol. 181, pp. 655-660, 2012, doi: https://doi.org/10.1016/j.cej.2011.12.033.
[143] F. R. Chambon, Franck Pinel, Catherine Cabiac, Amandine Guillon, Emmanuelle Essayem, Nadine, "Cellulose hydrothermal conversion promoted by heterogeneous Brønsted and Lewis acids: remarkable efficiency of solid Lewis acids to produce lactic acid," *Applied Catalysis B: Environmental*, vol. 105, no. 1-2, pp. 171-181, 2011, doi: https://doi.org/10.1016/j.apcatb.2011.04.009.
[144] F.-F. Wang, C.-L. Liu, and W.-S. Dong, "Highly efficient production of lactic acid from cellulose using lanthanide triflate catalysts," *Green chemistry*, vol. 15, no. 8, pp. 2091-2095, 2013, doi: https://doi.org/10.1039/C3GC40836A.
[145] X. Lei, F.-F. Wang, C.-L. Liu, R.-Z. Yang, and W.-S. Dong, "One-pot catalytic conversion of carbohydrate biomass to lactic acid using an ErCl3 catalyst," *Applied Catalysis A: General*, vol. 482, pp. 78-83, 2014, doi: https://doi.org/10.1016/j.apcata.2014.05.029.
[146] F.-F. Wang, J. Liu, H. Li, C.-L. Liu, R.-Z. Yang, and W.-S. Dong, "Conversion of cellulose to lactic acid catalyzed by erbium-exchanged montmorillonite K10," *Green Chemistry*, vol. 17, no. 4, pp. 2455-2463, 2015, doi: https://doi.org/10.1039/C4GC02131B.
[147] H. Li, Y. Qu, Y. Yang, S. Chang, and J. Xu, "Microwave irradiation–A green and efficient way to pretreat biomass," *Bioresource technology*, vol. 199, pp. 34-41, 2016.
[148] Y. Wang *et al.*, "Chemical synthesis of lactic acid from cellulose catalysed by lead (II) ions in water," *Nature Communications*, vol. 4, p. 2141, 2013, doi: https://doi.org/10.1038/ncomms3141.
[149] Z. Tang *et al.*, "Transformation of Cellulose and its Derived Carbohydrates into Formic and Lactic Acids Catalyzed by Vanadyl Cations," *ChemSusChem*, vol. 7, no. 6, pp. 1557-1567, 2014, doi: https://doi.org/10.1002/cssc.201400150.
[150] P. Wattanapaphawong, P. Reubroycharoen, and A. Yamaguchi, "Conversion of cellulose into lactic acid using zirconium oxide catalysts," *RSC Advances*, vol. 7, no. 30, pp. 18561-18568, 2017, doi: https://doi.org/10.1039/C6RA28568F.
[151] P. S. Wattanapaphawong, Osamu Sato, Koichi Mimura, Naoki Reubroycharoen, Prasert Yamaguchi, Aritomo "Conversion of Cellulose to Lactic Acid by Using ZrO2–Al2O3 Catalysts," *Catalysts*, vol. 7, no. 7, p. 221, 2017, doi: https://doi.org/10.3390/catal7070221.
[152] S. Zhang, F. Jin, J. Hu, and Z. Huo, "Improvement of lactic acid production from cellulose with the addition of Zn/Ni/C under alkaline hydrothermal conditions,"

Bioresource Technology, vol. 102, no. 2, pp. 1998-2003, 2011, doi: https://doi.org/10.1016/j.biortech.2010.09.049.

[153] R. Sakhuja, K. Pericherla, K. Bajaj, B. Khungar, and A. Kumar, "Ytterbium Triflate Catalyzed Synthesis of Heterocycles," *Synthesis*, vol. 48, no. 24, pp. 4305-4346, 2016, doi: https://doi.org/10.1055/s-0036-1588321.

[154] N. Narra, B. N. P. Rachapudi, S. P. B. Vemulapalli, and P. V. Korlipara, "Lewis-acid catalyzed synthesis and characterization of novel castor fatty acid-based cyclic carbonates," *RSC Advances*, vol. 6, no. 31, pp. 25703-25712, 2016, doi: https://doi.org/10.1039/C6RA00880A.

[155] Z. Fang, B. Liu, J. Luo, Y. Ren, and Z. Zhang, "Efficient conversion of carbohydrates into 5-hydroxymethylfurfural catalyzed by the chromium-exchanged montmorillonite K-10 clay," *Biomass and Bioenergy*, vol. 60, pp. 171-177, 2014, doi: https://doi.org/10.1016/j.biombioe.2013.12.002.

[156] X. Yang, L. Yang, W. Fan, and H. Lin, "Effect of redox properties of LaCoO3 perovskite catalyst on production of lactic acid from cellulosic biomass," *Catalysis Today*, vol. 269, pp. 56-64, 2016/07/01/ 2016, doi: https://doi.org/10.1016/j.cattod.2015.12.003.

[157] J. Wang *et al.*, "A highly selective and stable ZnO-ZrO2 solid solution catalyst for CO2 hydrogenation to methanol," *Science Advances*, vol. 3, no. 10, p. e1701290, 2017, doi: https://doi.org/10.1126/sciadv.1701290.

[158] S. Tosoni, H.-Y. T. Chen, A. Ruiz Puigdollers, and G. Pacchioni, "TiO2 and ZrO2 in biomass conversion: why catalyst reduction helps," *Philosophical Transactions of the Royal Society A: Mathematical, Physical and Engineering Sciences*, vol. 376, no. 2110, p. 20170056, 2017, doi: https://doi.org/10.1098/rsta.2017.0056.

[159] L. Yang, X. Yang, E. Tian, V. Vattipalli, W. Fan, and H. J. J. o. c. Lin, "Mechanistic insights into the production of methyl lactate by catalytic conversion of carbohydrates on mesoporous Zr-SBA-15," *Journal of Catalysis*, vol. 333, pp. 207-216, 2016, doi: https://doi.org/10.1016/j.jcat.2015.10.013.

[160] T. Werpy *et al.*, "Top value added chemicals from biomass. Volume 1-Results of screening for potential candidates from sugars and synthesis gas,," Department of Energy Washington DC, 2004.

[161] U. Omoruyi, S. Page, J. Hallett, and P. W. Miller, "Homogeneous catalyzed reactions of levulinic acid: to γ-valerolactone and beyond," *ChemSusChem*, vol. 9, no. 16, pp. 2037-2047, 2016, doi: https://doi.org/10.1002/cssc.201600517.

[162] J. Ahlkvist, "Formic and Levulinic Acid from Cellulose via Heterogeneous Catalysis," Doctoral thesis, comprehensive summary, Umeå universitet, Umeå, 2014. [Online]. Available: http://urn.kb.se/resolve?urn=urn:nbn:se:umu:diva-85216

[163] S. Wetzel, L. C. Duchesne, and M. F. Laporte, "Biochemicals," *Bioproducts from canada's forests: New Partnerships in the Bioeconomy*, pp. 61-69, 2006.

[164] J. W. Shen, Charles E "Hydrochloric acid-catalyzed levulinic acid formation from cellulose: data and kinetic model to maximize yields," *AIChE Journal*, vol. 58, no. 1, pp. 236-246, 2012, doi: https://doi.org/10.1002/aic.12556.

[165] R. Weingarten, W. C. Conner, and G. W. Huber, "Production of levulinic acid from cellulose by hydrothermal decomposition combined with aqueous phase dehydration with a solid acid catalyst," *Energy & Environmental Science*, vol. 5, no. 6, pp. 7559-7574, 2012.

[166] W. Liu *et al.*, "Efficient conversion of cellulose to glucose, levulinic acid, and other products in hot water using SO2 as a recoverable catalyst," *Industrial & Engineering Chemistry Research*, vol. 51, no. 47, pp. 15503-15508, 2012, doi: https://doi.org/10.1021/ie302317t.

[167] L. L. Peng, Lu Zhang, Junhua Zhuang, Junping Zhang, Beixiao Gong, Yan "Catalytic conversion of cellulose to levulinic acid by metal chlorides," *Molecules*, vol. 15, no. 8, pp. 5258-5272, 2010, doi: https://doi.org/10.3390/molecules15085258.
[168] B. Girisuta, L. Janssen, and H. Heeres, "Kinetic study on the acid-catalyzed hydrolysis of cellulose to levulinic acid," *Industrial & Engineering Chemistry Research*, vol. 46, no. 6, pp. 1696-1708, 2007, doi: https://doi.org/10.1021/ie061186z.
[169] S. S. Joshi, A. D. Zodge, K. V. Pandare, and B. D. Kulkarni, "Efficient Conversion of Cellulose to Levulinic Acid by Hydrothermal Treatment Using Zirconium Dioxide as a Recyclable Solid Acid Catalyst," *Industrial & Engineering Chemistry Research*, vol. 53, no. 49, pp. 18796-18805, 2014, doi: https://doi.org/10.1021/ie5011838.
[170] M. Xiang, Liu, J., Fu, W., Tang, T., & Wu, D. , "Improved activity for cellulose conversion to levulinic acid through hierarchization of ETS-10 zeolite.," *ACS Sustainable Chemistry & Engineering*, vol. 5, no. 7, pp. 5800-5809., 2017, doi: https://doi.org/10.1021/acssuschemeng.7b00529.
[171] D. M. G. Alonso, Jean Marcel R Mellmer, Max A Wettstein, Stephanie G Dumesic, James A "Direct conversion of cellulose to levulinic acid and gamma-valerolactone using solid acid catalysts," *Catalysis Science Technology*, vol. 3, no. 4, pp. 927-931, 2013, doi: https://doi.org/10.1039/C2CY20689G.
[172] Y. Zuo, Y. Zhang, and Y. Fu, "Catalytic conversion of cellulose into levulinic acid by a sulfonated chloromethyl polystyrene solid acid catalyst," *ChemCatChem*, vol. 6, no. 3, pp. 753-757, 2014, doi: https://doi.org/10.1002/cctc.201300956.
[173] S. G. Wettstein, D. M. Alonso, Y. Chong, and J. A. Dumesic, "Production of levulinic acid and gamma-valerolactone (GVL) from cellulose using GVL as a solvent in biphasic systems," *Energy & Environmental Science*, vol. 5, no. 8, pp. 8199-8203, 2012, doi: https://doi.org/10.1039/C2EE22111J.
[174] H. Ren, Y. Zhou, and L. Liu, "Selective conversion of cellulose to levulinic acid via microwave-assisted synthesis in ionic liquids," *Bioresource Technology*, vol. 129, pp. 616-619, 2013, doi: https://doi.org/10.1016/j.biortech.2012.12.132.
[175] Y. Shen, J.-K. Sun, Y.-X. Yi, B. Wang, F. Xu, and R.-C. Sun, "One-pot synthesis of levulinic acid from cellulose in ionic liquids," *Bioresource Technology*, vol. 192, pp. 812-816, 2015, doi: https://doi.org/10.1016/j.biortech.2015.05.080.
[176] H. Ren, B. Girisuta, Y. Zhou, and L. Liu, "Selective and recyclable depolymerization of cellulose to levulinic acid catalyzed by acidic ionic liquid," *Carbohydrate Polymers*, vol. 117, pp. 569-576, 2015, doi: https://doi.org/10.1016/j.carbpol.2014.09.091.
[177] Z. Sun *et al.*, "One-pot depolymerization of cellulose into glucose and levulinic acid by heteropolyacid ionic liquid catalysis," *Rsc Advances*, vol. 2, no. 24, pp. 9058-9065, 2012, doi: https://doi.org/10.1039/C2RA01328B.
[178] J. S. Potvin, Erin Hegner, Jessica DeBoef, Brenton Lucht, Brett L "Effect of NaCl on the conversion of cellulose to glucose and levulinic acid via solid supported acid catalysis," *Tetrahedron Letters*, vol. 52, no. 44, pp. 5891-5893, 2011, doi: https://doi.org/10.1016/j.tetlet.2011.09.013.
[179] D. Ding, J. Wang, J. Xi, X. Liu, G. Lu, and Y. Wang, "High-yield production of levulinic acid from cellulose and its upgrading to γ-valerolactone," *Green Chemistry*, vol. 16, no. 8, pp. 3846-3853, 2014.
[180] A. S. M. Khan, Zakaria Bustam, Mohamad Azmi Kait, Chong Fai Nasrullah, Asma Ullah, Zahoor Sarwono, Ariyanti Ahamd, Pervaiz Muhammad, Nawshad, "Dicationic ionic liquids as sustainable approach for direct conversion of cellulose to levulinic acid," *Journal of Cleaner Production*, vol. 170, pp. 591-600, 2018, doi: https://doi.org/10.1016/j.jclepro.2017.09.103.

[181] H. Lin *et al.*, "High yield production of levulinic acid by catalytic partial oxidation of cellulose in aqueous media," *Energy & Environmental Science,* vol. 5, no. 12, pp. 9773-9777, 2012, doi: https://doi.org/10.1039/C2EE23225A.
[182] D.-m. Lai, L. Deng, Q.-x. Guo, and Y. Fu, "Hydrolysis of biomass by magnetic solid acid," *Energy & Environmental Science,* vol. 4, no. 9, pp. 3552-3557, 2011, doi: https://doi.org/10.1039/C1EE01526E.
[183] A. M. R. A. Galletti, Claudia De Luise, Valentina Licursi, Domenico Nassi, Nicoletta "Levulinic acid production from waste biomass," *BioResources,* vol. 7, no. 2, pp. 1824-1835, 2012.
[184] S. S. Chen *et al.*, "Valorization of lignocellulosic fibres of paper waste into levulinic acid using solid and aqueous Brønsted acid," *Bioresource Technology,* vol. 247, pp. 387-394, 2018/01/01/ 2018, doi: https://doi.org/10.1016/j.biortech.2017.09.110.
[185] A. Yüksel Özşen, "Conversion of Biomass to Organic Acids by Liquefaction Reactions Under Subcritical Conditions," *Frontiers in Chemistry,* vol. 8, p. 24, 2020, doi: https://doi.org/10.3389/fchem.2020.00024.
[186] A. Mukherjee, M.-J. Dumont, and V. Raghavan, "Sustainable production of hydroxymethylfurfural and levulinic acid: Challenges and opportunities," *Biomass and Bioenergy,* vol. 72, pp. 143-183, 2015, doi: https://doi.org/10.1016/j.biombioe.2014.11.007.
[187] M. Akizuki, T. Fujii, R. Hayashi, and Y. Oshima, "Effects of water on reactions for waste treatment, organic synthesis, and bio-refinery in sub- and supercritical water," *Journal of Bioscience and Bioengineering,* vol. 117, no. 1, pp. 10-18, 2014/01/01/ 2014, doi: https://doi.org/10.1016/j.jbiosc.2013.06.011.
[188] U. Kaatze, "Water, the special liquid," *Journal of Molecular Liquids,* vol. 259, pp. 304-318, 2018/06/01/ 2018, doi: https://doi.org/10.1016/j.molliq.2018.03.038.
[189] M. Plaza and C. Turner, "Pressurized hot water extraction of bioactives," *Green Extraction Techniques: Principles, Advances and Applications,* vol. 76, p. 53e82, 2017, doi: https://doi.org/10.1016/j.molliq.2018.03.038.
[190] M. E. Zakrzewska, E. Bogel-Łukasik, and R. Bogel-Łukasik, "Ionic liquid-mediated formation of 5-hydroxymethylfurfural□ A promising biomass-derived building block," *Chemical Reviews,* vol. 111, no. 2, pp. 397-417, 2011, doi: https://doi.org/10.1021/cr100171a.
[191] F. Tao, H. Song, and L. Chou, "Hydrolysis of cellulose in SO3H-functionalized ionic liquids," *Bioresource Technology,* vol. 102, no. 19, pp. 9000-9006, 2011, doi: https://doi.org/10.1016/j.biortech.2011.06.067.
[192] K. B. Sidhpuria, A. L. Daniel-da-Silva, T. Trindade, and J. A. Coutinho, "Supported ionic liquid silica nanoparticles (SILnPs) as an efficient and recyclable heterogeneous catalyst for the dehydration of fructose to 5-hydroxymethylfurfural," *Green Chemistry,* vol. 13, no. 2, pp. 340-349, 2011, doi: https://doi.org/10.1039/C0GC00690D.
[193] S. Maiti *et al.*, "Microwave-assisted one-pot conversion of agro-industrial wastes into levulinic acid: An alternate approach," *Bioresource Technology,* vol. 265, pp. 471-479, 2018, doi: https://doi.org/10.1016/j.biortech.2018.06.012.
[194] S. Chatterjee, S. Gangopadhyay, S. Patra, and S. P. Chowdhury, "An overview of different approaches for sustainable production and convertibility of hydroxymethylfurfural," *International Journal of Research in Engineering and Technology,* vol. 5, no. 1, pp. 45-52, 2016.
[195] A. El Kadib, A. Finiels, and D. Brunel, "Sulfonic acid functionalised ordered mesoporous materials as catalysts for fine chemical synthesis," *Chemical Communications,* vol. 49, no. 80, pp. 9073-9076, 2013, doi: https://doi.org/10.1039/C3CC45160G.

[196] W. Zeng, D.-g. Cheng, F. Chen, and X. Zhan, "Catalytic conversion of glucose on Al–Zr mixed oxides in hot compressed water," *Catalysis Letters*, vol. 133, no. 1-2, p. 221, 2009, doi: https://doi.org/10.1007/s10562-009-0160-3.
[197] S. Van de Vyver *et al.*, "Catalytic production of levulinic acid from cellulose and other biomass-derived carbohydrates with sulfonated hyperbranched poly (arylene oxindole) s," *Energy & Environmental Science*, vol. 4, no. 9, pp. 3601-3610, 2011, doi: https://doi.org/10.1039/C1EE01418H.
[198] X. Hu, Wang, S., Westerhof, R. J., Wu, L., Song, Y., Dong, D., & Li, C. Z., "Acid-catalyzed conversion of C6 sugar monomer/oligomers to levulinic acid in water, tetrahydrofuran and toluene: Importance of the solvent polarity," *Fuel*, vol. 141, pp. 56-63., 2015, doi: https://doi.org/10.1016/j.fuel.2014.10.034.
[199] F. Menegazzo, E. Ghedini, and M. Signoretto, "5-Hydroxymethylfurfural (HMF) production from real biomasses," *Molecules*, vol. 23, no. 9, p. 2201, 2018.
[200] G. W. Huber, J. N. Chheda, C. J. Barrett, and J. A. Dumesic, "Production of liquid alkanes by aqueous-phase processing of biomass-derived carbohydrates," *Science*, vol. 308, no. 5727, pp. 1446-1450, 2005, doi: https://doi.org/10.1126/science.1111166.
[201] T. Kläusli, "On Platform Chemicals from Renewables. ," *ACS Network Chemistry Community Online*, 2014, doi: https://doi.org/10.1515/gps-2014-0029.
[202] A. I. Torres, P. Daoutidis, and M. Tsapatsis, "Continuous production of 5-hydroxymethylfurfural from fructose: a design case study," *Energy & Environmental Science*, vol. 3, no. 10, pp. 1560-1572, 2010, doi: https://doi.org/10.1039/C0EE00082E.
[203] H. Lü, X. Li, and M. Zhang, "Decomposition of cellulose to produce 5-hydroxymethyl-furaldehyde in subcritical water," *Transactions of Tianjin University*, vol. 14, no. 3, pp. 198-201, 2008, doi: https://doi.org/10.10.1007/s12209-008-0036-4.
[204] K. Ehara and S. Saka, "Decomposition behavior of cellulose in supercritical water, subcritical water, and their combined treatments," *Journal of Wood Science*, vol. 51, no. 2, pp. 148-153, 2005, doi: https://doi.org/10.1007/s10086-004-0626-2.
[205] P. Wang, H. Yu, S. Zhan, and S. Wang, "Catalytic hydrolysis of lignocellulosic biomass into 5-hydroxymethylfurfural in ionic liquid," *Bioresource Technology*, vol. 102, no. 5, pp. 4179-4183, 2011, doi: https://doi.org/10.1016/j.biortech.2010.12.073.
[206] X. Du, J. Zhang, Y. Wang, and Y. Qu, "Conversion of carbohydrates into platform chemicals catalyzed by alkaline ionic liquids," *Catalysts*, vol. 7, no. 9, p. 245, 2017, doi: https://doi.org/10.3390/catal7090245.
[207] K. Y. G. Nandiwale, Nitish D Thakur, Pratika Sawant, Sanjay D Zambre, Vishal P Bokade, Vijay V, "One-pot synthesis of 5-hydroxymethylfurfural by cellulose hydrolysis over highly active bimodal micro/mesoporous H-ZSM-5 catalyst," *ACS Sustainable Chemistry Engineering*, vol. 2, no. 7, pp. 1928-1932, 2014, doi: https://doi.org/10.1021/sc500270z.
[208] X. Zhang, D. Zhang, Z. Sun, L. Xue, X. Wang, and Z. Jiang, "Highly efficient preparation of HMF from cellulose using temperature-responsive heteropolyacid catalysts in cascade reaction," *Applied Catalysis B: Environmental*, vol. 196, pp. 50-56, 2016.
[209] X. Li, K. Peng, Q. Xia, X. Liu, and Y. Wang, "Efficient conversion of cellulose into 5-hydroxymethylfurfural over niobia/carbon composites," *Chemical Engineering Journal*, vol. 332, pp. 528-536, 2018, doi: https://doi.org/10.1016/j.cej.2017.06.105.
[210] Y. W. Zhao, Shurong Lin, Haizhou Chen, Jingping Xu, Hao "Influence of a Lewis acid and a Brønsted acid on the conversion of microcrystalline cellulose into 5-hydroxymethylfurfural in a single-phase reaction system of water and 1, 2-dimethoxyethane," *RSC Advances*, vol. 8, no. 13, pp. 7235-7242, 2018, doi: https://doi.org/10.1039/C7RA13387A.

[211] L. Yang, X. Yan, S. Xu, H. Chen, H. Xia, and S. Zuo, "One-pot synthesis of 5-hydroxymethylfurfural from carbohydrates using an inexpensive FePO 4 catalyst," *RSC Advances*, vol. 5, no. 26, pp. 19900-19906, 2015, doi: https://doi.org/10.1039/C4RA16145A.
[212] N. Shi, Q. Liu, Q. Zhang, T. Wang, and L. Ma, "High yield production of 5-hydroxymethylfurfural from cellulose by high concentration of sulfates in biphasic system," *Green Chemistry*, vol. 15, no. 7, pp. 1967-1974, 2013, doi: https://doi.org/10.1039/C3GC40667A.
[213] E. M. Leng, Ming Peng, Yang Li, Xiaomin Gong, Xun Zhang, Yang, "The Direct Conversion of Cellulose into 5-Hydroxymethylfurfural with CrCl3 Composite Catalyst in Ionic Liquid under Mild Conditions," *ChemistrySelect*, vol. 4, no. 1, pp. 181-189, 2019, doi: https://doi.org/10.1002/slct.201803130.
[214] W.-H. L. Hsu, Yin-Ying Peng, Wun-Huei Wu, Kevin C-W "Cellulosic conversion in ionic liquids (ILs): Effects of H2O/cellulose molar ratios, temperatures, times, and different ILs on the production of monosaccharides and 5-hydroxymethylfurfural (HMF)," *Catalysis Today*, vol. 174, no. 1, pp. 65-69, 2011, doi: https://doi.org/10.1016/j.cattod.2011.03.020.
[215] J. B. R. Binder, Ronald T "Fermentable sugars by chemical hydrolysis of biomass," *Proceedings of the National Academy of Sciences*, vol. 107, no. 10, pp. 4516-4521, 2010, doi: https://doi.org/10.1073/pnas.0912073107
[216] Z. S. Li, Kunmei Ren, Jun Yang, Dongjiang Cheng, Bowen Kim, Chan Kyung Yao, Xiangdong "Direct catalytic conversion of glucose and cellulose," *Green Chemistry*, vol. 20, no. 4, pp. 863-872, 2018, doi: https://doi.org/1010.1039/C7GC03318D.
[217] S. F. Eminov, Paraskevi Brandt, Agnieszka Wilton-Ely, James DET Hallett, Jason P "Direct catalytic conversion of cellulose to 5-hydroxymethylfurfural using ionic liquids," *Inorganics*, vol. 4, no. 4, p. 32, 2016, doi: https://doi.org/10.3390/inorganics4040032.
[218] S. Xiao, B. Liu, Y. Wang, Z. Fang, and Z. Zhang, "Efficient conversion of cellulose into biofuel precursor 5-hydroxymethylfurfural in dimethyl sulfoxide–ionic liquid mixtures," *Bioresource Technology*, vol. 151, pp. 361-366, 2014, doi: https://doi.org/10.1016/j.biortech.2013.10.095.
[219] S. Yin, Y. Pan, and Z. Tan, "Hydrothermal conversion of cellulose to 5-hydroxymethyl furfural," *International Journal of Green Energy*, vol. 8, no. 2, pp. 234-247, 2011, doi: https://doi.org/10.1080/15435075.2010.548888.
[220] L. S. Atanda, Adib Mukundan, Swathi Shrotri, Abhijit Torres-Torres, Gilberto Beltramini, Jorge "Catalytic behaviour of TiO 2–ZrO 2 binary oxide synthesized by sol–gel process for glucose conversion to 5-hydroxymethylfurfural," *RSC Advances*, vol. 5, no. 98, pp. 80346-80352, 2015, doi: https://doi.org/10.1039/C5RA15739K.
[221] S. Zhao, M. Cheng, J. Li, J. Tian, and X. Wang, "One pot production of 5-hydroxymethylfurfural with high yield from cellulose by a Brønsted–Lewis–surfactant-combined heteropolyacid catalyst," *Chemical Communications*, vol. 47, no. 7, pp. 2176-2178, 2011, doi: https://doi.org/10.1039/C0CC04444J.
[222] G. Portillo Perez, A. Mukherjee, and M.-J. Dumont, "Insights into HMF catalysis," *Journal of Industrial and Engineering Chemistry*, vol. 70, pp. 1-34, 2019/02/25/ 2019, doi: https://doi.org/10.1016/j.jiec.2018.10.002.
[223] H. Ma, F. Wang, Y. Yu, L. Wang, and X. Li, "Autocatalytic Production of 5-Hydroxymethylfurfural from Fructose-Based Carbohydrates in a Biphasic System and Its Purification," *Industrial & Engineering Chemistry Research*, vol. 54, no. 10, pp. 2657-2666, 2015, doi: https://doi.org/10.1021/ie504791x.

[224] A. Ranoux, K. Djanashvili, I. W. Arends, and U. Hanefeld, "5-Hydroxymethylfurfural synthesis from hexoses is autocatalytic," *ACS Catalysis*, vol. 3, no. 4, pp. 760-763, 2013, doi: https://doi.org/10.1021/cs400099a.
[225] R. P. Swatloski, S. K. Spear, J. D. Holbrey, and R. D. Rogers, "Dissolution of cellose with ionic liquids," *Journal of the American Chemical Society*, vol. 124, no. 18, pp. 4974-4975, 2002, doi: https://doi.org/10.1021/ja025790m.
[226] K. Z. Mousavi, Y. Yamini, and S. Seidi, "Dispersive liquid–liquid microextraction using magnetic room temperature ionic liquid for extraction of ultra-trace amounts of parabens," *New Journal of Chemistry*, vol. 42, no. 12, pp. 9735-9743, 2018, doi: https://doi.org/10.1039/C8NJ01154K.
[227] F. Z. Jiang, Qingjun Ma, Ding Liu, Xiumei Han, Xiuwen "Direct conversion and NMR observation of cellulose to glucose and 5-hydroxymethylfurfural (HMF) catalyzed by the acidic ionic liquids," *Journal of Molecular Catalysis A: Chemical*, vol. 334, no. 1-2, pp. 8-12, 2011, doi: https://doi.org/10.1016/j.molcata.2010.10.006.
[228] C. Li and Z. K. Zhao, "Efficient acid-catalyzed hydrolysis of cellulose in ionic liquid," *Advanced Synthesis & Catalysis*, vol. 349, no. 11-12, pp. 1847-1850, 2007, doi: https://doi.org/10.1002/adsc.200700259.
[229] M. W. Roman, William T, "Effect of sulfate groups from sulfuric acid hydrolysis on the thermal degradation behavior of bacterial cellulose," *Biomacromolecules*, vol. 5, no. 5, pp. 1671-1677, 2004, doi: https://doi.org/10.1021/bm034519.
[230] F. Parveen, T. Patra, and S. Upadhyayula, "Hydrolysis of microcrystalline cellulose using functionalized Bronsted acidic ionic liquids – A comparative study," *Carbohydrate Polymers*, vol. 135, pp. 280-284, 2016/01/01/ 2016, doi: https://doi.org/10.1016/j.carbpol.2015.08.039.
[231] F. Tao, H. Song, and L. Chou, "Hydrolysis of cellulose by using catalytic amounts of FeCl2 in ionic liquids," *ChemSusChem*, vol. 3, no. 11, pp. 1298-1303, 2010, doi: https://doi.org/10.1002/cssc.201000184.
[232] H. Abou-Yousef and P. Steele, "Rapid conversion of cellulose to 5-hydroxymethylfurfural using single and combined metal chloride catalysts in ionic liquid," *Journal of Fuel Chemistry Technology*, vol. 41, no. 2, pp. 214-222, 2013, doi: https://doi.org/10.1016/S1872-5813(13)60013-4.
[233] Z. M. Xue, Ming-Guo Li, Zhonghao Mu, Tiancheng "Advances in the conversion of glucose and cellulose to 5-hydroxymethylfurfural over heterogeneous catalysts," *RSC Advances*, vol. 6, no. 101, pp. 98874-98892, 2016, doi: https://doi.org/10.1039/C6RA20547J.
[234] J.-A. L. Chun, Jin-Woo Yi, Young-Byung Hong, Seong-Sig Chung, Chung-Han, "Catalytic production of hydroxymethylfurfural from sucrose using 1-methyl-3-octylimidazolium chloride ionic liquid," *Korean Journal of Chemical Engineering*, vol. 27, no. 3, pp. 930-935, 2010, doi: https://doi.org/10.1007/s11814-010-0167-x.
[235] Y. Li, X. Zhang, G. He, and F. Zhang, "Sulfonated poly (phenylene sulfide) grafted polysulfone proton exchange membrane with improved stability," *International Journal of Hydrogen Energy*, vol. 42, no. 4, pp. 2360-2369, 2017, doi: https://doi.org/10.1016/j.ijhydene.2016.09.183.
[236] J. Guan, Cao, Q., Guo, X., & Mu, X., "The mechanism of glucose conversion to 5-hydroxymethylfurfural catalyzed by metal chlorides in ionic liquid: A theoretical study," *Computational and Theoretical Chemistry*, vol. 963, no. 2-3, pp. 453-462, 2011, doi: https://doi.org/10.1016/j.comptc.2010.11.012.
[237] Q. W. Zhao, Lei Zhao, Shun Wang, Xiaohong Wang, Shengtian "High selective production of 5-hydroymethylfurfural from fructose by a solid heteropolyacid catalyst,"

Fuel, vol. 90, no. 6, pp. 2289-2293, 2011, doi: https://doi.org/10.1016/j.fuel.2011.02.022.
[238] X. Liu *et al.*, "The degradation and saccharification of microcrystalline cellulose in aqueous acetone solution with low severity dilute sulfuric acid," *Process Biochemistry*, vol. 68, pp. 146-152, 2018, doi: https://doi.org/10.1016/j.procbio.2018.02.011.
[239] E. Kontturi *et al.*, "Degradation and crystallization of cellulose in hydrogen chloride vapor for high-yield isolation of cellulose nanocrystals," *Angewandte Chemie International Edition*, vol. 55, no. 46, pp. 14455-14458, 2016, doi: https://doi.org/10.1002/anie.201606626.
[240] K. M. Hello and E. K. Hlial, "Modification of silica with sulfuric acid and phosphoric acid for cellulose hydrolysis," in *Journal of Physics: Conference Series*, 2019, vol. 1294, no. 5: IOP Publishing, p. 052013, doi: https://doi.org/10.1088/1742-6596/1294/5/052013.
[241] R. Weingarten *et al.*, "Selective conversion of cellulose to hydroxymethylfurfural in polar aprotic solvents," *ChemCatChem*, vol. 6, no. 8, pp. 2229-2234, 2014, doi: https://doi.org/10.1002/cctc.201402299.
[242] J. B. Binder and R. T. Raines, "Simple Chemical Transformation of Lignocellulosic Biomass into Furans for Fuels and Chemicals," *Journal of the American Chemical Society*, vol. 131, no. 5, pp. 1979-1985, 2009/02/11 2009, doi: https://doi.org/10.1021/ja808537j.
[243] W. Z. Deng, Qinghong Wang, Ye, "Catalytic transformations of cellulose and its derived carbohydrates into 5-hydroxymethylfurfural, levulinic acid, and lactic acid," *Science China Chemistry*, vol. 58, no. 1, pp. 29-46, 2015, doi: https://doi.org/10.1007/s11426-014-5283-8.
[244] S. Soltani, U. Rashid, S. I. Al-Resayes, and I. A. Nehdi, "Recent progress in synthesis and surface functionalization of mesoporous acidic heterogeneous catalysts for esterification of free fatty acid feedstocks: A review," *Energy Conversion and Management*, vol. 141, pp. 183-205, 2017, doi: https://doi.org/10.1016/j.enconman.2016.07.042.
[245] F. S. Asghari and H. Yoshida, "Dehydration of fructose to 5-hydroxymethylfurfural in sub-critical water over heterogeneous zirconium phosphate catalysts," *Carbohydrate Research*, vol. 341, no. 14, pp. 2379-2387, 2006, doi: https://doi.org/10.1016/j.carres.2006.06.025.
[246] C.-W. Z. Jiang, Xin Luo, Zheng-Hong "An improved kinetic model for cellulose hydrolysis to 5-hydroxymethylfurfural using the solid SO 4 2−/Ti-MCM-41 catalyst," *RSC Advances*, vol. 4, no. 29, pp. 15216-15224, 2014, doi: https://doi.org/10.1039/C4RA00167B.
[247] A. C. Chareonlimkun, V Shotipruk, A Laosiripojana, N "Reactions of C5 and C6-sugars, cellulose, and lignocellulose under hot compressed water (HCW) in the presence of heterogeneous acid catalysts," *Fuel*, vol. 89, no. 10, pp. 2873-2880, 2010, doi: https://doi.org/10.1016/j.fuel.2010.03.015.
[248] N. L. Shi, Qiying Wang, Tiejun Ma, Longlong Zhang, Qi Zhang, Qing "One-pot degradation of cellulose into furfural compounds in hot compressed steam with dihydric phosphates," *ACS Sustainable Chemistry & Engineering*, vol. 2, no. 4, pp. 637-642, 2014, doi: https://doi.org/10.1016/j.biortech.2015.05.080.
[249] X. Jia, X. Zhang, N. Rui, X. Hu, and C.-j. Liu, "Structural effect of Ni/ZrO2 catalyst on CO2 methanation with enhanced activity," *Applied Catalysis B: Environmental*, vol. 244, pp. 159-169, 2019, doi: https://doi.org/10.1016/j.apcatb.2018.11.024.

[250] Y. Román-Leshkov and J. A. Dumesic, "Solvent effects on fructose dehydration to 5-hydroxymethylfurfural in biphasic systems saturated with inorganic salts," *Topics in Catalysis*, vol. 52, no. 3, pp. 297-303, 2009.
[251] S. Y. Xu, Xiaopei Bu, Quan Xia, Haian "Highly efficient conversion of carbohydrates into 5-hydroxymethylfurfural using the bi-functional CrPO 4 catalyst," *RSC Advances*, vol. 6, no. 10, pp. 8048-8052, 2016, doi: https://doi.org/10.1039/C5RA23716E.
[252] J. B. Mensah, I. Delidovich, P. J. Hausoul, L. Weisgerber, W. Schrader, and R. Palkovits, "Mechanistic Studies of the Cu (OH)+-Catalyzed Isomerization of Glucose into Fructose in Water," *ChemSusChem*, vol. 11, no. 15, pp. 2579-2586, 2018, doi: https://doi.org/10.1002/cssc.201800483.
[253] M. Misono, "Unique acid catalysis of heteropoly compounds (heteropolyoxometalates) in the solid state," *Chemical Communications*, no. 13, pp. 1141-1152, 2001, doi: https://doi.org/10.1039/B102573M.
[254] E. Commission, "Accelerating the development of the market for bio-based products in Europe," 2007.
[255] P. Nelson, E. Hood, and R. Powell, "The bioeconomy: a new era of products derived from renewable plant-based feedstocks," *Plant Biomass Conversion*, pp. 1-20, 2011.
[256] R. Taylor *et al.*, "From the Sugar Platform to biofuels and biochemicals : Final report for the European Commission Directorate-General Energy," E4tech/Re-CORD/Wageningen UR, 2015. [Online]. Available: https://edepot.wur.nl/360244
[257] R. Chinthapalli *et al.*, "Biobased building blocks and polymers—Global capacities, production and trends, 2018–2023," *Industrial Biotechnology*, vol. 15, no. 4, pp. 237-241, 2019.
[258] IHS Markit, "Ethylene Glycols : Chemical Economics Handbook https://ihsmarkit.com/products/ethylene-glycols-chemical-economics-handbook.html," 2020.
[259] J. R. Ochoa-Gómez and T. Roncal, "Production of sorbitol from Biomass," in *Production of Platform Chemicals from Sustainable Resources*: Springer, 2017, pp. 265-309.
[260] N. von Weymarn, *Process Development for Mannitol Production by Lactid Acid Bacteria*. Helsinki University of Technology 2002.
[261] J. C. Van der Waal and E. de Jong, "Avantium Chemicals: The high potential for the levulinic product tree," *Ind Biorenewables*, vol. 4, pp. 97-120, 2016.
[262] D. Datta, M. E. Marti, D. Pal, and S. Kumar, "Equilibrium Study on the extraction of levulinic acid from aqueous solution with Aliquat 336 dissolved in different diluents: Solvent's polarity effect and column design," *Journal of Chemical & Engineering Data*, vol. 62, no. 1, pp. 3-10, 2017.
[263] A. Kumar, D. Z. Shende, and K. L. Wasewar, "Extractive separation of levulinic acid using natural and chemical solvents," *Chemical Data Collections*, p. 100417, 2020.
[264] L. Moens, "Sugar cane as a renewable feedstock for the chemical industry: challenges and opportunities," in *Advances in the chemistry and processing of beet and cane sugar: Proceedings of the 2002 Sugar Processing Research Conference held in New Orleans, Louisiana, USA, 10-13 March 2002*, 2002: Sugar Processing Research, Institute, Inc., pp. 26-41.
[265] D. J. Hayes, S. Fitzpatrick, M. H. Hayes, and J. R. Ross, "The biofine process–production of levulinic acid, furfural, and formic acid from lignocellulosic feedstocks," *Biorefineries–Industrial Processes and Product*, vol. 1, pp. 139-164, 2006.
[266] R. Taylor *et al.*, "From the sugar platform to biofuels and biochemicals: final report for the European Commission Directorate-General Energy," 492297, 2015.

[267] Plastics Technology, "100% biobased polyester charts course to commercialization https://www.ptonline.com/blog/post/100-biobased-polyester-charts-course-to-commercialization," 2014.
[268] T. Werpy and G. Petersen, "Top value added chemicals from biomass: volume I--results of screening for potential candidates from sugars and synthesis gas," National Renewable Energy Lab., Golden, CO (US), 2004.
[269] C. Antonetti, D. Licursi, S. Fulignati, G. Valentini, and A. M. Raspolli Galletti, "New frontiers in the catalytic synthesis of levulinic acid: from sugars to raw and waste biomass as starting feedstock," *Catalysts*, vol. 6, no. 12, p. 196, 2016, doi: https://doi.org/10.3390/catal6120196
[270] J. F. Leal Silva, R. Grekin, A. P. Mariano, and R. Maciel Filho, "Making levulinic acid and ethyl levulinate economically viable: a worldwide technoeconomic and environmental assessment of possible routes," *Energy Technology*, vol. 6, no. 4, pp. 613-639, 2018, doi: https://doi.org/10.1002/ente.201700594.
[271] F. D. Pileidis and M. M. Titirici, "Levulinic acid biorefineries: new challenges for efficient utilization of biomass," *ChemSusChem*, vol. 9, no. 6, pp. 562-582, 2016, doi: https://doi.org/10.1002/cssc.201501405.
[272] G. K. Beh *et al.*, "Flame-made amorphous solid acids with tunable acidity for the aqueous conversion of glucose to levulinic acid," *Green Chemistry*, vol. 22, no. 3, pp. 688-698, 2020, doi: https://doi.org/10.1039/C9GC02567G.
[273] M. Mikola, J. Ahola, and J. Tanskanen, "Production of levulinic acid from glucose in sulfolane/water mixtures," *Chemical Engineering Research and Design*, vol. 148, pp. 291-297, 2019, doi: https://doi.org/10.1016/j.cherd.2019.06.022.
[274] S.-H. Pyo, S. J. Glaser, N. Rehnberg, and R. Hatti-Kaul, "Clean Production of Levulinic Acid from Fructose and Glucose in Salt Water by Heterogeneous Catalytic Dehydration," *ACS Omega*, 2020, doi: https://doi.org/10.1021/acsomega.9b04406.
[275] H. Qu *et al.*, "Metal-organic framework containing Brønsted acidity and Lewis acidity for efficient conversion glucose to levulinic acid," *Fuel Processing Technology*, vol. 193, pp. 1-6, 2019, doi: https://doi.org/10.1016/j.fuproc.2019.04.035.
[276] D. W. Rackemann, J. P. Bartley, and W. O. Doherty, "Methanesulfonic acid-catalyzed conversion of glucose and xylose mixtures to levulinic acid and furfural," *Industrial Crops and Products*, vol. 52, pp. 46-57, 2014, doi: https://doi.org/10.1016/j.indcrop.2013.10.026.
[277] I. Thapa, B. Mullen, A. Saleem, C. Leibig, R. T. Baker, and J. B. Giorgi, "Efficient green catalysis for the conversion of fructose to levulinic acid," *Applied Catalysis A: General*, vol. 539, pp. 70-79, 2017, doi: https://doi.org/10.1016/j.apcata.2017.03.016.
[278] S. Kumar and R. B. Gupta, "Biocrude production from switchgrass using subcritical water," *Energy & Fuels*, vol. 23, no. 10, pp. 5151-5159, 2009, doi: https://doi.org/10.1021/ef900379p.
[279] G. Yildiz, F. Ronsse, R. Venderbosch, R. van Duren, S. R. Kersten, and W. Prins, "Effect of biomass ash in catalytic fast pyrolysis of pine wood," *Applied Catalysis B: Environmental*, vol. 168, pp. 203-211, 2015, doi: https://doi.org/10.1016/j.apcatb.2014.12.044.
[280] D. S. Scott, L. Paterson, J. Piskorz, and D. Radlein, "Pretreatment of poplar wood for fast pyrolysis: rate of cation removal," *Journal of Analytical and Applied Pyrolysis*, vol. 57, no. 2, pp. 169-176, 2001, doi: https://doi.org/10.1016/S0165-2370(00)00108-X.
[281] F. Shafizadeh, R. H. Furneaux, T. G. Cochran, J. P. Scholl, and Y. Sakai, "Production of levoglucosan and glucose from pyrolysis of cellulosic materials," *Journal of Applied Polymer Science*, vol. 23, no. 12, pp. 3525-3539, 1979, doi: https://doi.org/10.1002/app.1979.070231209.

[282] J. Piskorz, D. Radlein, and D. S. Scott, "On the mechanism of the rapid pyrolysis of cellulose," *Journal of Analytical and Applied pyrolysis*, vol. 9, no. 2, pp. 121-137, 1986, doi: https://doi.org/10.1016/0165-2370(86)85003-3.
[283] N. M. Kuzhiyil, "Pyrolytic sugars from cellulosic biomass," Doctoral thesis, Iowa State University, 2013. [Online]. Available: https://lib.dr.iastate.edu/etd/13644
[284] A. Mukherjee, G. Portillo-Perez, and M.-J. Dumont, "Synthesis of hydroxymethylfurfural and furfural from hardwood and softwood pulp using ferric sulphate as catalyst," *Frontiers of Chemical Science and Engineering*, vol. 13, no. 3, pp. 531-542, 2019, doi: https://doi.org/10.1007/s11705-019-1814-3.
[285] S. R. G. Oudenhoven, R. J. M. Westerhof, N. Aldenkamp, D. W. F. Brilman, and S. R. A. Kersten, "Demineralization of wood using wood-derived acid: Towards a selective pyrolysis process for fuel and chemicals production," *Journal of Analytical and Applied Pyrolysis*, vol. 103, pp. 112-118, 2013/09/01/ 2013, doi: https://doi.org/10.1016/j.jaap.2012.10.002.
[286] T. v. d. Weijde *et al.*, "The potential of C4 grasses for cellulosic biofuel production," *Frontiers in Plant Science*, vol. 4, p. 107, 2013, doi: https://doi.org/10.3389/fpls.2013.00107.
[287] A. Neelamegam, H. Al-Battashi, S. Al-Bahry, and S. Nallusamy, "Biorefinery production of poly-3-hydroxybutyrate using waste office paper hydrolysate as feedstock for microbial fermentation," *Journal of Biotechnology*, vol. 265, pp. 25-30, 2018, doi: https://doi.org/10.1016/j.jbiotec.2017.11.002.
[288] E. Nzediegwu and M.-J. Dumont, "Chemo-Catalytic Transformation of Cellulose and Cellulosic-Derived Waste Materials into Platform Chemicals," *Waste and Biomass Valorization*, pp. 1-27, 2020, doi: https://doi.org/10.1007/s12649-020-01179-y.
[289] D. A. Turner, I. D. Williams, and S. Kemp, "Greenhouse gas emission factors for recycling of source-segregated waste materials," *Resources, Conservation and Recycling*, vol. 105, pp. 186-197, 2015, doi: https://doi.org/10.1016/j.resconrec.2015.10.026.
[290] J. Buongiorno, "Projected effects of US tariffs on Canadian softwood lumber and newsprint imports: a cobweb model," *Canadian Journal of Forest Research*, vol. 48, no. 11, pp. 1351-1357, 2018, doi: https://doi.org/10.1139/cjfr-2018-0153.
[291] S. Dutta *et al.*, "Influence of green solvent on levulinic acid production from lignocellulosic paper waste," *Bioresource Technology*, vol. 298, p. 122544, 2020, doi: https://doi.org/10.1016/j.biortech.2019.122544.
[292] S. S. Chen *et al.*, "Valorization of lignocellulosic fibres of paper waste into levulinic acid using solid and aqueous Brønsted acid," *Bioresource Technology*, vol. 247, pp. 387-394, 2018, doi: https://doi.org/10.1016/j.biortech.2017.09.110.
[293] W. Lei *et al.*, "Cellulose nanocrystals obtained from office waste paper and their potential application in PET packing materials," *Carbohydr. Polym.*, vol. 181, pp. 376-385, 2018, doi: https://doi.org/10.1016/j.carbpol.2017.10.059.
[294] A. Sluiter *et al.*, "Determination of structural carbohydrates and lignin in biomass," *Laboratory analytical procedure*, no. TP-510-42618, 2010.
[295] S. C. Moldoveanu and V. David, "Derivatization methods in GC and GC/MS," in *Gas Chromatography-Derivatization, Sample Preparation, Application*: IntechOpen, 2018.
[296] J. Shen and C. E. Wyman, "Hydrochloric acid-catalyzed levulinic acid formation from cellulose: data and kinetic model to maximize yields," *AIChE Journal*, vol. 58, no. 1, pp. 236-246, 2012.
[297] D. Díez, A. Urueña, R. Piñero, A. Barrio, and T. Tamminen, "Determination of Hemicellulose, Cellulose, and Lignin Content in Different Types of Biomasses by Thermogravimetric Analysis and Pseudocomponent Kinetic Model (TGA-PKM

Method)," *Processes*, vol. 8, no. 9, p. 1048, 2020, doi: https://doi.org/10.3390/pr8091048.
[298] C. Borsoi, M. V. Zimmernnam, A. J. Zattera, R. M. Santana, and C. A. Ferreira, "Thermal degradation behavior of cellulose nanofibers and nanowhiskers," *Journal of Thermal Analysis and Calorimetry*, vol. 126, no. 3, pp. 1867-1878, 2016, doi: https://doi.org/10.1007/s10973-016-5653-x.
[299] G.-T. Jeong and D.-H. Park, "Production of sugars and levulinic acid from marine biomass Gelidium amansii," *Applied Biochemistry and Biotechnology*, vol. 161, no. 1-8, pp. 41-52, 2010, doi: https://doi.org/10.1007/s12010-009-8795-5.
[300] N. Sweygers, M. H. Somers, and L. Appels, "Optimization of hydrothermal conversion of bamboo (Phyllostachys aureosulcata) to levulinic acid via response surface methodology," *Journal of Environmental Management*, vol. 219, pp. 95-102, 2018, doi: https://doi.org/10.1016/j.jenvman.2018.04.105.
[301] M. E. M. Ali, H. Abdelsalam, N. S. Ammar, and H. S. Ibrahim, "Response surface methodology for optimization of the adsorption capability of ball-milled pomegranate peel for different pollutants," *Journal of Molecular Liquids*, vol. 250, pp. 433-445, 2018, doi: https://doi.org/10.1016/j.molliq.2017.12.025.
[302] S. X. Chin, C. H. Chia, S. Zakaria, Z. Fang, and S. Ahmad, "Ball milling pretreatment and diluted acid hydrolysis of oil palm empty fruit bunch (EFB) fibres for the production of levulinic acid," *Journal of the Taiwan Institute of Chemical Engineers*, vol. 52, pp. 85-92, 2015, doi: https://doi.org/10.1016/j.jtice.2015.01.028.
[303] B. Girisuta, B. Danon, R. Manurung, L. Janssen, and H. Heeres, "Experimental and kinetic modelling studies on the acid-catalysed hydrolysis of the water hyacinth plant to levulinic acid," *Bioresource Technology*, vol. 99, no. 17, pp. 8367-8375, 2008, doi: https://doi.org/10.1016/j.biortech.2008.02.045.
[304] Z. Yang *et al.*, "Dilute-acid conversion of cotton straw to sugars and levulinic acid via 2-stage hydrolysis," *Industrial Crops and Products*, vol. 46, pp. 205-209, 2013, doi: https://doi.org/10.1016/j.indcrop.2013.01.031.
[305] K. Salmenoja, O. Poukka, and M. Battegazorre, "Management of non-process elements in eucalyptus Kraft pulp mills," in *42nd Pulp and Paper International Congress and Exhibition*, 2009.
[306] S. R. J. Petroudy and H. Resalati, "Newsprint from soda bagasse pulp in admixture with hardwood CMP pulp," *BioResources*, vol. 6, no. 3, pp. 2483-2491, 2011.
[307] S. Rivas, A. M. Raspolli-Galletti, C. Antonetti, V. Santos, and J. C. Parajó, "Sustainable production of levulinic acid from the cellulosic fraction of Pinus pinaster wood: Operation in aqueous media under microwave irradiation," *Journal of Wood Chemistry and Technology*, vol. 35, no. 5, pp. 315-324, 2015, doi: https://doi.org/10.1080/02773813.2014.962152.
[308] A. M. R. Galletti, C. Antonetti, V. De Luise, D. Licursi, and N. Nassi, "Levulinic acid production from waste biomass," *BioResources*, vol. 7, no. 2, pp. 1824-1835, 2012.
[309] E. S. Lopes *et al.*, "Kinetic insights into the lignocellulosic biomass-based levulinic acid production by a mechanistic model," *Cellulose*, vol. 27, pp. 5641-5663, 2020.
[310] C.-Y. Guan, S. S. Chen, T.-H. Lee, C.-P. Yu, and D. C. Tsang, "Valorization of biomass from plant microbial fuel cells into levulinic acid by using liquid/solid acids and green solvents," *Journal of Cleaner Production*, vol. 260, p. 121097, 2020, doi: https://doi.org/10.1016/j.jclepro.2020.121097.
[311] E. Nzediegwu, G. Portillo-Perez, and M.-J. Dumont, "Valorization of decationized newsprint to levulinic acid," *Cellulose*, pp. 1-19, 2021, doi: https://doi.org/10.1007/s10570-021-04061-9.

[312] J. S. Kim, Y. Lee, and T. H. Kim, "A review on alkaline pretreatment technology for bioconversion of lignocellulosic biomass," *Bioresource Technology*, vol. 199, pp. 42-48, 2016, doi: https://doi.org/10.1016/j.biortech.2015.08.085.
[313] R. Sindhu, A. Pandey, and P. Binod, "Alkaline treatment," in *Pretreatment of biomass*: Elsevier, 2015, pp. 51-60.
[314] M. Li *et al.*, "The effect of liquid hot water pretreatment on the chemical–structural alteration and the reduced recalcitrance in poplar," *Biotechnology for Biofuels*, vol. 10, no. 1, pp. 1-13, 2017, doi: https://doi.org/10.1186/s13068-017-0926-6.
[315] Q. Cai, L. Jothinathan, S. Deng, S. Ong, H. Ng, and J. Hu, "Fenton-and ozone-based AOP processes for industrial effluent treatment," in *Advanced Oxidation Processes for Effluent Treatment Plants*: Elsevier, 2021, pp. 199-254.
[316] P. Jain and N. Vigneshwaran, "Effect of Fenton's pretreatment on cotton cellulosic substrates to enhance its enzymatic hydrolysis response," *Bioresource Technology*, vol. 103, no. 1, pp. 219-226, 2012, doi: https://doi.org/10.1016/j.biortech.2011.09.110.
[317] S. R. Pouran, A. A. A. Raman, and W. M. A. W. Daud, "Review on the application of modified iron oxides as heterogeneous catalysts in Fenton reactions," *Journal of Cleaner Production*, vol. 64, pp. 24-35, 2014, doi: https://doi.org/10.1016/j.jclepro.2013.09.013.
[318] K. Walter, M. Paulsson, and P. Hellström, "Acid hydrogen peroxide treatment of Norway spruce TMP: a model study using free ferrous ions and ferric ions chelated with EDTA as catalysts," *Journal of wood chemistry and technology*, vol. 33, no. 4, pp. 267-285, 2013, doi: https://doi.org/10.1080/02773813.2013.792840.
[319] O.-K. Lee, "Mechanistic studies of the oxidation of lignin and cellulose models," 2003.
[320] Z. Tang and J. Su, "Direct conversion of cellulose to 5-hydroxymethylfurfural (HMF) using an efficient and inexpensive boehmite catalyst," *Carbohydrate Research*, vol. 481, pp. 52-59, 2019, doi: https://doi.org/10.1016/j.carres.2019.06.010.
[321] C. Wang, Q. Zhang, Y. Chen, X. Zhang, and F. Xu, "Highly efficient conversion of xylose residues to levulinic acid over FeCl3 catalyst in green salt solutions," *ACS Sustainable Chemistry & Engineering*, vol. 6, no. 3, pp. 3154-3161, 2018, doi: https://doi.org/10.1021/acssuschemeng.7b03183.
[322] Z. Zhi, N. Li, Y. Qiao, X. Zheng, H. Wang, and X. Lu, "Kinetic study of levulinic acid production from corn stalk at relatively high temperature using FeCl3 as catalyst: A simplified model evaluated," *Industrial Crops and Products*, vol. 76, pp. 672-680, 2015, doi: https://doi.org/10.1016/j.indcrop.2015.07.058.
[323] Y. Zhang, H. Li, X. Li, M. E. Gibril, and M. Yu, "Chemical modification of cellulose by in situ reactive extrusion in ionic liquid," *Carbohydrate Polymers*, vol. 99, pp. 126-131, 2014, doi: https://doi.org/10.1016/j.carbpol.2013.07.084.
[324] G. Dobele, G. Rossinskaja, T. Dizhbite, G. Telysheva, D. Meier, and O. Faix, "Application of catalysts for obtaining 1, 6-anhydrosaccharides from cellulose and wood by fast pyrolysis," *Journal of Analytical and Applied Pyrolysis*, vol. 74, no. 1-2, pp. 401-405, 2005, doi: https://doi.org/10.1016/j.jaap.2004.11.031.
[325] M. Yang *et al.*, "Fenton reaction-modified corn stover to produce value-added chemicals by ultralow enzyme hydrolysis and maleic acid and aluminum chloride catalytic conversion," *Energy & Fuels*, vol. 33, no. 7, pp. 6429-6435, 2019, doi: https://doi.org/10.1021/acs.energyfuels.9b00983.
[326] N. Sweygers, R. Dewil, and L. Appels, "Production of levulinic acid and furfural by microwave-assisted hydrolysis from model compounds: effect of temperature, acid concentration and reaction time," *Waste and Biomass Valorization*, vol. 9, no. 3, pp. 343-355, 2018, doi: https://doi.org/10.1007/s12649-016-9797-5.

[327] A. S. Khan *et al.*, "Dicationic ionic liquids as sustainable approach for direct conversion of cellulose to levulinic acid," *Journal of Cleaner Production*, vol. 170, pp. 591-600, 2018, doi: https://doi.org/10.1016/j.jclepro.2017.09.103.
[328] Q. Qing, Q. Guo, P. Wang, H. Qian, X. Gao, and Y. Zhang, "Kinetics study of levulinic acid production from corncobs by tin tetrachloride as catalyst," *Bioresource Technology*, vol. 260, pp. 150-156, 2018, doi: https://doi.org/10.1016/j.biortech.2018.03.073.
[329] M. J. McGrath *et al.*, "Calculation of the Gibbs free energy of solvation and dissociation of HCl in water via Monte Carlo simulations and continuum solvation models," *Physical Chemistry Chemical Physics*, vol. 15, no. 32, pp. 13578-13585, 2013, doi: https://doi.org/10.1039/C3CP51762D.
[330] W. Wang, A. Mittal, H. Pilath, X. Chen, M. P. Tucker, and D. K. Johnson, "Simultaneous upgrading of biomass-derived sugars to HMF/furfural via enzymatically isomerized ketose intermediates," *Biotechnology for biofuels*, vol. 12, no. 1, pp. 1-9, 2019, doi: https://doi.org/10.1186/s13068-019-1595-4.
[331] L. Yan, A. A. Greenwood, A. Hossain, and B. Yang, "A comprehensive mechanistic kinetic model for dilute acid hydrolysis of switchgrass cellulose to glucose, 5-HMF and levulinic acid," *Rsc Advances*, vol. 4, no. 45, pp. 23492-23504, 2014, doi: https://doi.org/10.1039/C4RA01631A.
[332] Q. Xiang, Y. Lee, P. O. Pettersson, and R. W. Torget, "Heterogeneous aspects of acid hydrolysis of α-cellulose," in *Biotechnology for Fuels and Chemicals*: Springer, 2003, pp. 505-514.
[333] A. Mukherjee and M.-J. e. Dumont, "Levulinic acid production from starch using microwave and oil bath heating: a kinetic modeling approach," *Industrial & Engineering Chemistry Research*, vol. 55, no. 33, pp. 8941-8949, 2016.
[334] B. Girisuta, K. Dussan, D. Haverty, J. Leahy, and M. Hayes, "A kinetic study of acid catalysed hydrolysis of sugar cane bagasse to levulinic acid," *Chemical Engineering Journal*, vol. 217, pp. 61-70, 2013.
[335] C. Wang *et al.*, "A kinetic study on the hydrolysis of corncob residues to levulinic acid in the FeCl 3–NaCl system," *Cellulose*, vol. 26, no. 15, pp. 8313-8323, 2019.
[336] X. Zheng, Z. Zhi, X. Gu, X. Li, R. Zhang, and X. Lu, "Kinetic study of levulinic acid production from corn stalk at mild temperature using FeCl3 as catalyst," *Fuel*, vol. 187, pp. 261-267, 2017.
[337] J. Li, H. Xiu, M. Zhang, H. Wang, Y. Ren, and Y. Ji, "Enhancement of cellulose acid hydrolysis selectivity using metal ion catalysts," *Current Organic Chemistry*, vol. 17, no. 15, pp. 1617-1623, 2013.
[338] J. Li, X. Zhang, M. Zhang, H. Xiu, and H. He, "Ultrasonic enhance acid hydrolysis selectivity of cellulose with HCl–FeCl3 as catalyst," *Carbohydrate Polymers*, vol. 117, pp. 917-922, 2015, doi: https://doi.org/10.1016/j.carbpol.2014.10.028.
[339] L. Peng, L. Lin, J. Zhang, J. Zhuang, B. Zhang, and Y. Gong, "Catalytic conversion of cellulose to levulinic acid by metal chlorides," *Molecules*, vol. 15, no. 8, pp. 5258-5272, 2010, doi: https://doi.org/10.3390/molecules15085258.
[340] B. Lindman, B. Medronho, L. Alves, C. Costa, H. Edlund, and M. Norgren, "The relevance of structural features of cellulose and its interactions to dissolution, regeneration, gelation and plasticization phenomena," *Physical Chemistry Chemical Physics*, vol. 19, no. 35, pp. 23704-23718, 2017, doi: https://doi.org/10.1039/C7CP02409F.
[341] C. Liu, X. Lu, Z. Yu, J. Xiong, H. Bai, and R. Zhang, "Production of levulinic acid from cellulose and cellulosic biomass in different catalytic systems," *Catalysts*, vol. 10, no. 9, p. 1006, 2020, doi: https://doi.org/10.3390/catal10091006.

[342] F. Hammerer *et al.*, "Rapid mechanoenzymatic saccharification of lignocellulosic biomass without bulk water or chemical pre-treatment," *Green Chem.*, vol. 22, no. 12, pp. 3877-3884, 2020, doi: https://doi.org/10.1039/D0GC00903B.
[343] E. Nzediegwu and M.-J. Dumont, "Optimization and mechanistic kinetic model: Toward newsprint waste conversion to levulinic acid," *J. Environ. Chem. Eng.* , vol. 9, no. 6, p. 106637, 2021, doi: https://doi.org/10.1016/j.jece.2021.106637.
[344] S. Takkellapati, T. Li, and M. A. Gonzalez, "An overview of biorefinery-derived platform chemicals from a cellulose and hemicellulose biorefinery," *Clean Technol Environ Policy.*, vol. 20, no. 7, pp. 1615-1630, 2018, doi: https://doi.org/10.1007/s10098-018-1568-5.
[345] Y. Zhao, K. Lu, H. Xu, L. Zhu, and S. Wang, "A critical review of recent advances in the production of furfural and 5-hydroxymethylfurfural from lignocellulosic biomass through homogeneous catalytic hydrothermal conversion," *Renew. Sust. Energ. Rev.*, vol. 139, p. 110706, 2021, doi: https://doi.org/10.1016/j.rser.2021.110706.
[346] A. Shivhare, A. Kumar, and R. Srivastava, "Metal phosphate catalysts to upgrade lignocellulose biomass into value-added chemicals and biofuels," *Green Chem.*, vol. 23, no. 11, pp. 3818-3841, 2021, doi: https://doi.org/10.1039/D1GC00376C.
[347] X. Lyu *et al.*, "Energy efficient production of 5-hydroxymethylfurfural (5-HMF) over surface functionalized carbon superstructures under microwave irradiation," *Chem. Eng. J.*, vol. 428, p. 131143, 2022, doi: https://doi.org/10.1016/j.cej.2021.131143.
[348] H. Wu, T. Huang, F. Cao, Q. Zou, P. Wei, and P. Ouyang, "Co-production of HMF and gluconic acid from sucrose by chemo-enzymatic method," *Chem. Eng. J.*, vol. 327, pp. 228-234, 2017, doi: https://doi.org/10.1016/j.cej.2017.06.107.
[349] D. P. Duarte, R. Martínez, and L. J. Hoyos, "Hydrodeoxygenation of 5-hydroxymethylfurfural over alumina-supported catalysts in aqueous medium," *Ind. Eng. Chem.*, vol. 55, no. 1, pp. 54-63, 2016, doi: https://doi.org/10.1021/acs.iecr.5b02851.
[350] X. Li *et al.*, "Valorization of corn stover into furfural and levulinic acid over SAPO-18 zeolites: Effect of Brønsted to Lewis acid sites ratios," *Ind Crops Prod.*, vol. 141, p. 111759, 2019, doi: https://doi.org/10.1016/j.indcrop.2019.111759.
[351] A. E. Eseyin and P. H. Steele, "An overview of the applications of furfural and its derivatives," 2015.
[352] O. He *et al.*, "Experimental and kinetic study on the production of furfural and HMF from glucose," *Catalysts*, vol. 11, no. 1, p. 11, 2020, doi: https://doi.org/10.3390/catal11010011.
[353] J. Arciszewski and K. Auclair, "Mechanoenzymatic Reactions Involving Polymeric Substrates or Products," *ChemSusChem*, 2022, doi: https://doi.org/10.1002/cssc.202102084.
[354] S. Kaabel, J. D. Therien, C. E. Deschênes, D. Duncan, T. Friščić, and K. Auclair, "Enzymatic depolymerization of highly crystalline polyethylene terephthalate enabled in moist-solid reaction mixtures," *Proc. Natl. Acad. Sci. U.S.A.*, vol. 118, no. 29, 2021, doi: https://doi.org/10.1073/pnas.2026452118.
[355] M. Pérez-Venegas and E. Juaristi, "Mechanoenzymology: State of the Art and Challenges towards Highly Sustainable Biocatalysis," *ChemSusChem*, vol. 14, no. 13, pp. 2682-2688, 2021, doi: https://doi.org/10.1002/cssc.202100624.
[356] M. Pérez-Venegas and E. Juaristi, "Mechanochemical and mechanoenzymatic synthesis of pharmacologically active compounds: A green perspective," *ACS Sustain. Chem. Eng.*, vol. 8, no. 24, pp. 8881-8893, 2020, doi: https://doi.org/10.1021/acssuschemeng.0c01645.

[357] C. G. Avila-Ortiz, M. Pérez-Venegas, J. Vargas-Caporali, and E. Juaristi, "Recent applications of mechanochemistry in enantioselective synthesis," *Tetrahedron Lett.*, vol. 60, no. 27, pp. 1749-1757, 2019, doi: https://doi.org/10.1016/j.tetlet.2019.05.065.
[358] C. Bolm and J. G. Hernández, "From synthesis of amino acids and peptides to enzymatic catalysis: a bottom-up approach in mechanochemistry," *ChemSusChem*, vol. 11, no. 9, pp. 1410-1420, 2018, doi: https://doi.org/10.1002/cssc.201800113.
[359] F. Hammerer *et al.*, "Solvent-free enzyme activity: quick, high-yielding mechanoenzymatic hydrolysis of cellulose into glucose," *Angew. Chem.*, vol. 130, no. 10, pp. 2651-2654, 2018, doi: https://doi.org/10.1002/ange.201711643.
[360] F. Hammerer, S. Ostadjoo, T. Friščić, and K. Auclair, "Towards Controlling the Reactivity of Enzymes in Mechanochemistry: Inert Surfaces Protect β-Glucosidase Activity During Ball Milling," *ChemSusChem*, vol. 13, no. 1, pp. 106-110, 2020, doi: https://doi.org/10.1002/cssc.201902752.
[361] S. Ostadjoo, F. Hammerer, K. Dietrich, M.-J. Dumont, T. Friscic, and K. Auclair, "Efficient enzymatic hydrolysis of biomass hemicellulose in the absence of bulk water," *Molecules*, vol. 24, no. 23, p. 4206, 2019, doi: https://doi.org/10.3390/molecules24234206.
[362] J. D. Therien, F. Hammerer, T. Friščić, and K. Auclair, "Mechanoenzymatic Breakdown of Chitinous Material to N-Acetylglucosamine: The Benefits of a Solventless Environment," *ChemSusChem*, vol. 12, no. 15, pp. 3481-3490, 2019, doi: https://doi.org/10.1002/cssc.201901310.
[363] R. Musule *et al.*, "Chemical composition of lignocellulosic biomass in the wood of Abies religiosa across an altitudinal gradient," *J. Wood Sci.*, vol. 62, no. 6, pp. 537-547, 2016, doi: https://doi.org/10.1007/s10086-016-1585-0.
[364] U. Tyagi, N. Anand, and D. Kumar, "Synergistic effect of modified activated carbon and ionic liquid in the conversion of microcrystalline cellulose to 5-Hydroxymethyl Furfural," *Bioresour. Technol.*, vol. 267, pp. 326-332, 2018, doi: https://doi.org/10.1016/j.biortech.2018.07.035.
[365] H. J. Kim, S. B. Kim, and C. J. Kim, "The effects of nonionic surfactants on the pretreatment and enzymatic hydrolysis of recycled newspaper," *Biotechnol. Bioprocess Eng.*, vol. 12, no. 2, pp. 147-151, 2007.
[366] M. K. Purkait and D. Haldar, *Lignocellulosic Biomass to Value-Added Products: Fundamental Strategies and Technological Advancements*. Elsevier, 2021.
[367] J.-L. Do and T. Friščić, "Mechanochemistry: a force of synthesis," *ACS Cent. Sci.*, vol. 3, no. 1, pp. 13-19, 2017, doi: https://doi.org/10.1021/acscentsci.6b00277.
[368] I. Halasz *et al.*, "In situ and real-time monitoring of mechanochemical milling reactions using synchrotron X-ray diffraction," *Nat. Protoc.*, vol. 8, no. 9, pp. 1718-1729, 2013, doi: http://www.nature.com/doifinder/10.1038/nprot.2013.100.
[369] H. Kulla, M. Wilke, F. Fischer, M. Röllig, C. Maierhofer, and F. Emmerling, "Warming up for mechanosynthesis–temperature development in ball mills during synthesis," *ChemComm.*, vol. 53, no. 10, pp. 1664-1667, 2017, doi: https://doi.org/10.1039/C6CC08950J.
[370] K. Užarević *et al.*, "Enthalpy vs. friction: heat flow modelling of unexpected temperature profiles in mechanochemistry of metal–organic frameworks," *Chem. Sci.*, vol. 9, no. 9, pp. 2525-2532, 2018, doi: https://doi.org/10.1039/C7SC05312F.
[371] S. Lukin, K. Užarević, and I. Halasz, "Raman spectroscopy for real-time and in situ monitoring of mechanochemical milling reactions," *Nat. Protoc.*, vol. 16, no. 7, pp. 3492-3521, 2021, doi: https://doi.org/10.1038/s41596-021-00545-x.

[372] T. Di Nardo and A. Moores, "Mechanochemical amorphization of chitin: impact of apparatus material on performance and contamination," *Beilstein J. Org. Chem.*, vol. 15, no. 1, pp. 1217-1225, 2019, doi: https://doi.org/10.3762/bjoc.15.119.
[373] S. Roy Goswami, M.-J. Dumont, and V. Raghavan, "Microwave assisted synthesis of 5-hydroxymethylfurfural from starch in AlCl3· 6H2O/DMSO/[BMIM] Cl system," *Ind. Eng. Chem.*, vol. 55, no. 16, pp. 4473-4481, 2016, doi: https://doi.org/10.1021/acs.iecr.6b00201.
[374] L. Liu, H.-m. Chang, H. Jameel, J.-Y. Park, and S. Park, "Catalytic conversion of biomass hydrolysate into 5-hydroxymethylfurfural," *Ind. Eng. Chem.*, vol. 56, no. 49, pp. 14447-14453, 2017, doi: https://doi.org/10.1021/acs.iecr.7b03635.
[375] K. Yan, G. Wu, T. Lafleur, and C. Jarvis, "Production, properties and catalytic hydrogenation of furfural to fuel additives and value-added chemicals," *Renew. Sust. Energ. Rev.* , vol. 38, pp. 663-676, 2014, doi: https://doi.org/10.1016/j.rser.2014.07.003.
[376] M. J. Antal Jr, W. S. Mok, and G. N. Richards, "Mechanism of formation of 5-(hydroxymethyl)-2-furaldehyde from D-fructose and sucrose," *Carbohydr. Res*, vol. 199, no. 1, pp. 91-109, 1990, doi: https://doi.org/10.1016/0008-6215(90)84096-D.
[377] C. Van Nguyen *et al.*, "Combined treatments for producing 5-hydroxymethylfurfural (HMF) from lignocellulosic biomass," *Catal. Today*, vol. 278, pp. 344-349, 2016, doi: https://doi.org/10.1016/j.cattod.2016.03.022.
[378] X. Qi, M. Watanabe, T. M. Aida, and R. L. Smith Jr, "Fast transformation of glucose and di-/polysaccharides into 5-hydroxymethylfurfural by microwave heating in an ionic liquid/catalyst system," *ChemSusChem*, vol. 3, no. 9, pp. 1071-1077, 2010, doi: https://doi.org/10.1002/cssc.201000124.
[379] T. D. Swift, C. Bagia, V. Choudhary, G. Peklaris, V. Nikolakis, and D. G. Vlachos, "Kinetics of homogeneous Brønsted acid catalyzed fructose dehydration and 5-hydroxymethyl furfural rehydration: a combined experimental and computational study," *ACS Catal.*, vol. 4, no. 1, pp. 259-267, 2014, doi: https://doi.org/10.1021/cs4009495.
[380] T. D. Swift, H. Nguyen, A. Anderko, V. Nikolakis, and D. G. Vlachos, "Tandem Lewis/Brønsted homogeneous acid catalysis: conversion of glucose to 5-hydoxymethylfurfural in an aqueous chromium (iii) chloride and hydrochloric acid solution," *Green Chem.*, vol. 17, no. 10, pp. 4725-4735, 2015, doi: https://doi.org/10.1039/C5GC01257K.
[381] C. Lupo, S. Boulos, and L. Nyström, "Influence of partial acid hydrolysis on size, dispersity, monosaccharide composition, and conformation of linearly-branched water-soluble polysaccharides," *Molecules*, vol. 25, no. 13, p. 2982, 2020, doi: https://doi.org/10.3390/molecules25132982.
[382] K. Lamminpää, J. Ahola, and J. Tanskanen, "Kinetics of xylose dehydration into furfural in formic acid," *Ind. Eng. Chem. Res*, vol. 51, no. 18, pp. 6297-6303, 2012, doi: https://doi.org/10.1021/ie2018367.
[383] Z. Chen, W. Zhang, J. Xu, and P. Li, "Kinetics of xylose dehydration into furfural in acetic acid," *Chin. J. Chem. Eng*, vol. 23, no. 4, pp. 659-666, 2015, doi: https://doi.org/10.1016/j.cjche.2013.08.003.
[384] N. L. da Costa *et al.*, "Phosphotungstic acid on activated carbon: A remarkable catalyst for 5-hydroxymethylfurfural production," *Mol. Catal.*, vol. 500, p. 111334, 2021, doi: https://doi.org/10.1016/j.mcat.2020.111334.
[385] A. Rusanen, K. Lappalainen, J. Kärkkäinen, and U. Lassi, "Furfural and 5-Hydroxymethylfurfural Production from Sugar Mixture Using Deep Eutectic

Solvent/MIBK System," *ChemistryOpen,* vol. 10, no. 10, pp. 1004-1012, 2021, doi: https://doi.org/10.1002/open.202100163.
[386] J. Hidalgo-Carrillo, A. Marinas, and F. J. Urbano, "Chemistry of Furfural and Furanic Derivatives," in *Furfural: An Entry Point of Lignocellulose in Biorefineries to Produce Renewable Chemicals, Polymers, and Biofuels*: World Scientific, 2018, pp. 1-30.
[387] H. Hoydonckx, W. Van Rhijn, W. Van Rhijn, D. De Vos, and P. Jacobs, "Furfural and derivatives," *Ullmann's encycl. ind. path,* 2000, doi: https://doi.org/10.1002/14356007.a12_119.pub2.
[388] Q. Tian, T. Shi, and Y. Sha, "CuO and Ag2O/CuO catalyzed oxidation of aldehydes to the corresponding carboxylic acids by molecular oxygen," *Molecules,* vol. 13, no. 4, pp. 948-957, 2008, doi: https://doi.org/10.3390/molecules13040948.
[389] W. Fan, C. Verrier, Y. Queneau, and F. Popowycz, "5-Hydroxymethylfurfural (HMF) in organic synthesis: a review of its recent applications towards fine chemicals," *Curr. Org. Synth.,* vol. 16, no. 4, pp. 583-614, 2019, doi: https://doi.org/10.2174/1570179416666190412164738.
[390] B. A. Smith, P. Champagne, and P. G. Jessop, "A Semi-Batch Flow System for the Production of 5-Chloromethylfurfural," *Chemistry-Methods,* vol. 1, no. 10, pp. 438-443, 2021, doi: https://doi.org/10.1002/cmtd.202100031.
[391] A. Baliani *et al.*, "Design and synthesis of a series of melamine-based nitroheterocycles with activity against trypanosomatid parasites," *J. Med. Chem.*, vol. 48, no. 17, pp. 5570-5579, 2005, doi: https://doi.org/10.1021/jm050177+.
[392] K. I. Galkin, F. A. Kucherov, O. N. Markov, K. S. Egorova, A. V. Posvyatenko, and V. P. Ananikov, "Facile chemical access to biologically active norcantharidin derivatives from biomass," *Molecules,* vol. 22, no. 12, p. 2210, 2017, doi: https://doi.org/10.3390/molecules22122210.
[393] C. Rosenfeld *et al.*, "Hydroxymethylfurfural: A key to increased reactivity and performance of fructose-based adhesives for particle boards," *Industrial Crops and Products,* vol. 187, p. 115536, 2022.
[394] C. Rosenfeld, J. Konnerth, W. Sailer-Kronlachner, P. Solt, T. Rosenau, and H. W. van Herwijnen, "Current situation of the challenging scale-up development of hydroxymethylfurfural production," *ChemSusChem,* vol. 13, no. 14, pp. 3544-3564, 2020.
[395] Y. Zhang *et al.*, "Direct conversion of biomass-derived carbohydrates to 5-hydroxymethylfurural over water-tolerant niobium-based catalysts," *Fuel,* vol. 139, pp. 301-307, 2015.
[396] N. Sweygers, J. Harrer, R. Dewil, and L. Appels, "A microwave-assisted process for the in-situ production of 5-hydroxymethylfurfural and furfural from lignocellulosic polysaccharides in a biphasic reaction system," *J. Clean. Prod,* vol. 187, pp. 1014-1024, 2018, doi: https://doi.org/10.1016/j.jclepro.2018.03.204.
[397] J. Slak, B. Pomeroy, A. Kostyniuk, M. Grilc, and B. Likozar, "A review of bio-refining process intensification in catalytic conversion reactions, separations and purifications of hydroxymethylfurfural (HMF) and furfural," *Chem. Eng. J,* vol. 429, p. 132325, 2022, doi: https://doi.org/10.1016/j.cej.2021.132325.
[398] Y. Yang, C.-w. Hu, and M. M. Abu-Omar, "Conversion of carbohydrates and lignocellulosic biomass into 5-hydroxymethylfurfural using AlCl 3· 6H 2 O catalyst in a biphasic solvent system," *Green Chem.*, vol. 14, no. 2, pp. 509-513, 2012, doi: https://doi.org/10.1039/C1GC15972K.
[399] Q. Ji, X. Yu, L. Chen, A. E. A. Yagoub, and C. Zhou, "Aqueous choline chloride/γ-valerolactone as ternary green solvent enhance Al (III)-catalyzed

hydroxymethylfurfural production from rice waste," *Energy Technol,* vol. 8, no. 12, p. 2000597, 2020, doi: https://doi.org/10.1002/ente.202000597.
[400] J. G. Lynam, C. J. Coronella, W. Yan, M. T. Reza, and V. R. Vasquez, "Acetic acid and lithium chloride effects on hydrothermal carbonization of lignocellulosic biomass," *Bioresour Technol,* vol. 102, no. 10, pp. 6192-6199, 2011, doi: https://doi.org/10.1016/j.biortech.2011.02.035.
[401] B. Frank, "Corrugated box compression—A literature survey," *Packag. Technol. Sci,* vol. 27, no. 2, pp. 105-128, 2014, doi: https://doi.org/10.1002/pts.2019.
[402] K. K. Gaikwad, S. Singh, and Y. S. Lee, "Functional corrugated board with organic and inorganic materials in food packaging applications: a review," *Korean Journal of Pakaging Science & Technology,* vol. 22, no. 3, pp. 49-58, 2016, doi: https://doi.org/10.20909/kopast.2016.22.3.49.
[403] Y. Ma and J. Cao, "Facile preparation of magnetic porous carbon monolith from waste corrugated cardboard box for solar steam generation and adsorption," *Biomass Convers. Biorefin.*, pp. 1-18, 2020, doi: https://doi.org/10.1007/s13399-020-00739-5.
[404] J. F. Saeman, "Kinetics of wood saccharification-hydrolysis of cellulose and decomposition of sugars in dilute acid at high temperature," *Ind. Eng. Chem.,* vol. 37, no. 1, pp. 43-52, 1945.
[405] Y. Zheng, Z. Pan, and R. Zhang, "Overview of biomass pretreatment for cellulosic ethanol production," *Int. J. Agric. Biol. Eng.,* vol. 2, no. 3, pp. 51-68, 2009, doi: https://doi.org/10.3965/j.issn.1934-6344.2009.03.051-068.
[406] U. Tyagi and N. Anand, "Conversion of Babool wood residue to 5-Hydroxymethyl Furfural: Kinetics and Process modelling," *Bioresource Technology Reports,* vol. 14, p. 100674, 2021.
[407] D. Licursi, C. Antonetti, M. Martinelli, E. Ribechini, M. Zanaboni, and A. M. R. Galletti, "Monitoring/characterization of stickies contaminants coming from a papermaking plant–Toward an innovative exploitation of the screen rejects to levulinic acid," *Waste Manage.,* vol. 49, pp. 469-482, 2016, doi: https://doi.org/10.1016/j.wasman.2016.01.026.
[408] L. Fan, Y. H. Lee, and D. H. Beardmore, "Mechanism of the enzymatic hydrolysis of cellulose: effects of major structural features of cellulose on enzymatic hydrolysis," *Biotechnol. Bioeng.,* vol. 22, no. 1, pp. 177-199, 1980, doi: https://doi.org/10.1002/bit.260220113.
[409] P. Kanchanalai, G. Temani, Y. Kawajiri, and M. J. Realff, "Reaction kinetics of concentrated-acid hydrolysis for cellulose and hemicellulose and effect of crystallinity," *Bioresources,* vol. 11, no. 1, pp. 1672-1689, 2016.
[410] G. G. Millán *et al.*, "Furfural production in a biphasic system using a carbonaceous solid acid catalyst," *Appl. Catal. A: Gen,* vol. 585, p. 117180, 2019, doi: https://doi.org/10.1016/j.apcata.2019.117180.
[411] Y. Yang, C. W. Hu, and M. M. Abu-Omar, "Synthesis of furfural from xylose, xylan, and biomass using AlCl3· 6 H2O in biphasic media via xylose isomerization to xylulose," *ChemSusChem,* vol. 5, no. 2, pp. 405-410, 2012.
[412] B. Saha and M. M. Abu-Omar, "Advances in 5-hydroxymethylfurfural production from biomass in biphasic solvents," *Green Chem.,* vol. 16, no. 1, pp. 24-38, 2014, doi: https://doi.org/10.1039/C3GC41324A.
[413] M. Li, W. Li, Y. Lu, H. Jameel, H.-m. Chang, and L. Ma, "High conversion of glucose to 5-hydroxymethylfurfural using hydrochloric acid as a catalyst and sodium chloride as a promoter in a water/γ-valerolactone system," *RSC Adv.,* vol. 7, no. 24, pp. 14330-14336, 2017, doi: https://doi.org/10.1039/C7RA00701A.

[414] F. Gomes, L. Pereira, N. Ribeiro, and M. Souza, "Production of 5-hydroxymethylfurfural (HMF) via fructose dehydration: Effect of solvent and salting-out," *Braz. J. Chem. Eng.*, vol. 32, pp. 119-126, 2015, doi: https://doi.org/10.1590/0104-6632.20150321s00002914.
[415] Y. Román-Leshkov and J. A. Dumesic, "Solvent effects on fructose dehydration to 5-hydroxymethylfurfural in biphasic systems saturated with inorganic salts," *Top. Catal.*, vol. 52, no. 3, pp. 297-303, 2009, doi: https://doi.org/10.1007/s11244-008-9166-0.
[416] A. Mittal, H. M. Pilath, and D. K. Johnson, "Direct conversion of biomass carbohydrates to platform chemicals: 5-hydroxymethylfurfural (HMF) and furfural," *Energy Fuels*, vol. 34, no. 3, pp. 3284-3293, 2020, doi: https://doi.org/10.1021/acs.energyfuels.9b04047.
[417] X. Zhang, D. Zhang, Z. Sun, L. Xue, X. Wang, and Z. Jiang, "Highly efficient preparation of HMF from cellulose using temperature-responsive heteropolyacid catalysts in cascade reaction," *Appl. Catal. B*, vol. 196, pp. 50-56, 2016, doi: https://doi.org/10.1016/j.apcatb.2016.05.019.
[418] E. Nzediegwu, M. Pérez-Venegas, K. Auclair, and M.-J. Dumont, "Semisynthetic production of hydroxymethylfurfural and furfural: The benefits of an integrated approach," *J. Environ. Chem. Eng.*, p. 108515, 2022, doi: https://doi.org/10.1016/j.jece.2022.108515.
[419] Z.-D. Ding, J.-C. Shi, J.-J. Xiao, W.-X. Gu, C.-G. Zheng, and H.-J. Wang, "Catalytic conversion of cellulose to 5-hydroxymethyl furfural using acidic ionic liquids and co-catalyst," *Carbohydr. Polym*, vol. 90, no. 2, pp. 792-798, 2012, doi: https://doi.org/10.1016/j.carbpol.2012.05.083.
[420] T. Zhang, W. Li, H. Xin, L. Jin, and Q. Liu, "Production of HMF from glucose using an Al3+-promoted acidic phenol-formaldehyde resin catalyst," *Catal. Commun.*, vol. 124, pp. 56-61, 2019, doi: https://doi.org/10.1016/j.catcom.2019.03.001.
[421] J. Zha, B. Fan, J. He, Y.-C. He, and C. Ma, "Valorization of Biomass to Furfural by Chestnut Shell-based Solid Acid in Methyl Isobutyl Ketone–Water–Sodium Chloride System," *Appl. Biochem. Biotechnol.*, vol. 194, no. 5, pp. 2021-2035, 2022, doi: https://doi.org/10.1007/s12010-021-03733-3.
[422] X. Li *et al.*, "Conversion of waste lignocellulose to furfural using sulfonated carbon microspheres as catalyst," *Waste Manage.*, vol. 108, pp. 119-126, 2020, doi: https://doi.org/10.1016/j.wasman.2020.04.039.
[423] H. Ma, Z. Li, L. Chen, and J. Teng, "LiCl-promoted-dehydration of fructose-based carbohydrates into 5-hydroxymethylfurfural in isopropanol," *RSC Adv*, vol. 11, no. 3, pp. 1404-1410, 2021, doi: https://doi.org/10.1039/D0RA08737H.
[424] P. Wang, H. Yu, S. Zhan, and S. Wang, "Catalytic hydrolysis of lignocellulosic biomass into 5-hydroxymethylfurfural in ionic liquid," *Bioresour. Technol*, vol. 102, no. 5, pp. 4179-4183, 2011, doi: https://doi.org/10.1016/j.biortech.2010.12.073.
[425] J. Wang, H. Cui, J. Wang, Z. Li, M. Wang, and W. Yi, "Kinetic insight into glucose conversion to 5-hydroxymethyl furfural and levulinic acid in LiCl· 3H2O without additional catalyst," *Chem. Eng. J*, vol. 415, p. 128922, 2021, doi: https://doi.org/10.1016/j.cej.2021.128922.
[426] J. B. Binder and R. T. Raines, "Simple chemical transformation of lignocellulosic biomass into furans for fuels and chemicals," *J. Am. Chem. Soc*, vol. 131, no. 5, pp. 1979-1985, 2009, doi: https://doi.org/10.1021/ja808537j.
[427] T. Chen and L. Lin, "Conversion of Glucose in CPL-LiCl to 5-Hydroxymethylfurfural," *Chin. J. Chem. Eng*, vol. 28, no. 9, pp. 1773-1776, 2010, doi: https://doi.org/10.1002/cjoc.201090299.

[428] N. Sweygers, M. Kamali, T. M. Aminabhavi, R. Dewil, and L. Appels, "Efficient microwave-assisted production of furanics and hydrochar from bamboo (Phyllostachys nigra “Boryana”) in a biphasic reaction system: effect of inorganic salts," *Biomass Convers. Biorefin.*, vol. 12, no. 1, pp. 173-181, 2022, doi: https://doi.org/10.1007/s13399-021-01372-6.
[429] W. Daengprasert, P. Boonnoun, N. Laosiripojana, M. Goto, and A. Shotipruk, "Application of sulfonated carbon-based catalyst for solvothermal conversion of cassava waste to hydroxymethylfurfural and furfural," *Ind. Eng. Chem. Res.*, vol. 50, no. 13, pp. 7903-7910, 2011, doi: https://doi.org/10.1021/ie102487w.
[430] G. Qiu, B. Chen, C. Huang, N. Liu, and X. Sun, "Tin-modified ionic liquid polymer: A novel and efficient catalyst for synthesis of 5-hydroxymethylfurfural from glucose," *Fuel*, vol. 268, p. 117136, 2020.
[431] E. Nzediegwu and M.-J. Dumont, "Optimization and mechanistic kinetic model: Toward newsprint waste conversion to levulinic acid," *Journal of Environmental Chemical Engineering*, vol. 9, no. 6, p. 106637, 2021.
[432] G. Yang, C. Wang, G. Lyu, L. A. Lucia, and J. Chen, "Catalysis of glucose to 5-hydroxymethylfurfural using Sn-beta zeolites and a Brønsted acid in biphasic systems," *BioResources*, vol. 10, no. 3, pp. 5863-5875, 2015.
[433] L. Zhang, G. Xi, J. Zhang, H. Yu, and X. Wang, "Efficient catalytic system for the direct transformation of lignocellulosic biomass to furfural and 5-hydroxymethylfurfural," *Bioresource technology*, vol. 224, pp. 656-661, 2017.
[434] Z. Xu *et al.*, "Conversion of corn stalk into furfural using a novel heterogeneous strong acid catalyst in γ-valerolactone," *Bioresource technology*, vol. 198, pp. 764-771, 2015.
[435] Y. Lu *et al.*, "Directional synthesis of furfural compounds from holocellulose catalyzed by sulfamic acid," *Cellulose*, vol. 28, pp. 8343-8354, 2021.
[436] P. Bhaumik and P. L. Dhepe, "Efficient, stable, and reusable silicoaluminophosphate for the one-pot production of furfural from hemicellulose," *ACS Catalysis*, vol. 3, no. 10, pp. 2299-2303, 2013.
[437] J. Zha, B. Fan, J. He, Y.-C. He, and C. Ma, "Valorization of Biomass to Furfural by Chestnut Shell-based Solid Acid in Methyl Isobutyl Ketone–Water–Sodium Chloride System," *Applied Biochemistry and Biotechnology*, vol. 194, no. 5, pp. 2021-2035, 2022.
[438] L. Ji, Z. Tang, D. Yang, C. Ma, and Y.-C. He, "Improved one-pot synthesis of furfural from corn stalk with heterogeneous catalysis using corn stalk as biobased carrier in deep eutectic solvent–water system," *Bioresource Technology*, vol. 340, p. 125691, 2021.
[439] Z. Zhang *et al.*, "Conversion of carbohydrates into 5-hydroxymethylfurfural using polymer bound sulfonic acids as efficient and recyclable catalysts," *RSC advances*, vol. 3, no. 24, pp. 9201-9205, 2013.
[440] L. Huang *et al.*, "Production of furfural and 5-hydroxymethyl furfural from Camellia oleifera fruit shell in [Bmim] HSO4/H2O/1, 4-dioxane biphasic medium," *Ind Crops Prod.*, vol. 184, p. 115006, 2022, doi: https://doi.org/10.1016/j.indcrop.2022.115006.
[441] L. Shuai and J. Luterbacher, "Organic solvent effects in biomass conversion reactions," *ChemSusChem*, vol. 9, no. 2, pp. 133-155, 2016.
[442] J. E. Morinelly, J. R. Jensen, M. Browne, T. B. Co, and D. R. Shonnard, "Kinetic characterization of xylose monomer and oligomer concentrations during dilute acid pretreatment of lignocellulosic biomass from forests and switchgrass," *Ind. Eng. Chem. Res.*, vol. 48, no. 22, pp. 9877-9884, 2009, doi: https://doi.org/10.1021/ie900793p.
[443] B. Lavarack, G. Griffin, and D. Rodman, "The acid hydrolysis of sugarcane bagasse hemicellulose to produce xylose, arabinose, glucose and other products," *Biomass*

Bioenergy, vol. 23, no. 5, pp. 367-380, 2002, doi: https://doi.org/10.1016/S0961-9534(02)00066-1.

[444] X. Li, Q. Liu, C. Luo, X. Gu, L. Lu, and X. Lu, "Kinetics of furfural production from corn cob in γ-valerolactone using dilute sulfuric acid as catalyst," *ACS Sustain Chem Eng*, vol. 5, no. 10, pp. 8587-8593, 2017, doi: https://doi.org/10.1021/acssuschemeng.7b00950.